NATIONAL TECHNICAL UNIVERSITY OF ATHENS

SCHOOL OF NAVAL ARCHITECTURE AND MARINE ENGINEERING

Probabilistic Assessment of Ship Dynamic Stability in Waves

by

Nikolaos I. Themelis

Doctoral Thesis

Athens, October 2008

NATIONAL TECHNICAL UNIVERSITY OF ATHENS

SCHOOL OF NAVAL ARCHITECTURE AND MARINE ENGINEERING

Probabilistic Assessment of Ship Dynamic Stability in Waves

by

Nikolaos I. Themelis

Doctoral Thesis

Advisory Committee:

Konstantinos J. Spyrou, *Associate Professor* (Supervisor)

Gerasimos A. Athanassoulis, *Professor*

Georgios D. Tsabiras, *Professor*

Athens, October 2008

Meanwhile the boat was still booming through the mist, the waves curling and hissing around us like the erected crests of enraged serpents.

Herman Melville
Moby Dick; or, the Whale, 1851

ACKNOWLEDGMENTS

The current thesis represents my scientific research effort and knowledge obtained during the period of my postgraduate studies at the School of Naval Architecture and Marine Engineering. In the School I found a lot of encouragement and support for my studies and I am indebted to its academic, research and administrative staff.

This thesis has been partly funded by the Greek Scholarship Foundation, the NTUA Committee of Basic Research through the project THALIS (NTUA Project No. 65/118900) and the European Commission through the integrated project SAFEDOR (Design, Operation and Regulation for Safety, IP-516278, sub-project SP 2.3: Probabilistic assessment of intact stability).

I would also specially express my gratitude to my supervisor, Prof. Kostas Spyrou, for his genuine support, inspiration and guidance during all these years. He has been a great academic teacher, helping me to advance my scientific knowledge as well as to express thoroughly my ideas and work in writing and oral form. Our collaboration was characterised by spirit of mutual understanding and determination for innovative research. Furthermore, I am indebted for his trust and for the opportunities which he gave to me for teaching and scientific work.

Moreover, I would like to thank the other members of the Advisory Committee, Prof. Gerasimos Athanassoulis and Prof. Georgios Tsabiras for their interesting and valuable remarks during the period of my work at NTUA. I am also grateful to the members and staff of the Ship Design Laboratory for their help.

Of profound importance has been my collaboration with Giannis Tigkas, Panos Poulios and Stavros Niotis. Except from their continuous encouragement, working in the same place for the major part of my thesis proved to be quite essential for my academic progress. Moreover we have built a strong friendship which I am sure will last for years.

Last but not least, I would like to thank my family, my father Ilias and my sister Eleni, for all the assistance and support they offered to me during my studies. It would be very difficult to arrive to the end without their help.

This thesis is dedicated to my mother Kaiti, whose memory is indelible.

CONTENTS

LIST OF FIGURES

LIST OF TABLES

Chapter 1:

Introduction

The development of a practical and yet scientifically sound methodology for the probabilistic assessment of ship dynamic stability in waves is the main objective of this thesis. The basic motivation came from the feeling that key advances in the knowledge of ship stability and stochastic wave theory could be integrated within a single framework where their strengths can be exploited and augmented concurrently. The general belief is that current stability criteria reflect little of the state-or-the-art in ship dynamics and in the modeling of sea waves. Moreover, there is necessity of fundamental rethinking of the criteria arising from the new ship design trends, generating new requirements and the potential of unexpected types of behaviour that could set in danger lives, the environment and properties. It appears that the time has come for setting new stability requirements and international consensus is currently built that these should be of probabilistic type, as discussions at IMO reveal. This thesis aims to contribute towards this direction.

As a major aspect of ship design and operation, the dynamics of ship rolling continually challenge the research community since the first published cornerstone works of Moseley (1850) and Froude (1861). It is obvious that fundamental understanding of this area is essential for establishing stability criteria that hold a rational basis. Basic research efforts towards comprehending the root mechanisms of ship instabilities have been carried out mainly in a deterministic context, regarding the excitation, as this offered a more rigorous basis for understanding and analyzing the underlying physics. Nevertheless, the seaway incurs probabilistic wind and wave loads on a ship and moreover, several operational uncertainties influence behaviour. Efforts to integrate these important elements are not novel, however the issue is still considered open.

The stochastic nature of the seaway is well reflected by a number of parametric models that abound in the literature of sea wave statistics. Nonetheless, deriving the probabilistic properties of the response is impeded by the nonlinear and multidimensional nature of mathematical models of extreme ship dynamics. Knowing the probability density functions (pdf) of wind and waves in the vicinity of a ship is not sufficient for deducing the exact pdf of

her responses, especially if the latter are large. Thus, a number of simplifications are usually necessary and the sort of simplifications defines in essence the research philosophy on the subject.

Those mathematically inclined often prefer to focus narrowly on an elementary version of the problem, assuming a simple structure for the mathematical model and certain idealizing properties for the random excitation. These enable a rigorous treatment, permitting sometimes analytical solution as regards the pdf of the response. However, generalizations towards more realistic conditions and sheer treatment of instabilities are restricted. At the other end, and impelling for practicality, those of engineering background often lean towards a "brute force" simulation approach, without considering the complexities of dynamical phenomena that govern the occurrence of various instabilities. The general feeling is that still, there is no reliable probabilistic method for ship stability assessment with the entailed depth and breadth for general engineering application.

The current approach represents an attempt to fill this gap by interfacing the deterministic analyses of ship dynamics with the wealth of probabilistic wave models and statistics. The study has relied on the following framework. Basic instabilities modes should be individually addressed where scientific findings of the nature of these instabilities obtained by deterministic ship stability analyses and tools have to be exploited. Furthermore the assessment should not focus on a single type of modeling of ship motions while appropriate state-of-the art sea wave statistics and models would be incorporated in the procedure. Finally practicality has to be satisfactory.

The inspiration for the idea driving this approach comes from a number of observations from the field of ship dynamics and wave:

- Subject to satisfying well-known relationships between the range of frequencies that appear in the excitation and the system's natural frequencies, near regularity of excitation is conducive to large amplitude responses.
- As noted by Draper (1971), higher waves tend to appear in groups.
- For certain instabilities to appear, some regularity in the excitation is required where the amplitude is built-up gradually (beam-sea resonance, parametric roll, cumulative broaching). Other instabilities are the outcome of the encounter of a single critical wave that is capable to disturb the ship from her safe bounded motion (capsize in breaking waves, pure-loss of stability, direct broaching). A final case is the cumulative

effect of random waves (accumulation of water on deck for intact or damaged ships).

Considering the above statements, the principal idea underlying this approach is described as follows: the probability of occurrence of some instability event could be assumed as equal to the probability of encountering the critical (or "worse") wave groups that generate this instability. Subsequently, the task could be disassembled into two parts:

- a mainly deterministic one, for producing the specification of critical wave groups as represented by their height, period and run-length, obtained entirely from ship motion dynamics; and
- a genuinely probabilistic, focusing on statistical wave models, in order to calculate the probability to encounter these critical wave groups.

Driven by these considerations, the thesis has been developed as follows: Firstly, in Chapter 2 is presented a review of the relevant scientific fields. This includes a brief introduction to the main intact ship stability problems, the methods and tools for their study with emphasis on the mathematical models, (both analytical and numerical) such as nonlinear dynamics techniques and simulation codes. A short analysis also of the current regulatory "instrument", the so-called weather criterion is also provided, aiming to present how the maritime community faces up the problem. Finally, a comprehensive review of the probabilistic treatment of ship rolling, which attempts to cover the main research branches of this vast area, is presented, where some conceptually relevant to the proposed approach references are critically discussed. Next, in Chapter 3 are outlined briefly the aims of the current thesis.

In Chapter 4 a detailed description of the proposed assessment methodology, rationally split into a number of steps that formalize the procedure, is provided. Illustration of each step of the methodology as well as the required definitions and examples are given, aiming to better unfold the structure of the novel assessment.

Chapter 5 is devoted to the analysis of the probabilistic properties of wave groups and specifically presents the basic theory and related works that will be employed for the current assessment. It should be noted that this approach takes advantage and combines properly methods and tools of this area, yet without contributing to new theoretical results. However, the integration of these techniques is not trivial, considering that it has never been achieved, as far as is known, in a similar methodology.

In the following Chapter, the deterministic ship dynamics tools that have been incorporated hitherto in this assessment are analyzed. As part of this thesis is the study of ship intact

stability, a mathematical model for the coupled large amplitude roll motion in beam seas has been developed, providing an “in house” numerical tool which could be fitted in the procedure. As it was decided that the assessment should not be biased towards a single type modeller of ship motions, a well known commercial panel code has also been employed. In addition two analytical criteria arising from key results of ship dynamics and providing properly input for two types of ship instability have been integrated into the analysis.

Application of the assessment has been demonstrated by means of two examples presented in Chapter 7. A ROPAX ferry and a post panamax containership have been investigated for specific routes in two different geographical areas while head seas parametric rolling, beam seas resonance and pure loss of stability have been studied using the calculation tools presented in the previous Chapter. A novel type of stability assessment diagram has been produced providing information about the probability of exhibiting instability of some selected type for individual stages of the journey.

In the final Chapter are examined various technical aspects of the assessment like the effect of weather parameters on the probability figures for a selected type of instability as well as the very interesting subject of how the initial state of the ship affects the outcome of the assessment procedure. Furthermore a critical comparison of the prediction capabilities of two calculation tools and its reflection on the probability calculations has been carried out.

The development of this approach and its applications have been documented in a number of papers which are cited as (Spyrou and Themelis 2005, 2006; Themelis and Spyrou 2006, 2007; Spyrou et al 2007a, 2007b).

Chapter 2:

Critical review

In this Chapter a review of studies related with aspects of importance to this thesis is presented. These studies can be categorized in two areas: the first is related with dynamic ship stability analyses and the second with the probabilistic treatment of ship rolling. Furthermore, a short review on the development of the "weather criterion" and some remarks concerning its basic philosophy is provided. The "weather criterion" constitutes the current intact stability requirement and thus it is the best representative of the regulatory framework. A significant topic also of the thesis is the probabilistic properties of wave groups. However, it was preferred to present these studies together with the analysis carried out in the relevant Chapter. Moreover, due to the extend of the field of these topics, only a characteristic sample of studies is provided, aiming both to consolidate, supplement and reinforce the theoretical basis of the current study and to present different approaches that may have potential for application in the future.

2.1 Dynamic stability of displacement-type ships

As the basic scope of this study is the development of an assessment for the dynamic ship stability in waves, it is elementary to explore the dynamics of extreme rolling motion which can incur capsize. At this point it should be noticed that ship instability in the current context is mainly connected with the direction of transverse rotation (rolling) which may resulted either by direct excitation by the wave or by instability in another mode of motion which is coupled with roll and produces then roll growth. Therefore, one could briefly distinguish the main types of ship instabilities by the angle of encounter between ship and waves as follows (Spyrou 2006):

Beam waves

Includes the classical resonance of a driven nonlinear oscillator, whereas shift of cargo can also result in excessive rolling motion due to the generation of strong bias. Water on deck is also included where decreased metacentric height is combined with dynamic interaction of ship and liquid motion. Furthermore impact loading by breaking wave acted on side of the ship may be experienced.

Following waves

In steep waves, roll restoring may obtain time dependence which can bear either pure loss of stability experienced as a lack of restoring on wave crest when the frequency of encounter is near to zero, or parametric resonance, which is fundamentally a Mathieu type phenomenon if the wave tuning is right (Spyrou 2004). Moreover nonlinear surging in following waves can force the ship to move at the same speed with the wave; this phenomenon is known as surf - riding. From this instability, loss of steerability may be produced leading to a tight turn towards the beam sea condition; this instability in the horizontal plane is known as broaching. Finally bow – diving can be caused induced by lack of pitch restoring due to a slender bow part.

Head waves

Parametric resonance can also occur; however in this case heave and pitch fluctuations are more pronounced and can contribute to the development of roll motion.

Of course combinations of these instabilities are also possible. Analytical presentation and mathematical modeling of such phenomena are however beyond the scope of this work. Belenky and Sevastianov (2007) provide a thorough discussion of the state-of-the-art in these topics. Furthermore, a concise presentation of important papers that contributed to the development of the theory of dynamic stability of ships, starting from the middle of 19th century with Moseley, including also Froude and Krylov, is presented in the appendix of Spyrou (2006).

Regarding the stability assessment that has been adopted formally by the maritime community and specifically by the International Maritime Organization (IMO), this involves the adoption in 1969 of the well known general stability criteria which are in fact empirical requirements addressing the righting arm. They were supplemented in 1985 by the so – called "weather criterion" which represents a treatment of roll dynamics of a ship that is exposed in wind and waves coming from abeam and based on a criterion developed in the '50s for Japanese passenger ships. Although it represents a dynamic viewpoint of the problem, its empirical nature does not account correctly for modern designs and especially large passenger ships. IMO proceeded recently to an "upgrade" of this criterion. Nevertheless these criteria stand far away from the current state of scientific knowledge and it is high time for more profound stability assessment to arise. A more detailed discussion of these topics is presented in the following section. It is also remarkable that other instabilities are not involved in a regulatory framework, except from a guidance to the Master issued by IMO (1995) regarding dangerous

situations in following seas, while a classification society developed recently a guide for the avoidance of parametric rolling for containerships (ABS 2004).

Generally, one of the most established methods of investigating and understanding ship stability dynamics and their underlying physics is through mathematical modeling. Besides it is argued that it is through deterministic analysis that one can obtain insight of the mechanics of capsize or instabilities modes. Contemporary research could be classified in two categories; the first regards relatively simple models which entail basic parameters of the problem, however they are suitable for rigorous dynamic analysis of the nonlinear behaviour by means of analytical and geometrical techniques. Their advantage is their capability prediction of basic nonlinear effects such as jumps of response and the phenomenon of sudden erosion of the safe basin, Thompson (1997). 'Threshold' relationships in closed form between key parameters can be produced in certain cases, offering aid at the early design stage. Nevertheless their simplified modelling of various aspects of the problem limits their implementation in detailed applications. The second area of mathematical modeling regards detailed numerical simulation codes that rely on a fuller set of motion equations, taking into account couplings with other degrees of freedom. More elaborated consideration of ship hull shape and ship – wave hydrodynamic interactions is achieved employing a first principles approach combined with engineering empiricism. Nonetheless, their usual practise reduces the process to simple simulation "runs" which may not be sufficient for identification of nonlinear dynamic phenomena.

At this point some key works for the study of nonlinear dynamic analyses are presented. Thompson (1997) presented and summarized the main global geometrical techniques of nonlinear dynamics aiming at providing criteria for hull design against capsize in beam seas. It is well known that capsize in beam waves is modelled by an escape of a driven oscillator from a potential well. Two of the most significant results of nonlinear dynamics in this field are sudden jumps of the response due to multiplicity of the responses and the sudden erosion of the safe area in the phase basin. For example Figure 2.1 shows a roll response curve, where x axis stands for the scaled wave frequency, that is encounter wave frequency over the natural roll frequency (undamped). Further increase of the frequency at position B will lead to a sudden jump to position C due to multiexistence of the response. Besides it was derived that the transient response is more critical regarding capsize as realized for lower levels of excitation and broader region of frequencies, therefore steady state analysis may overestimate the safety level.

The sudden loss of safe area is connected with the transformation of basin boundaries to fractal where the threshold in terms of excitation is predicted by Melnikov theory (Wiggins 1988). Further increase of excitation induces rapid erosion of the "integrity" of the system, a phenomenon known as "Dover cliff" (Thompson 1997). This is shown in the relevant integrity curves, which represent the ratio of safe area to the initial safe area (Figure 2.2). In this figure are also shown the rapid change of the safe basin area due to a small increase in the excitation and the fractal character of the erosion.

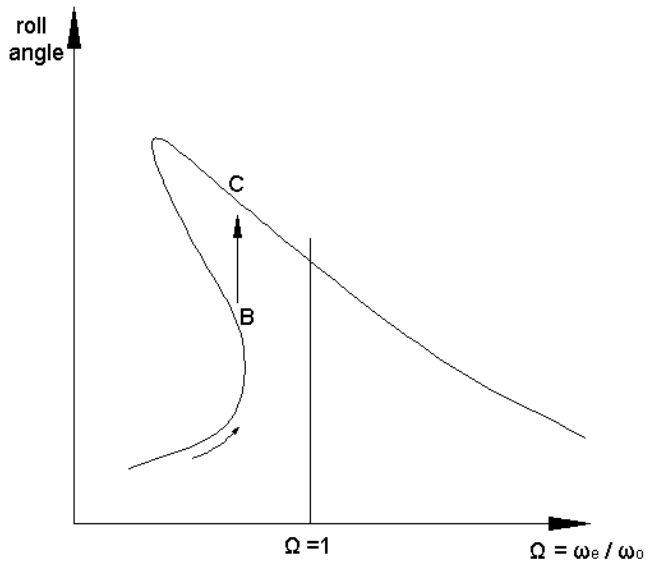

Figure 2.1: Schematic presentation of a roll response curve where sudden jumps can occur.

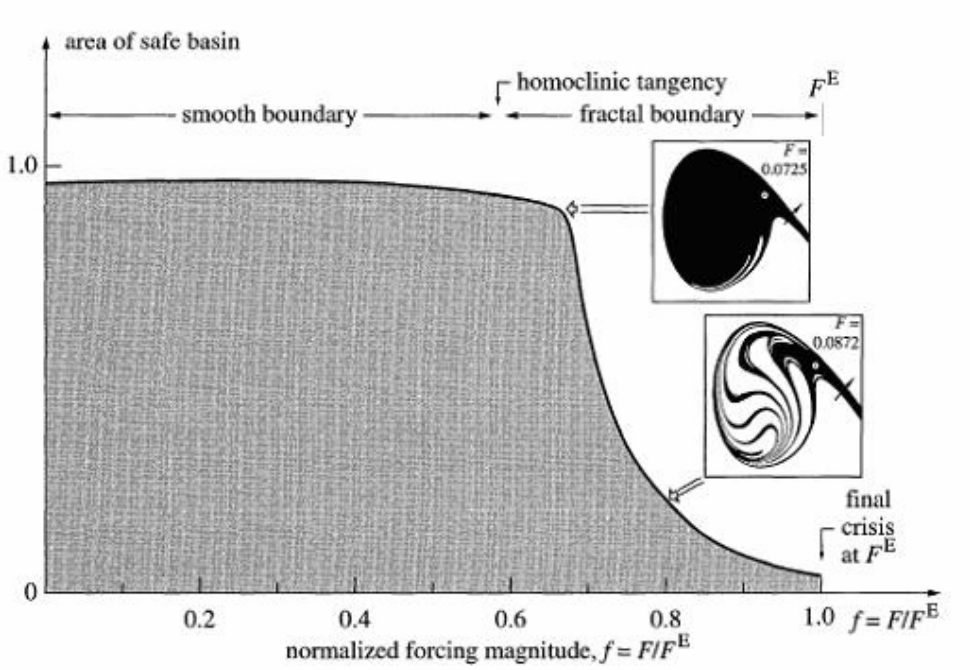

Figure 2.2: Engineering integrity curve and erosion of the safe basin of attraction, extracted by Thompson and Soliman (1990).

Damping can delay the point the "Dover cliff" appears in terms of excitation amplitude. A simple formula that connects characteristics of the ship, such as the angle of vanishing stability and the roll damping, with the critical wave slope based upon the above analysis was produced. Finally it was pointed out that a mean bias in roll, in terms of the required wave excitation for capsize compared with the unbiased case, can be crucial for capsize occurrence.

Besides, Falzarano et al (1992) had originally applied analytical global analysis techniques for the study of nonlinear behaviour. In particular they discussed how the roll damping and roll restoring affect the invariant manifolds of the system, which determine the limits of the safe and unsafe area in state space (safe basin boundary). However, the basin boundaries formed by stable manifolds can be fractal when stable and unstable manifolds intersect and become tangled. For example, Figure 2.3 shows the homoclinic tangency of a pair of manifolds arising for the same saddle. Once an intersection has taken place, an infinitive number of intersections will follow, creating a significant change in the safe basin area. In this case two adjacent points might belong to different domains of attraction which explain the fractal erosion of the safe basin. Melnikov's method can be used then, which in fact calculates the separation between the stable and unstable manifolds. When this separation distance changes sign, the manifolds have crossed, therefore transverse intersection points exist which bring about chaotic dynamics and a quick erosion of the safe basin. Melnikov's method produces an expression that connects system parameters (damping and metacentric height) and the critical forcing amplitude.

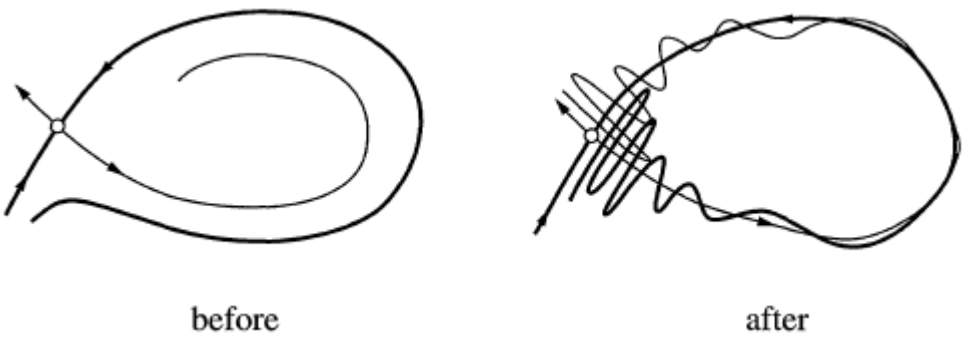

Figure 2.3: Intersection of invariant manifolds with increase of excitation amplitude (taken from Spyrou and Thompson 2000).

A collection of articles that share the same viewpoint in their approach are found in (Spyrou and Thompson 2000). In their introductory paper, the necessity of nonlinear analyses is explained through phenomena which linear dynamics cannot capture. These include for example, unexpected and violent transient motions leading to system capsize, irregular

response under regular excitation, subtle boundaries between the domains of coexisting responses and sensitive dependence on the initial conditions. Relevant aspects are also the coexistence of more than one response for the same parameter values of the system, bifurcation theory which investigates how the system can change its behaviour qualitatively as some influential parameters are varied, mechanisms that can lead to chaotic behaviour (e.g. period doubling). A reference work for chaotic motion that can lead to capsize is that of Virgin (1987). Techniques such as Poicaré maps as well as numerical simulations have been utilized for the study of chaotic motion induced by harmonic excitation.

Transient response has been considered as quite significant for the study of ship dynamic response. For example, Soliman (1990) ascertained that the critical wave height for capsize is smaller than the required for losing stability in steady state. In addition, a small regular wave train encountered with the right tuning is more dangerous for incurring capsize compared with stochastic excitation of same energy. Furthermore it is undeniable that this represents a more realistic scenario in ocean waves than a large number of regular wave cycles which are necessary for achieving steady state. This is supported also by the fact that roll damping is relatively small, so steady state is unlikely to be experienced, especially in real seas. From steady state analysis the bifurcation diagram can be calculated, providing knowledge of the behaviour of the system, while for transient response the transient capsize diagram has been proposed. This diagram estimates the critical wave excitation in terms of wave frequency for which capsize occur within a small number of wave encounters (e.g. 8 cycles), assuming that after these wave encounters capsize is unlikely to be experienced.

Various studies have been carried out attempting to investigate nonlinear roll dynamic behaviour in beam waves when couplings with other motions are preserved. In fact these studies try to apply techniques of nonlinear dynamical systems theory in a similar manner with one dimensional model and search for relevant phenomena as those presented in the above studies. For example Thompson et al (1992) developed a model from first principles taking into account roll, sway and heave motion. Supposing that the ship follows the rotational motion of the water particles and wave pressures are not disturbed by her presence, the concept of the effective gravitational field is introduced, which is supposed to be perpendicular to the water surface, allowing for the *GZ* characteristics derived in calm water to be used. In Appendix A the validity of this hypothesis is studied. Assuming also static balance in heave, a single roll equation is produced which contains implicitly a slave variation in heave coordinate. Furthermore, this model includes both direct excitation generated by the

rotational acceleration of the wave normal and parametric excitation produced by the fluctuating gravitational field. Steady state and transient response has been studied on the basis of this rolling equation, where nonlinear behaviour characteristics such as sudden jumps of the response and safe basin erosion were examined. Moreover a biased ship condition has been examined and due to the consideration of parametric forcing the biased ship is no longer insensitive to the direction of propagation of beam seas.

Chen et al (1999) also assembled a sway-heave-roll model in beam seas from first principles. After deriving the general three degree of freedom model, rescaling and nondimensionalization of the system led to a form that various time scales are taken into account. With this systematic reduction of the original system, a single degree of freedom model is obtained where roll motion was dominant while quasi static heave dynamics and sway velocity were taken into account. Invariant manifold theory of dynamical systems were used then finding out that the single d.o.f ship model can be regarded as the dynamics on a 2-D invariant manifold of the coupled ship system. Specifically they deduced that within the angles of vanishing stability, trajectories in the state space will quickly approach the slow invariant manifold which describes the roll/sway motion and after about 15 wave periods roll dynamics become dominant. But of course it is unlikely such a regular scenario to be realised in a real seaway.

McCue & Troesch (2003) developed a sway-heave-roll model with the hydrodynamic coefficients obtained from the linear seakeeping program SHIPMO of the University of Michigan. They investigated the development of integrity diagrams that could be suitable for a 3-degree of freedom system. For this reason the effect of the transverse and vertical position of the ship on the wave, through the sway/sway velocity and heave/heave velocity, on the erosion of the safe basin was studied. It was found that in some cases a stable ship can be significantly affected by her initial position on the waves.

Some recent studies that discuss specific aspects of ship stability problems follow. For example Kuroda and Ikeda (2002) studied experimentally and numerically the effect of drift motion. The wave induced drift force was determined with a panel method while lateral resistance was determined on the basis of vortex shedding using semi-empirical formulae developed earlier by Ikeda. Interesting jumps between high and low drift velocities leading to different rolling characteristics were observed. This behaviour may arise from the fact that different encounter frequencies can be experienced for the same wave due to the possibility of realising low and high drift velocities. Furthermore they concluded that the ratio of natural

roll period to natural heave period is important for roll resonance because of their coupled interaction in the restoring variation of each motion.

Special stability problems such as water on deck and its impact on roll motion have gathered attention. Water-on-deck can incur serious problems especially for small ships like the fishing vessels. Dillingham (1980) examined the dynamic behaviour of ship motion in beam waves when an amount of water is trapped and moves on her deck. A roll – sway model was used for ship motion while for the 2D motion of water-on-deck, shallow water equations were used. Hydraulic jumps and dry points on the deck are treated utilizing Glimm's method, which is a method for handling nonlinear hyperbolic systems. The relative position of water surface and deck openings is estimated, assuming steady flow. For small roll angles, a small amount of water on the deck might act as an antirolling device, as hydraulic jumps result in energy dissipation. However for a large amount of water flow, the coupling rolling motion becomes larger due to action of deck water.

On the other hand, more detailed models regarding the ship motion can be incorporated for the study of water on deck. For example Belenky et al (2003) utilized the code LAMP, which is a 3-D time-domain potential flow panel method based on a body-nonlinear formulation, for the study of nonlinear rolling motion considering water on deck and deck in water effects. Except from hydrostatic and Froude – Krylov forces acted due to these effects, dynamic flow on deck has been modelled. Firstly, the flow on the deck is estimated taking into account the relative motion of the ship, the incident wave at the deck edge and the motion of the deck. Then the water on deck motion is modeled with a finite volume technique assuming shallow water and allowing the calculation of the respective forces acted on the ship due to this effect. Some motion stability and some preliminary bifurcation analysis are also attempted.

Numerical codes for the simulation of ship motion are becoming popular, yet not fully reliable tools, for the study of extreme ship behaviour or capsize. An earlier review of this area is provided by Beck and Reed (2001). On the other hand ITTC Specialist Committee on Stability in Waves has carried out recently two benchmark studies (2002 and 2005) concerning numerical time domain tools for the study of extreme behaviour and capsizing of intact ships. Participants reflect the current state of the art in this field even though the level of detail and sophistication of the mathematical modelling varies. Emphasis has been given both in the accuracy of the predictions compared with experimental results and to the capability of identifying specific instabilities in various wave headings. It seems that further progress will be required before achieving satisfactory quantitative accuracy.

2.2 "Weather criterion" and some remarks on its probabilistic aspects

2.2.1 Basic philosophy

At this point a brief introduction of the current tool of the intact stability regulatory framework, the "weather criterion", as well as discussions of its basic philosophy and some of its probabilistic properties will be presented. Marine community had been long ago aware of the necessity of intact stability standards and the importance of stability requirements for the avoidance of ship accidents; see for example Kobylinski and Kastner (2003) for a historical review. Driven often by ship casualties, various attempts for determining minimum stability characteristics had been presented mainly between the two World Wars considering as more important the work of Rahola (1935). His approach was based on the analysis of the stability parameters of ships lost even 70 years ago with those of ships considered safe leading to a set of criteria regarding the righting arm curve which indeed are of statistical type. A summary of other attempts is presented in Kobylinski and Kastner (2003) and Brown and Deybach (1998). On the other hand various countries had developed intact stability criteria, for example USSR (1961), Japan – presented by Yamagata (1959) and USA (1962). In the framework of IMO, stability requirements were set in 1969 with the resolution A.167, following the spirit of the Rahola – type criteria. However at that time national stability criteria, like the above mentioned, had been developed which were based on more rational approaches, taking into account for example some ship roll dynamics. The need of more lucid requirements led to the adoption of the weather criterion as Resolution A.562 by IMO's assembly in 1985, applying to passengers and cargo ships over 24 meters in length. In particular the weather criterion has been based on Yamagata's work "Standard of stability adopted in Japan", cited as Yamagata (1959), while some contribution can be found back in Watanabe's (1938) work. Furthermore some technical part, that will be discussed later, emanated by the Russian stability requirements (USSR 1961). Even the weather criterion did not reflect in that period, and much more at our times, the state of the art in stability assessment approaches, is generally considered as a step – forward in the context of stability requirements. Resolutions of A. 167 and A.562 combined with those for ships carrying timber cargo (A. 206) and fishing vessels (A.168) in a unified intact stability code as Resolution A.749 (IMO 1993).

The main scope of the weather criterion is to determine the ability of a ship to withstand severe wind and rolling from abeam by comparing heeling and righting moments. This method of developing stability standards premises the correct calculation of the external heeling moments, while simplifications regarding the physics of the ship in a seaway are

necessary, for example righting moments are estimated in calm water.

In particular the weather criterion assumes that the ship is subjected to a steady side wind pressure obtaining a stationary heeling angle θ_0 estimated by the steady heeling wind arm l_{w1} which does not depend on the heeling angle (Figure 2.4). The steady wind speed velocity is $26\ \mathrm{m/s^2}$, a value that as will be mentioned later presents a kind of "average" condition between the center of typhoon and the following steady wind zone. The heeling angle of equilibrium θ_0 should be limited to a certain value; as a guide, 16^0 or 80% of the angle of deck immersion, whichever is less is suggested.

From this angle the ship performs resonant rolling motion due to wave action reaching to a maximum heeling angle θ_1 windward and then is subjected to a gust wind pressure represented by a lever $l_{w2} = 1.5\ l_{w2}$, a value discussed also next, acting at least for a half roll cycle. The criterion proposes that letting the ship roll freely from the position θ_1 with zero roll velocity, the potential energy should be sufficient in order to prevent the ship to roll leeward beyond the limiting angle θ_2. This is achieved when the area b is greater than the area a (Figure 2.4). The limiting angle θ_2 should be the minor of 50^0, the angle of downflooding or θ_c. As mentioned by Spyrou (2002), the ship is assumed to be released in still water from the off equilibrium position θ_1 as wave action is not taken into account at the leeward motion, thus only potential energies are accounted in the energy balance.

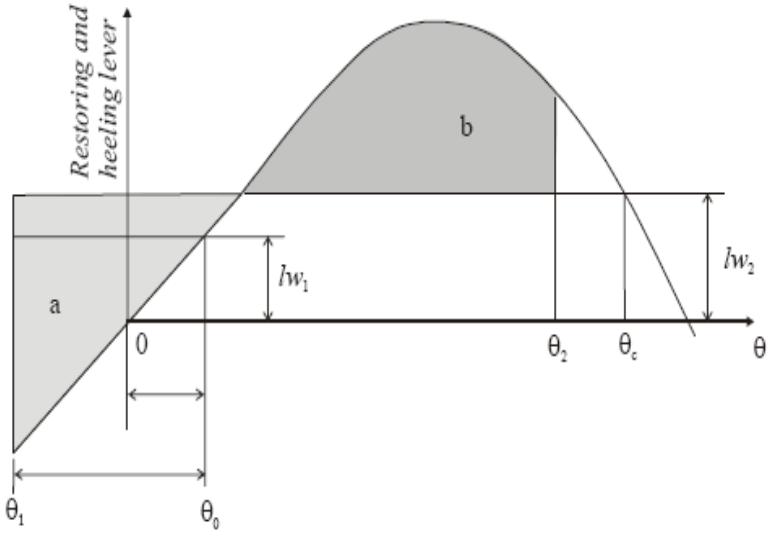

Figure 2.4: The weather criterion (taken from Spyrou 2002).

One of the most essential parts of the weather criterion is the calculation of the rolling amplitude θ_1 (roll back angle) whose value is derived by the next formula:

$$\theta_1 = 109kX_1X_2\sqrt{rs} \tag{2.1}$$

In fact this formula has been derived by the combination of the calculation methods proposed by Japan and USSR, based on the works of Yamagata (1959) and Lugovsky (1963) respectively. Yamagata (1959) expressed the amplitude of synchronous rolling in regular waves in terms of the effective wave slope r, wave steepness s and Bertin's extinction coefficient N. Due to the realistic seaway environment, a reduction for irregular waves has been considered, so the rolling amplitude θ_{1a} should be 70% of the synchronous rolling amplitude. This reduction is discussed later as it constitutes one of the probabilistic aspects of the criterion.

$$\theta_{1a} = \sqrt{\frac{138rs}{N}} \tag{2.2}$$

Yamagata's approach relates wave steepness with wave period through wave age (wave speed / wind speed), so for resonant rolling the respective wave steepness estimated by the natural roll period. Furthermore roll damping is expressed by Bertin's coefficient N, however Yamagata assumed it constant due to lack of a reliable formula. On the other hand, in the USSR approach rolling amplitude was estimated by the variance of rolling given a sea spectrum and knowing the transfer function. Furthermore, correction coefficients X_1, X_2 and k related with the breadth to draft ratio, block coefficient and bilge keel area respectively are involved in the calculation procedure, correlating ship parameters with the rolling amplitude. These coefficients are estimated by respective tables derived from a series of ships. Finally IMO combined Japan's method for the calculation of rolling amplitude with the correction coefficients of USSR approach leading to eq. 2.1 included in Resolution A.562.

Recently IMO proceeded, through the SLF Sub – Committee sessions, to a modification of the procedure of calculating rolling amplitude regarding the tables related with factors r and s, as they were quite unfavorable for new Ro/Ro ship designs. Large windage area, high position of center's of gravity and large roll periods were not characteristic of the series of ships used in the development of the coefficients of the criterion making it rather stringent for this type of ships. A fruitful discussion on this area has been provided by Franscescutto et al (2001). From a different viewpoint, Spyrou (2002) presented an approach as an alternative to

the weather criterion based on nonlinear dynamics theory. Specifically the engineering integrity concept and Melnikov's method are utilized aiming at the specification of the critical wave slope for capsize in terms of the wind –induced heel and damping. Wind loading is represented by a bias in the GZ curve, while direct numerical identification of the critical combinations of parameters through basin plots has been also used. This method provides also the opportunity to set fractional integrities (e.g. 90% integrity) which could be quite appropriate in setting stability criteria as the sustainable wave slope will reflect various levels of safety. The approach is based on global dynamics and stands beyond the "limited" performance based methods or the compliance with prescribed limits. However a number of issues should be refined, such as problem of selecting a limiting angle lower than the vanishing angle.

2.2.2 Probabilistic background

Following the work of Yamagata (1959), the main probabilistic aspect of the criterion regards the calculation of the maximum rolling angle in irregular waves. As known the criterion firstly estimates the synchronous rolling angle among regular waves as a function of wave steepness, effective wave slope coefficient, damping and other shape coefficients. However, the irregularity of sea waves should be considered. One could observe that in regular excitation the roll response curve has a steep crest in the region of synchronism. However in the case of irregular waves the curve is significantly lower as the necessary waves to cause exact synchronism are unlikely to be encountered successively. On the other hand, outside the region of synchronism, waves with periods near to the resonance period could come, even with a small probability. It would be then rational to make a reduction in the rolling amplitude; otherwise it would be too severe to consider the rolling angle at synchronism. This reduction is estimated supposing firstly a series of regular waves with height equal to the significant wave height of an assumed sea spectrum. Then the response rolling curve is estimated. Following the work of St. Dennis and Pierson (1953), which is also mentioned next, when irregular waves are taken into account the maximum rolling amplitude within 20 to 50 rolling oscillations can be estimated by the above rolling energy density and is about 0.7 times the rolling amplitude amongst regular waves. Thus this reduction value is considered for the estimation of rolling amplitude in irregular waves using the synchronous rolling amplitude. One could also assume that the choice of the steady wind and gust values holds a probabilistic basis. In the criterion the steady wind velocity has been selected as the middle point between the center of typhoon and the following steady wind zone. This selection was

based on the fact that in the center of a typhoon even the wind velocities have extreme values, the undeveloped sea results in the occurrence of highly irregular waves. On the following wind zone, wind velocities decrease but waves grow and become developed leading to more intense rolling. The middle case among these linearly connected situations was selected. Finally, "gustiness" or else the fluctuation of wind velocity, was determined as the average value observed for a typhoon, as it would be too harsh to select its maximum value. Furthermore, the critical gusts are of duration of half the typical natural roll periods and it is observed that more intense are the gusts with longer duration.

2.3 Probabilistic methods for ship rolling

St Denis and Pierson (1953) were the first to apply stochastic process theory in linear seakeeping. They exploited the Wiener – Khinchin theorem (e.g. Price and Bishop 1974) which, for a linear system, supplies the relationship between the spectra of excitation and response. As no general method has been developed yet for treating rigorously nonlinear systems driven by stochastic processes, several concepts were proposed for dealing with it in an approximate way.

In an effort to use results from linear theory, linearization techniques have been developed, where the idea is that the original nonlinear system is substituted with a linear equivalent. One method is statistical linearization; see for example Vassilopoulos (1971). Here, the stochastic excitation is assumed ergodic, while nonlinear roll restoring is substituted with an equivalent linear, under the requirement that the mean square of the error incurred is minimal. The linear response is, like the excitation, Gaussian with mean value zero and its variance should be minimized in order to obtain the "equivalent" linear coefficient. Another method based on linearization techniques is the energy statistical linearization of Gerasimov (1979) cited in Belenky and Sevastianov (2007). This method assumes equivalence of statistical characteristics in terms of work/energy balance. Specifically, the concept of energy equivalent cycle is proposed where a linear undamped and unforced oscillation with frequency equal to the averaged frequency of the original system and same roll velocity variance is sought. A drawback of these methods is that the output process is assumed Gaussian, which is not representative for a nonlinear system even though the input due to the wave surface elevation could be adequately assumed as a Gaussian process.

Analytical calculation of the probability distribution of the response is often attempted by assuming a stochastic "Markov process". This means that the current value of the process

depends only on the value in a previous moment of time and not on the previous history of the process. A Markov process can be fully characterized by the conditional distribution at two consecutive moments of time; and the function of the conditional distribution $f(t_1, x_1; t_2, x_2)$ can be considered as a solution of two partial differential equations [the so-called Fokker – Planck – Kholmogorov (FPK) equations], referring to a previous and to the current moment of time. Stationary solutions of the FPK equations for the case of nonlinear rolling under the assumption of Markov process were presented for example in Haddara (1974) and Roberts (1982). However, a disadvantage of this approach is that the excitation has to be modeled as an ideal white noise process in order to obtain analytically the stationary solution. Sea wave spectra have usually a distinct peak and limited bandwidth. Appropriate forming filters should then be used to describe the wave input. Even so, to derive analytic formulas in manageable form, the procedure has to be applied successfully for one degree of freedom. Problems arise also if nonlinear damping is assumed (Haddara and Zhang 1994).

In order to overcome these difficulties while keeping the assumption of a Markov process, numerous treatments have been presented. Roberts (1982) considered the energy envelope of the response, using the assumption that the energy of the envelope is a slowly varying parameter of time. Applying then a stochastic averaging technique, the two dimensional FPK equations are reduced to one for the energy envelope, implying that the process of the energy envelope is modeled approximately as one dimensional Markov process. This equation can be solved for any type of nonlinearity while the input process is not necessarily assumed as white noise. A stationary joint distribution for the roll displacement and roll velocity was obtained considering a related phase process. Haddara and Nassar (1986) combined also the averaging technique with the FPK approach to formulate the partial differential equation describing the conditional probability distribution for roll amplitude and employing also the Galerkin technique in order to derive the related distribution.

Other analytical methods dealing with the problem are non - Gaussian closure techniques which can be incorporated in order to develop expressions for the probability density functions for nonlinear systems (Ibrahim 1985). Another analytical method is Hermitte's which is based on diffusion process theory and it can be utilized for deriving the non - Gaussian response statistics of nonlinear systems driven by Gaussian or non Gaussian excitation (Ness et al 1989).

In particular for parametrically excited ship rolling, stability criteria have been developed

taking into account damping and characteristics of the spectrum of the fluctuating metacentric height. A popular definition of stability is the "almost sure" asymptotic stability. Assuming that the evolution of the system is represented as a diffusion Markov process, the stochastic Lyapunov functions can be used for producing criteria. For example Vinje (1976) derived a criterion for the standard deviation of *GM* variation, assuming that is Gaussian distributed. Furthermore, asymptotic stability depends on the exponential growth rate of the response of the system, which is determined by the sign of the maximum Lyapunov exponent λ. This is estimated as the stochastic analogue of the real part of the largest eigenvalue of a linearized system under deterministic excitation. Namachchivaya and Ramakrishnan (2003) derived a criterion where after estimating the maximum Lyapunov exponent λ, the requirement of $\lambda < 1$ leads to a critical value of damping involving the natural roll frequency and the spectrum density of the fluctuating *GM* process at twice the natural roll frequency. A relevant analysis can provide the moment Lyapunov exponent, in order to obtain information on the rate of convergence or the stability of moments (Nolan and Ramakrishnan 1999).

Naito et al. (2006) proposed a non linear relationship of a certain form between the short-term significant wave height and the standard deviation of ship response, where the two parameters could be identified from measurements; or on the basis of the severest outcome. Thereafter long-term response could be obtained with linear superposition of short-term exceedence probabilities. Assessments by this philosophy where a limited number of short-term sea states are used for obtaining a long-term assessment are popular also in neighboring fields (see for example Baarholm and Jensen 2004). The log normal can be a satisfactory model for the probability distribution of the significant wave height, while the three-parameter Weibull is believed to be suitable for extreme significant heights (Ochi 1998). For the joint distribution, scatter diagrams that present information of the combined values of significant wave height and average zero-crossing period are sometimes available. The joint log-normal distribution is a popular fit, although it seems to diverge for severe sea states (Ochi 1978). The joint distribution could be obtained from the product of the marginal distribution of significant wave height and the conditional distribution of mean period for a specific significant wave height. Mathiesen and Bitner – Gregersen (1990) used the three dimensional Weibull for the marginal and the log normal for the conditional. This field however concerns a vast part of wave statistics and will not analyzed further. For more details for the methods and related aspects for calculating joint pdf of these types from marginal distribution are given in (Athanassoulis et al 1994; Ochi 1998).

From another standpoint, Arnold et al (2004) discussed how some concepts from the theory of dynamical systems like attractors and bifurcations are generalized in the case when a system is perturbed by random noise. Then, the statistical behaviour of the random dynamical system is described by invariant measures, which in this case are probability measures. Furthermore, Lyapunov exponents as already mentioned, random attractors and their domain of attraction as well as stochastic bifurcation theory are utilized to describe the random system and possible qualitative changes of behaviour. In nonlinear dynamical systems' theory is rooted also the work of Hsieh et al. (1994) who have used the Melnikov function for a randomly excited system in order to assess the tendency of a ship for capsize (Simiu 2002). As it was referred, Melnikov's function expresses the distance between the stable and unstable invariant manifolds (Wiggins 1988; Falzarano et al. 1992). Their intersection generates chaos and potentially capsize. In this approach, the time-fluctuating part of the Melnikov function is associated with the stochastic excitation and specifically as the Melnikov function is a linear transformation of excitation, thus it is a random process. Assuming that wave elevation is a stationary ergodic Gaussian random process and using linear hydrodynamics the roll excitation is also a Gaussian process. Therefore Melnikov function is a stationary ergodic Gaussian process, so its mean and the variance uniquely determine its statistics. The mean proved to be zero, while after some manipulation the spectrum of this Melnikov part can be estimated. A probabilistic measure of capsize tendency was proposed; the rate of phase space flux, which is a measure of the amount of phase space transported, and hence, of the system's propensity for chaos. The result for the average rate states that the area under the positive part of the Melnikov function represents the area that transported out of the safe basin. It is interesting that there is a finite amount of phase space flux for every non zero excitation and after a certain critical value of significant wave height, the flux becomes important and increases in an asymptotic linear way. Similar studies for stochastic excitation have been performed also by Jiang et al (1996, 2000), where in their first study a biased ship is examined and in the second study the memory dependence of hydrodynamic coefficients have been included combing the extended state space technique with the phase space transport ideas.

On the other hand, numerical simulation techniques based e.g. on the Monte-Carlo method turn to be nowadays more popular. A profound advantage of these techniques is that there are fewer constraining assumptions about the type of the mathematical model. Generally, Monte-Carlo simulations are a kind of stochastic simulations that use a random generator. For

irregular rolling a generator of irregular waves is needed and then the rolling equation is solved numerically. However a large number of realizations are needed while the results depend strongly on satisfactory representation of the random excitation (Belenky et al. 2006). The analytical piece-wise linear method of Belenky (1994), including the fluctuating part of wind's excitation, was used by Paroka and Umeda (2006) for comparisons with numerical predictions and for testing the effectiveness of Monte-Carlo simulations. A Poisson flow for the upcrossings of the capsize limit within a given period time was assumed.

Repetitive numerical simulations are contemporarily a practical choice for estimating the probability of capsize. For example, McTaggart and DeKat (2000) used a well-known simulation code, FREDYN, and the random wave phase approach for generating wave realizations in order to estimate the probability of capsize. They adopted the Gumbel distribution in order to fit the maximum roll angles from each realization. However, the number of realizations can affect the Gumbel fit especially when hourly probabilities are greater than 10^{-3}. They examined different scenarios of speed, heading and weather and obtained practical polar diagrams of capsize probability. Whilst embodying a "black-box" approach and being short of accounting for factors like the initial conditions, polar diagrams are a popular means within the naval architecture community for expressing capsize tendency. Recent approaches like the time-to-capsize concept of Ayyub et al (2006) may enhance the potential of this assessment philosophy.

In order to overcome practicality problems related with the direct calculation of the probability of capsize, Belenky and Weems (2008) have introduced the so called "time split" method in which the problem is recast in two parts with different time scales. Since capsize is generally considered as a "rare" event, the methodology targets firstly the conditions leading to exceedence of GZ_{max}. Hence, the first part employs typical numerical simulations of ship motions in irregular waves where the "non-rare" events of upcrossing critical roll angles are calculated, while in the second part the "rare" event of capsize is addressed, examining the probability of capsize given the exceedence of $GZ_{max.}$ Essential for the approach is the assumption of Poisson flow for the upcrossings. This was tested and the sensitivity of the results on the crossing level was verified. On the other hand, in quartering seas, Poisson flow seems to be rather inappropriate as the response process holds a distinct group structure. This physics-based consideration of capsize as a sequence of two events presents also a similar insight with the process of wave group impact on ship response, which is the core element of the current thesis.

The significance of the group structure of random waves in the occurrence of instabilities and unacceptable behaviour has been noticed by some studies that are nearer to the spirit of the current thesis. Blocki (1980) attempted to correlate wave group occurrence with parametric roll experience. In this study the amplitude of the critical initial roll velocity that will lead to the critical roll angle was deterministically estimated by the approximated analytical solution of a non linear parametric equation for various group lengths while Goda's theory (Goda 1976), was used for the calculation of the probability of occurrence of the wave groups with these lengths. However, a drawback of this assessment is that there is no connection of the heights of the waves in the group with the phenomenon of parametric rolling as they are taken into account arbitrarily. Nevertheless, the crossing level of the wave height significantly affects the probability of occurrence for a given sea state. Furthermore the sequence of waves exceeding the critical level is assumed uncorrelated. Nonetheless the interesting point is the fact that initial conditions were treated as random variables connected to the wave environment; yet the initial roll angle is set always to zero. This may underestimate the probability of exceeding the critical threshold as many critical wave groups may not be considered.

Tikka and Paulling (1990) contemplated the analysis of parametric rolling in terms of the encounter of a high run of waves and referred also to the combination of ship's speed and heading that could lean toward such an encounter combined with mean group velocity. DeKat (1994) referred also to the use of joint distributions of wave length and steepness for predicting the encounter of critical combinations. Also he mentioned how in astern seas forward speed effects can result to a type of regular roll excitation during the passage of a wave group despite the inherent spatial irregularities, which may lead, depending on the length of the encountered wave group, to parametric resonance.

Boukhanovsky and Degtyarev (1996) studied statistical issues related with the group structure of waves and their correlation with the group structure of parametric roll response in longitudinal seas. They claimed that a sequence of short groups with similar periods is more dangerous than one long wave group, repeating also that swell seas are more propitious to the development of wave groups than wind waves.

Furthermore, Myrhaug et al (2000) investigated synchronous rolling by using joint distributions of successive wave periods. Providing a simple formula for the increase of roll amplitude in synchronous conditions, they presented how a joint pdf of periods could be embodied in a simplified manner for probabilistic calculations without however considering

the magnitude of critical wave heights.

Takaishi et al (2000) have also considered “high runs” of wave groups as dangerous encountered passages in following and quartering seas. Especially they correlated the dangerous zone, shown on the operation guidance issued by IMO (1995), determined mainly by the ratio V/T , i.e. ship speed/ wave period, with the probability of encountering groups of “high runs”. Encountered spectrum in a specific range of speeds can be very narrow, leading to a wave energy concentration which increases significantly the probability of encountering wave groups with the respective wave frequencies. Long – crested seas are more favor in this phenomenon as the directional distribution of wave energy diminishes the concentration of energy. However the ratio V/T cannot be the only connection parameter with the probability of a “high run” as the number of waves in the group as well as their wave height also contributes to the development of the examined ship instability.

Spyrou (2004) has also pointed out the relevance of wave groups with the growth of parametric rolling describing how wave group length and height in group waves could be connected with a criterion for roll growth.

Chapter 3:

Objectives

The objectives of the thesis can be stated as follows:

- To develop a probabilistic assessment methodology of ship intact stability capable of addressing the main instability modes, with sufficient practicality and which can be embedded upon a risk assessment framework.
- To study the scientific areas that underlie the methodology; such as, ship dynamic stability and especially nonlinear dynamics techniques and the mechanics that govern the main capsize modes; main probabilistic methods of ship rolling, stochastic waves and particularly wave group theory.
- To develop and test the required calculation tools for efficient implementation of the new methodology.
- To demonstrate the practicality of the assessment method through applications, supported by various parametric studies and investigations of technical issues.

Chapter 4:

Concept and description of the new methodology

4.1 Introducing the concept

Several thoughts and ideas have contributed to the development of the current assessment procedure. For example, it is essential the main ship instabilities to be individually addressed. This will enhance the methodology, as different ship types are prone to exhibiting potentially different modes of instability. As mentioned in the introduction, practical, engineering probabilistic treatments of extreme ship rolling motions that address the basic instabilities have not yet reached a reliable level. On the other hand, numerical simulation codes of ship motions under random wave excitation present several limitations, concerning mainly the assumed stationarity of the modeled stochastic waves and the targeted nonlinear roll responses. Lengthy simulation runs, representing for example a long voyage response time history, are time consuming and results are sensitive to the modeled process of random waves.

Thus one could think that a reasonable alternative would be to determine firstly the critical wave events that incur undesirable or excessive responses and then calculate the probability of occurrence of these events from wave statistics. The envisaged separation of ship motion dynamics from the stochastic wave excitation allows flexibility in the use of ship dynamics, without affecting the essence of the probabilistic calculation process. Furthermore, use of more than one tool should result in a more informed decision about the specification of the critical wave events.

The above conception holds also a solid scientific basis; for certain instabilities to appear, such as beam seas resonance and parametric rolling, rightly tuned wave trains should be encountered. The tuning concerns the range of wave frequencies and their relationship with system's natural frequencies, while the near regularity in the excitation is favourable for large amplitude responses when also high waves appear. Such wave occurrences are known also as wave groups. More specifically, a wave group is a sequence of waves with heights exceeding some preset level and having nearly equal periods (Masson and Chandler 1993; Ochi 1998). The tendency of large waves to appear in groups has been widely observed; see for example Draper (1971), while their importance for marine safety has motivated many research studies

regarding their probabilistic occurrence and they will be presented in the next Chapter. On the other hand, for other instabilities, such as that owed to the breaking of a wave at the side of a ship, the single encounter of a critical wave could disturb the bounded ship motion.

Subsequently, taking into account these remarks, the concept of the methodology could be summarized as follows: the probability of occurrence of some instability event could be assumed as equal to the probability of encountering the critical (or "worse") wave groups (or single wave) that generate this instability. The specification of the characteristics of the critical wave groups from, in the first instance, deterministic ship motion dynamics constitutes the first part of the envisaged solution, while the second entails the calculation of the probability to encounter these critical wave groups from suitable stochastic wave models.

In a probabilistic ship stability assessment various aspects should be taken into account. Therefore the methodology has been arranged in a number of steps that take care of these features. For example, a set of stability criteria addressing the main ship instabilities should be included. In order the criteria to be functional, unsafe behaviour should be specified by the setting of norms representing limiting values regarding ship response and her cargo's shifting. The safety limits could be escalated according to levels of risk; for example limits for a Ro/Ro ferry could range from passenger comfort criteria up to capsize heeling angles.

Of course, the considered time of exposure to the environment is also one of the parameters that determine the type of the assessment as well as the type of the required weather parameters data. Thus statistical, forecast or hindcast wave data can be used according to the assumed assessment scenario. Another point of the assessment is the representation of the weather conditions, along a specific route or in the wider navigational area. This could be done by a grid of weather nodes. Performing calculations for each point of the grid, prediction of the type of ship instabilities that may occur in the area around each node, and thus at specific parts along the route can be obtained. Therefore, useful information for design or for operational measures is produced. The basic steps of the assessment methodology are shown schematically in the flow chart of Figure 4.1. A detailed presentation and explanation of the proposed steps and their options follows.

4.2 Type of assessment

Assuming as known, at least in general terms, the specification of the ship under investigation, different perspectives are possible concerning the character of her assessment, determined by the length of time of the ship's exposure to the environment. In the current

context, as "short-term" will be labeled an assessment where stability is gauged during a single voyage. Therefore a route, or alternative routes, need to be specified beforehand and the assessment will be driven by the "few hours" forecast of the representative environmental parameters, in the vicinity of the prescribed route(s).

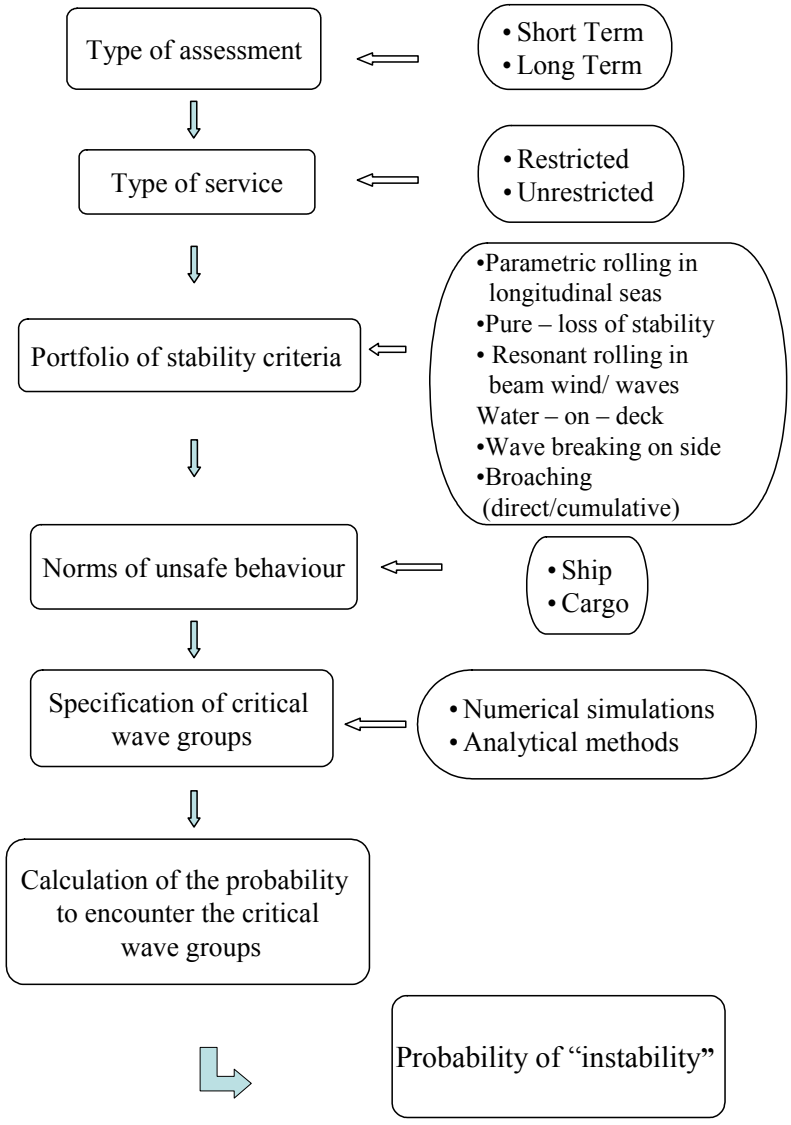

Figure 4.1: Flow – chart of the methodology.

Besides, an assessment based on hindcast weather data could be also performed. "Short-term" assessment could support decision-making concerning ship departure control (Spyrou et al. 2004) or weather routing in terms of stability performance. A note of caution is needed here: whilst short-term wave data are an essential input of this assessment, one should not confuse the, say, one hour validity concerning stationarity, of short-term wave data with the reference duration of a short-term stability assessment under the current methodology which could last for several hours as "fresh" environmental data continually feed the model. Therefore, from

the ship's stability point of view a short term assessment could include many short term weather data input along the route in order changing of weather conditions in time and place to be adequately captured. If one would like to characterize this type of assessment from a wave statistics viewpoint, then a middle timescale should be used among short and long term and thus a possible expression would be "middle – term" assessment.

On the other hand, "long-term" assessments might be undertaken for a variety of reasons. Probabilities of occurrence of instability on a seasonal or annual basis, either for specific reference routes or for wider areas of operation, can be determined with obvious utility at corporal and national administration levels. Moreover, by projecting the annual statistics to the ship's life-span, a long-term assessment could be tied to ensuring a satisfactory stability safety level in a design process. For example estimations of the stability performance might be carried out for different bilge keel designs helping in the decision stage of the design. This type of study requires long term weather statistics of the geographical area of interest. At this point it should be mentioned again that the procedure could be embodied within a risk – based framework whether it regards decisions in weather routing or in design level.

4.3 Type of service and grid of weather nodes

The anticipated service profile needs to be specified amongst restricted and unrestricted. Restricted service refers to operation on specific routes (e.g. the standard route of a Ro/Ro ferry in the Mediterranean Sea). Unrestricted service sets no narrow limits for the navigational area, e.g. the North Atlantic, and thus it might lead to a different assessment result while it concerns long – term assessment mainly.

The procedure "assumes" mapping of the weather data (representing a forecast, hindcast or statistical information) on a grid of "weather nodes". For a restricted ship service profile they should be placed, with sufficient density, close enough to the route; otherwise, for unrestricted service they should be scattered in the wider navigational area that is under consideration. In this case one should fit a probabilistic distribution for the ship to lie in a specific node and time. Each node "influences" an area that surrounds it and it will be assumed that inside an area of this kind, the weather conditions are uniform, represented by the weather at the node. The usual weather parameters considered are the significant wave height H_S, the wave peak period T_P, the mean wave direction Θ_M while mean wind speed and direction can also be taken into account when wind excitation is examined. Then, the voyage is split into a number of segments whose number depends on the distance between nodes in the "weather grid".

This notion is illustrated in Figure 4.2. The dots correspond to the nodes while the rectangle around the dots to their influence area. For a short-term assessment, stationarity of wave data can reasonably be assumed if a sufficiently dense grid has been generated, so the ship moves to the next grid area before weather conditions changed.

Following the placement of weather nodes, the time that the ship spends in the vicinity of each node as a percentage of the duration of the voyage in beam, following and head seas is taken place. The time spent by the ship within the influence area of some arbitrary node S depends on the length inside the corresponding rectangle (obtained with a simple geometrical calculation) and the speed sustained by the ship in that part of the journey. Then, the time of exposure to beam, head and following seas can be deduced taking into account the heading of the ship (according to the defined route) and the distribution of mean direction of the local wave field around each node. For this reason a convention for the wave direction and the encounter angle should be assumed like the one of Figure 4.3. Moreover given the density of the mean wave direction, the probability of exposure to head seas for example, will be estimated by the area between the limiting angles that define the "head-seas" encounter (Figure 4.4). The time of exposure to specific wave scenarios then scaled with reference to the duration of the whole voyage.

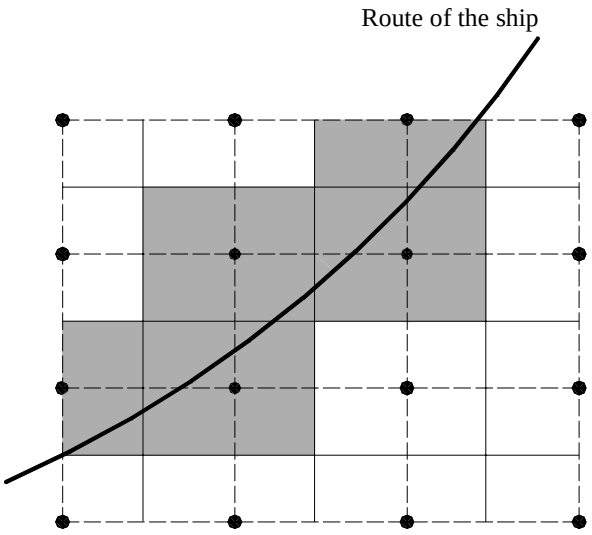

Figure 4.2: Weather nodes with their areas of influence.

$$\tau_{S\ \text{head}} = \frac{\text{time spent in head seas in the } S \text{ node}}{\text{whole duration of the voyage}} \tag{4.1}$$

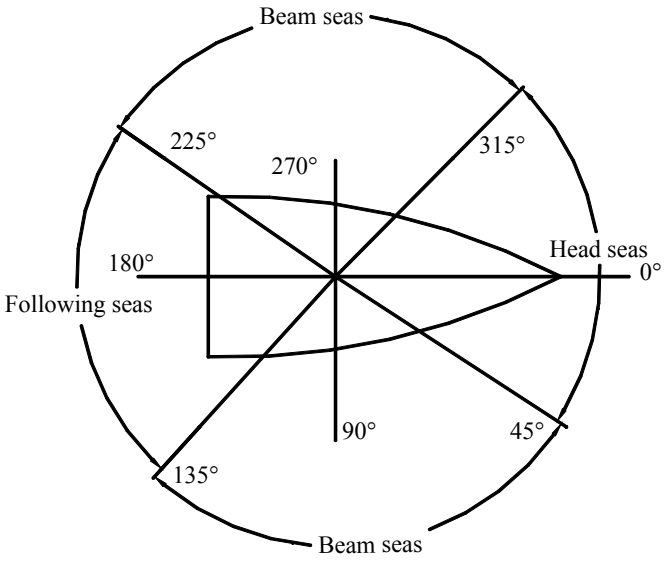

Figure 4.3: Example of the convention for wave direction (0^0 waves coming from North, 90^0 East).

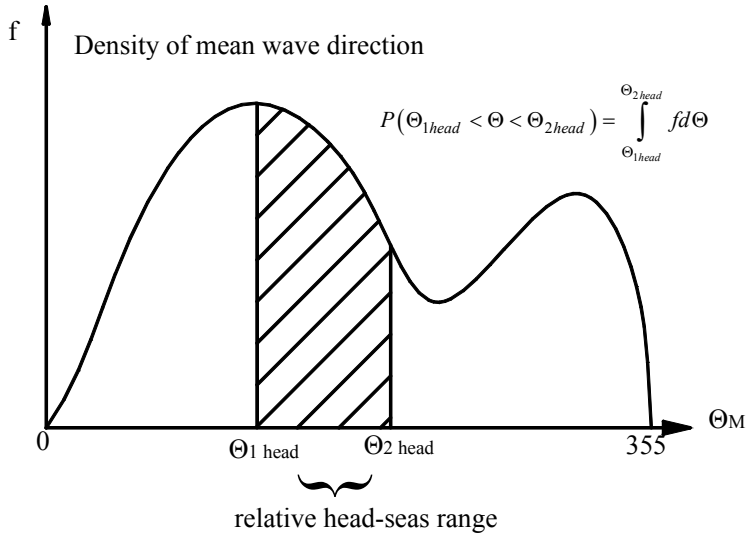

Figure 4.4: Example of probability of exposure time to head-seas.

4.4 Portfolio of stability criteria

In theory, instabilities of a different nature could arise during a voyage. Furthermore, different ship types often present different tendencies for unstable behaviour. Acknowledging these, the criteria of the assessment will be linked to the occurrence of the known types of instability. A portfolio of stability criteria reflecting the main instability phenomena are thus incorporated into the assessment. A recommended generic set of stability criteria should include resonance instabilities (beam-sea resonance and parametric rolling in longitudinal seas); pure – loss of stability on a wave crest in following seas; for smaller vessels, instability

due to breaking waves from the side and "water-on-deck"; lastly broaching (including also the cumulative type). So, ship stability performance can be attended per criterion. Finally in the current methodology the criteria that have been implemented are beam seas resonance, parametric rolling in longitudinal seas and pure loss of stability.

4.5 Norms of unsafe behaviour

For the criteria to become meaningful, norms representing quantified levels of unsafe behaviour should be "attached" to each one of them. One could envisage the setting of quantitative "warning" and "failure" levels per criterion and ship type, on the basis of threshold angular and linear displacements and accelerations, referring respectively to the safety of the ship and her cargo. A warning level should play a cautionary role and its exceedence should be permitted with controlled probability. To the contrary, failure levels should not be exceeded for the acceptable level of risk. Nevertheless in the current thesis risk analysis will not be performed. An example for probable norms of unsafe behaviour of a Ro/Ro ferry is shown in Figure 4.5. The norm of cargo is established because shift of cargo is treated as an inability of the ship to carry out her mission even if this will not bring about capsize. Moreover, the norm of ship will specify an limiting roll angle which maybe not connected directly with capsize in the strict sense, but the exceedence of this angle will not assure the safe operation of the ship (e.g. angle of immersion of deck openings).

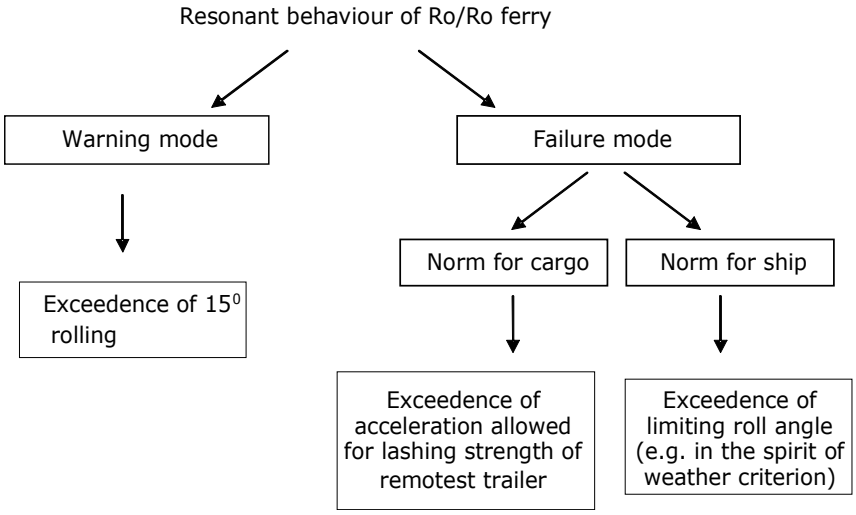

Figure 4.5: Possible safety norms of a Ro/Ro ferry.

4.6 Specification of critical wave groups

This step deals with the specification of critical wave groups, which will be represented by the number of waves in the group (group run-length), the threshold wave height and period. In Figure 4.6 is shown schematically a wave group comprised of three successive waves (i.e. the run length is equal to three) with periods lying within a predefined time interval and corresponding wave heights above a threshold height that had been determined in advance as critical. Individual waves are measured here using the standard zero – upcrossing method, with their height taken as the maximum vertical excursion of the surface elevation between two zero – upcrossings; and their period, as the time interval separating these two events. It should be mentioned at this point that focusing in the main stability criteria under consideration (beam seas resonance, parametric rolling in longitudinal seas and pure loss of stability) the wave height is more relevant variable than the wave crest as it totally contributes to the wave excitation of the ship. In the case of combinations of instabilities or for other types of excitation as water on deck or breaking waves, wave crests or other wave parameters could be of more importance. For this reason the group analysis will be concentrated on the wave heights and periods. An introduction to wave groups and their probabilistic properties will be presented in the next Chapter.

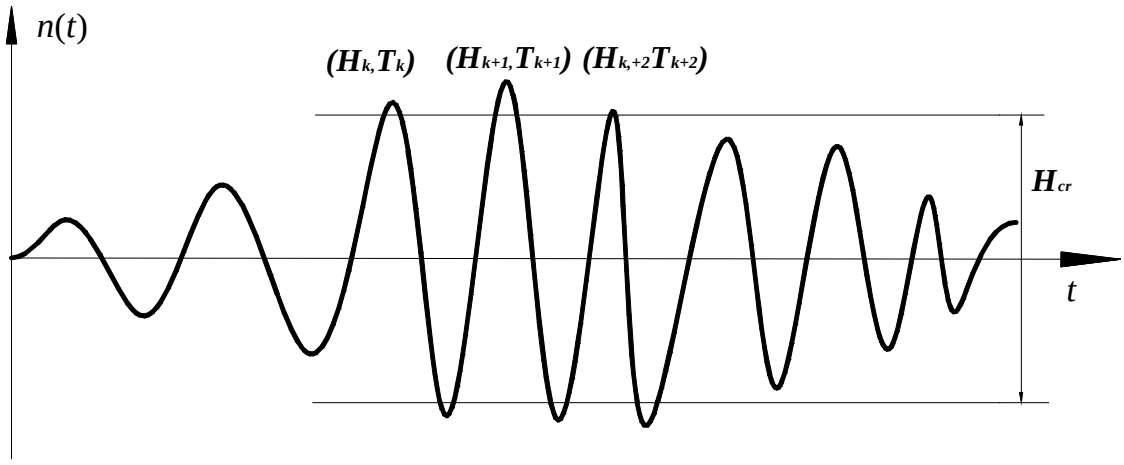

Figure 4.6: Example of a wave group.

In this step of the assessment, advantage is taken of the strengths of deterministic analyses. With a specific instability mode in mind (criterion) one could subject the ship to a wave group and observe the outcome in terms of exceedence of the threshold values (norms). For this part of the study, wave groups are represented by a regular wave train, thus all waves have the same height and period. Numerical simulation tools can be employed for this, based on

detailed mathematical models of large-amplitude ship motions. Alternatively, analytical techniques that capture the key systems dynamics may be utilized; for example analytical expressions of the growth of roll amplitude per encounter wave cycle. Different methods have their own strengths and weakness. However the conceptual disengagement of ship dynamics from the probabilistic seaway allows one to reach an informed decision about what constitutes the critical wave environment for a ship, on the basis of more than one tool. Therefore, results from different simulation codes or combinations of simulation with rigorous stability analysis techniques could be used. In a following Chapter, a detailed presentation of the tools that have been utilized in the application part of the procedure will be provided. In the next sections further details of the procedure for identifying critical wave groups will be discussed.

4.6.1 Formalization of the calculation

As it was referred earlier, the specification of critical wave groups regards their group length, threshold wave height and wave period. Notably, critical wave groups are specified for the entire range of wave periods that could be met in a realistic seaway. Firstly, the range of wave periods is discretised in, say, ℓ, equal parts, with step δT. Then, the set of wave groups that satisfy the critical norm is determined utilizing simulations or direct analytical methods as mentioned earlier. More specifically, the critical surface of Figure 4.7 is determined according to the following procedure:

- Consider a wave period T_i in the defined range.
- Take n waves in the group.
- Calculate the corresponding critical wave height $H_{cr}\left(T_i, n\right)$.
- Continue for run length $n+1$.
- Take the next wave period $T_{i+1} = T_i + \delta T$ until the whole range is spanned.

Firstly it should be noticed that for resonance phenomena a sequence of waves is needed, so the number of waves in the group should be at least two. Increasing the run length will result to a lower necessary critical wave height, however wave groups with large run length are rare. The wave period range assumed, $\left[T_A, T_B\right]$ according to Figure 4.7, shall contain the realistic wind wave periods and especially for beam seas resonance a range among the natural roll period where large amplitude response is expected. The specification of this range in advance will reduce the number of the required calculations. Furthermore, as the transient response is targeted, initial conditions should be set and in particular a probabilistic distribution can be specified.

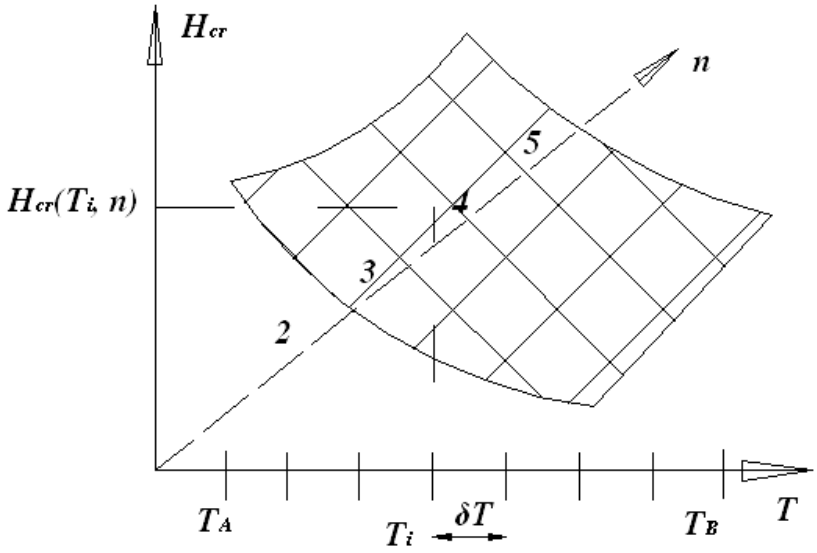

Figure 4.7: Critical surface of wave group characteristics.

For each case the procedure will be repeated and the total probability will be derived by the weighted sum of all cases. However for beam seas resonance, as it is a directly excited mode, one could assume the ship unbiased and upright with zero roll velocity when the wave group approaches her. This state will decrease the computational effort and there is some theoretical background from ship dynamics in support of adopting this initial condition (Rainey and Thompson 1991). They ascertained that for a practical investigation, the upright state is sufficient for the estimation of the critical wave height that will incur rapid loss of the safe area of the transient safe basin. Nonetheless, alternative initial conditions may affect the derived probabilities and for this reason an investigation based on first principles for this effect has been carried out and will presented in a following Chapter.

The procedure can be repeated for other loading conditions on the basis of the loading profile of the ship. Moreover, rather than a single speed U, a range of speeds may be deemed necessary to be examined, especially for a longitudinal sea where speed affects seriously the frequency of encounter.

For the specification of the critical wave groups for parametric instability in longitudinal seas, the range of critical wavelengths λ as well as the wave period range, like the $[T_A, T_B]$ of Figure 4.7, that could give rise to parametric resonance should be determined for each examine discrete value of speed U. Therefore, in order to realize parametric resonance, the frequency of encounter ω_e can be identified from the condition:

$a^2 = 4\omega_o^2 / \omega_e^2$, where $a = 1, 2, ...$ (4.2)

For exact principal parametric resonance $a = 1$, so $\omega_e = 2\omega_0$ and thereafter the critical wave length and wave period are calculated respectively by:

$$\lambda = \frac{2\pi}{\omega_e}(c + U\cos\psi) \tag{4.3}$$

$$T = \sqrt{\frac{2\pi\lambda}{g}} \tag{4.4}$$

Symbols are used with their customary meaning: ω_0 is ship's natural roll frequency, $c = \sqrt{g/k}$ is wave celerity where g, k are gravity's acceleration and wave number respectively and finally ψ is the heading angle relatively to the wave direction of propagation (0^0 for head-seas). Here it should be pointed out that a range of values around $a = 1$ for the case of exact principal parametric resonance is favorable to be considered as in this range parametric rolling could also arise (Spyrou et al 2007).

As parametric rolling is a non-directly excited mode, some (probabilistic) initial heel angle should be assumed; otherwise, even within the instability region, no growth of roll could be expected, so critical wave groups are determined for each initial discretised heel range. Generally, for all parameters that integrated in the procedure, such as ship's speed U or the loading condition some distribution of their values should be assumed.

For pure loss of stability, the characteristics of the single critical wave encounter will be estimated on the basis the wave period lie in a range where the wave length is about ship's length and also the frequency of encounter is enough low. This will result the ship to stay long enough on the wave crest and if the wave height surpass a critical value then the restoring moment can become negative. If the ship stays long enough with negative restoring in the vicinity of the wave crest, then a failure heeling angle can be reached from an initial heel disturbance.

4.7 Calculation of probability of critical wave groups

Generally, for the calculation of the probabilities to encounter the critical wave groups for a given sea state will rely on spectral methods where appropriate multivariate conditional and joint probability density functions of wave periods and heights $\left(f(\boldsymbol{\tau}|h), f(\mathbf{h})\right)$ will be

utilized. For the case of a single wave encounter, joint probability density functions (pdf) $f(h,\tau)$ will be used instead. Symbols in bold corresponds to vector variables. A detailed presentation of the probabilistic properties of wave groups as well as of the relevant utilized pdfs is going to be presented in a next Chapter. The analysis entails also a frequency spectrum.

4.7.1 Probabilities according to stability criteria

From the previous step critical wave groups with the following characteristics have been determined and their probability occurrence needs to be estimated:

- wave groups with n successive waves in group (maximum considered run length k),
- periods within the group lying in an time interval $\left[T_i, T_j\right]$, where $T_j - T_i = \delta T$
- wave heights exceeding the critical height: $H_n \geq H_{cr}$.

The associated probability P will be derived by the calculation of the following probabilities:

$$P = P_1 \cdot P_2 \tag{4.5}$$

$$P_1 = P\left[T_1, T_2, ..., T_k \left| H_n > H_{cr} \right.\right] = \underbrace{\int_{\tau_i}^{\tau_j} \int ... \int_{\tau_i}^{\tau_j}}_{k} f\left(\boldsymbol{\tau} \left| h_n > h_{cr} \right.\right) d\tau,\ n = 1, ..., k \tag{4.6}$$

$$P_2 = P\left[H_1 > H_{cr}, ..., H_k > H_{cr}\right] = \int_{h_{cr}}^{\infty} ... \int_{h_{cr}}^{\infty} f\left(h_1, ..., h_k\right) dh_1 ... dh_k \tag{4.7}$$

where $\boldsymbol{\tau} = \left[\tau_1, \tau_2, ..., \tau_k\right]^T$ and $\tau = T/T_m$, $h = H/H_{rms}$ are respectively dimensionless wave period and height. T_m and H_{rms} stand for mean spectral period and root–mean–square wave height respectively. All the above calculations will be derived by the frequency spectra information. For phenomena where the period of encounter is different from the wave period, the above calculations should be based of course on the encountered spectrum.

For instability modes like pure – loss of stability, a single critical wave with the next characteristics has been specified:

- wave period lying in a time interval $\left[T_i, T_j\right]$ so that the wave length is around the ship length.
- wave height exceeding a critical height: $H \geq H_{cr}$

The related probability will be estimated according to the next formula:

$$P\left[H_{cr},T\right]=\int_{h_{cr}}^{\infty}\int_{\tau_i}^{\tau_j} f\left(h,\tau\right)dhd\tau \tag{4.8}$$

4.7.2 Summation of probabilities of different scenarios

To illustrate the calculation procedure, let us assume a scenario of beam-sea resonance where $\ell \times k$ critical wave groups have been determined, with ℓ corresponding to the number of the discretised segments of the wave period range and k to the number of considered wave group run lengths in each segment. The probability P_S for some arbitrary weather node S is expressed as:

$$P_S=\sum_{r=1}^{\ell}\sum_{n=2}^{k} P_{r,n} \tag{4.9}$$

where P_r corresponds to probabilities of different segments of the wave period range, while P_n represent probabilities of different run lengths. Probabilities for each segment are summed up. Events of wave-group-encounter in a range $r\in\left[T_i,\,T_j\right]$ with $n=2,3,...,k$ successive waves are treated as independent but not mutually exclusive. This treatment prevents the summation from including the probability of a wave group occurrence more times. So, the internal sum follows the well-known rule:

$$\begin{aligned} P_r=&\sum_{n=2}^{k}P\left[A_n\right]-\sum_{n=2}^{k-1}\sum_{m=n+1}^{k}P\left[A_nA_m\right]+\sum_{n=2}^{k-2}\sum_{m=n+1}^{k-1}\sum_{q=m+1}^{k}P\left[A_nA_mA_q\right]-...\\ &+(-1)^k P\left[A_nA_mA_q...A_k\right],\quad r\in\left[1,2,...,\ell\right] \end{aligned} \tag{4.10}$$

where $A_nA_m=A_n\cap A_m$ is the intersection of the events and A_n refers to the event of encountering of a critical wave group that has a certain specification. As these events could be assumed as independent, $P\left[A_n\cap A_m\right]=P\left[A_n\right]P\left[A_m\right]$. Furthermore, the probabilities from each discretised wave range part r are mutually exclusive as wave groups whose periods lie in different ranges are not overlapped. Thus the total probability for some weather node S is obtained by summing up according to eq. (4.9). In the case where a discretised probabilistic distribution of initial conditions $\left(\varphi_0,\dot{\varphi}_0\right)$ has been considered in the procedure, eq. (4.9) will be transformed to eq. 4.11.

$$P_{S(beam)}=\sum_{\varphi_0}\sum_{\dot{\varphi}_0}\sum_{r}\sum_{n}\left(P_{r,n|(\varphi_0,\dot{\varphi}_0)}\times P_{(\varphi_0,\dot{\varphi}_0)}\right) \tag{4.11}$$

where $P_{r,n|(\varphi_0,\dot{\varphi}_0)}$ is the conditional probability for the given initial state and $P_{(\varphi_0,\dot{\varphi}_0)}$ is the probability for this initial state to be exist when the wave group approach the ship.

When additional scenarios have been involved, as for example in parametric rolling, the probability in the area of influence of some weather node S will be:

$$P_{S(parametric)} = \sum_{\varphi_0}\sum_{U}\sum_{r}\sum_{n}\left(P_{r,n|\varphi_0,U} \times P_{\varphi_0} \times P_U\right) \tag{4.12}$$

In this case the speed determines also the wave periods where parametric resonance could occur and hence it affects the probability calculation. Also, initial roll angles φ_0 have been considered. The wave period range for parametric resonance is also specified by the parameter a which takes care of frequency tuning, but only through the wave frequency. So, the selection of the values of parameter a should not lead to an overlap with the wave period range determined by the speed. Similarly, probabilistic ranges of the ship speed P_U and of the initial heel disturbance P_{φ_0} have been assumed in the calculation procedure.

Finally for the case where a single critical wave encounter has been determined, as in pure – loss of stability, the associated probability will be estimated by eq. 4.13, where the subscript r stands for the wave period range for which pure loss of stability is expected.

$$P_{S(pure\ loss)} = \sum_{\varphi_0}\sum_{U}\sum_{r}\left(P_{r|(\varphi_0,U)} \times P_{\varphi_0} \times P_U\right) \tag{4.13}$$

If more parameters have been integrated, such as different loading conditions, the probabilities of wave groups will be conditioned on these parameters and then are multiplied with the probability of the selected parameter occurrence.

4.7.3 Critical time ratio and probability of instability

Arguably, it is more meaningful to transform and express these probabilities (which by definition refer to the number of encountered waves irrespectively of their periods) into a representation that conveys the percentage of time that the ship is expected to be in peril, with respect to the entire time of exposure. This magnitude shall be called as “critical time ratio”. The calculation is based (approximately) on the next simple transformation, where T is the examined period of a certain sub range and T_{m2} is the average zero-crossing period.

$$\overline{t}_{cr} = \frac{t_{cr}}{t_{tot}} = \frac{N_{crit} \cdot T}{N_{tot} \cdot T_{m2}} = P\frac{T}{T_{m2}} \tag{4.14}$$

Therefore, regarding beam seas resonance and for an arbitrary node S the respective critical time ratio is given by eq. 4.15, where the upright state has been only assumed.

$$\overline{t}_{S(beam)} = \sum_{r=1}^{\ell} P_r \frac{T_r}{T_{m2}} \tag{4.15}$$

If along the considered route m weather nodes have been placed, then the total probability for beam-sea resonance and respectively the total critical time will be calculated by eq. 4.16 and 4.17 respectively, where $\tau_{S\ bean}$ is the percentage of exposure to beam seas (similar to eq. 4.1).

$$P_{beam} = \sum_{S=1}^{m} P_{S(beam)} \tau_{S\ beam} \tag{4.16}$$

$$\overline{t}_{beam} = \sum_{S=1}^{m} \overline{t}_S\ \tau_{S\ beam} \tag{4.17}$$

Summing up all the probabilities for each stability criterion, the total probability is derived.

So far, probability values are expressed as number of critical waves over the total number of encountered waves. Thus, to determine the probability of instability, a suitable transformation is entailed. Therefore one should estimate the average number of waves to be encountered, determined as zero – crossings events. For the arbitrary node S, it will be derived as follows:

$$N_S = \frac{t_S}{T_{m2(S)}} \tag{4.18}$$

where t_S is the time the ship spends in the vicinity area of node S. If the summed probability, including all the instability nodes for the node S is P_S, then the probability of instability for the whole voyage is:

$$P_{instability} = \sum_{S} P_S N_S \tag{4.19}$$

4.7.4 Projection of probabilities for long term assessment

If the character of the assessment is long-term, scatter diagrams or fitted joint distributions of significant wave height and peak period $P_L\left(H_S, T_P\right)$, per node for example, will be necessary. The long term probability of encountering the critical wave groups will de derived as an accumulation of the short term cases $P_{Short\ \text{term}}\left(H_S, T_P\right)$, however as pointed out by Ochi (1998), the number of waves N of each short term case has to be taken into account. This

arises from the fact that while short term sea state can be assumed as a steady random process, this is not the case for long term statistics. Therefore, to obtain (per node S) the long-term probability the following summation should be performed.

$$\overline{P}_S = \frac{\sum_{H_S}\sum_{T_P} N\, P_{Short\ \text{term}}\left(H_S, T_P\right)\, P_L\left(H_S, T_P\right)}{\sum_{H_S}\sum_{T_P} N\, P_L\left(H_S, T_P\right)} \tag{4.20}$$

where N is the number of waves in each short term case that depends on the duration t and calculated according to eq. 4.18. The dominator of eq. (4.20) accounts for the total number of waves encountered during the assumed long–term period (e.g. one year). Arguably, the long term statistics of the mean wave direction characterised, say by $P_L\left(\Theta_M\right)$, can be implemented in the above summation.

Chapter 5:

Probabilistic treatment of wave groups – Spectral methods

In the current Chapter, a comprehensive presentation of the probabilistic quantities of the wave groups will be presented focusing on the available methods and tools for the calculation of group's statistics. The task of the calculation of the probability of occurrence of the specified critical wave groups is one of the most essential parts of the assessment, thus it has been considered helpful to analyze the relevant properties of wave groups. Furthermore, for the calculation of the related group statistics and probabilities, the so-called spectral methods will be employed, so all the necessary information for the estimation of these quantities can be extracted from the frequency wave spectrum. Hence, no time series analysis is necessary which adds to the versatility of the methodology of the procedure. Next, two well-known spectral approaches are briefly presented as an introduction to stochastic analysis of wave groups. A review on the probability density functions that are incorporated in the calculation procedure of the estimation of wave group probability occurrence is presented at the last part of the Chapter.

5.1 The wave group phenomenon

As mentioned earlier, the phenomenon of a sequence of high waves having nearly equal periods is known as wave group or group wave (Ochi 1998). Wave groups have been reported in the open ocean during storm waves, see for example Rye (1974) and it has been ascertained that they can incur serious problems to marine safety. This arises mainly due to the near resonance response of the structure by the wave group excitation and less due to the uncommonly high waves of the group. A physical explanation for the group structure of waves has not been established clearly. However among others, Mollo – Christensen and Ramamonjiarisoa (1978) refer that the wave field does not consist of independently propagating Fourier waves but encloses wholly or in a part wave groups of permanent type and this may be attributed to the higher phase velocities than those predicted by linear theory.

The stochastic analysis of wave groups focuses mainly on the estimation of the frequency occurrence of the groups and most of the studies are sorted under two approaches. The first

one treats the wave groups as a level crossing problem related with the envelope of a random process, while the second assumes the sequence of waves as a Markov chain. The envelope approach is based on the works of Rice (1945) and of Longuet Higgins (1957, 1984) and relates the exceedence of the envelope of a wave train above a certain level with a wave group occurrence. Various studies that follow this viewpoint have been presented targeting on mean values of wave group parameters. On the other hand, the Markov chain representation for the sequence of high waves allows for a correlation among them where the value of a wave height depends only on the values of the immediately previous waves. According to Sawhney (1962) the Markov characteristic of ocean waves disappears practically after 8 wave cycles. A cornerstone work of this approach is that of Kimura (1980) which is often combined with the modification study by Battjes and van Vledder (1984).

Nevertheless, both approaches target the estimation of a standard measure of wave groupiness, the mean group length $\overline{j}$ obtained by averaging the number of consecutive waves exceeding a threshold height H_{cr} over a record of sea surface elevation. The mean group length is related through the narrow spectral bandwidth approximation to some characteristics of the wave spectrum; the spectral bandwidth parameter v for the first approach and the spectral correlation coefficient γ_s for the second.

It is worth to mention here that the group analysis according to these two approaches is restricted to linear wave theory and therefore, wave group formation as a result of nonlinear instability is not considered. Usually, in linear theory, wave groups are assumed to be associated with wave components concentrated around the peak frequency and thus, in these approaches, only unimodal spectra are appropriate for wave group analysis (Masson and Chandler 1993). Fruitful discussions and comparison studies of various parameters of wave group statistics are presented in Medina and Hudspeth (1990) and Masson and Chandler (1993).

5.2 Envelope approach

In this approach waves are considered to be a stationary ergodic Gaussian random process; thus wave profiles are distributed following the normal probability distribution with zero mean and a variance representing the sea severity. The spectrum is also concentrated at a particular frequency, i.e. the wave spectral density function is “narrow banded”.

Longuet Higgins (1957, 1984) developed an estimate of the average number of waves in a

group, $\bar{N}_G$ in terms of the spectral bandwidth parameter. Sea surface elevation $n(t)$ can be represented as the sum of sinusoidal components with angular frequency ω_n:

$$n(t) = \mathrm{Re}\left(\sum_n c_n e^{i(\omega_n t + \varepsilon_n)} \right) \tag{5.1}$$

where the random phases ε_n are uniformly distributed over the range $[0, 2\pi]$. The amplitude is estimated from the frequency spectrum $S(\omega)$ according to: $c_n = \sqrt{2S(\omega)\delta\omega}$ where $\delta\omega$ is the frequency increment. Selecting a carrier wave frequency $\bar{\omega}$, the mean frequency $\omega_m = m_1/m_0$ may be a representative midband value, $n(t)$ may be written as:

$$n(t) = \mathrm{Re}\left(e^{i\bar{\omega}t} \sum_n c_n e^{\left[(\omega_n - \bar{\omega})t + \varepsilon_n\right]} \right) = \mathrm{Re}\left(R(t) e^{i\bar{\omega}t} \right) \tag{5.2}$$

A wave envelope function can be specified as:

$$R(t) = a(t) e^{i\phi(t)} \tag{5.3}$$

$a(t)$ is the amplitude of the envelope function and $\phi(t)$ is its phase. The variation of the wave envelope function $R(t)$ with time is slow compared to the carrier wave $e^{i\bar{\omega}t}$ and the wave crests and troughs assumed tightly to follow the surface elevation $n(t)$. Firstly, the average number of crossings of a reference level $H^*/2$ will be estimated. Knowing the joint probability density function of the displacement and velocity of the envelope $f(a, \dot{a})$, it will be:

$$\bar{N}_{H^*/2} = \int_0^\infty \dot{a} \cdot f(H^*/2, \dot{a}) d\dot{a} \tag{5.4}$$

Furthermore, the wave envelope amplitude a and its time derivative $\dot{a}$ follow the Rayleigh and Gaussian distribution respectively and assumed independent.

$$f(a) = \frac{a}{m_0} e^{-\frac{a^2}{2m_0}} \tag{5.5}$$

$$f(\dot{a}) = \frac{1}{\sqrt{2\pi\mu_2}} e^{-\frac{\dot{a}^2}{2\mu_2}} \tag{5.6}$$

where in general the j^{th} spectral moment and central moment about the mean frequency are respectively:

$$m_j = \int_0^\infty \omega^j S(\omega) d\omega \tag{5.7}$$

$$\mu_j = \int_0^\infty (\omega - \bar{\omega})^j S(\omega) d\omega \tag{5.8}$$

From the above equations the average number of crossings of the reference level $A^* = H^*/2$ is:

$$\bar{N}_{A^*} = \sqrt{\frac{\mu_2}{2\pi}} \frac{A^*}{m_0} e^{-\frac{A^{*2}}{2m_0}} \tag{5.9}$$

The average time interval between two upcrossings $\bar{\tau}_{A^*}$ is the inverse of $\bar{N}_{A^*}$. The average number then of waves in a group $\bar{N}_G$ per unit time will be derived by the average time of a wave group to occur $\bar{\tau}_{A_+^*}$ divided by the average wave period $T_{m2} = 2\pi\sqrt{m_0/m_2}$. $\bar{\tau}_{A_+^*}$ is estimated multiplying the amount of time the envelope exceeds the preset level with $\bar{\tau}_{A^*}$:

$$\bar{\tau}_{A_+^*} = \bar{\tau}_{A^*} \int_{A^*}^\infty f(a) da = \sqrt{\frac{2\pi}{\mu_2}} \frac{m_0}{A^*} \tag{5.10}$$

So, $\bar{N}_G$ will be:

$$\bar{N}_G = \frac{\bar{\tau}_{A_+^*}}{T_{m2}} = \frac{1}{A^*\sqrt{2\pi}} \sqrt{\frac{m_o m_2}{\mu_2}} = \frac{1}{A^*\sqrt{2\pi}} \frac{\sqrt{1+v^2}}{v} \sqrt{m_0} \tag{5.11}$$

where spectral bandwidth parameter v, is defined as:

$$v = \sqrt{\frac{m_2 m_0}{m_1^2} - 1} \tag{5.12}$$

However, the groupiness parameter $\bar{N}_G$ derived by the continuous envelope theory is defined in a different way compared to the parameter $\bar{j}$ that is based on discrete counting. Therefore, if the time duration in which the envelope exceeds the preset level is short, then no discrete wave could be accounted. Vanmarcke (1975) and Goda (1976) provided a discrete counting

correction expression assuming a Poisson probability distribution for the parameter $\bar{N}_G$ supposing that successive upcrossings of the preset level are uncorrelated. This assumption will hold when the time interval between the occurrence of two wave groups is large compared with the mean wave period $2\pi/\bar{\omega}$. First it is assumed that an envelope group with $i < N_G < i+1$ with $i = 0,1,2,3...$ corresponds to a group with run length j of i or $i+1$ waves. Then the probability of a wave group with N_G to be associated with a group of either i or $i+1$ discrete waves is $(i+1-N_G)$ and $(N_G - i)$ respectively. So, the mean number of waves per group will be:

$$\bar{j} = \frac{\sum_{i=1}^{\infty}(p_{i1} + p_{i2})i}{\sum_{i=1}^{\infty}(p_{i1} + p_{i2})} \tag{5.13}$$

with

$$p_{i1} = \int_{i-1}^{i} (N_G - i + 1)p(N_G)d(N_G) \tag{5.14}$$

$$p_{i2} = \int_{i}^{i+1} (i + 1 - N_G)p(N_G)d(N_G) \tag{5.15}$$

and as mentioned before, the probability distribution of N_G for narrow spectra is approximated by a Poisson distribution:

$$p(N_G) = N_G e^{-\frac{N_G}{\bar{N}_G}} \tag{5.16}$$

Combing eq (5.13 – 5.16), the mean number per wave group transformed to the next expression:

$$\bar{j} = \frac{1}{1 - e^{-\frac{1}{\bar{N}_G}}} \tag{5.17}$$

and for the limiting value $N_G -> \infty$ this expression relieved to the one proposed by Longuet – Higgins (1984) for discrete counting:

$$\bar{j} \approx \bar{N}_G + 0.5 \tag{5.19}$$

At this point it should be noticed that the above analysis concerns the estimation of the expected values of group parameters. Moreover, it has been implied that the envelope crossing will constitute a wave group, however as it was mentioned before a single wave crest or even no wave crest may be occurred during that time. For this reason, Ochi and Sahinoglou (1989a, 1989b) carried out an analysis for the statistical properties of wave groups considering also the exceedence of at least two wave crests above the preset level. This condition allows for a more realistic approach of the wave group concept. Furthermore, instead of the expected values of group properties, the analytical calculation of the probability density functions of these parameters, like the time duration of a wave group is examined. As the derivation of the pdfs is quite laborious and lengthy, details can be found at the above papers.

5.3 Wave group as a Markov chain sequence

In this approach the sequence of wave heights is treated as a Markov chain, allowing for non-zero correlation between consecutive waves. Generally, the most traditional way of the presentation of sea waves as a stochastic process is as a Fourier series of expansion given a spectrum as was described in the previous section. This approach bears some assumptions like the stationarity and the Gaussian character of the process. A different presentation of the sea waves is through an autoregression model (ARM) where the value of a realization in any moment of time is evaluated by the history plus a small random disturbance in the present moment of time (e.g. Belenky, 1998; Wist et al, 2004). This approach stands for any type of process. Taking into account all moments of the history, the value of the process Y at time t using an ARM model is presented as:

$$Y_t = \sum_{j=1}^{\infty} \Phi_j Y_{t-j} + \varepsilon_t \tag{5.20}$$

where Φ_j are parameters of the autoregression and represent the correlation and dependence among the value of the process at the present moment of time and the past value, while ε_t is white noise with zero mean value. If one does assume that events that have taken place in a long time before cannot affect the values at the present time, then eq. 5.20 may be transformed to a limited number of series expansion and is characterized as autoregressive process of order N :

$$Y_t = \sum_{j=1}^{N} \Phi_j Y_{t-j} + \varepsilon_t \tag{5.21}$$

This representation holds a physical meaning in which the first part of eq. 5.21 expresses the inertial characteristic of sea surface and the second part reflects the stochastic contribution from wind reaction and other disturbances. Now, if the value of the process depends only on the previous one, then it is characterized as a Markov process or first order autoregressive process:

$$Y_t = \Phi \cdot Y_{t-1} + \varepsilon_t \tag{5.22}$$

Markov process can be regarded as a first expansion of the real stochastic process and for such a process the Markov chain property stands and expressed in terms of probability as:

$$P\left(Y(t) = y_t \,|Y(0) = y_0, ..., Y(t-1) = y_{t-1}\right) = P\left(Y(t) = y_t \,|Y(t-1) = y_{t-1}\right) \tag{5.23}$$

In the work of Kimura (1980), time series of wave height are treated as a Markov chain, where the transition probabilities can be represented by the bivariate Rayleigh distribution. A run of high waves is a wave train in which all the wave heights exceed a preset value, which is in other words a wave group as stated earlier. In general, the transition equation for a Markov chain is presented as follows:

$$p_n = p_0 P^n \tag{5.24}$$

where p_0 is the initial distribution, p_n is the distribution after n time and P is the transition probability matrix. Now the wave height train $H_j, \left(j = 1,2,3,...\right)$ can be classified in states on the basis of a reference wave height H^*, for example state 1 will hold for $0 < H_j \le H^*$, state 2 for $H^* < H_j \le 2H^*$ and state i for $(i-1)H^* < H_j \le i \cdot H^*$. Then the transition probability matrix will be derived as:

$$P = \begin{pmatrix} P_{11} & P_{12} & P_{13} & \cdots \\ P_{21} & P_{22} & P_{23} & \cdots \\ P_{31} & P_{32} & P_{33} & \cdots \\ \vdots & \vdots & \vdots & \ddots \end{pmatrix} \tag{5.25}$$

where

$$P_{ij} = \int_{(j-1)H^*}^{j \cdot H^*} \int_{(i-1)H^*}^{i \cdot H^*} f(H_1, H_2) dH_1 dH_2 \,/ \int_{(i-1)H^*}^{i \cdot H^*} q(H_1) dH_1, \ (i, j = 1,2,3,...) \tag{5.26}$$

Kimura proposed the bivariate Rayleigh distribution for the joint pdf of successive wave

heights $f(H_1, H_2)$ and the Rayleigh distribution for the marginal pdf $q(H)$ of wave height respectively.

$$f(H_1, H_2) = \frac{4H_1H_2}{(1-\kappa^2)H_{rms}^4} e^{-\frac{(H_1^2+H_2^2)}{(1-\kappa^2)H_{rms}^2}} I_0\left(\frac{2\kappa H_1 H_2}{(1-\kappa^2)H_{rms}^2}\right) \tag{5.27}$$

$$q(H) = \frac{2H}{H_{rms}^2} e^{\left(-\frac{H^2}{H_{rms}^2}\right)} \tag{5.28}$$

In the above equations, κ is a correlation parameter, H_{rms} the root–mean-square wave height and I_0 the modified Bessel function of zeroth order. The correlation parameter κ is a function of the linear correlation coefficient between successive wave heights γ_h, which in time domain can be derived from:

$$\gamma_h = \frac{\frac{1}{N-1}\sum_{i=1}^{N-1}(H_i - H_{rms})(H_{i+1} - H_{rms})}{\frac{1}{N}\sum_{i-1}^{N}(H_i - H_{rms})^2} \tag{5.29}$$

According to Kimura (1980), the correlation parameter κ is associated with the correlation coefficient of successive wave heights γ_h.

$$\gamma_h = \frac{E(\kappa) - (1-\kappa^2)\frac{K(\kappa)}{2} - \frac{\pi}{4}}{1-\frac{\pi}{4}} \simeq \frac{\pi}{16-4\pi}\left(\kappa^2 + \frac{\kappa^4}{16} + \frac{\kappa^6}{64}\right) \tag{5.30}$$

E, K are complete elliptic integrals of the first and second kind respectively. The approximation [second part of eq. (5.30)] is according to Stansell et al (2002). For the calculation of the probability distribution of the run of high waves and the mean length of high runs $\bar{j}$, Kimura (1980) used a two state Markov chain process. There are four cases for two successive wave heights H_i, H_{i+1}, relatively to a specified wave height H^*, and the transition matrix becomes:

$$P = \begin{pmatrix} P_{11} & P_{12} \\ P_{21} & P_{22} \end{pmatrix} \tag{5.31}$$

where

$$P_{11} = \Pr\left\{H_{i+1} < H^* \middle| H_i < H^*\right\} = \int_0^{H^*}\int_0^{H^*} f(H_1, H_2)dH_1dH_2 \Big/ \int_0^{H^*} q(H_1)dH_1 \tag{5.32}$$

$$P_{12} = \Pr\left\{H_{i+1} > H^* \middle| H_i < H^*\right\} = \int_{H^*}^{\infty}\int_0^{H^*} f(H_1, H_2)dH_1dH_2 \Big/ \int_0^{H^*} q(H_1)dH_1 \tag{5.33}$$

$$P_{21} = \Pr\left\{H_{i+1} < H^* \middle| H_i > H^*\right\} = \int_0^{H^*}\int_{H^*}^{\infty} f(H_1, H_2)dH_1dH_2 \Big/ \int_{H^*}^{\infty} q(H_1)dH_1 \tag{5.34}$$

$$P_{22} = \Pr\left\{H_{i+1} > H^* \middle| H_i > H^*\right\} = \int_{H^*}^{\infty}\int_{H^*}^{\infty} f(H_1, H_2)dH_1dH_2 \Big/ \int_{H^*}^{\infty} q(H_1)dH_1 \tag{5.35}$$

If a high run is considered which starts when $H_i > H^*$, so $H_{i-1} < H^*$, then the initial distribution is $p_0 = (0,1)$ and from eq. 5.24 for $n = 1,2$ respectively

$$p_1 = (P_{21}, P_{22}) \tag{5.36}$$

$$p_2 = \left(P_{21}P_{11} + P_{22}P_{21}, P_{21}P_{12} + P_{22}^2\right) \tag{5.37}$$

For runs of high waves, the elements P_{11} and P_{12} are not involved, so the transition matrix becomes:

$$P = \begin{pmatrix} 0 & 0 \\ P_{21} & P_{22} \end{pmatrix} \tag{5.38}$$

Then the probability of a high run to have length 2, thus two consecutive waves exceeds H^* and the next one is lower than H^* is:

$$p(2) = P_{22}P_{21} = P_{22}(1 - P_{22}) \tag{5.39}$$

Finally the probability that a wave group has a run length j is:

$$p(j) = P_{22}^{j-1}(1 - P_{22}) \tag{5.40}$$

Then the average number of waves exceeding H^* as a group, that will be the mean length of high runs or mean group length will be:

$$\bar{j} = \sum_{j=1}^{\infty} j \cdot p(j) = \frac{1}{1 - P_{22}} \tag{5.41}$$

A disadvantage of Kimura's analysis is that the group properties are not connected with the

properties of an energy spectrum but depend on the parameter γ_h computed from the series of discrete wave heights. In order to overcome this drawback, Battjes and Van Vledder (1984), based on the work of Arhan and Ezraty (1978), modified Kimura's theory, introducing a new correlation parameter κ_s, determined by the frequency spectrum as follows:

$$\kappa_s^2 = \frac{\sqrt{X^2 + Y^2}}{m_0} \tag{5.42}$$

$$X = \int_0^\infty S(\omega)\cos(\omega \cdot T_{m2})d\omega \tag{5.43}$$

$$Y = \int_0^\infty S(\omega)\sin(\omega \cdot T_{m2})d\omega \tag{5.44}$$

Using this spectral parameter κ_s, a new correlation coefficient γ_s can be estimated in a similar way according to eq. 5.30. In fact, the spectral parameter γ_s represents the value of the autocorrelation of the wave envelope $a(t)$ for points separated by the time interval T_{m2} and is expressed as:

$$\gamma_s = \frac{1}{\sigma^2(a)} \int_0^\infty \int_0^\infty (a_1 - \bar{a})(a_2 - \bar{a}) f(a_1, a_2) da_1 da_2 \tag{5.45}$$

where $a_1 = a(t),\ a_2 = a(t + T_{m2})$ and $\sigma(a),\ \bar{a}$ are the variance and the mean of the wave envelope function respectively. The joint pdf $f(a_1, a_2)$ follows the bivariate Rayleigh distribution similar with eq. 5.27 with the correlation parameter κ to be equal to κ_s. Therefore, the correlation coefficient between discrete waves is replaced by the correlation coefficient between points of the wave envelope. These two parameters are identical under the following assumptions.

- The amplitude of the discrete waves obeys the envelope function.
- The waves are separated by a time interval approximately constant and equal to T_{m2}.
- The wave heights can be approximated by twice the value of the envelope function.

These assumptions are strictly satisfied in the limit of very narrow spectra. Masson and Chandler (1993) carried out an analysis in order to examine the difference in the values between the discrete and spectral correlation coefficient for both field and numerically

simulated data. Furthermore they examined how and in which way the above assumptions generate possible discrepancies. Generally, the study showed that the spectral correlation coefficient was underestimated compared with that calculated from the discrete waves. Regarding possible reasons for this deviation, the main cause revealed to be the estimation of the height of discrete waves as twice the value of the envelope at the time of the crest. Thus, a more appropriate estimate of the wave height is needed by taking points of the envelope separated not only by the time interval T_{m2} but also on other appropriate intervals as the half wave period. This improved estimate of wave height may arise from the definition of wave height as the distance between the maximum and minimum surface elevation within a wave period. This sampling technique was used also by Tayfun (1990) in order to derive the statistical distribution of zero – upcrossing wave heights, while Van Vledder (1993) presented this new "averaged" estimate of the spectral correlation coefficient between successive waves where it depends not only on the values of the autocorrelation of the wave envelope at T_{m2} but also on the values at $1/2$ and $3/2$ of this time lag, thereafter it can be produced according to the following expression:

$$\bar{\gamma}_s = \frac{\gamma_s(T_{m2}/2) + 2\gamma_s(T_{m2}) + \gamma_s(3T_{m2}/2)}{2 + 2\gamma_s(T_{m2}/2)} \tag{5.46}$$

A similar study carried out by Stansell et al (2002), where time domain field data are compared in terms of group statistics with spectral predictions methods. This study sustained the usage of the refined estimate of the spectral correlation coefficient $\bar{\gamma}_s$ as it improves the prediction spectral values compared with the time series analysis. They have also concluded that the bivariate Rayleigh distribution provides a sufficient model for the adjacent wave heights when narrow and moderate broad band spectra are involved. Furthermore, Sobey (1996) performed an analysis in order to check the adequacy of the two critical assumptions of the above presented Kimura approach; the Markov process for the sequence of individual wave heights and the bivariate Rayleigh distribution for consecutive wave heights. The study was based on the analysis of water surface records and revealed that the data set of the sequence of wave heights were described reasonably well by an linear first order autoregressive model, thus the Markov process model of Kimura approach. Besides, simulated data were used for studying the appropriateness of the bivariate Rayleigh distribution taking into account various spectral shapes. The estimates were narrower and more sharply at the peak than the estimate by the bivariate Rayleigh, however it can

satisfactorily be used for the calculation of group properties. Furthermore one more similar analysis has been presented by Rodriguez and Soares (2001) for the study of the correlation structure of waves where however mixed sea states, thus additionally wind and swell part, have also been considered.

5.4 Probability distribution functions

Apart from the wave group properties, like the average group length, the calculation of the probability of occurrence of a single critical wave or a critical wave group (dependending on the examined stability criterion) given specific sea conditions is the aim of this task. For this reason suitable multivariate conditional and joint probability density functions of wave periods and heights $\left(f\left(\boldsymbol{\tau}|h\right), f\left(h,\tau\right)\right)$ should be sought from the literature. Symbols in bold corresponds to vector variables. It should be noticed here that a variety of joint, conditional or marginal distributions of wave parameters, like the wave steepness or wavelength, can be derived. However, in the current procedure and due to the character of the examined stability criteria, the wave parameters that are incorporated are the wave height and the wave period which are defined according the standard zero upcrossing method. Thus, only joint distributions of the above parameters are included in this study.

A variety of joint distributions of wave height and associated wave period have been proposed, for example Lindgren and Rychlic (1982), Longuet – Higgins (1975, 1983), Cavanié et al. (1976), Tayfun (1993) and Stansell et al (2004). A more theoretical treatment of the problem has been presented by Memos (1994), while a review on various joint distributions is provided by Massel (1990). A critical comparison of the first three above mentioned studies with observational data has been performed by Srokosz and Challenor (1987). A brief review of some of these approaches follows. For the presentation of pdfs the next normalized variable of height and period are used respectively:

$$\xi = H/\sqrt{m_0},\ \tau = T/T_m \tag{5.47}$$

where $T_m = 2\pi\dfrac{m_0}{m_1}$ is the mean spectral period.

Longuet Higgins (1983) developed the joint distribution of wave height (peak to trough excursions) and associated wave period by taking into account the joint distribution of the envelope amplitude and the time derivative of the envelope phase $f\left(a,\dot{\phi}\right)$. Waves are expressed similar to eq. 5.2 as:

$$n(t) = \mathrm{Re}\left(a(t) e^{i\phi(t)} e^{i\omega_m t} \right) \tag{5.48}$$

The envelope phase can be expressed in terms of a frequency which in turn can be related with a period. Under the narrow band approximation $\left(\nu^2 << 1\right)$ the total phase, according to eq. 5.48, is an increasing function of time. It can be shown that the time derivative of the envelope phase is enough small compared with the mean frequency, $\left(\dot{\phi} << \omega_m\right)$, so the period can be approximated by $T = \dfrac{2\pi}{\omega_m + \dot{\phi}}$ Then the derived joint pdf is:

$$f\left(\xi,\tau\right) = \frac{1}{8\sqrt{2\pi}\nu}\left(1+\frac{\nu^2}{4}\right)\left(\frac{\xi}{\tau}\right)^2 \exp\left(-\frac{\xi^2}{8}\left[1+\frac{1}{\nu^2}\left(1-\frac{1}{\tau}\right)^2\right]\right) \tag{5.49}$$

where it has been considered that integration of the density over the sample space should be unity. Stansell et al (2004) presented an improvement of the distributions derived by Longuet – Higgins (1983) by adjusting the sampling frequency from the wave envelope than keeping it constant.

Cavanié et al. (1976) derived a distribution of positive maxima and the time interval between them, thus for non – narrow band process where in that case, multiple crests can be exist. They derived their pdf by considering the joint distribution of positive maxima and the associated second derivatives. A transformation then is needed for the second derivative and the time interval in order to obtain the pdf of maxima and time interval. However further assumptions are needed for the wave height to be evolved and this regards that twice the positive maxima is wave height, which is in fact a form of narrow band approximation; sinusoidal profile for each wave and consideration only of positive maxima. The obtained pdf for wave height and period has the form:

$$f\left(\xi,\tau\right) = C\frac{\xi^2}{\tau^5}\exp\left\{-\frac{\xi^2}{8\varepsilon^2\tau^4}\left[\left(\tau^2 - \left(\frac{1-\varepsilon^2}{1+\nu^2}\right)\right)^2 + \beta^2\left(\frac{1-\varepsilon^2}{1+\nu^2}\right)\right]\right\} \tag{5.50}$$

where

$$C = \frac{1}{4}(1-\varepsilon^2)\frac{1}{\sqrt{2\pi}\varepsilon\cdot a\cdot(1+\nu^2)^2} \tag{5.51}$$

$$\varepsilon^2 = 1 - \frac{m_2^2}{m_0 m_4} \tag{5.52}$$

$$a = \frac{1}{2}\left[1+\sqrt{1-\varepsilon^2}\right] \tag{5.53}$$

$$\beta = \varepsilon^2 \Big/ \left(1-\varepsilon^2\right) \tag{5.54}$$

On the other hand, Lindgren and Rychlic (1982) based mainly on a series of works of Lindgren, developed a statistical theory for evaluating the joint pdf of height and period given the covariance function of the process and assuming Gaussian waves. The result can not be written in closed analytical form and even it is mathematically elaborated, it is not practical for engineering purposes. Briefly, the approach based on using a "model process" for the examination of the behaviour of the surface near a local maximum (crest) of a given height. Then the joint pdf of height and period can be derived conditioned on the crest height, while integrating for all possible crest heights the final pdf produced. Contrary to the previously described pdf, this result depends on the entire covariance function and its first four derivatives. According to the comparison study of Srokosz and Challenor (1987), Longuet Higgins and Cavanié's distributions present good agreement for narrow band seas and zero upcrossing defined waves while Lindgren accounts for wider bandwidths and thus better approaches the crest to trough heights and periods.

From another viewpoint Tayfun (1993) proposed a joint pdf of wave height and period that according to his study is appropriate for large wave heights. This joint pdf comes from the product of the marginal pdf f_ξ of large wave heights (Tayfun 1990) and the conditional pdf $f_{\tau|\,\xi}$. His main idea was to obtain a more accurate representation for the distribution of large wave heights than that of Longuet Higgins (1975, 1983) which will be not limited only in very narrow banded waves. Tayfun (1990) derived this pdf which is suitable for predictions for wave heights larger than the mean wave height, proving a better estimate of the zero upcrossing wave period and taking into account the correlation parameter κ_a between two linear successive wave amplitudes which is calculated by eq. 5.42 through eq. 5.44 for $T_{m2}/2$. This result to a modified distribution compared with the Rayleigh and has the following form:

$$f_\xi = \frac{\xi}{2[2\kappa_a(1+\kappa_a)]^{1/2}}\left(1+\frac{1-\kappa_a^2}{4\kappa_a\xi^2}\right)\exp\left(-\frac{\xi^2}{4(1+\kappa_a)}\right) \tag{5.55}$$

where $\xi > \overline{\xi}$, $\overline{\xi}$ is the normalized mean wave height. If $\kappa_a = 1$, eq. 5.55 transformed to the Rayleigh distribution. Then the joint pdf of wave height and period will be deduced by:

$$f_{\xi\tau} = f_{\xi} f_{\tau|\xi} \tag{5.56}$$

Regarding the conditional $f_{\tau|\xi}$, Longuet Higgins (1975) derived a pdf which presented a satisfactory qualitative representation of periods in terms of their symmetry and spread about a mean value, however for large ξ the mean periods are underpredicted as observed values show (Srokosz and Challenor 1987) by 25 - 30%. The conditional density of τ given ξ of Longuet Higgins (1975) is:

$$f\left(\tau|\xi\right) = \frac{\xi}{2\sqrt{2\pi\nu}} \exp\left[-\frac{\xi^2}{8\nu^2}\left(\tau-1\right)^2\right] \tag{5.57}$$

In fact this is the Gaussian with the conditional mean and standard deviation as follows:

$$\mu_{\tau|\xi} = 1 \tag{5.58}$$

$$\sigma_{\tau|\xi} = \frac{2\nu}{\xi} \tag{5.59}$$

As mentioned, for large ξ the observed $f_{\tau|\xi}$ presents a characteristic symmetry about a mean value $\mu_{t|\xi}$, that can be larger than $\mu_{t|\xi} = 1$ by as much as 25 – 30% depending on spectrum's bandwidth ν. One possible reason of this effect may be ascribed possibly to nonlinearities and to an assumption of the theory of Longuet Higgins where the wave phase in a given zero – upcrossing cycle always increases with time as also previously noticed. Nevertheless, this is valid only for $\nu -> 0$, which is not the case for wind waves where phases can decrease or reverse direction (Tayfun 1993). Additionally, nonlinear effects modify wave phases in a manner that their distribution is no longer uniform over $[0, 2\pi]$. Furthermore, Tayfun (1990) mentioned that it unlikely for zero – upcrossing wave periods to be larger than $2T_m$, so after all he proposed that it is justified to approximate $f_{\tau|\xi}$ by a Gaussian form, modifying the conditional mean and standard deviation as follows

$$f_{\tau|\xi} = C_1 \exp\left(-\frac{1}{2}\left(\frac{\tau-\mu_{\tau|\xi}}{\sigma_{\tau|\xi}}\right)^2\right) \tag{5.60}$$

where $\xi > \overline{\xi}$, $0 < \tau < 2$ and C_1 is a parameter in order the following condition to be satisfied:

$$\int_0^2 f_{\tau|\xi} d\tau = 1 \tag{5.61}$$

In eq. 5.60 the conditional mean and standard deviation are respectively:

$$\mu_{\tau|\xi} = 1 + \nu^2 (1+\nu^2)^{-3/2} \tag{5.62}$$

$$\sigma_{\tau|\xi} = \frac{2\nu}{\xi(1+\nu^2)} \tag{5.63}$$

According to eq. 5.61 the parameter C_1 approaches the value $C_1 \approx 1/\left(\sqrt{2\pi}\sigma_{\tau|\xi}\right)$. The explicit form of the joint pdf of large wave height and associated period then is:

$$f_{\xi\tau}(\xi,\tau) = C_T \xi \left(1 + \frac{1-\kappa_a^2}{4\kappa_a \xi^2}\right) \exp\left(-\frac{1}{2}\left[\frac{\xi^2}{2(1+\kappa_a)} + \left(\frac{\tau - \mu_{\tau/\xi}}{\sigma_{\tau/\xi}}\right)^2\right]\right) \tag{5.64}$$

where $\xi > \overline{\xi}$, $0 < \tau < 2$ and C_T a normalizing factor such that:

$$C_T = \frac{1}{2\sqrt{4\pi\kappa_a(1+\kappa_a)}\sigma_{\tau|\xi}} \tag{5.65}$$

The form of the $f_{\tau|\xi}$ proposed by Tayfun implies that the modal period τ_{mod}, which corresponds to the maximum of $f_{\tau|\xi}$, is identical with the mean $\tau_{1/p}$ of periods associated with the $1/p$ highest ξ and both given by $\mu_{\tau|\xi}$, while the modal period of Longuet Higgins (1975) model was $\tau_{\text{mod}} = 1$.

At this point it should be noticed that all the above equations can be represented if instead of the parameter $\xi = H/\sqrt{m_0}$ for the wave height, the parameter $h = H/H_{rms}$ is used in order to be consistent with the equations of section 5.3. For example the joint pdf of Tayfun (eq. 5.64) will be described by:

$$f_{h\tau}(h,\tau) = C_T h \left(1 + \frac{1-\kappa_a^2}{32\kappa_a h^2}\right) \exp\left(-\frac{1}{2}\left[\frac{4h^2}{1+\kappa_a} + \left(\frac{\tau - \mu_{\tau/h}}{\sigma_{\tau/h}}\right)^2\right]\right) \tag{5.66}$$

where now

$$\sigma_{\tau|h} = \frac{2\nu}{\sqrt{8}h(1+\nu^2)},\ \mu_{\tau|h} = 1+\nu^2(1+\nu^2)^{-3/2} \tag{5.67}$$

$$C_T = \frac{2\sqrt{2}}{2\sqrt{4\pi\kappa_a(1+\kappa_a)}\sigma_{\tau|h}} \tag{5.68}$$

As it is presented, Tayfun (1993) approximated the conditional distribution of wave period given the wave height on the basis of the Gaussian distribution. Wist et al. (2004) utilized this statement and proposed that the multivariate Gaussian distribution could be a satisfactory model of the conditional distribution of successive wave periods given the associated wave heights exceeds a threshold level. Analyses of field data sustain the practical adequacy of this concept. The proposed conditional pdf of p successive wave periods $\mathbf{T} = \left[T_1,...,T_p\right]^T$, given that each wave height in the group exceeds the threshold H_{cr}, is given below by eq. 5.69. It is worth to mention that a general formula for variable threshold $H_{cr,i}$ per wave in the group could also be extracted. This is of interest since it could lead to a more realistic representation of a wave group; however the present analysis, keeping in mind the specification of wave groups through the stability criteria of the assessment, assumes each wave in the group to exceed the same threshold.

$$f_{\mathbf{T}|\mathbf{H}}\left(\boldsymbol{\tau}\,|h_i > h_{cr}\right) = \frac{1}{(2\pi)^{p/2}\left|\Sigma_{\tau|h_{cr}}\right|^{1/2}} e^{\left(-\frac{1}{2}\left(\boldsymbol{\tau}-\boldsymbol{\mu}_{\tau|h_{cr}}\right)^T \Sigma^{-1}_{\tau|h_{cr}}\left(\boldsymbol{\tau}-\boldsymbol{\mu}_{\tau|h_{cr}}\right)\right)} \tag{5.69}$$

$\Sigma_{\tau|h_{cr}}$ is the matrix of covariance given as:

$$\Sigma_{\tau|h_{cr}} = \begin{bmatrix} \sigma^2_{\tau|h_{cr}} & \mathrm{Cov}\left[T_1,T_2\,|H_{cr}\right] & \mathrm{Cov}\left[T_1,T_p\,|H_{cr}\right] \\ & \cdots & \\ \mathrm{Cov}\left[T_1,T_p\,|H_{cr}\right] & \cdots & \sigma^2_{\tau|h_{cr}} \end{bmatrix} \tag{5.70}$$

and $\mathrm{Cov}\left[T_i,T_j\,|H_{cr}\right] = \rho_{ij}\sigma^2_{\tau|h_{cr}}$. The mean values $\boldsymbol{\mu}_{\tau|h_{cr}}$ and the standard deviations $\sigma_{\tau|h_{cr}}$ are calculated from by the above formulas. The correlation coefficient ρ_{ij} corresponds to the correlation of wave periods whose sequence also forms a Markov chain (Kimura 1980):

$$\rho_{1j} = \rho_{12}^{j-1},\ j \geq 2 \tag{5.71}$$

For the study of distributions of successive wave periods, few works have been presented; Kimura (1980) and Myrhaung and Rue (1993, 1998) have followed similar approaches.

Specifically, the work of Myrhaung and Rue (1993) is based on Bretschneider's (1959) assumption that the square of the wave period T is Rayleigh distributed. Providing a non dimensional form of the wave period $\tau = T / T_m$, the marginal pdf is obtained by:

$$f(\tau) = 4\tau^3 e^{-\tau^4} \tag{5.72}$$

The above pdf has been considered according to the above references as a good distribution for practical engineering approaches. Then, the joint distribution of successive wave periods is obtained by transforming a two-dimensional Rayleigh distribution, whose marginal pdfs are given from eq. 5.72. The resulting pdf is (Kotz et al 2000; Middleton 1960):

$$f(\tau_1, \tau_2) = \frac{16\tau_1^3 \tau_2^3}{1-\kappa^2} \exp\left(-\frac{\tau_1^4 + \tau_2^2}{1-\kappa^2}\right) I_0\left(\frac{2\kappa\tau_1^2\tau_2^2}{1-\kappa^2}\right) \tag{5.73}$$

According to Middleton (1960) the correlation coefficient of successive wave periods ρ_{12} is given by:

$$\rho_{12} = \frac{\Gamma^2\left(\frac{1}{4}\right)}{8\sqrt{\pi} - \Gamma^2\left(\frac{1}{4}\right)}\left[F\left(-\frac{1}{4}, -\frac{1}{4}; 1; \kappa^2\right) - 1\right] \tag{5.74}$$

where Γ is the Gamma function and F is the Gaussian hypergeometric function. Generally, the hypergeometric function is given by a series of expansion that converges within a certain interval. In the current analysis the relevant calculation performed in a Mathematica environment where special functions as the gamma and the hypergeometric are supported providing their arguments.

It should be also noticed that the above analysis for the wave periods can be generalised by assuming a Weibull and a two dimensional Weibull distribution respectively (Kimura 1980; Myrhaung and Rue 1998), however the shape parameters of the marginal pdf should be provided and thus are not suitable for implementation for a practical approach.

5.5 Calculating the occurrence of critical wave events

As mentioned in the previous Chapter, the probability of occurrence of a wave group with the next characteristics will be calculated:

- wave groups with n successive waves in group (maximum considered run length k),
- periods within the group lying in an time interval $\left[T_i, T_j\right]$, where $T_j - T_i = \delta T$.

- wave heights exceeding the critical height: $H_n \geq H_{cr}$.

$$P = P_1 \cdot P_2 \tag{5.75}$$

where

$$P_1 = P\left[T_1, T_2, ..., T_k \left| H_n > H_{cr} \right.\right] = \underbrace{\int_{\tau_i}^{\tau_j} \int ... \int}_{k}_{\tau_i}^{\tau_j} f\left(\boldsymbol{\tau} \left| h_n > h_{cr} \right.\right) d\boldsymbol{\tau},\ n = 1, ..., k \tag{5.76}$$

$$P_2 = P\left[H_1 > H_{cr}, ..., H_k > H_{cr}\right] = \int_{h_{cr}}^{\infty} ... \int_{h_{cr}}^{\infty} f\left(h_1, ..., h_k\right) dh_1 ... dh_k \tag{5.77}$$

In the first probability, the multivariate conditional pdf of eq 5.69 will be utilized. For the calculation of the second probability, the multivariate joint pdf $f(\mathbf{h})$ or $f\left(h_1, ..., h_k\right)$ will be estimated according to:

$$f\left(h_1, h_2, ..., h_k\right) = f(h_k \left| h_{k-1} \right.) .... f(h_2 \left| h_1 \right.) f(h_1) \tag{5.78}$$

where the conditional bivariate pdf are derived from:

$$f\left(h_{i+1} \left| h_i \right.\right) = \frac{f\left(h_i, h_{i+1}\right)}{f\left(h_i\right)} \tag{5.79}$$

The joint pdf $f\left(h_i, h_{i+1}\right)$ is estimated by the bivariate Rayleigh distribution for successive wave heights (eq. 5.27), while for $f\left(h_i\right)$ the Rayleigh distribution is used. Therefore, the Markov chain concept allows for the estimation of the multivariate joint pdf through eq 5.78 by the combination of the conditional bivariate pdfs.

For instability modes like pure – loss of stability, a single critical wave encounter with the next characterictics will have been specified:

- wave period lying in a time interval $\left[T_i, T_j\right]$ so that the wave length is around the ship length.
- wave height exceeding a critical height: $H \geq H_{cr}$

The related probability will be estimated according to the next formula:

$$P\left[H_{cr}, T\right] = \int_{h_{cr}}^{\infty} \int_{\tau_i}^{\tau_j} f\left(h, \tau\right) dh d\tau \tag{5.80}$$

For the joint density of wave height and period, one can select one of the presented $f\left(h, \tau\right)$.

In the current methodology and in the application part, the respective pdf proposed by Tayfun (1993) has been employed (eq. 5.66), as large wave heights are expected to be specified for this ship instability.

Chapter 6:

Calculation tools for the specification of critical wave groups

In this Chapter, the utilized tools that have been incorporated in the assessment for the specification of the critical wave groups are presented. As it has been mentioned, numerical tools for time domain simulations based on detailed mathematical models or analytical criteria aiming at the key systems dynamics can be employed, each of them have strength and weakness. It is the deterministic character of this step of the assessment that allows one to estimate the characteristics of critical wave groups based on more than one tool which can contain different levels of detail in terms of mathematical modelling. For example, more than one numerical code for time domain simulations can be used or even one can compare results from numerical and analytical tools and make a more sound decision. Thus, the assessment does not depend on a specific mathematical model for this step.

At this stage, two numerical tools and two analytical methods have been utilized. One of the objectives of this thesis has been the development of a mathematical model for the simulation of the coupled roll, sway and heave motion in beam seas under regular waves. This will enhance the understanding of ship dynamics while targeting at large amplitude transient rolling motion. The second numerical tool is a commercial panel code, SWAN2 2002, which however has not been used in such type of stability analysis. The thought of employing such a code was firstly to provide time domain simulations in other wave headings than beam seas and then to perform an investigation for the prediction capability for head seas parametric rolling between the panel code and an analytical method. On the other hand, two analytical techniques that exploit key results for deterministic analyses have been implemented. The first provides a robust relationship for the critical excitation to experience specific parametric roll growth, whereas the second, in the similar spirit, estimates critical parameters for pure loss of stability in following seas. A presentation of each tool follows.

6.1 Mathematical model of coupled roll in beam seas

An analytical description of the mathematical model for the coupled rolling motion in regular beam seas follows. The model has three degrees of motion freedom; roll, heave and sway.

Here, it should be noticed that a coupled model is more appropriate for the study of large amplitude roll motion, due to the limitations entailed from the assumptions of the one degree of freedom models. In Appendix A an examination of these limitations is carried out leading to the adoption of the 3 d.o.f system.

Firstly the equations of motions are derived for the assumed coordinate system and then are described and analyzed the relevant forces that are involved in the problem. The obtained mathematical model is programmed completely in a Mathematica environment where the geometry of the ship is modeled through panels and the derived differential equations are numerically solved.

6.1.1 Equations of motion

The equations of motion will be derived from applying the second law of Newton, assuming that the ship is a rigid body, for an inertial system and then appropriately transformed for a body fixed system. Figure 6.1 presents the inertial (*OYZ*) and body fixed (*Gyz*) coordinate systems. The first one (*OYZ*) lies on calm water and the *OZ* axis is directed upward, while the origin of the second one (*Gyz*) is located at the center of gravity *G* of the body.

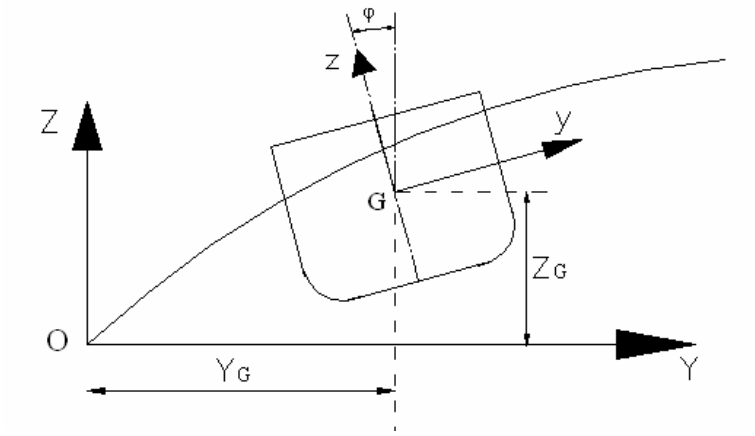

Figure 6.1: Convention of the coordinate systems.

Let $(\vec{J},\vec{K})$, $(\vec{j},\vec{k})$ be the unit vectors of the inertial and body fixed system respectively. According to the above convention Y_G, Z_G are the sway and heave displacement measured from the inertial system and the angle φ is the absolute heel angle, which defined as the rotation from an axis (unit vector $\vec{i}$) which pass from *G* and is vertical to the plane *Gyz* . If v, w are the sway and heave instantaneous velocities of the ship's centre of gravity in the directions of *Gy* and *Gz* axis respectively, $\dot{\varphi}$ is the roll angular velocity and m is the mass of the ship, then from basic kinematics the equation of translational motions is:

$$m\left(\dot{\vec{u}}_G + \dot{\vec{\varphi}} \times \vec{u}_G\right) = \sum \vec{F} \tag{6.1}$$

where in the specific case:

$$\dot{\vec{\varphi}} = \dot{\varphi} \cdot \vec{i} \tag{6.2}$$

$$\vec{u}_G = v \cdot \vec{j} + w \cdot \vec{k} \tag{6.3}$$

The equation of sway and heave motion are then according to:

$$m(\dot{v} - \dot{\varphi} w) = \sum F_y \tag{6.4}$$

$$m(\dot{w} + \dot{\varphi} v) = \sum F_z \tag{6.5}$$

For the rotational motion, if I_G is the mass moment of inertia around the longitudinal axis *x* of the ship that passes from the centre of gravity and as only one rotational velocity exists, the equation of the rolling motion is derived from:

$$I_G \ddot{\vec{\varphi}} + \dot{\vec{\varphi}} \times I_G \dot{\vec{\varphi}} = I_G \ddot{\varphi} = \sum M_G \tag{6.6}$$

The well-known transformation between the inertial and body fixed coordinate systems is applied:

$$\begin{pmatrix} \dot{Y}_G \\ \dot{Z}_G \\ \dot{\varphi} \end{pmatrix} = \begin{pmatrix} \cos\varphi & -\sin\varphi & 0 \\ \sin\varphi & \cos\varphi & 0 \\ 0 & 0 & 1 \end{pmatrix} \begin{pmatrix} v \\ w \\ \dot{\varphi} \end{pmatrix} \tag{6.7}$$

6.1.2 Formulation of the body – waves interaction problem and relevant forces

In general, the two forces and the moment (about the center of gravity) that appear at the right-hand-side of eq. 6.4 - 6.6 can be decomposed as follows:

$$\sum F = F_{Hs} + F_W{}^{FK} + F_W^D + F_R + F_V \tag{6.8}$$

where F_{Hs} is hydrostatic, F_W^{FK} is Froude – Krylov, F_W^D is diffraction, F_R is radiation and F_V is the viscous force. Next a brief discussion for the body – waves interaction problem will be presented, for a more detailed analysis see for example Belenky and Sevastianov (2007).

In the context of linear wave theory, the total fluid velocity potential is the sum of the potentials of incident wave Φ_I, diffraction Φ_D and radiation Φ_R. The incident wave potential describes the wave flow which is not disturbed by the presence of the ship. The diffracted wave potential describes the fluid flow that generated by the reflection of waves

due to the presence of the ship which assumed fixed. The radiation potentials $\Phi_{R(i)}$ express the flow of the generated waves due to the forced ship motion for every motion freedom i in still water.

$$\Phi = \Phi_I + \Phi_D + \sum_{i=1}^{6} \Phi_{Ri} \tag{6.9}$$

The pressure distribution in the flow field, assuming incompressible and irrotational fluid flow, can be estimated by the Bernoulli equation:

$$P = -\rho\left(gz + \frac{\partial \Phi}{\partial t} + \frac{1}{2}\nabla\Phi\nabla\Phi \right) \tag{6.10}$$

As usual, ρ is seawater density and g is acceleration of gravity, while the first part of the eq. 6.10 is the hydrostatic pressure and the remaining part is the hydrodynamic pressure. The forces (and moments) that act on the body due to the interaction with the wave are calculated by integrating the pressures acted on the ship over its wetted surface:

$$\vec{F} = \iint_{S(t)} P\vec{n}ds \tag{6.11}$$

where $\vec{n}$ is the unit vector (vertical towards the body) and $S(t)$ is the instantaneous wetted surface. The relevant moments will be derived by replacing $\vec{n}$ with $\vec{r}\times\vec{n}$, where $\vec{r}$ determines the examined position on the wetted surface (from the center of gravity *G*). The surface elevation due of the incoming linear harmonic wave that travels parallel to axis Gy will be as known:

$$\zeta = A\cos(kY - \omega_w t) \tag{6.12}$$

where A ω_w, k are the wave amplitude, wave cyclic frequency and the wave number.

6.1.3 Hydrostatic forces

The hydrostatic forces, which are in fact restoring forces, estimated by the integration of the static pressure component, therefore:

$$F_{HSi}(t) = -\rho g \iint_{S(t)} Z^* \vec{n}_i ds, \text{ for } i=2, 3, 4 \tag{6.13}$$

where Z^* is the vertical distance from the water surface calculated by:

$$Z^* = Z - A\cos(kY - \omega_w t) \tag{6.14}$$

Moreover the index $i = 2,3,4$ correspond respectively to sway, heave and roll motion, so $\vec{n}_i$ are projections of the unit vector $\vec{n}$ to the i direction, however as mentioned above $\vec{n}_4 = \vec{r} \times \vec{n}$.

6.1.4 Froude - Krylov forces

The Froude Krylov forces or else forces due to the undistributed wave are estimated by the incident dynamic pressure P_I, so:

$$F_{Wi}^{FK}(t) = \iint_{S(t)} P_I \vec{n}_i ds, \text{ for } i=2, 3, 4 \tag{6.15}$$

$$P_I = -\rho\left(\frac{\partial \Phi_I}{\partial t} + \frac{1}{2}\left(\nabla \Phi_I\right)^2\right) \tag{6.16}$$

For regular waves, the incident wave potential is calculated from:

$$\Phi_I = \frac{Ag}{\omega_w} e^{kZ^*} \sin(kY - \omega_w t) \tag{6.17}$$

Thus eq. 6.16 is transformed to:

$$P_I = \rho g A e^{kZ^*} \cos(kY - \omega_w t) + \rho\left(\frac{Agk}{\omega_w}\right)^2 e^{2kZ^*} (\cos(kY - \omega_w t))^2 \tag{6.18}$$

It should be noted that the integration is performed over the instantaneous wetted surface and pressures are calculated from the exact wave elevation. As a matter of fact, nonlinear restoring forces and at least some of the nonlinear part of the wave excitation (Froude – Krylov) is taken into account, which is important for more accurate simulation of large motions. Furthermore, when the nonlinear part of the Froude-Krylov forces is considered, a nonzero mean during the time of excitation period may be exist, therefore a steady lateral drift force is present, which may introduce a bias to the rolling motion.

6.1.5 Diffraction forces

The hydrodynamic diffraction forces are generated by the possibly reflected waves due to the presence of the ship, which is assumed unmovable. When the wavelength λ of the incoming waves are long compared with a characteristic dimension of ship, as the breadth B, then the so called Froude - Krylov or long wave assumption may be valid $(\lambda/B \geq 6)$ where the ship tends to follow the motion of water particles and does not disturb the wave field, so diffraction forces might be not play significant role. See also Appendix A for a relevant analysis. Furthermore, when the ratio λ/B decreases, the reflection of waves is more intense

and steady lateral drift force is generated (Maruo 1960; Newman 1967). According to the references mentioned, the drift force is proportional to the square of the wave amplitude and increasing vice-versa with λ/B. In this mathematical model diffraction forces were not calculated, however for their calculation treatment one could follow for example the works of DeKat and Paulling (1989), Grochowalski et al (1998) and Belenky and Sevastianov (2007).

6.1.6 Radiation forces

The radiation forces are produced by the generation of waves due to the forced movement of the ship in calm water and their radiation away from her. They are also known as hydrodynamic force of added mass and damping. Let this force analysed in two components, one having the same phase with the velocity $\dot{s}_k$ of the ship and the other with the acceleration $\ddot{s}_k$ where the subscript refers to the k direction of motion. If A_{jk}, B_{jk} are the coefficients of added mass and damping respectively in the direction j due to the motion in direction k, then the hydrodynamic force due to the radiation of waves can be calculated as follows:

$$F_{Rj} = -\sum_{k=2}^{4} A_{jk}\ddot{s}_k + B_{jk}\dot{s}_k \tag{6.19}$$

The hydrodynamic coefficients of added mass and damping are calculated according to strip theory and can be available by frequency domain commercial codes. However, these coefficients are frequency dependent and so the radiation forces, hence eq. 6.19 stands exactly in the steady state and when the response is a harmonic function of time. Thus, assuming the hydrodynamic coefficients as constants can lead to inaccurate results, especially when studying the transient behaviour, so a transformation from the frequency domain to the time domain is necessary.

In the time domain the linear radiation forces are estimated using an impulse response function, obtained as the Fourier transform of the frequency dependent radiation transfer function, the radiation forces will be (Cummins 1962):

$$F_{Rj}(t) = -A_{jk}(\infty)\ddot{s}_k - \int_0^{+\infty} K_{jk}(\tau)\dot{s}_k(t-\tau)d\tau, \text{ for } j,k = 2,3,4 \tag{6.20}$$

$$K_{jk}(\tau) = \frac{2}{\pi}\int_0^{\infty} B_{jk}(\omega_e)\cos(\omega_e\tau)d\omega \tag{6.21}$$

where it is considered above that the damping $B_{jk}(\infty)$ at infinite frequency is negligible. The convolution integral is the well-known memory effect as it reflects the dependence of the

radiation force not only of the instantaneous velocity but also by the time history of the motion and this effect is cumulative and will be present for sometime before it dies out. Specifically, the kernel $K(t)$ of the convolution integral express the time history of the radiation force when an impulsive change in the velocity is generated at the time moment $t = 0$ and for this reason is usually referred as impulse response function. In the above relationships, $A_{jk}(\infty)$ is the added mass coefficient calculated at an infinite frequency limit, while it is preferable the damping coefficients to be estimated using the encounter frequency ω_e due to the possible drift velocity of the ship.

In the present model the frequency dependent added mass and damping coefficients are approximated in the time domain with extended state space variables. The relevant analysis and model are presented in Appendix B and based in the currently developed PhD thesis of Tigkas (2007).

6.1.7 Forces due to viscous effects

An important role in the estimation of ship response keeps the damping forces due to viscous flow effects. The above analysis has not included them as all the forces are calculated through the relevant potential flow velocities. Furthermore it is well known that especially for the roll motion and also for sway motion the damping viscous forces are the main component of damping as the wave making part is significantly small. Thus a proper calculation of this kind of forces is necessary.

The main components of roll damping and respectively for the other motions are: the wave making damping which calculated by the radiation forces, eddy making damping, skin friction and bilge keel or generally appendage damping (Figure 6.2). It is a common practise roll damping viscous forces to be expressed through an equivalent linearized damping coefficient assuming a roll response amplitude and semi empirical expressions for the relevant calculations (Himeno 1981). However in a mathematical model for the coupled roll motion, the estimation of damping due to the other motions as the sway drag force or due to cross coupling effects, for example roll damping from sway motion, needs to be determined. So, in the presented model, a method for the calculation of these forces based on Lloyd (1989) has been implemented where analytical estimated the force (and moments) of each component of damping taking into account the detailed geometry of the hull. The calculation of the three components of viscous damping follows while more details on the method are presented in the Appendix B.

Principally, viscous forces are proportional with the square of the relative velocities, so the method takes into account the local relative velocities along the hull, using the sway, heave and roll velocities ($\dot{Y}_G, \dot{Z}_G, \dot{\varphi}$), the wave particle velocities u_2 and u_3 as well as the detailed geometry of the hull. According to Figure 6.3, the relative velocities in terms of the transverse and vertical axis of a point on the hull whose distance from the center of mass of the ship G is r, are estimated by:

$$\dot{Y}_R = \dot{Y}_G - \dot{\varphi} \cdot r \sin(\theta_1 + \theta_2)\cos(\theta_2) - u_2 \tag{6.22}$$

$$\dot{Z}_R = \dot{Z}_G - \dot{\varphi} \cdot r \sin(\theta_1 + \theta_2)\sin(\theta_2) - u_3 \tag{6.23}$$

$$u_2 = \frac{\partial \Phi_I}{\partial y} \tag{6.24}$$

$$u_3 = \frac{\partial \Phi_I}{\partial z} \tag{6.25}$$

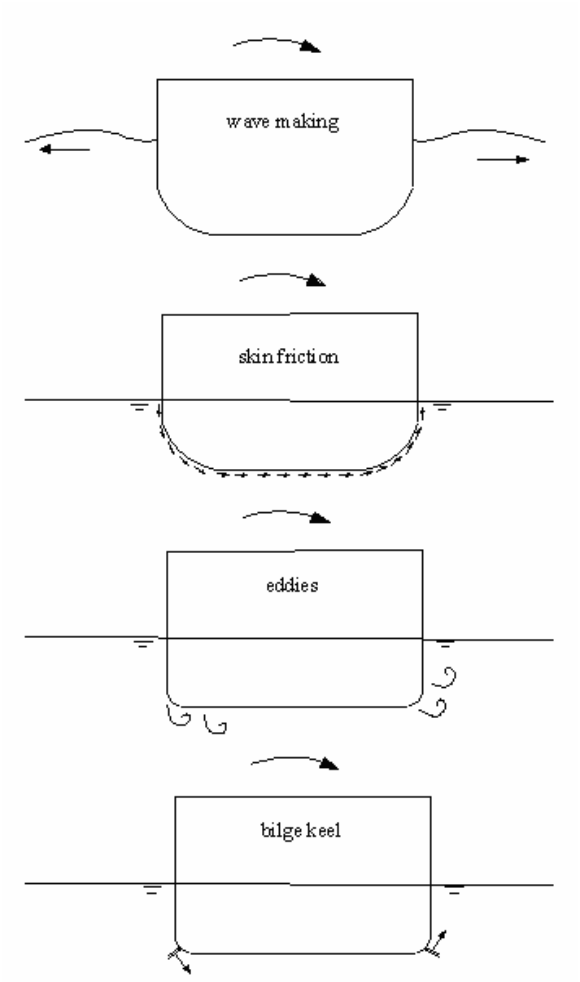

Figure 6.2: Roll damping components, inspired by Lloyd (1989).

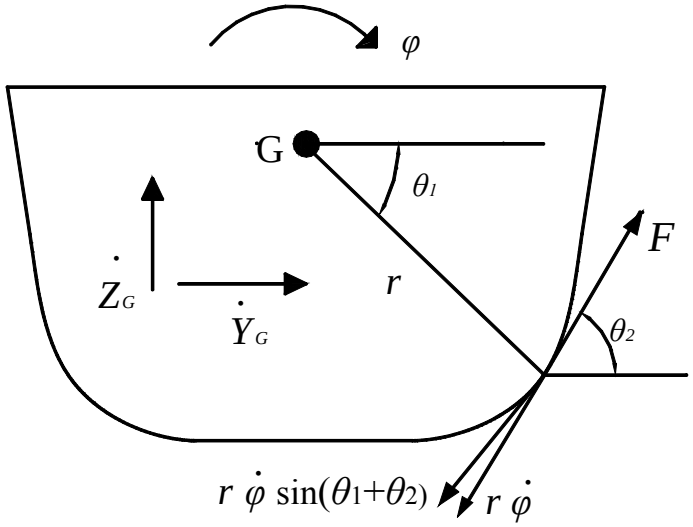

Figure 6.3: Relative velocities on the hull.

Damping forces due to bilge keels

The viscous damping forces due to the existence of bilge keels are in fact drag forces when the ship has no forward speed, while a lift component exists otherwise. If the drag forces considered, then according to the next figure they will be calculated as follows:

$$F_{BY} = \frac{1}{2}\rho(\dot{Y}_G - r_A\,\dot{\varphi}\cos(\theta) - u_2)\left|\dot{Y}_G - r_A\,\dot{\varphi}\cos(\theta) - u_2\right| C_D A_{BK} \tag{6.26}$$

$$F_{BZ} = \frac{1}{2}\rho(\dot{Z}_G - r_A\,\dot{\varphi}\sin(\theta) - u_3)\left|\dot{Z}_G - r_A\,\dot{\varphi}\sin(\theta) - u_3\right| C_D A_{BK} \tag{6.27}$$

$$F_B = \sqrt{F_{YB}^2 + F_{ZB}^2} \tag{6.28}$$

$$M_B = -r_A\left(F_{BY}\sin\theta_1 + F_{BZ}\cos\theta_1\right) \tag{6.29}$$

C_D is the drag coefficient and A_{BK} is the examined bilge keel area. Other symbols are explained in Figure 6.4.

Damping forces due to eddy making

The forces due to the generation of eddies at the points of the hull where the geometry is changed sharply and whose distance from the center G is r_b are estimated by:

$$F_{eY} = \frac{1}{2}\rho\dot{Y}_R\left|\dot{Y}_R\right| sC_E dx_b \tag{6.30}$$

$$F_{eZ} = \frac{1}{2}\rho \dot{Z}_R \left|\dot{Z}_R\right| s C_E dx_b \tag{6.31}$$

$$M_e = -r_b \left(F_{eZ}\cos\theta_1 + F_{eY}\sin\theta_1\right) \tag{6.32}$$

where s, dx_b are the radius and the length of the section of the ship and C_E is a drag coefficient that depends on the shape of the section.

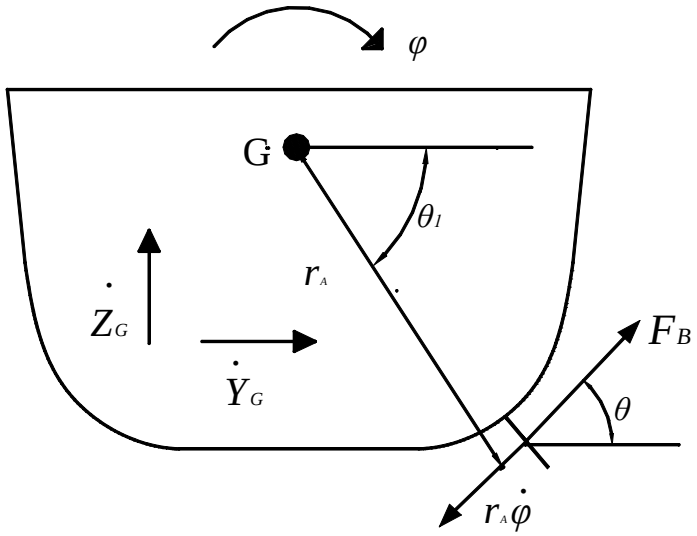

Figure 6.4: Bilge keel damping forces.

Forces due to skin friction damping

The fluid flow on the section surface incurs friction forces. For a section part ds whose distance from G is r the forces that are produced due to friction are:

$$F_{SY} = \frac{1}{2}\rho \dot{Y}_R \left|\dot{Y}_R\right| ds C_F dx \tag{6.33}$$

$$F_{SZ} = \frac{1}{2}\rho \dot{Z}_R \left|\dot{Z}_R\right| ds C_F dx \tag{6.34}$$

$$M_S = -r\left(F_{SZ}\cos\theta_1 + F_{SY}\sin\theta_1\right) \tag{6.35}$$

Integration for the complete wetted surface will produce the total force due to skin friction, while C_F is a friction coefficient. A detailed presentation of the method, the calculation procedure and of the related parameters will be provided in the Appendix B.

6.1.8 Brief description of the numerical code

The numerical model is programmed completely in a Mathematica environment, which is an advanced programming language. The structure of the code is as follows: firstly, the geometry of the hull is inserted through a number of sections, described by coordinates of points. Then loading characteristics such as her mass and her distribution, the draft and the vertical position of the center of gravity are also introduced, while regarding the incident regular wave, its height and frequency.

The code creates panels over the hull, including the deck, using the points of the sections (Figure 6.5). For each panel and time step, the coordinates of the center of the panel and the angle β between the horizontal plane and the normal vector of the panel are estimated. Then it is checked whether these points are located instantaneously beneath the water surface by calculating the value of Z^* and then the static and dynamic pressures are evaluated at each successive time step (Figure 6.6). Furthermore the points where the water surface intersects the hull are estimated, so the relevant panels are extended up to these points and thus the instantaneous wetted surface is taken into account in the calculation of the nonlinear restoring and Froude – Krylov forces.

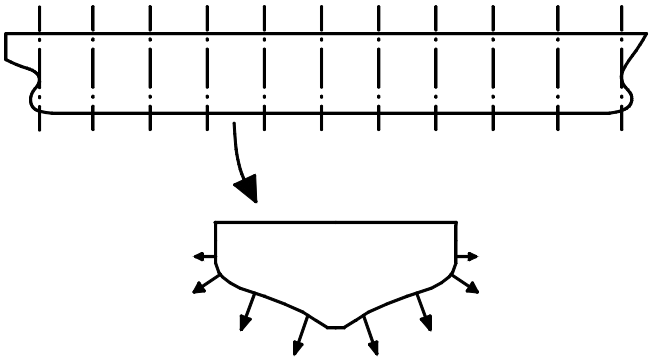

Figure 6.5: Sections and generation of panels.

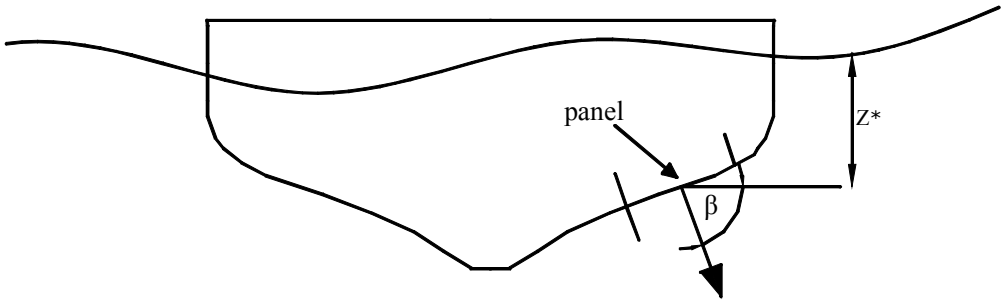

Figure 6.6: Angle between normal vector and horizontal plane and distance from the water surface.

Moreover the water pressure (as estimated by the Bernoulli equation) that acts on the submerged part of the deck is considered without however other effects as the motion of water on deck to be taken into account. Regarding the calculation of viscous forces, the points where bilge keels exists and whereon eddies can be generated, in fact where the geometry of the hull changes rapidly, have been beforehand specified. Finally, since the total forces have been evaluated, the code solves numerically the system of ordinary differential equation using a classic fourth order Runge - Kutta method.

As mentioned before, in Appendix B more details about the calculation procedure for the viscous forces are provided, whereas an application of the mathematical model through predictions of the response for a fishing vessel exposed to harmonic beam waves will be presented in Appendix C. The relevant analysis has been also presented in the deliverable report of the project THALIS (Themelis and Spyrou 2005).

6.2 A time domain panel code: SWAN2

In this section, the time domain panel code SWAN2 (2002) will be briefly presented. It should be noticed at this point that this code has been treated only as a detailed numerical tool for the specification of the critical wave groups without having any control in his source code or aiming in his refinement. Any other similar time domain tool could be used, having in mind how one would apply the methodology with the help of a well known commercial code. A detailed presentation about the theory and computation method of the code can be found in Sclavounos (1996), while for more practical affairs the user's manual SWAN2 (2002) is proposed.

SWAN2 is a numerical code for the analysis of the steady and unsteady "zero-speed" and "forward-speed" free surface flows past ships which are stationary or cruising in water of infinite or finite depth or in a channel. SWAN2 solves the steady and unsteady free-surface potential flow problems around ships using a three-dimensional Rankine Panel Method in the time domain using a distribution of quadrilateral panels over the ship hull and the free surface. The developers of the software argue that the numerical solution algorithms lead to convergent, accurate and efficient wave flow simulations without problems related with numerical dissipation. The ship hull input to SWAN2 is in the form of standard Computer Aided Design (CAD) generated offsets. Moreover, the creation of the panel mesh over the ship hull and the free surface is performed internally by suitable routines of the program (Figure 6.7).

Water depth may be either infinite or finite with uniform water depth. The supported ship types include mono hulls, catamaran, trimaran and SES. Mono hull is supposed to be longitudinal symmetric and stern type may be selected between cruiser or transom designs.

The free-surface flows are solved about the reference coordinate system fixed at the ship mean position while a uniform stream with velocity U flows in the negative x-direction. Travelling waves form an encountering angle β relative to the positive x axis (Figure 6.8). Two input files are necessary; a hull offset file and a job control parameters file that contains mainly sea wave characteristics (wave height and period) and operational information (ship mass, speed and etc).

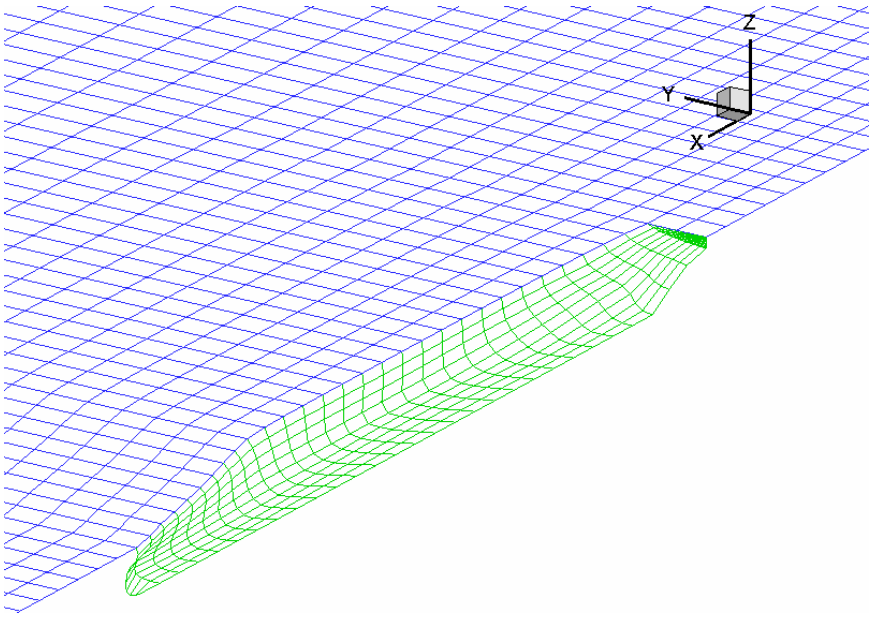

Figure 6.7: 3D view of the geometry of the semi hull as well as the distribution of the panels on the hull and the free surface.

In terms of the output files, the grid information on the computational mesh, the principal ship hydrostatic particulars and inertial properties are included. Other output files regard a time history of the global motions as well as of the global forces and moments acting on the body.

Physical constraints are reported in SWAN2 (2002). In particular, ship's speed, wave heading and period specify the reduced frequency $\tau = \frac{U\omega}{g}$. Above a critical value, $\tau = 0.25$, no waves travel upstream from the ship while below this value there will be a system of long waves travelling upstream. Near the critical value, the linear formulation used in SWAN2 requires careful discretization of the free surface. When the critical value must be approached,

executions should be carried with free surface panel meshes which extend over larger distances in the transverse and upstream/downstream directions. This will lead to improved accuracy in the SWAN2 predictions near the value of $\tau = 0.25$. Finite depth H could present another limitation when the depth Froude number $F_H = \frac{U}{\sqrt{gH}}$ approaches the value of 1.

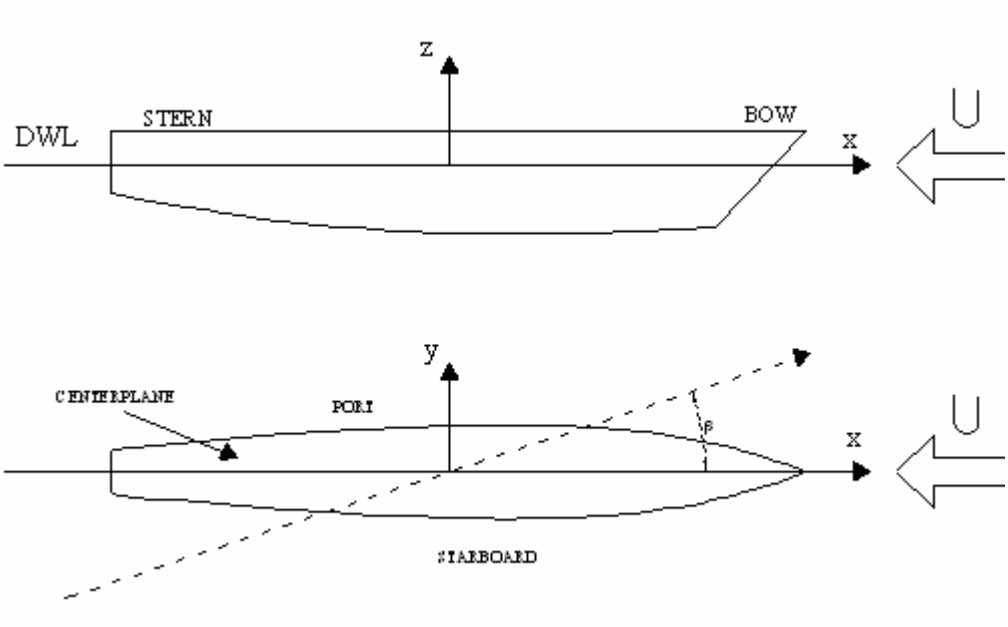

Figure 6.8: Reference coordinate system (taken from SWAN2 2002).

Numerical constraints and stability problems have been identified as in the case of large panel aspect ratio where the discrete solution of the wave flow may become unstable which affects negatively the accuracy of the solution. For these reason numerical convergence studies have been performed, according to the above references, in order to ensure that these kinds of errors are negligible.

6.3 An analytical criterion for parametric rolling

In this section, the study focuses on a specific stability criterion, parametric rolling in longitudinal seas, and demonstrates how key findings from deterministic dynamic analysis can be suitably utilized in the framework of the current methodology in a rational manner.

In particular, a convenient analytical formula that connects the transient part (growth) of parametric rolling with the number of wave encounters is used. Before presenting the analytical formula, a short introduction for this dynamic instability that reveals the connection with the current concept of wave groups follows.

The region that is customarily identified with principal parametric resonance is in the hollow part of curves (a) and (b) in Figure 6.9. This boundary is in fact a bifurcation locus (types shown on the figure) where loss of stability of the upright position equilibrium is generated. Depending on the initially hardening (case shown) or softening character of the restoring curve, the marked bifurcation types are interchanged. Usually analytical or numerical prediction methods target this linear boundary where, $a = 4\omega_0^2 / \omega_e^2$ and h is representative of the intensity of fluctuation of the restoring.

These boundaries refer to long-term dynamic behaviour which is unlikely to be reached in a realistic seaway as an "infinitive" number of wave encounters is required. Therefore it is more significant to know from a technical viewpoint whether roll oscillations can grow to a dangerous level within a few waves. This statement leads to a sound interface with the probabilistic wave group analysis. Therefore, transient response boundaries should be sought, like the curve (c) which has been drawn in a qualitative sense in Figure 6.9 , and that normally lie higher than the boundary curves obtained through the customary stability analysis of steady-states. The values of h for a transient boundary depend on the required number of wave encounters in order to "reach" the required roll growth. To determine such 'transient' boundaries entails some understanding of the mechanism of parametric roll growth, i.e. of the law of transient response. A closed form expression could be derived if the permissible roll angle is not set too high (which however leaves out the nonlinear oscillations that exist in the high amplitude region) and will be presented next. The derived formula will supply the critical magnitude of parametric excitation h_{cr} that is sufficient for realising q-fold increase from an initial roll disturbance, within a set number, say p, of roll cycles.

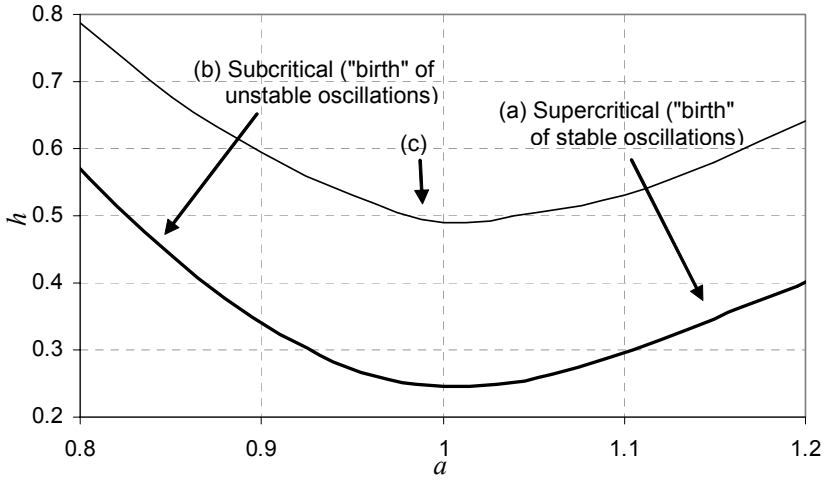

Figure 6.9: Region of principal parametric instability of damped nonlinear Mathieu-type system.

The following analysis is based on Spyrou (2005). The gross assumption that a rudimentary linear Mathieu-type model can describe adequately parametric rolling has been made. The undamped system will be studied first: for the first region of instability, the unstable motion should build up according to the following approximate general solution (Hayashi 1986):

$$\varphi(t) = c_1 e^{\mu\omega_0 t} \sin(\omega_0 t - \sigma) + c_2 e^{-\mu\omega_0 t} \sin(\omega_0 t + \sigma) \tag{6.36}$$

where c_1, c_2 determined by the initial conditions. The parameters μ, σ are functions of frequency and parametric excitation (a, h) and they can be determined by the next relationships (only first-order terms are kept):

$$\cos 2\sigma \approx \frac{2(a-1)}{ah} \quad (-\frac{\pi}{2} \le \sigma \le 0) \tag{6.37}$$

$$\mu \approx -\frac{\sqrt{a^2 h^2 - 4(a-1)^2}}{4} \tag{6.38}$$

In fact μ denotes how deeply inside the instability region one lies, whereas the phase σ which ranges from 0 to $-\pi/2$ indicates the distance from the side of the boundary (0 stands for the right and $-\pi/2$ for the left respectively of Figure 6.9)

For exact resonance $(a=1)$, parameters μ, σ obtain the specific values $\mu = -h/4$ and $\sigma = -\pi/4$. Subsequently the corresponding growth per roll cycle is captured by the following expression:

$$\frac{\varphi(T_0)}{\varphi(0)} = \frac{\frac{\sqrt{2}}{2}\left(c_1 e^{\frac{\pi h}{2}} - c_2 e^{-\frac{\pi h}{2}} \right)}{\frac{\sqrt{2}}{2}(c_1 - c_2)} \tag{6.39}$$

Assuming the initial conditions $\varphi(0) = \varphi_0$ and $\dot{\varphi}(0) = 0$, the growth of roll amplitude after p roll cycles should be according to eq. 6.39:

$$\frac{\varphi(pT_0)}{\varphi_0} = \frac{e^{\frac{p\pi h}{2}} + e^{-\frac{p\pi h}{2}}}{2} \tag{6.40}$$

Introducing linear damping, k is the linear 'half-dimensional' roll damping, the roll model becomes:

$$\ddot{\varphi} + 2k\dot{\varphi} + \omega_0^2 \left[1 - h\cos(\omega_e t)\right]\varphi = 0 \tag{6.41}$$

Setting $\varphi = we^{-kt}$ the above is transformed to an equivalent Mathieu equation with no explicit damping term:

$$\ddot{w} + \left(\omega_0^2 - k^2\right)\left(1 - \frac{\omega_0^2}{\omega_0^2 - k^2} h\cos\omega_e t\right) w = 0 \tag{6.42}$$

Then, the growth of roll amplitude after p roll cycles for the condition of exact resonance while taking into account roll damping can be produced combing eq. 6.40 and eq. 6.42:

$$\varphi\left(pT_0\right) = w(pT_0)e^{-\frac{2p\pi k}{\omega_0}} \simeq \left(\frac{e^{\frac{p\pi h}{2}} + e^{-\frac{p\pi h}{2}}}{2}\right) e^{-\frac{2p\pi k}{\omega_0}} \varphi_0 \tag{6.43}$$

A $q = \dfrac{\varphi\left(pT_0\right)}{\varphi_0}$ fold increase then in the roll amplitude from an initial roll disturbance will be derived from:

$$\ln q \simeq -\frac{2p\pi k}{\omega_0} + \ln\left(\frac{e^{\frac{p\pi h}{2}} + e^{-\frac{p\pi h}{2}}}{2}\right) \tag{6.44}$$

Given that the experienced growth is dominated by the positive eigenvalue of the characteristic equation, thus the exponential term with the negative sign can be dropped, the above can be approximated by:

$$\ln q \simeq -\frac{2p\pi k}{\omega_0} + \frac{p\pi h}{2} - \ln 2 \tag{6.45}$$

So, the following expression precise the critical parametric excitation h_{cr} for achieving q-fold growth within p roll cycles.

$$h_{cr} = \frac{4k}{\omega_0} + \frac{0.693 + \ln q}{1.571\, p} \tag{6.46}$$

Finally it should be noted than in order to realize p parametric roll cycles, a wave encounter, therefore a wave group with run length equal to $2p$ has to be encountered; i.e. for, say, 4 parametric roll cycles, approximately 8 successive critical waves will be needed.

6.4 An analytical criterion for pure loss of stability

This criterion correlates the time that it takes to reach a large inclination, assuming an initial roll disturbance, during a pure-loss event, with the time spent by the ship in the vicinity of a wave crest with negative restoring, leading to a relationship for the identification of the critical fluctuation of restoring curve.

Pure-loss of stability in astern seas is based on the single encounter of a critical wave and in this respect this phenomenon can be treated separately from parametric rolling although both accrue from the fluctuating righting-arm. Especially, it occurs in followings and stern seas when the speed of the ship is relatively near to the wave celerity, while a negative restoring moment can incur a sudden heel from the upright position. If the frequency of encounter is "sufficiently" low, the ship would have the time to reach large heel angles from where overturning cannot be avoided, before moving in a wave trough and thus positive restoring starts to act. The following analysis is based on Spyrou (2000).

The simplest equation that models the above behaviour is Mathieu equation, in non-dimensional form, with the parametric amplitude $h>1$ and the considered time range covers the passage from wave crest:

$$\ddot{z}+2k\dot{z}+\omega_0^2\left(1-h\cos(\omega_e t)\right)z=0,\ h>1 \tag{6.47}$$

where z is the roll angle scaled by the angle of vanishing stability. The time the ships spend with negative restoring is estimated by the following condition:

$$h\cos(\omega_e t)>1 \tag{6.48}$$

Then solving for time:

$$t_{nr}=\frac{2\arccos\left(\frac{1}{h}\right)}{\omega_e} \tag{6.49}$$

Then a linear roll equation is considered with an equivalent linear 'restoring' coefficient c for the region where the latter receives negative values, $c<0$

$$\ddot{z}+2k\dot{z}+c\dot{z}=0 \tag{6.50}$$

Its solution is given by:

$$z=a_1e^{\left(-k-\sqrt{k^2-c}\right)t}+a_2e^{\left(-k+\sqrt{k^2-c}\right)t} \tag{6.51}$$

To define a_1, a_2, the initial conditions should be specified, so the ship must have a small initial roll angle $z(0)$ and/or a roll velocity $\dot{z}(0)$, which is also a prerequisite in order the amplitude to grow up. These coefficients can be derived from the next equations:

$$a_1 = \frac{-k+\sqrt{k^2-c}}{2\sqrt{k^2-c}} z(0) - \frac{1}{2\sqrt{k^2-c}} \dot{z}(0) \tag{6.52}$$

$$a_2 = \frac{k+\sqrt{k^2-c}}{2\sqrt{k^2-c}} z(0) + \frac{1}{2\sqrt{k^2-c}} \dot{z}(0) \tag{6.53}$$

For negative restoring $c<0$, the first term of eq. 6.51 is bounded and contributes much less than the second term which is unbounded. Therefore in order to estimate analytically the time that it takes to reach the critical scaled roll angle z_{cr}, the first term of eq. 6.51 can be neglected, so for $z = z_{cr}$, the following solution is obtained for t:

$$t_{cr} \approx \frac{\ln z_{cr} - \ln\left(\frac{k+\sqrt{k^2-c}}{2\sqrt{k^2-c}} z(0) + \frac{1}{2\sqrt{k^2-c}} \dot{z}(0) \right)}{-k+\sqrt{k^2-c}} \tag{6.54}$$

Next the equivalent constant linear restoring coefficient c has to be determined. This can be derived by the following idea; in the region of negative restoring to balance the potential energy of the exact system with time dependent stiffness with the potential energy of the equivalent system with linear stiffness $c \cdot z$. The exact system (eq. 6.47), taken into account the phase where the ship moves to the negative restoring region is given by:

$$\ddot{z} + 2k\dot{z} + \omega_0^2 \left(1 - h\cos\left(\omega_e t - \arccos\frac{1}{h} \right) \right) z = 0 \tag{6.55}$$

The above mentioned equality of potential energies is expressed as:

$$\int_0^{z_{cr}} \int_0^{t_{nr}} c z dz dt = \int_0^{z_{cr}} \int_0^{t_{nr}} \omega_0^2 \left[1 - h\cos\left(\omega_e t - \arccos\frac{1}{h} \right) \right] z dz dt \tag{6.56}$$

Using also eq. 6.49 and solving for c,

$$c = \omega_0^2 \left[1 - \frac{\sqrt{h^2-1}}{\arccos\frac{1}{h}} \right] \tag{6.57}$$

The instability condition, thus the critical value of h obtained, is produced finally by requesting

$$t_{nr} \geq t_{cr} \tag{6.58}$$

It is worth to mention that a nonlinear version of the above analysis is also possible; but unfortunately the expressions obtained lack simplicity.

Chapter 7:

Application of the assessment methodology

To demonstrate the viability and the various facets of the developed methodology, two applications have been undertaken. In the first one a ROPAX ferry has been examined in a fictitious route in the Mediterranean Sea, on a seasonal basis, hence a "long-term" assessment study, for winter operation. The second application concerns a large post panamax containership operated in North Atlantic during specific days of "bad weather" extracted by hindcast data, thus short – term assessment is studied. Weather data have been provided for both applications for the geographical area that covers these routes.

The stability criteria that have been selected for 'running' the current application are: beam-sea resonance, parametric rolling and pure-loss of stability. This portfolio of stability criteria has been selected as a reference one without knowing a priori that these ships present tendency for these types of instabilities.

Limiting values of roll amplitude and transverse acceleration were set in an objective manner, based on relevant ship and cargo data. The norms of cargo will be obtained by assuming trailer and TEU shifting respectively for each application. For the specification of the critical wave groups, the calculation tools described in the previous Chapter have been utilized and will be mentioned respectively in each application and stability criterion.

Probabilities and corresponding critical time ratios for the three modes of instability have been calculated, leading to the generation of a new "probabilistic" diagram for ship stability assessment. By these diagrams one can easily deduce which type of instability is more likely to occur at any specific stage of the journey, therefore can be helpful for several assessments. For example they could support decision-making at various levels

Finally it should be noticed here that all the data regarding the ship as well as the weather conditions have been provided during the integrated project SAFEDOR (relevant sub-project: "SP 2.3: Probabilistic assessment of intact stability), mentioned also by the respective deliverable reports, where details can be found, in the reference section (Behrens 2006; Athanassoulis et al 2007; Spyrou and Themelis 2006; Themelis et al 2007).

7.1 Application 1: A ROPAX ferry in the Mediterranean Sea

7.1.1 Basic characteristics of the ship

The first examined ship is a recently built ROPAX ferry that is currently operating in the Western Mediterranean Sea. The basic particulars of the ferry are collected in Table 7.1. To reduce the volume of calculations, one draft corresponding to full-load departure has been considered. In Figure 7.1 are shown rendered views from different angles (stern and bow) of the hull-form of this ROPAX ferry extracted by the commercial code Maxsurf 11. Also, in Figure 7.2 is presented her general arrangement.

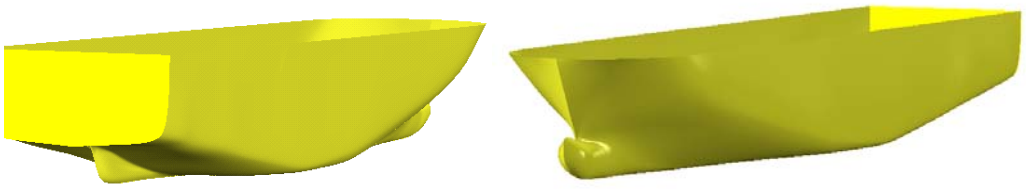

Figure 7.1: Rendered views of the hull-form of the examined ROPAX, generated by Maxsurf.

Table 7.1: Basic particulars of the ROPAX ferry.

L_{BP} (length)	157 m	GM (metacentric height, corrected)	2.08 m
B (beam)	26.2 m	T_0 (natural roll period)	15.26 s
D (depth to upper deck)	9.2 m	b_{BK}, l_{BK} (breadth, length of bilge keels)	0.26 m, 60.9 m
T_d (mean draught)	6.2 m	KG (vertical position of the center of gravity above keel)	12.72 m
C_b (block coeff.)	0.626	Trailers	99
V_S (speed)	22.5 kn	Cars	166

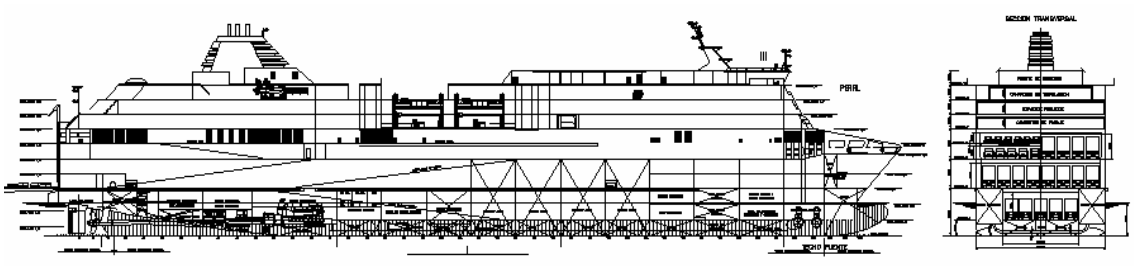

Figure 7.2: General arrangement of ROPAX.

7.1.2 Ship route, weather data and time of exposure to each node

The route Barcelona – Piraeus was selected and in Figure 7.3 it is schematically shown on a Google-Earth (2005) map of the Mediterranean Sea. The length of the trip was calculated as 1209.30 nautical miles. Given the service speed and ignoring any voluntary or involuntary speed reduction, it should be covered theoretically in 53.75 hours.

The objective was to assess the ship in the "long-term" concerning her winter operability. Mediterranean wave statistics have been accounted through placement of "weather nodes" along the selected route, a concept explained in Chapter 4. Each node lies at the centre of an assumed square "influence" area (Figure 7.4). To ensure sufficient resolution, a grid with density 1^0 x 1^0 has been built surrounding the route. In total, 23 nodes were cast. Tagged (per node) wave statistics were contributed by Athanassoulis et al (2006). In particular, univariate distributions of significant wave height H_S, peak period T_P and mean wave direction Θ_M were taken into account. The obtained mean weather values for winter season along the route are shown in Figure 7.5 to Figure 7.7 (preliminary analysis confirmed that, in this region, the most extreme values of wave parameters arise in winter).

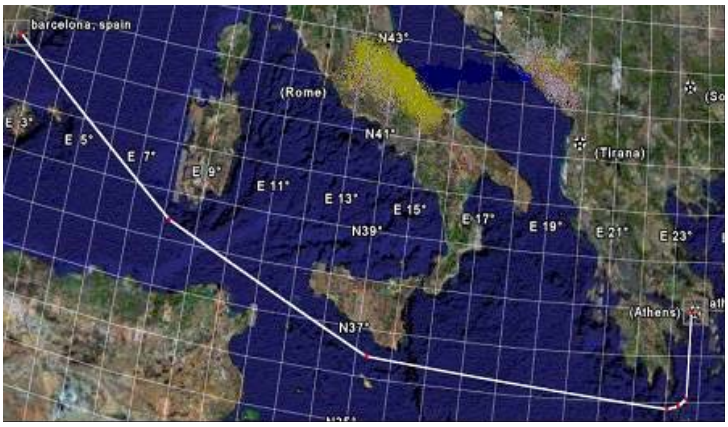

Figure 7.3: Barcelona – Piraeus route.

At this point it should be mentioned that probabilities figures will be estimated on the mean winter values of H_S, T_P and Θ_M assuming their univariate distribution and without taking into account their joint probabilistic occurrence.

The time spent by the ship within the influence area of some arbitrary node depends on the route's length that is inside the associated rectangle (obtained with a simple geometrical calculation) and the speed sustained by the ship in that part of the journey. Judging from the values of the most probable significant wave heights and periods, the assumption of constant

speed is not completely unrealistic. In Table 7.2 are summarized the segmented travel times associated with the 23 nodal points. Thereafter, the time of exposure to beam, head and following seas can be deduced taking into account the heading of the ship (according to the defined route) and the distribution of mean direction of the local wave field around each node. The convention for wave direction follows that of Figure 4.3. The time of exposure to specific wave scenarios, scaled with reference to the duration of the whole voyage, is shown in Figure 7.8.

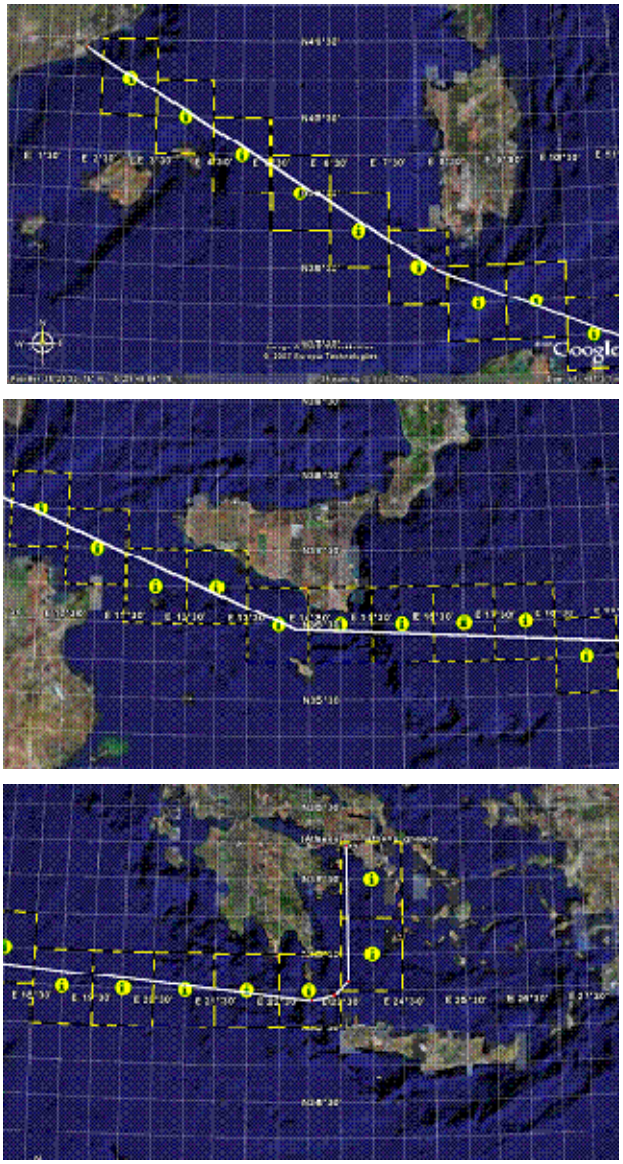

Figure 7.4: The selected route, placed weather nodes and their areas of influence.

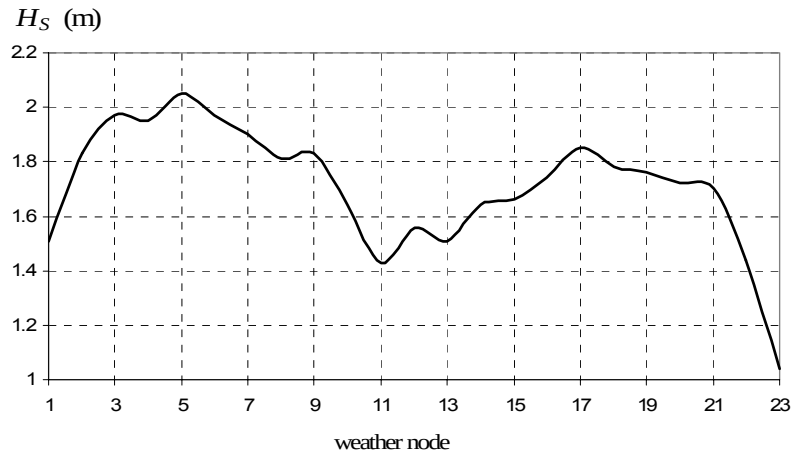

Figure 7.5: Variation of mean value of H_S along the route for winter.

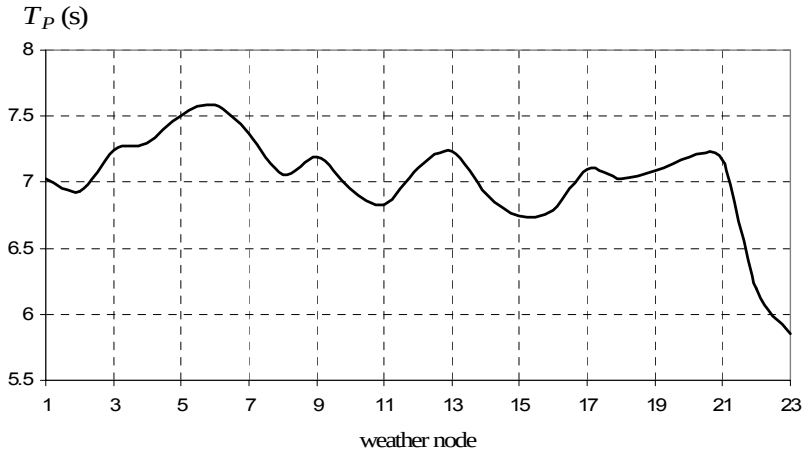

Figure 7.6: Variation of mean value of T_P, as above.

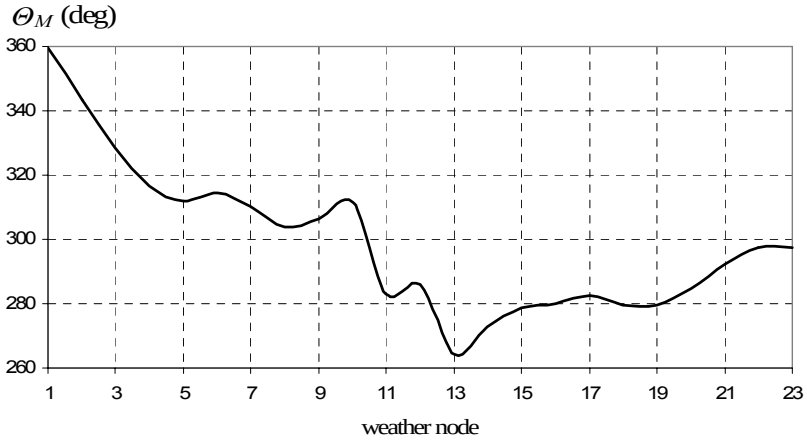

Figure 7.7: Variation of mean Θ_M (0^0 waves coming from North, 90^0 East).

Table 7.2: Time spent in each grid sub-area.

	Distance (nm)	Time (hr)	%
node 1 (41^0N, 03^0E)	68.56	3.05	5.67
node 2 (40.5^0N,04^0E)	53.28	2.37	4.41
node 3 (40^0N,05^0E)	54.43	2.42	4.50
node 4 (39.5^0N,06^0E)	54.64	2.43	4.52
node 5 (39^0N,07^0E)	55.71	2.48	4.61
node 6 (38.5^0N,08^0E)	54.62	2.43	4.52
node 7 (38^0N,09^0E)	50.78	2.26	4.20
node 8 (38^0N,10^0E)	51.21	2.28	4.23
node 9 (37.5^0N,11^0E)	52.00	2.31	4.30
node 10 (37^0N,12^0E)	52.01	2.31	4.30
node 11 (37^0N,13^0E)	52.76	2.34	4.36
node 12 (36.5^0N,14E)	51.81	2.30	4.28
node 13 (36.5^0N,15^0E)	48.37	2.15	4.00
node 14 (36.5^0N,16^0E)	48.50	2.16	4.01
node 15 (36.5^0N,17^0E)	48.57	2.16	4.02
node 16 (36.5^0N,18^0E)	48.31	2.15	3.99
node 17 (36^0N,19^0E)	48.81	2.17	4.04
node 18 (36^0N,20^0E)	48.48	2.15	4.01
node 19 (36^0N,21^0E)	48.87	2.17	4.04
node 20 (36^0N,22^0E)	48.95	2.18	4.05
node 21 (36^0N,23^0E)	51.00	2.27	4.22
node 22 (36.5^0N,24^0E)	60.84	2.70	5.03
node 23 (37.5^0N,24^0E)	56.79	2.52	4.70
Total	1209.30	53.75	100.0

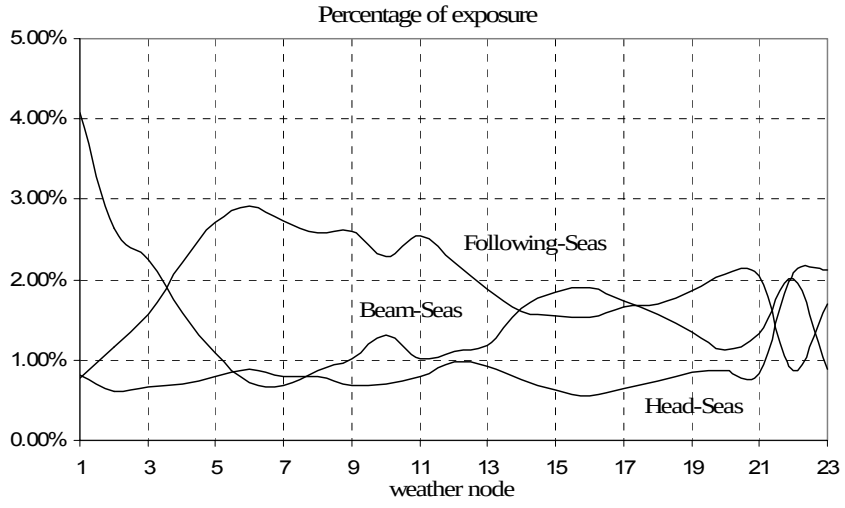

Figure 7.8: Percentage of exposure to weather nodes.

7.1.3 Norms of unsafe response for ship and cargo

Failure norms are formally establishing addressing the safety of the ship and of her cargo. These norms are expressed respectively through a critical roll angle for the ship and a critical acceleration for the cargo (in this case trailer) as explained next:

Direct capsize threshold

To determine a critical roll angle as a threshold of imminent "capsize", the principle of the weather criterion has been adopted (Figure 7.9). On the basis of hydrostatic calculation performed for the ROPAX it was concluded that, as ship capsize should be considered the exceedence of the minor of: the angle of vanishing stability determined as $\varphi_c = 63^0$; the flooding angle $\varphi_f = 35^0$; the ultimate angle of $\varphi_a = 50^0$ that is prescribed in the application of the weather criterion for balancing work against potential energy.

Shift of cargo threshold

The tendency of the most prone, regarding its position on ship, trailer for transverse sliding and tipping was checked for three different lashing arrangements regarding the vertical securing angle x (Figure 7.10). The specific angles examined were $(30^0, 45^0, 60^0)$ which span the permissible range. The background calculations are based on IMO (1991) cargo securing manual and the relevant calculation procedure can be found for example in (DNV 2002b; Themelis and Spyrou 2003). The lashing arrangement contains three lashings symmetrically located on each side, assumed with 100 kN strength, which is the lower strength limit (DNV 2002b). Trailer's mass, its centre of gravity above the deck as well as the friction coefficient between the deck and trailer's rubber are also involved. Trailer and lashing arrangement parameters that are essential for the current analysis are collected in Table 7.3. The assumed mass of the trailer and the coordinates of its remote position on the deck follow the Load Conditions and Intact Stability report that accompanied ship data. The most critical transverse acceleration $\left(a_y = 6.04 \text{ m/s}^2\right)$ was found corresponding to transverse sliding and a vertical securing angle of 60^0 (Figure 7.11).

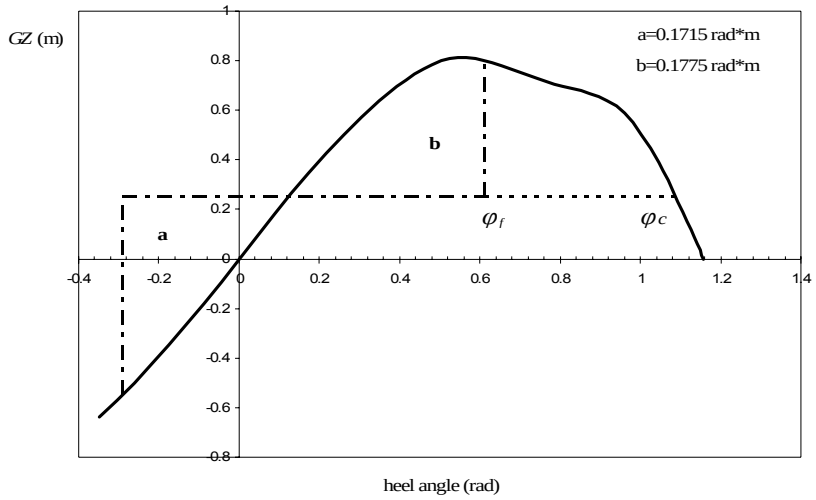

Figure 7.9: Application of the weather criterion.

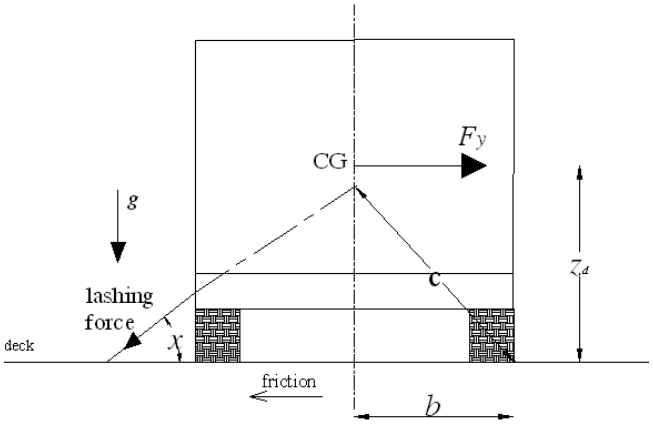

Figure 7.10: Lashing arrangement (transverse) and relevant forces.

Table 7.3: Trailer and lashings characteristics.

Trailer mass:	m_t = 49 t
Most arduous position of trailer (according to GA):	x = 57.2 m (from mid-ship section) y=10.2 m z_{bl} = 14.84 m (from base-line)
Centre of gravity above deck:	z_d = 2.36 m
Lever-arm for tipping:	b = 1.261 m
Frictional coefficient:	μ = 0.3 (rubber against steel)
Lashing arrangement:	3 chains with maximum securing load 100 kN on each side, symmetrical. Vertical securing angle: x = 30°/45°/60°

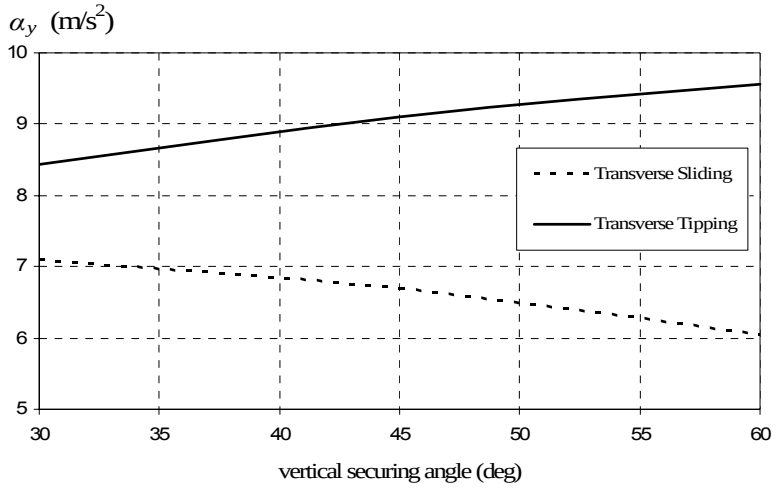

Figure 7.11: Critical transverse accelerations (with respect to sliding and tipping) for a range of angles of lashing arrangement.

7.1.4 Critical wave group characteristics identification

As it was referred, in the current application, critical wave groups have been identified for the following stability criteria: beam-sea resonance, parametric rolling in longitudinal seas and pure-loss of stability.

Wave groups leading to beam seas resonance

The calculation tool for this stability criterion is the mathematical model for the numerical deterministic simulation of the coupled roll, heave and sway motion, which developed during the thesis and described in detail in Chapter 6. Generally transient response was targeted and repetitive runs were carried out. So critical wave heights were estimated checking whether exceedence of the inspected norm, in each case, realised within the allowed number of wave encounters and the assume wave period range. Figure 7.12 presents a roll response simulation time history excited by one of the identified critical wave groups. The ship was assumed initially unbiased and the realistic range of periods of ocean waves has been spanned. It should be noted however that, in the low range of periods (about $T_w < 8.5$ s), it was not feasible to determine critical heights because the required steepness exceeded the wave breaking limit of Airy waves $\left(H/\lambda \simeq 1/7\right)$. In Figure 7.13 and Figure 7.14 are summarized the obtained critical wave heights, parameterized with respect to wave period and run length. They have been identified by taking into account ship response (Figure 7.13) and trailer shift (Figure 7.14).

Wave groups inciting parametric rolling with critical amplitude

For the assumed speed of $V_S = 22.5$ kn the ship could be liable to head-sea parametric rolling at the principal region of instability when the wavelength receives values like those shown in Figure 7.15. The diagram was obtained by setting the frequency parameter $a = 4\omega_0^2 / \omega_e^2$, to a value around 1.0 so that, one of the conditions of principal resonance is satisfied.

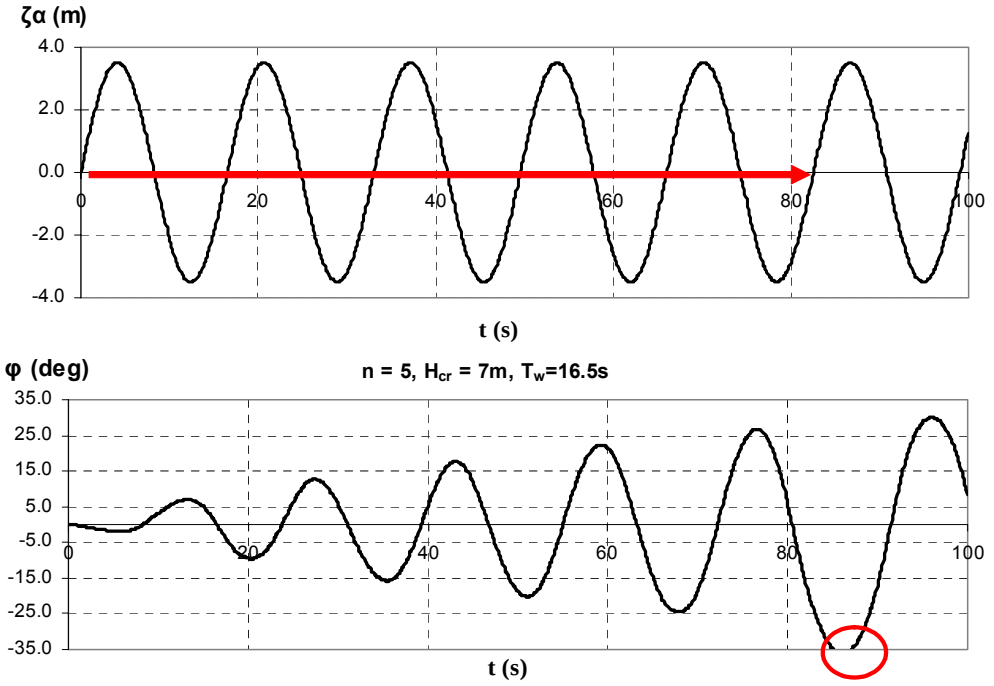

Figure 7.12: Time histories of wave elevation and roll response, where the exceedence of the specified norm has been marked.

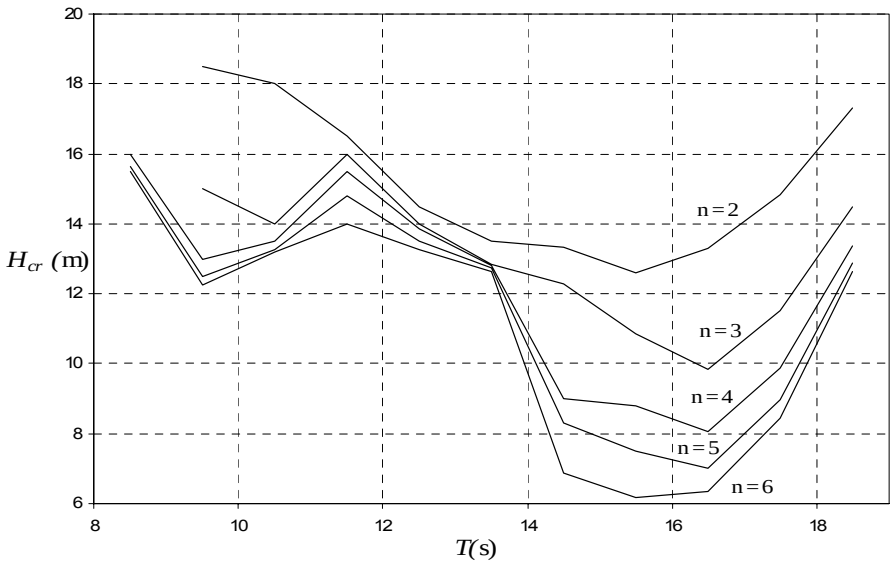

Figure 7.13: Wave groups producing critical ship inclination.

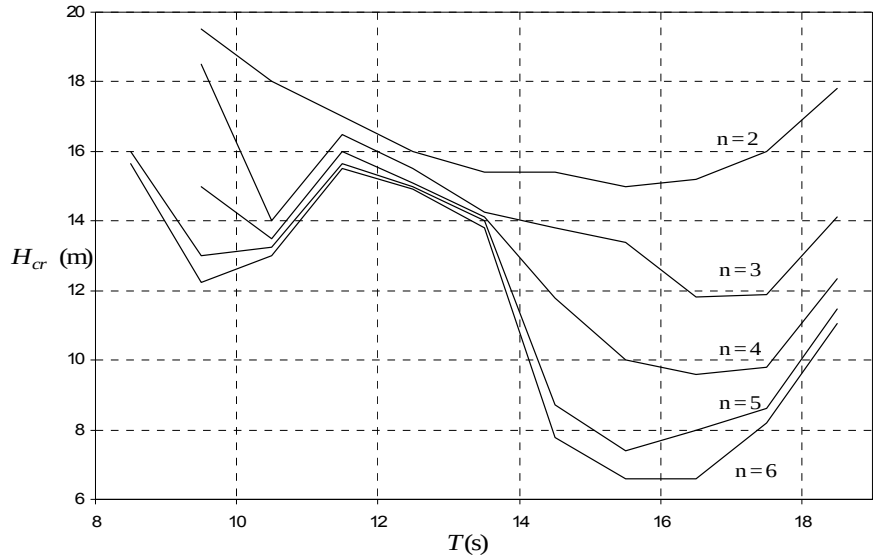

Figure 7.14: Wave groups producing critical cargo acceleration.

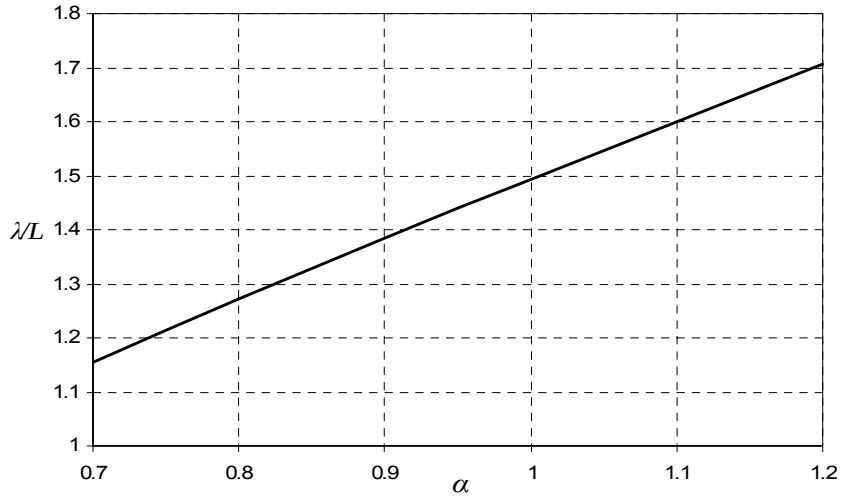

Figure 7.15: Wavelengths conducive to principal parametric rolling.

The analytical criterion targeting the transient part (growth) of parametric rolling, which has been presented in the previous Chapter, has been employed for the specification of critical wave heights. This criterion indeed produces the critical magnitude of parametric excitation h_{cr} that is necessary for realising a q - fold increase of an initial roll disturbance, within p roll cycles and was applied here for a wide range of a values ($a \in [0.7,1.2]$). It should be noticed that the form of the criterion for $a \neq 1$ is not practical for presentation and relevant calculations performed with the assistance of Mathematica. The parametric excitation h is linked exclusively to the fluctuation of GM, in accordance to the following formula:

$h = \dfrac{GM_{trough} - GM_{crest}}{2GM_{mean}}$. As well known, roll damping plays a critical role for the inception of parametric rolling and its value should be obtained with care. The value of roll damping divided by roll moment of inertia (mass plus hydrodynamic) was obtained according to the numerical code of beam-sea rolling referred-to earlier, using the viscous forces estimation methodology. An equivalent linear damping coefficient has been estimated around natural roll frequency, with no forward speed and its estimation was $k = 0.01039$ s^{-1}. It is also noticed that, at a high speed in head-seas, the heave and pitch effects should be important and a coupled model should be more appropriate. Here it is not intended to elaborate on this aspect further as the emphasis was set on the workings of the probabilistic method. A comparative study among the findings of a coupled detailed model and the analytical criterion follows in a next Chapter.

The targeted q-fold increase can be presented as the ratio of the critical roll angle (35^0 or the amplitude of roll oscillation during which the critical acceleration $a_y = 6.04$ m/s^2 is realised) to an uncertain initial roll disturbance which may be assumed during operation in a rough sea by the ship. This disturbance was considered to be distributed in the range $\varphi_0 = 0^0$ - 6^0 with 3^0 discretisation step and equal probability for each sub-range. In Figure 7.16 is shown the obtained critical parametric amplitude for the sub-range φ_0=3^0 - 6^0. Up to 4 parametric roll cycles, approximately 8 successive critical waves have been targeted. Should this be combined with a requirement of high waves in the group, such an encounter would constitute a very low probability event.

In the next step, the identified critical parametric excitations need to be converted into critical wave heights taking into account the ship form. Relevant calculations have been executed through the commercial code Maxsurf. Characteristic variations of submerged volume as the ship passes from a crest and from a trough, for one of the critical combinations of wave steepness and length ratio, is shown in Figure 7.17. For example, in Figure 7.18 are collected representative righting-arm variations showing the sensitivity in wave heights for two critical cases. The obtained critical wave heights according to run length are shown in Figure 7.19.

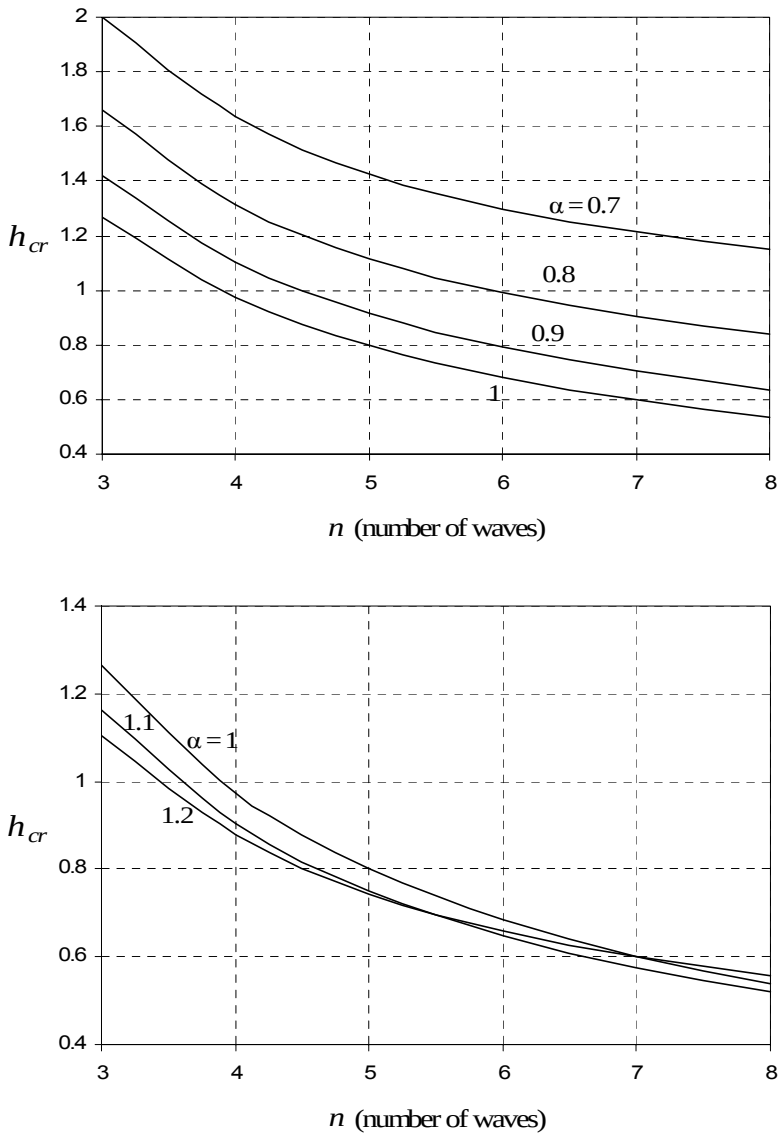

Figure 7.16: Critical parametric roll amplitudes assuming an initial roll angle in the range φ_0=3^0 - 6^0.

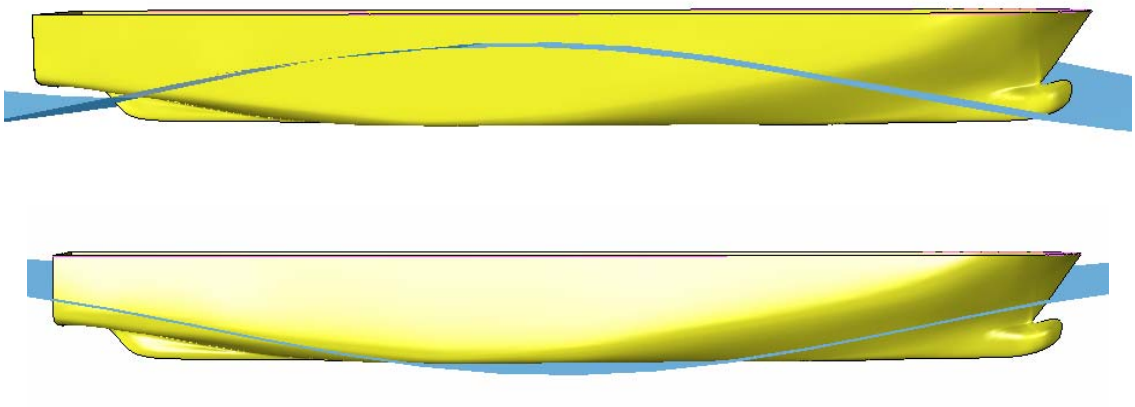

Figure 7.17: Variation of the wetted part of the hull in a wave ($H/\lambda = 0.065$, $\lambda/L = 1.493$).

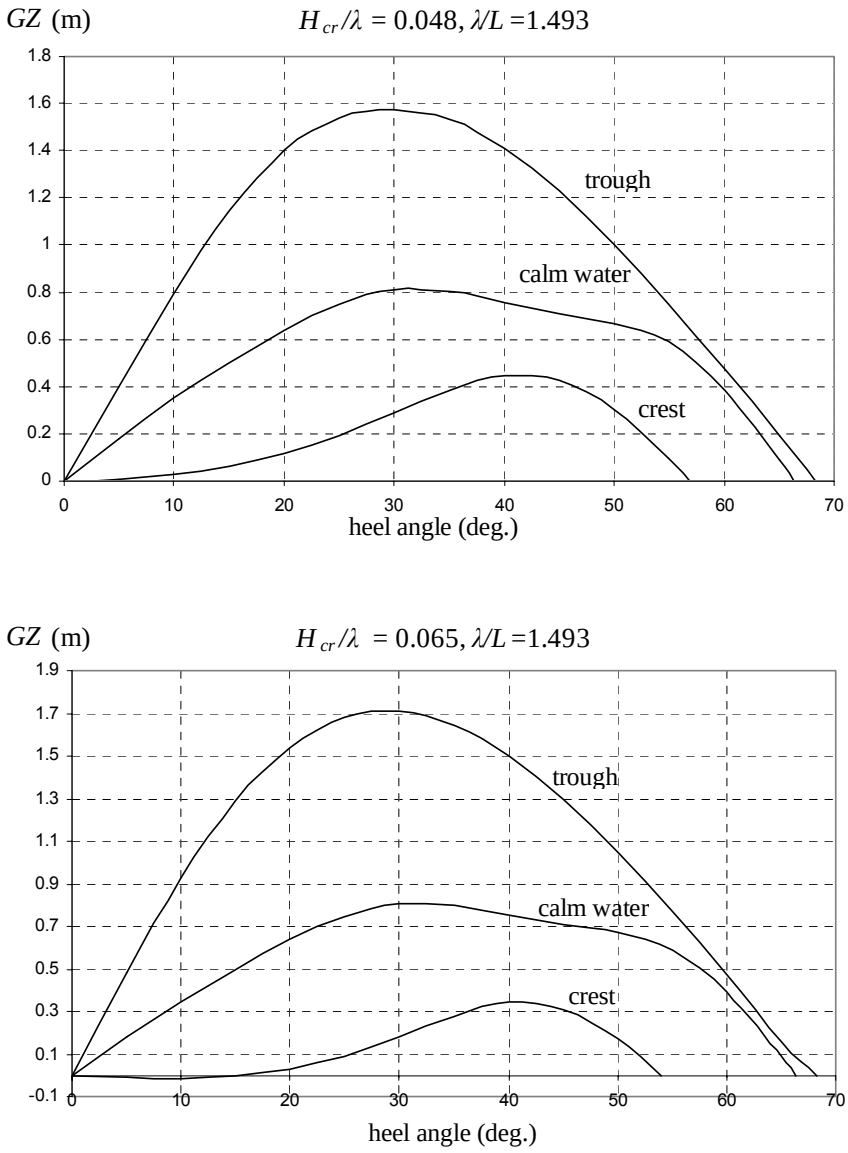

Figure 7.18: Variation of the *GZ* curve for $a = 1$ and two different wave heights.

Critical wave encounters for pure – loss of stability

The critical wave characteristics are determined utilizing the analytical criterion for pure loss of stability which has been presented in Chapter 6. Unlike a resonance phenomenon, this growth is relatively slow and the condition on the ship norm should prevail over the condition on the cargo. The same as in parametric rolling probabilistic initial roll disturbance was considered, while critical wavelength range was specified so that the encounter frequency to be low for the considered ship's speed. The critical wave height for several values of the length ratio λ/L was determined according to the relevant criterion for pure loss of stability (Chapter 6), taking into account the detailed form of the *GZ* curve. In Figure 7.20 is shown

the calculated h_{cr} for various values of λ/L. Its reflection in terms of wave height for the ROPAX ferry can be obtained from Figure 7.21.

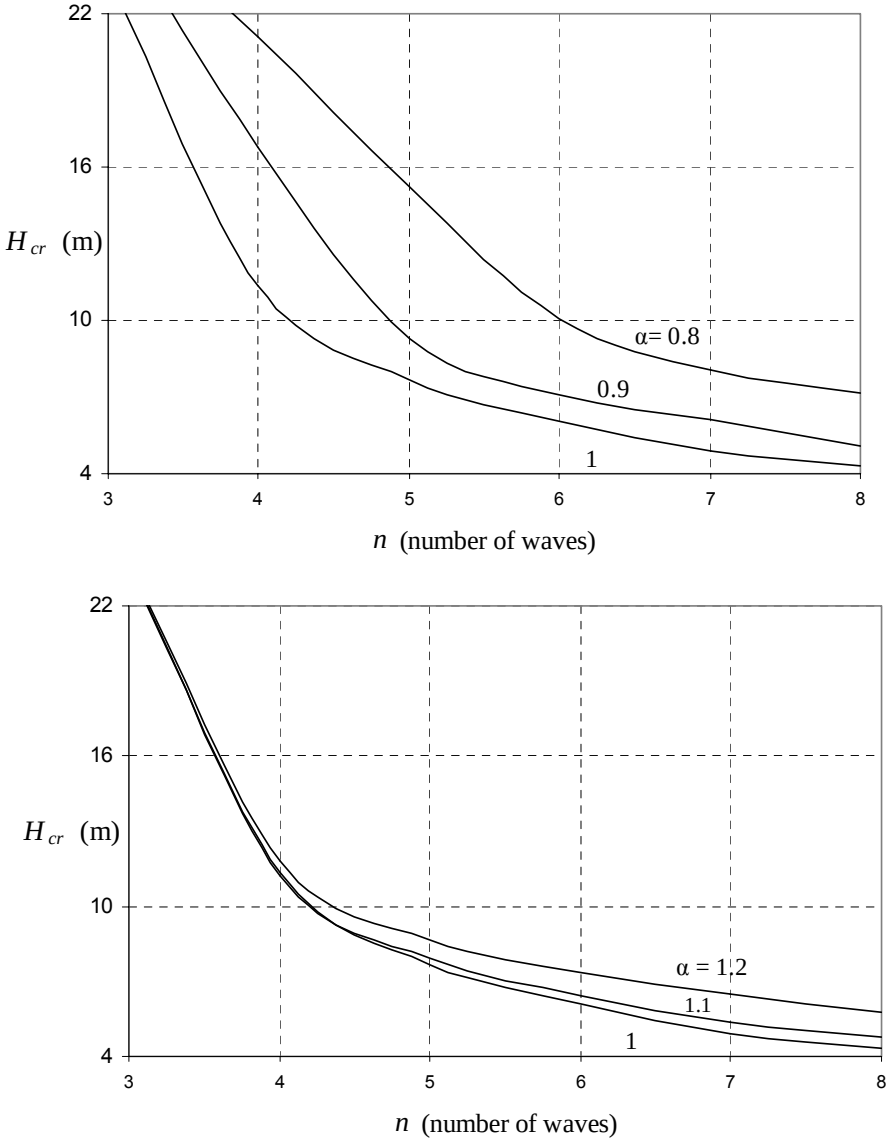

Figure 7.19: Corresponding wave height for reaching the critical roll angle.

7.1.5 Probability of "instability" per mode

The identification of critical wave groups per stability criterion (with reference to the corresponding limit-state parameter and norm) should be followed by the calculation of the probability of encountering these (or "worse") wave groups as well as the associated critical time ratio of ship exposure. The assumption of JONSWAP spectrum underlies the ensuing calculation of probabilities (Hasselmann et al 1973). As is well-known, its spectral density function is expressed as:

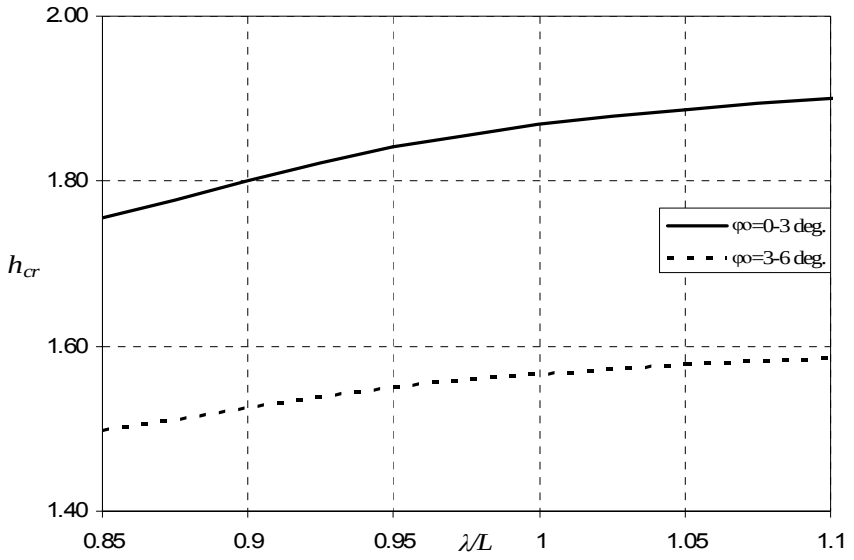

Figure 7.20: Critical values of h for pure-loss of stability for the two ranges of initial roll angles.

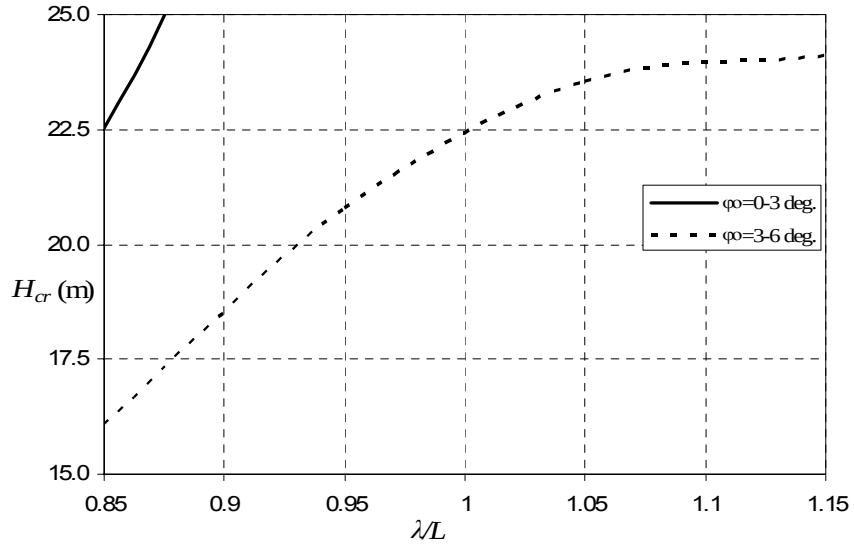

Figure 7.21: Extreme wave heights for realizing pure-loss of stability.

$$S(\omega) = a_w\, g^2 \omega^{-5} \exp\left(-\frac{5}{4}\left(\frac{\omega}{\omega_p}\right)^{-4}\right)\gamma^{\exp\left(-0.5\left(\frac{\omega-\omega_p}{\sigma\omega_p}\right)^2\right)} \tag{7.1}$$

where

$$a_w = \frac{5}{16}\left(\frac{H_S^2\omega_p^4}{g^2}\right)A_\gamma \tag{7.2}$$

$$A_\gamma \cong 1 - 0.287\ln(\gamma) \tag{7.3}$$

$$\sigma = \begin{cases} 0.07 \text{ if } \omega \le \omega_{\mathrm{p}} \\ 0.09 \text{ if } \omega > \omega_{\mathrm{p}} \end{cases} \tag{7.4}$$

a_w is the generalized Philips' constant, A_γ a normalizing factor, γ the peakness parameter, σ the spectral width parameter and ω_p the angular spectral peak frequency. For the peakness parameter γ the following formulas can be used (DNV 2002a).

$$\gamma = \begin{cases} 5 \text{ for } \dfrac{T_P}{\sqrt{H_S}} \le 3.6 \\ e^{5.75-1.15\frac{T_P}{\sqrt{H_S}}} \text{ for } 3.6 \le \dfrac{T_P}{\sqrt{H_S}} \le 5 \\ 1 \text{ for } 5 \le \dfrac{T_P}{\sqrt{H_S}} \end{cases} \tag{7.5}$$

The encounter spectrum is obtained by the next transformation:

$$S(\omega_e, \psi) = \frac{S(\omega)}{\left| 1 - \dfrac{2\omega U \cos\psi}{g} \right|} \tag{7.6}$$

Resonance in beam-seas

The probability calculations gave the inspiration to propose a new type of ship stability performance diagram, illustrating the variation of the critical time ratio at various locations along the desired route (Figure 7.22). The concept of the critical time ratio has been described in Chapter 4. The applied time scaling was local, in accordance to the time spent in the vicinity of the nearest node; i.e. within the associated rectangle. It is obvious that for a major part of the journey the probability is practically zero. Nonetheless it has been preferred to show this curve, in order to indicate the qualitative variation along the route which provides a hint also for conditions of harsher sea-states. Moreover all then presented diagrams are in a logarithmic scale.

Head-seas parametric rolling

For a more meaningful calculation of probabilities, some fluctuation of speed ± 1 kn around the service speed $\left(V_S = 22.5 \text{ kn}\right)$ has been assumed, given that this affects the frequency of encounter which, in a random seaway, is a probabilistic quantity. The obtained diagram of critical time ratio for head-seas parametric rolling can be seen in Figure 7.23. As expected, for

most part of the journey the ratio of critical time is negligibly small.

Pure-loss of stability

In Figure 7.24 is shown the probability of occurrence of a "pure-loss" event.

7.1.6 Collective probability of instability (all considered modes)

The percentage of time spent in beam, head and following seas is shown in Figure 7.25. The three critical time ratio curves are overlaid in Figure 7.26 for the ship norm and in Figure 7.27 for the cargo norm respectively. The probability of exhibiting instability of anyone of the considered types may thus be determined. The last figures are very illuminating also about the ship's propensity to instability of some selected type for individual stages of the journey. From this diagram one can easily deduce which type of instability is more likely to occur at any specific stage of the journey. Such a "localised" probabilistic figure of instability could be a valuable piece of information for weather routeing and decision support.

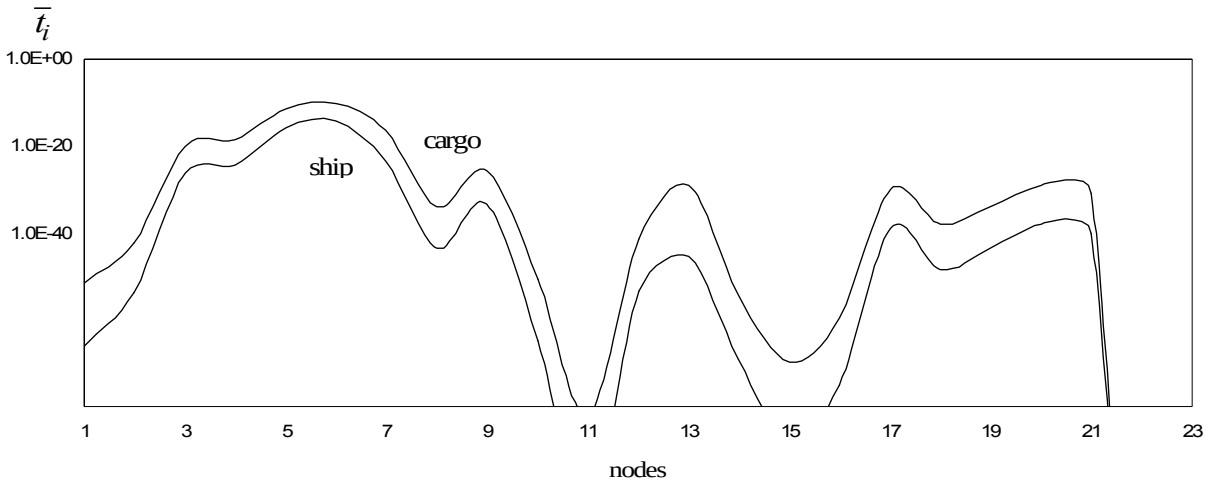

Figure 7.22: Variation of critical time ratio during voyage, for extreme rolling in beam-seas (ship and cargo norms).

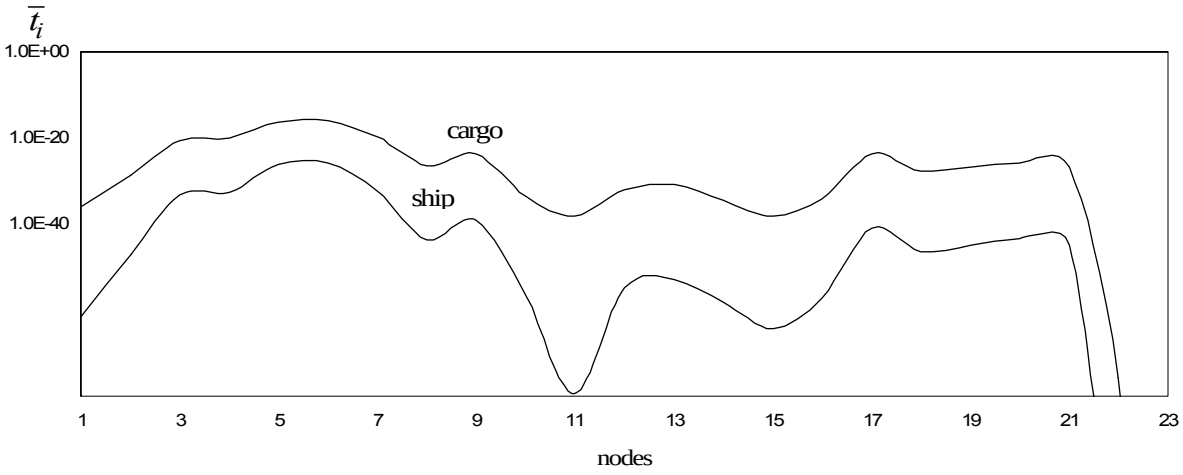

Figure 7.23: Critical time ratio curves for head-seas parametric rolling (ship and cargo norms).

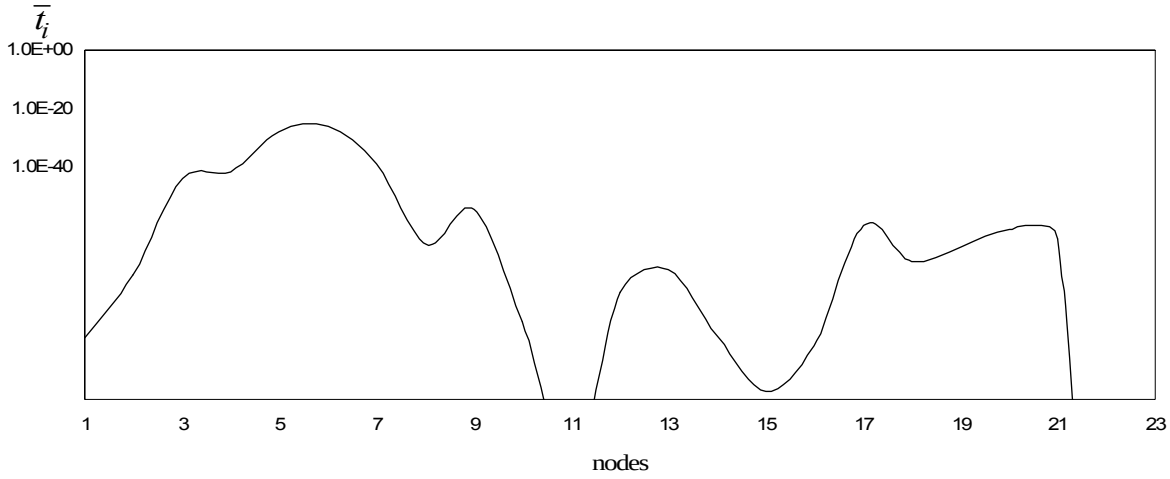

Figure 7.24: Critical time ratio for pure-loss of stability (ship norm).

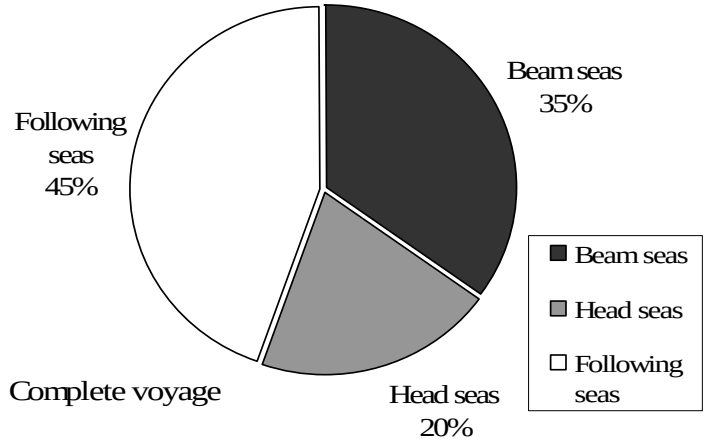

Figure 7.25: Percentage of time in beam, head and following seas.

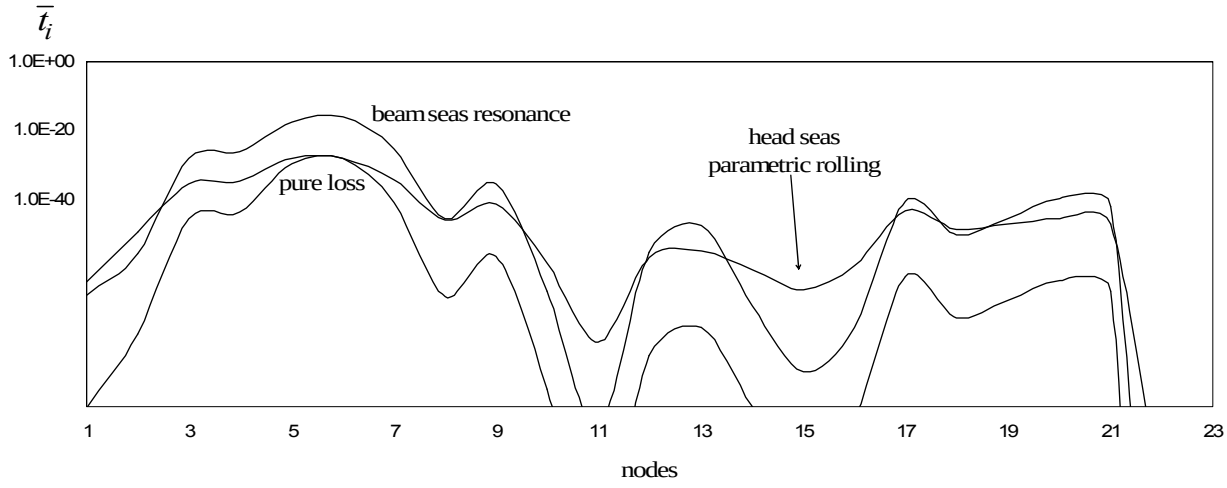

Figure 7.26: Comparison of tendencies for different types of instability during journey (ship norm).

Finally, the tendency for instability concerning the entire voyage can be characterized from the probability values shown in Table 7.4.

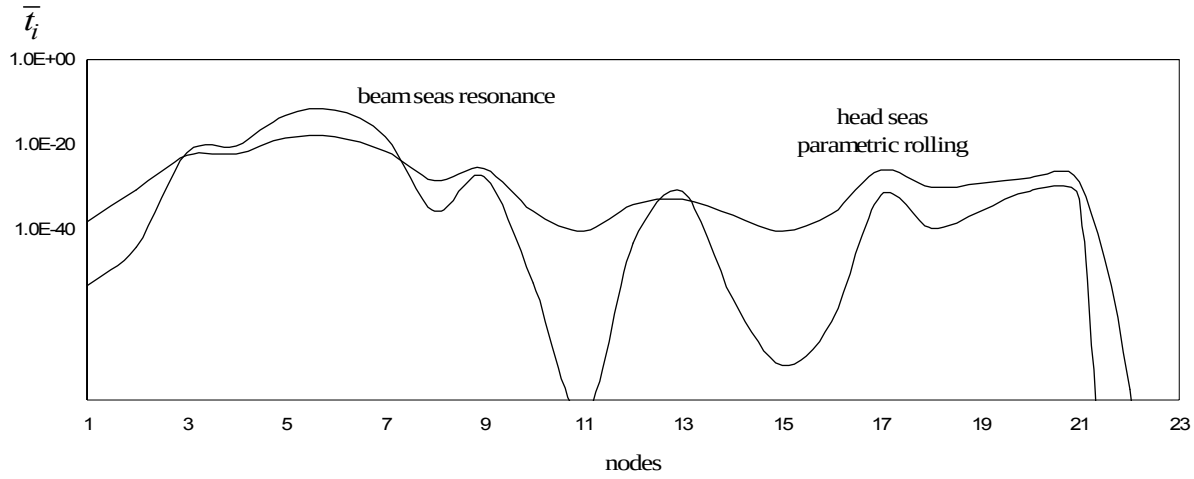

Figure 7.27: Comparison of tendencies for different types of instability during journey (cargo norm).

Table 7.4: Summed probability and associated critical time ratio for entire journey.

	P_i	$\overline{t_i}$
Ship: ($\varphi > 35^0$)	6.58 x 10^{-17}	9.55 x 10^{-17}
Cargo: ($a_y > 6.04$ m/s^2)	7.84 x 10^{-13}	1.14 x 10^{-12}

Probability values are expressed as number of critical waves over the total number of encountered waves. Thus, to determine the probability of a single loss given a certain period of exposure, a suitable transformation is entailed. Let's give a simple example and assume 25 years of exposure (winter operability) and let service time represent 60% of the actual time. A mean upcrossing wave period of 6.5 s along the route leads to 0.6 x 25 (years) x 3 (months) x 30 (days) x 24 (hr) x 3600 (s) / 6.5 (s) = 1.8 x 10^7 encountered waves approximately. Then the life-time probability of a single cargo shift event (this is the worst case according to Table 7.4) is about 1.43 x 10^{-5}.

7.2 Application 2: A post panamax containership in North Atlantic

7.2.1 Basic characteristics of the ship

The post panamax containership is currently operates in North Atlantic. Basic data concerning the assessed containership are shown in Table 7.5. Unfortunately, no information of her bilge keels was available, so a bare hull was only considered. Hull-form of the containership is shown respectively in Figure 7.28. Service speed was set to 24 kn.

Table 7.5: Ship data.

L_{BP} (length)	264.4 m	V_S (speed, calm water)	24 kn
B (beam)	40 m	$KG_{cor.}$ (corrected center of gravity above keel)	18.79 m
D (depth, upper deck)	24.3 m	$GM_{cor.}$ (metacentric height, corrected)	0.61 m
T (mean draught)	13.97 m	Number of TEUs	5048
C_b (block coef.)	0.600	T_0 (calculated natural roll period – based on roll radius of gyration 0.381B)	39.12 s

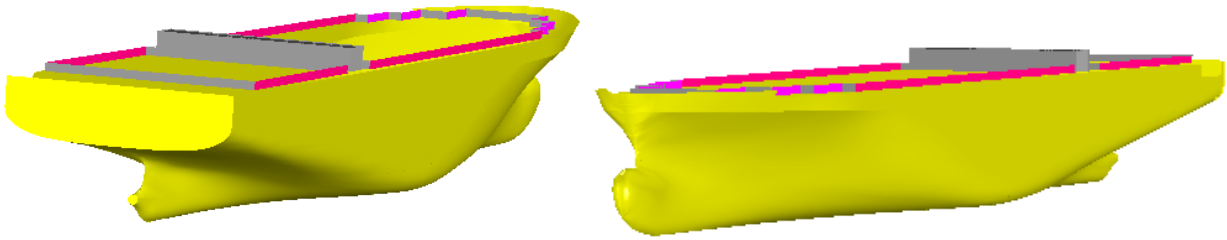

Figure 7.28: Rendered views of the hull form of the containership.

7.2.2 Ship route, weather data and time of exposure to each node

The selected route between Hamburg and New York is a rather popular one for containerships, although here the unusual choice of going over the Shetlands has been made due to the lack of weather data in the British Channel. Then the route follows a straight line until the southern coast of Newfoundland. Then it is bent slightly so that a course near to the coastline is maintained, until New York is reached. The total length of this route is 3422.86 nautical miles, covered in 142.82 hours if the service speed of 24 kn is kept. Due to the considerably longer distance, a grid with step in longitude of 3^0 and variable step in latitude (so that the nodes are cast as near to the route as possible, with 0.5^0 minimum step due to the spatial resolution of available wave statistics). In Figure 7.29 is shown the entire route,

overlaid on a Google Earth map. In total 27 “weather nodes” were cast along this route (example of the nodes with their area of influence shown for a middle part of the route, Figure 7.30), while in Table 7.6 are summarized the segmented travel times associated with the 27 nodal points.

Wave hindcast data for the North Atlantic referring to the period between 1990 and 1999 has been provided (Behrens 2006). In the current application a “short-term” assessment was performed. It should be mentioned here that despite the lengthy duration of these voyages, “fresh” short-term wave data can be imported as soon as the ship moves into a new rectangle of the discretised sea area. If, following a first distribution of nodes, it was found that the weather characteristics inside a rectangle change significantly while the ship is still inside this rectangle, the resolution can be adjusted by placing more nodes, so that a balance is achieved between the number of nodes and the requirement for practical stationarity of the wave field.

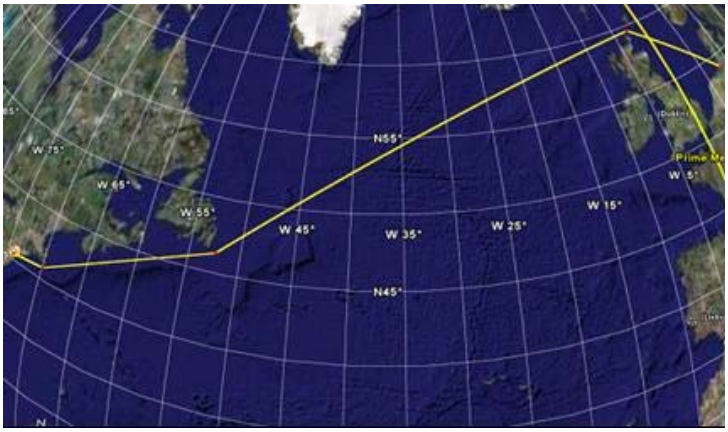

Figure 7.29: Hamburg - New York route.

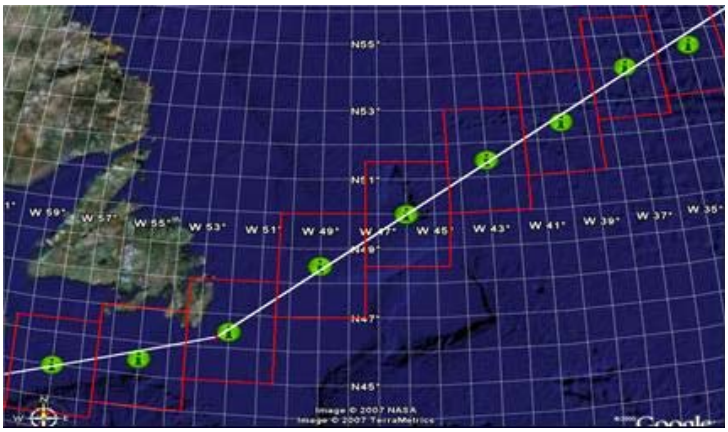

Figure 7.30: Part of route showing weather nodes and their areas of influence.

Then the data was searched in order to find specific days of bad weather at places near to the

ship's route. It was found that waves of significant height exceeding 10 m should have been realised in some part of the route, in the period between 13/01/1991 and 18/01/1991. The variation of H_S, T_P and of the mean wave direction Θ_M in the vicinity of the defined route, are presented in Figure 7.31 to Figure 7.33. It is clarified that the wave parameters account for total values, meaning that both the wind and swell part of the sea have been included and also it is worth noting that these values reflect the condition of the sea only at the time interval that the ship operates in the vicinity of a corresponding node, i.e. they refer in fact to different times.

The percentage of the ship's scaled time of exposure to beam, head and following seas per node had then to be worked out on the basis of ship heading (as defined by the route) and the distribution of mean direction of the local wave field around each node Θ_M, weighted by the time spent in its area of influence (Figure 7.34). For the distribution of Θ_M a hyperbolic-cosine spreading function, defined as follows (Athanassoulis 2004), has been considered.

$$D(\theta;\Theta_m) = \frac{1}{2}\beta \cosh^{-2}\left[\beta(\theta - \Theta_m)\right] \tag{7.7}$$

where the parameter β is defined by:

$$\beta = \begin{cases} 2.61(f/f_p)^{1.3}, & \text{for } 0.562 \le f/f_p < 0.95 \\ 2.28(f/f_p)^{-1.3}, & \text{for } 0.95 \le f/f_p < 1.60 \\ 1.24, & \text{otherwise} \end{cases} \tag{7.8}$$

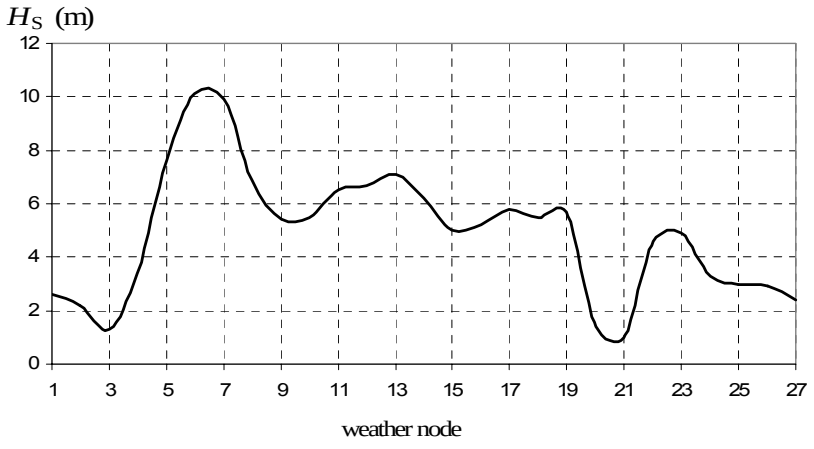

Figure 7.31: Variation of significant wave height per node.

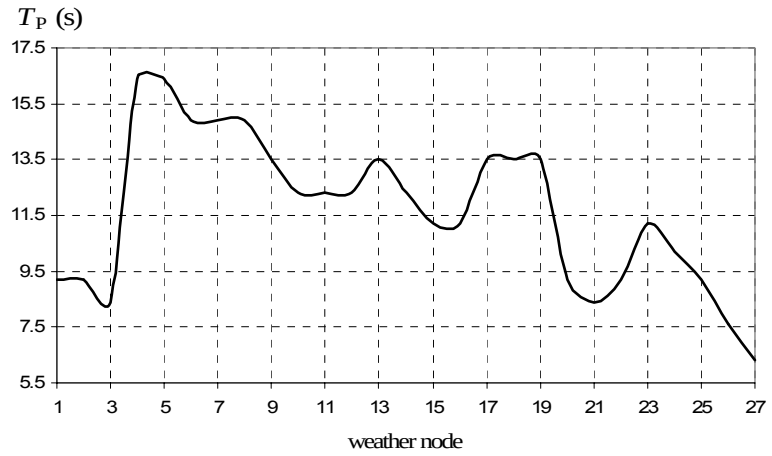

Figure 7.32: Variation of peak period.

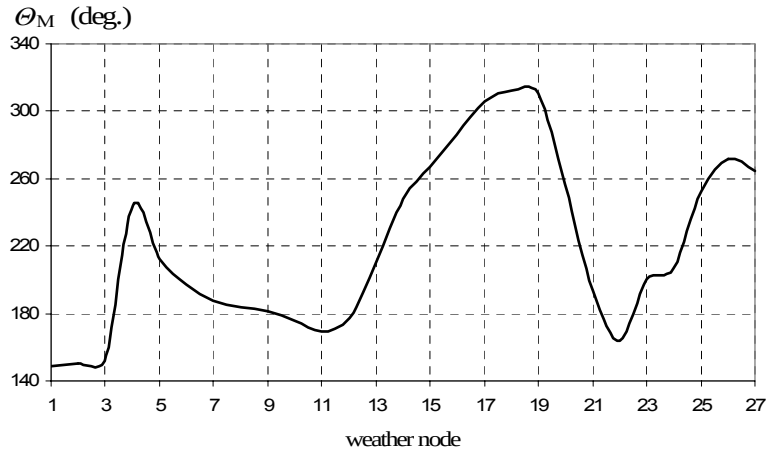

Figure 7.33: Variation of mean wave direction (0^0 waves coming from North, 90^0 East).

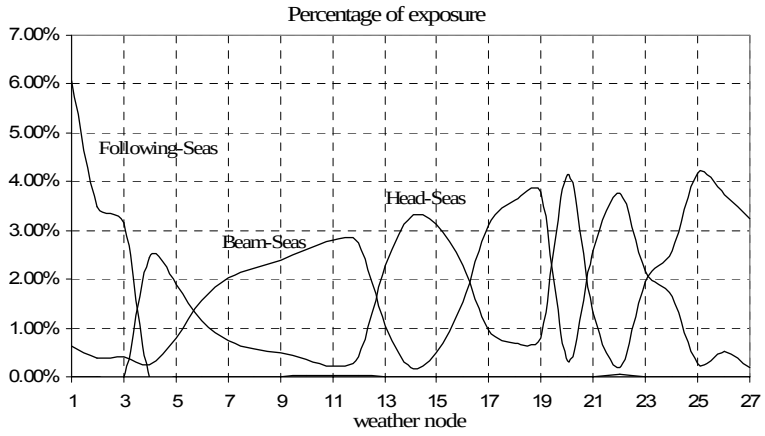

Figure 7.34: Exposure to beam, head and following seas.

Table 7.6: Time spent in each grid sub-area.

	Distance (nm)	Time (hr)	%
node 1 (56^0N, 05^0E)	229.79	9.57	6.71%
node 2(57.5^0N,02^0E)	132.79	5.53	3.88%
node 3 (59^0N,01^0W)	122.31	5.10	3.57%
node 4 (59.5^0N,04^0W)	92.53	3.86	2.70%
node 5 (59.5^0N,07^0W)	91.85	3.83	2.68%
node 6 (59.5^0N,10^0W)	93.20	3.88	2.72%
node 7 (59^0N,13^0W)	94.59	3.94	2.76%
node 8 (58.5^0N,16^0W)	96.72	4.03	2.83%
node 9 (58^0N,19^0W)	98.91	4.12	2.89%
node 10 (57.5^0N,22^0 W)	101.78	4.24	2.97%
node 11 (57^0N,25^0 W)	104.60	4.36	3.06%
node 12 (56.5^0N,28^0 W)	108.59	4.52	3.17%
node 13 (55.5^0N,31^0 W)	113.40	4.73	3.31%
node 14 (54.5^0N,34^0 W)	118.08	4.92	3.45%
node 15 (54^0N,37^0 W)	124.02	5.17	3.62%
node 16 (52.5^0N,40^0 W)	131.15	5.46	3.83%
node 17 (51.5^0N,43^0 W)	138.97	5.79	4.06%
node 18 (50^0N,46^0 W)	147.45	6.14	4.31%
node 19 (48.5^0N,49^0 W)	157.07	6.54	4.59%
node 20 (46.5^0N,52^0 W)	153.24	6.39	4.48%
node 21 (45.5^0N,55^0 W)	133.33	5.56	3.90%
node 22 (45^0N,58^0 W)	137.03	5.71	4.00%
node 23 (44^0N,61^0 W)	141.51	5.90	4.13%
node 24 (43^0N,64^0 W)	145.65	6.07	4.26%
node 25 (42^0N,67^0 W)	151.49	6.31	4.43%
node 26 (40.5^0N,70^0 W)	145.78	6.07	4.26%
node 27 (40.5^0N,73^0 W)	117.03	4.88	3.42%
Total	3422.86	142.62	100.0

7.2.3 Norms of unsafe response for ship and cargo

Direct "capsize" threshold

For the identification of the critical roll angle of the containership the same principle as in the previous application was applied. However, in this case the flooding angle was assumed to correspond to the least transverse inclination (with submerged volume preserved) at which the highest point of a hatch coaming is immersed. According to the drawings, hatch coamings rise 1.7 m above the deck. A rendered view of the hull (with some key deck structures) inclined to that angle is shown schematically in Figure 7.35. Hydrostatic calculations have produced that this angle should be 35^0. Bearing in mind that the angle of vanishing stability was determined at 52^0, the above flooding angle is much lower than the vanishing angle as well as than the

prescriptive absolute limit of 50^0 that appears in the weather criterion. Thus the critical roll angle to be used henceforth is 35^0.

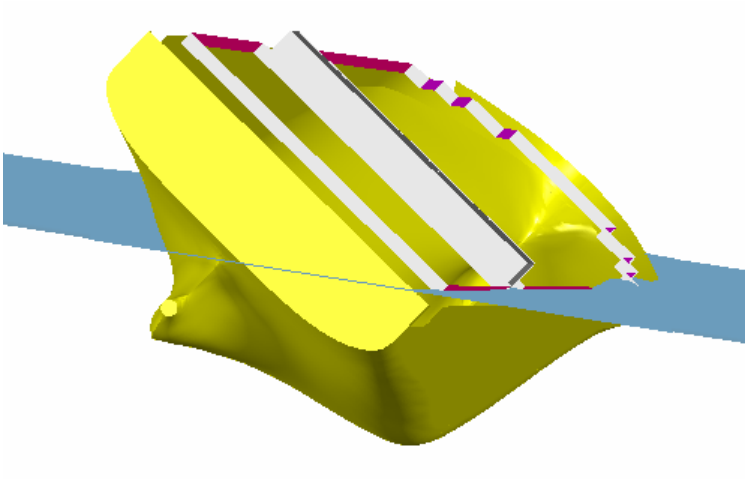

Figure 7.35: Critical heel angle for immersion of hatch coaming.

Shift- of-cargo threshold

In this case, the critical acceleration that could result in damage of the lashings of containers placed on the deck needs to be determined. This calculation was based on roll motion alone since this is known to be the dominant source of cargo excitation, although combined rolling and pitching might also lead sometimes to dangerous situations. The acceleration due to rolling motion has been estimated for tiers of 4, 5 and 6 TEUs placed on the deck. The relevant calculations have been carried out according to Cargo Securing Manual (DNV 2002b). Specifically, the capability of lashings' arrangement in terms of transverse sliding and tipping of the tier has been checked. The lashing arrangement is shown in Figure 7.36. In Table 7.7 have been collected the principal parameters that enter into the calculations. It is noted that the mass per unit of TEUs is in accordance to the Load Conditions and Intact Stability booklet of the ship and is consistent with the loading condition for the specified metacentric height. The most critical condition was identified to correspond to transverse sliding for a tier of 6 TEUs (Figure 7.37). The specific value of this critical acceleration was calculated as $a_y = 4.02$ m/s^2 .

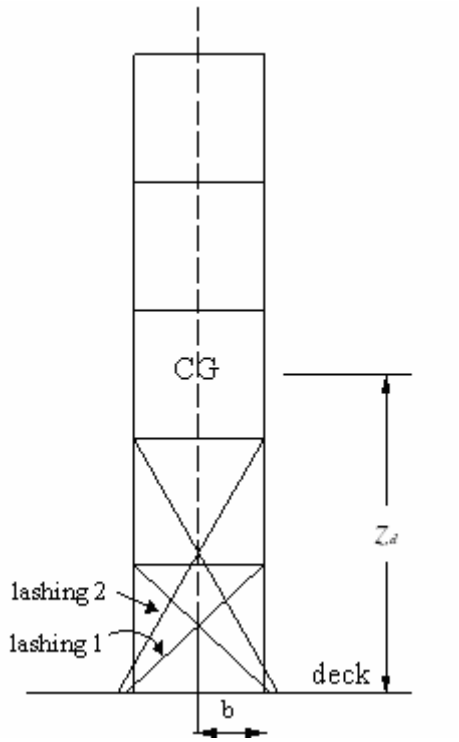

Figure 7.36: TEUs in a tier and lashing arrangement.

Table 7.7: Cargo and lashings characteristics.

Total number of TEUs: 5048	Total weight of TEUs: 51100t
Cargo mass: (4/5/6 TEUs in tier)	m = 40.49/ 50.61/ 60.74 t
Most severe position of trailer:	y=18.28 m z=24.3 m (from base line)
Centre of gravity above deck:	z_d = 4.88/ 6.10/ 7.32 m
lever-arm of tipping:	b = 1.219 m
Coefficient of friction:	Steel – steel: μ = 0.1
Lashing arrangement:	2 chains with MSL = 100 kN on each side, symmetrical vertical securing angle per lashing: 43°/60°

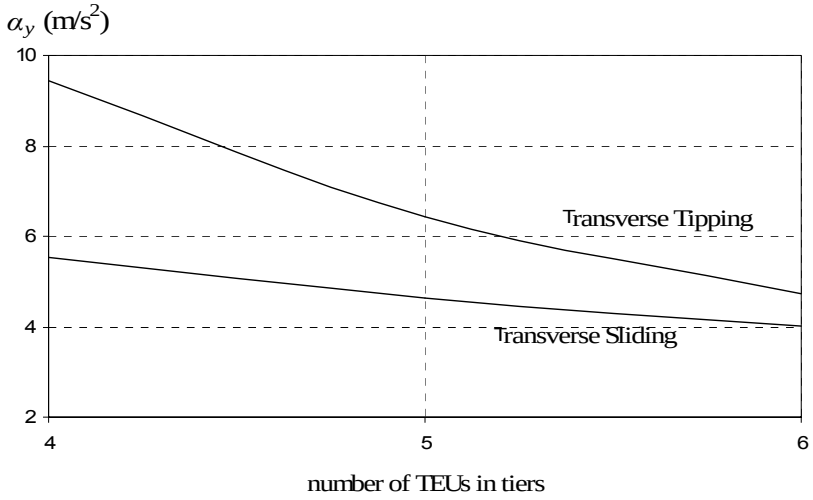

Figure 7.37: Critical transverse accelerations for sliding and tipping for three cases of cargo stowage.

7.2.4 Critical wave group characteristics identification

Critical wave groups have been specified for the following types of instability: beam-sea resonance, parametric rolling in longitudinal seas and pure-loss of stability. Their characteristics were found from numerical simulations, using the panel code SWAN2 (2002), which has been presented in the previous Chapter. Figure 7.38 shows characteristic 3D plots mesh generation of the containership, as obtained with SWAN2.

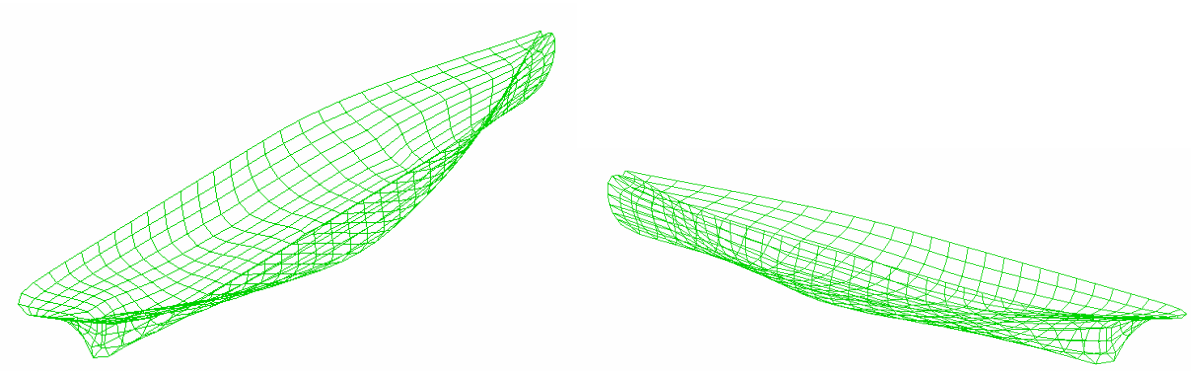

Figure 7.38: 3D plots mesh generation of containership by SWAN2.

Wave groups leading to beam seas resonance

To determine the critical combinations of wave height, period and group run length that could generate exceedence of a stability norm, deterministic numerical simulations have been carried out. The ship was assumed with no initial rolling. The practical range of wave periods that could be realised in the specific sea region has been spanned. Figure 7.39 presents a

rolling response to one of the identified as critical wave groups. Figure 7.40 and Figure 7.41 present the key characteristics of identified critical wave groups, referring respectively to ship and trailer responses. It should be reminded that no bilge keels have been considered, while nonlinear Froude-Krylov forces have been included in the calculation.

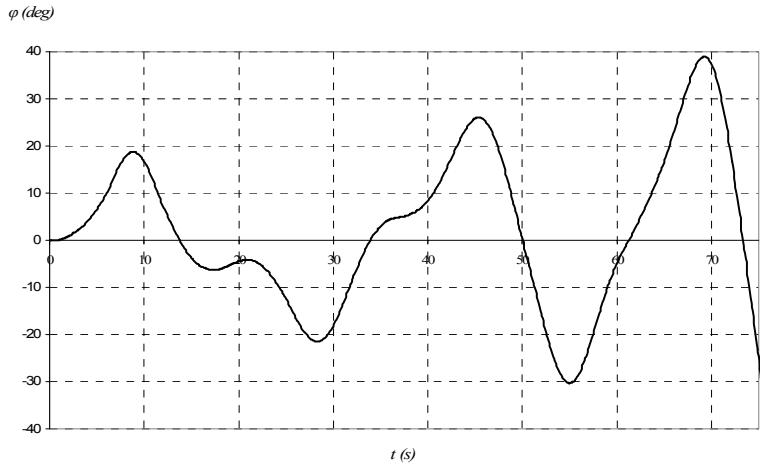

Figure 7.39: Response in beam waves for *T*=15.5 s and *H* =9.6 m.

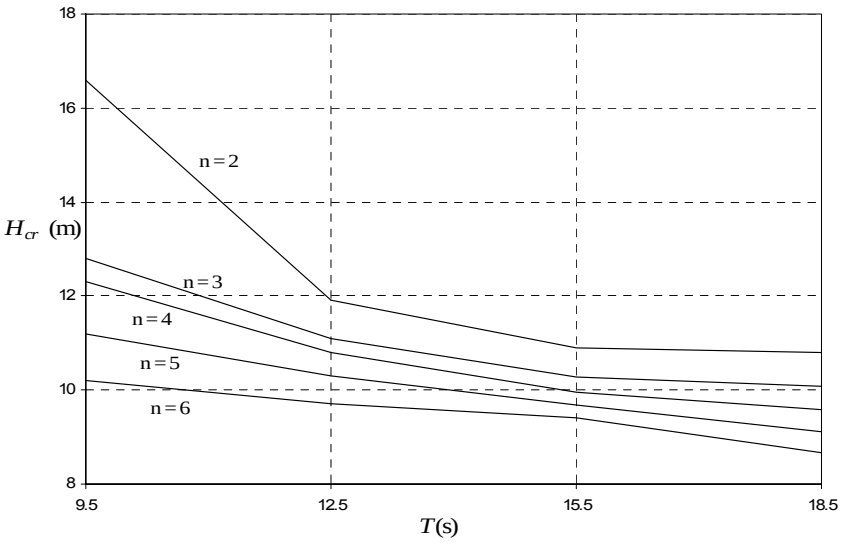

Figure 7.40: Critical wave groups of containership with reference to the limiting roll angle (ship).

Wave groups leading to head seas parametric rolling

For the assumed speed of $V_S = 24$ kn the ship could be prone to head-seas parametric rolling and specifically, the principal mode of parametric instability can be realised when the wavelength obtains values likes those shown in Figure 7.42. The required wavelengths are extremely long. An uncertain initial roll disturbance range was considered in order to realize

growth of roll amplitude, the same as in the previous assessment application. Up to a sequence of 8 wave encounters has been examined; because having more waves in a group is of truly negligible probability when the waves are high. The characteristics of critical wave groups were determined from repetitive numerical simulations, taking record whenever roll growth up to the critical norm was realised, within the allowed number of wave encounters. An example is shown in Figure 7.43. The variation of critical height and run length in the vicinity of exact principal resonance can be seen in Figure 7.44.

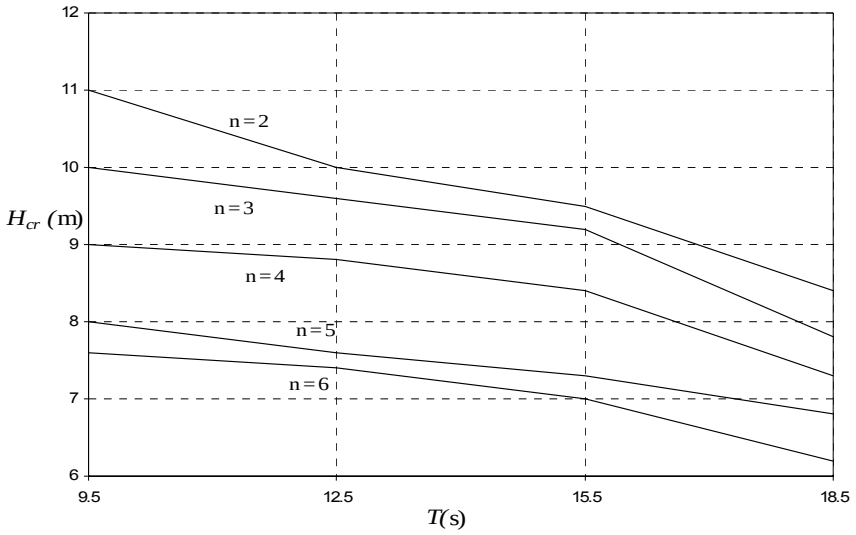

Figure 7.41: Critical wave groups of containership for the limiting transverse acceleration (cargo).

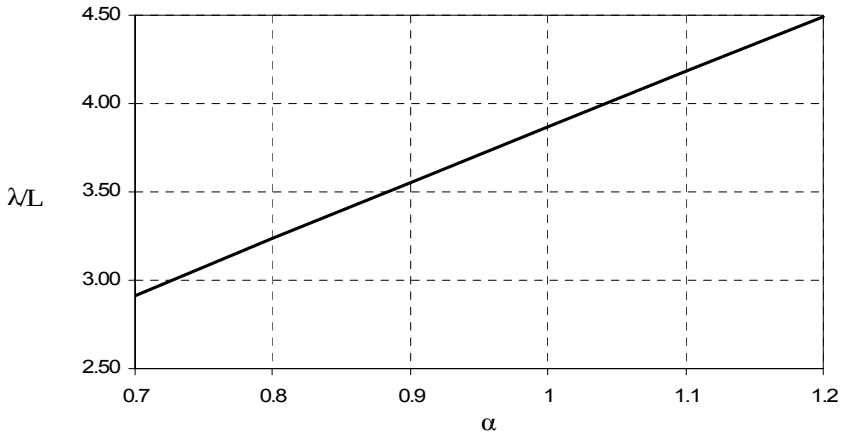

Figure 7.42: Critical wavelengths for head-seas parametric rolling (principal resonance).

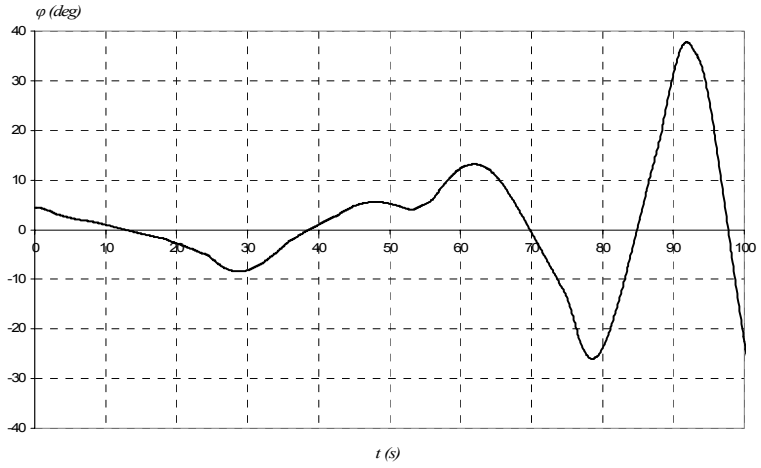

Figure 7.43: Parametric roll growth in head waves 80 % off principal resonance and for *H*=14 m.

Critical wave encounters for pure – loss of stability

As the panel code is not suitable for use at very low frequencies of encounter, the relevant analytical criterion of pure loss of stability was used. In Figure 7.45 is shown the calculated critical fluctuation of *GM*, h_{cr} for various values of λ/L. The respective critical wave heights were calculated taking into account the restoring variation on the waves using Maxsurf 11. However their values were extremely high and so had very small probability to be met.

7.2.5 Calculation of probability of instability per mode and total probability

Following the same procedure as in the previous application the calculation of probabilities and respective critical time ratios has been performed. The JONSWAP spectrum has been assumed again in order to expedite the calculation procedure, while for head seas parametric rolling a range of speeds $\pm 5\%$ around the service speed $(V_S = 24 \text{ kn})$ has been considered. The same as in the previous application probabilistic distributions for initial conditions ranges were assumed. Taking also into account the percentage of exposure to beam, head and following seas for the complete voyage (Figure 7.46), in Figure 7.47 and Figure 7.48 are overlaid the three obtained "critical time ratio" curves, for the ship and her cargo respectively. In Table 7.8 are presented the total probabilities and critical time ratios for the complete voyage.

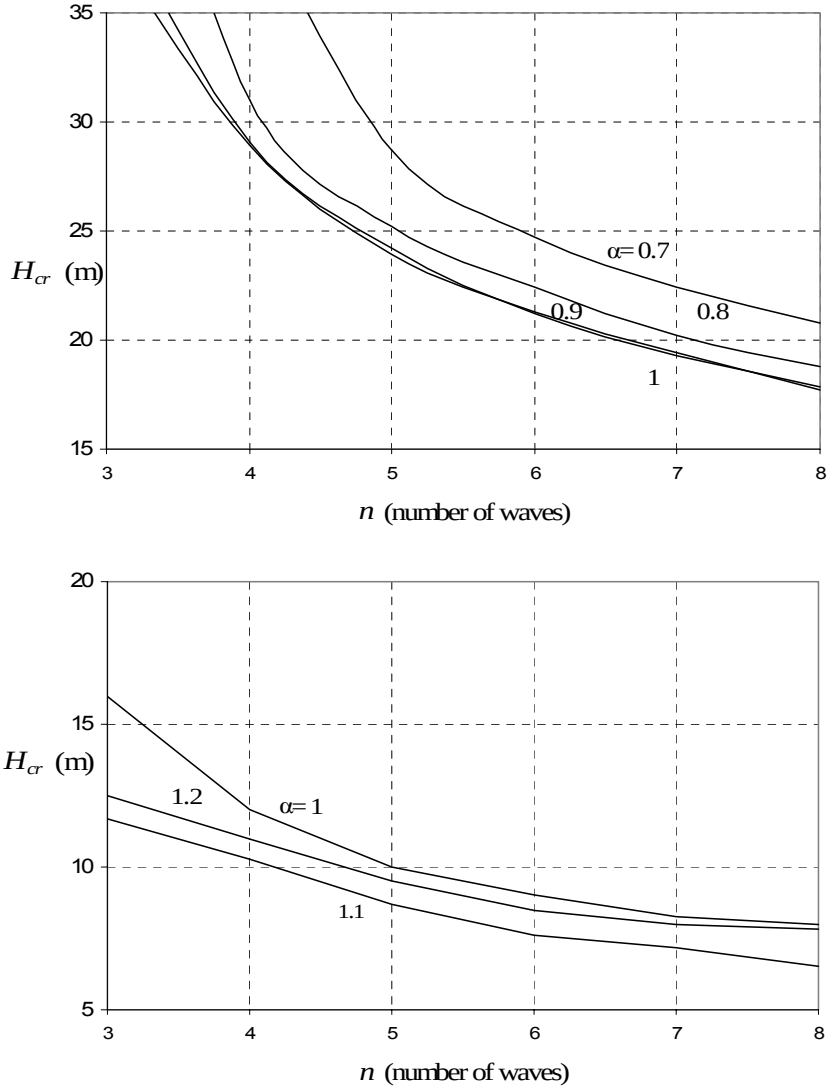

Figure 7.44: Required wave height for reaching the critical roll angle from an initial roll disturbance "around" 4.5^0.

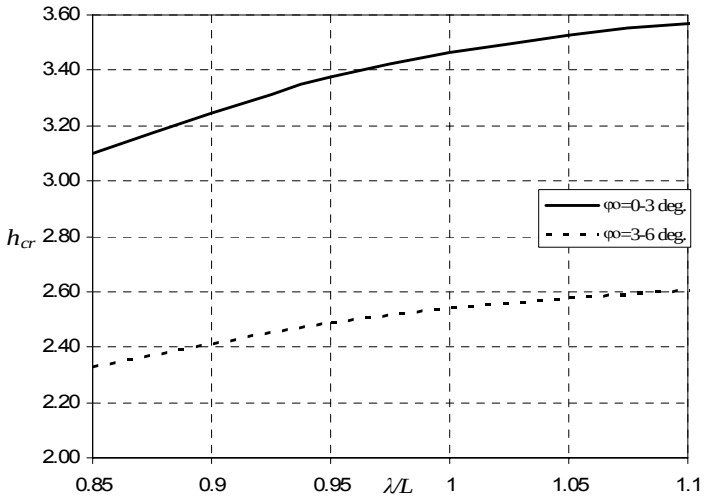

Figure 7.45: Critical values of h for pure-loss-of-stability.

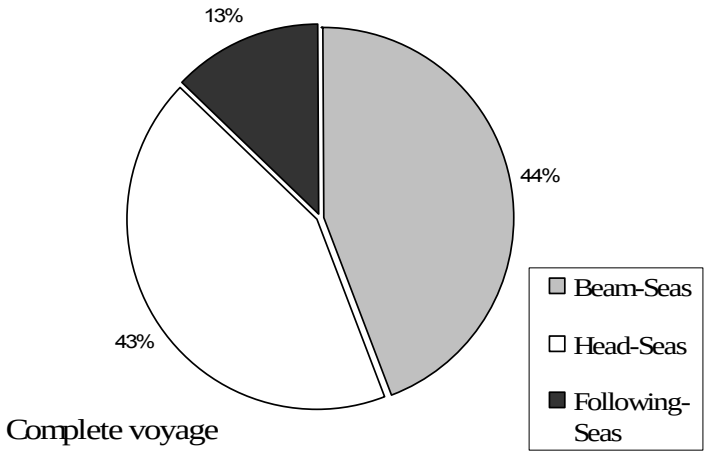

Figure 7.46: Percentage of time in beam, head and following seas.

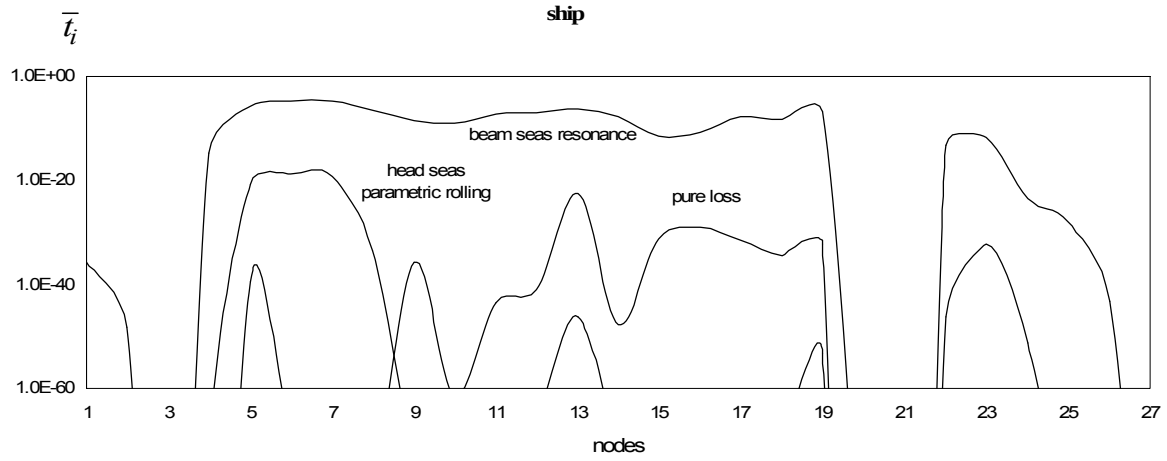

Figure 7.47: Collective view of "critical time ratio" diagrams for the ship norm.

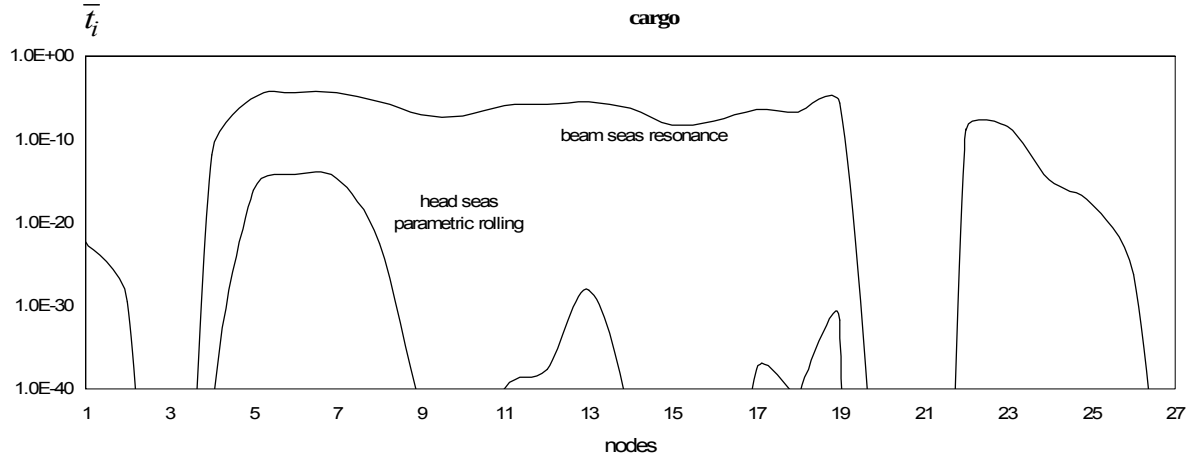

Figure 7.48: Collective view of "critical time ratio" diagrams for the cargo norm.

Table 7.8: Summed probability and associated critical time ratio for entire journey.

	P_i	$\overline{t_i}$
Ship: ($\varphi > 35^0$)	3.33 x 10^{-4}	3.95 x 10^{-5}
Cargo: ($a_y > 4$ m/s^2)	9.38 x 10^{-4}	1.11 x 10^{-4}

As in the previous application an example of the calculation of the probability of "instability" with reference to a specific part of the route is presented. Take for example the part covered by the area of node 5 whereabouts the time spent is 3.83 hr. The sea state is characterized by $H_S = 7.6m$ and $T_P = 16.4\ s$. The probability of critical waves for that node and for cargo shifting is 7.23 x 10^{-5}. For the assumed speed, the average zero upcrossing encounter wave period is 12.66 s and the number of waves encountered by the ship should be $13777(\mathrm{s})/12.66(\mathrm{s}) = 1089$. Hence the probability of instability for this time of exposure should be 7.88% which is quite a high value (one recalls here of course that the bilge-keels were not considered, which would reduce this number substantially).

Chapter 8:

Further studies

In this Chapter three studies which treat different aspects of the methodology will be presented. In the previous section two "practical" applications of the assessment have been demonstrated, which however include the basic calculation steps of the methodology. In this section, emphasis will be given in the technical points of the assessment.

The first study concerns the effect of weather conditions and specifically that of significant wave height H_S and wave peak period T_P on the probability to encountering the critical wave groups. The analysis will concentrate on a single instability mode; head seas parametric rolling, whereas relevant calculations for the characteristics of wave groups will be relied upon the analytical criterion. Different scenarios of wave parameters will be examined in a systematic way intending to check the method's sensitivity to these variations.

The next section regards a comparison study between two different calculation tools for the identification of critical wave groups; the numerical code SWAN2 and the analytical formula for parametric rolling, aiming in investigating their capability predictions in the critical wave events than incur parametric rolling. Possible discrepancies in the targeted estimation parameters will be reflected on the probabilities figures for a realistic seaway scenario.

Finally, a preliminary, yet systematic study based on a first principles approach, for the effect of different initial conditions on the calculated probabilities will be presented. This issue constitutes a technical aspect of the assessment in the task of specifying the characteristics of critical wave groups and presents special interest as this study intends to understand and examine how significant is the role of a set of initial conditions and how could be connected with the prevailed weather conditions.

8.1 Influence of weather parameters on the occurrence of head seas parametric rolling of a post panamax containership

The examined ship is a post- panamax containership (Figure 8.1). Her particulars are collected in Table 8.1. This ship had been known to exhibit parametric instability in head seas and at low speed while has been used as a reference ship in relative studies in ITTC. The

objective of this study, as it was mentioned, is to test the capability of the method to account realistically the severity of the environment in the calculation of the probability of instability. Taking as basis "North Atlantic" conditions of navigation, parametric studies will be performed for a range of significant wave heights H_S and peak periods T_P. These will be assumed to represent uniformly the wave environment. No specific route will be defined. The calculation tool selected for this study is the analytical criterion for parametric rolling.

Figure 8.1: Hull form of the examined containership, extracted by Maxsurf 11.

Table 8.1: Ship particulars.

L_{BP} (length)	288.87 m	Δ (displacement)	113,956 t
B (beam)	42.80 m	To (natural roll period)	30.26 s
D (depth, upper deck)	24.40 m	KG (vertical position of the center of gravity above keel)	18.83 m
T_d (mean draught)	14.00 m	GM (metacentric height)	1.08 m

No probabilistic treatment of the selected values of H_S and T_P has been considered, for example they could have been obtained by means of weather forecasting. Thus their values are taken as certain (probability equal to 1.0). A roll angle of 15^0 has been specified as the value whose exceedence should be avoided, a value that could connected as a warning level according to the proposed procedure (Chapter 4). Furthermore, as this angle is not set too high, the strengths of the analytical criterion used are exploited as the parametric amplitude variation h arises from the variation of GM. Critical values of h_{cr} that could provoke such roll motion within a limited number of wave cycles have been calculated for a range of initial angular disturbances ($\varphi_0 = 0^0$ - 6^0). A 2^0 discretization step and 50%, 30% and 20% probabilities for the first, second and third range respectively have been assumed.

Furthermore, rather than a single speed, a range of speeds $V_S \in [0,8]$ kn has been considered,

due to its effect on the encounter frequency which is a probabilistic quantity. To reduce the number of calculations, two equal sub-ranges were assumed; with 60% probability of occurrence for the first sub-range and 40% for the second. Here, it should be mentioned that a connection between the sustained ship speed and the encountered weather conditions based on estimations of involuntary speed loss due to "bad weather" could be implemented in the approach, leading to a more rational probabilistic distribution of ship speed.

The ship has been examined without bilge keels and the linear roll damping coefficient k, in fact the half dimensional damping divided by the roll moment of inertia plus the added moment, has been determined as $k = 0.0129\ s^{-1}$. This calculation has been carried out by the mathematical model of coupled roll motion (Chapter 6) using the viscous forces estimation methodology. An equivalent linear damping coefficient has been estimated around natural roll frequency, with no forward speed, which is subsequently introduced into the analytical criterion. As the speed effect was not taken into account in this calculation method, the roll damping coefficient that appears in the application of the analytical criterion is essentially a constant. At this point it has to be noticed that when using the analytical criterion for parametric rolling, a constant damping coefficient has to be assumed otherwise Mathieu equation can not be solved analytically.

The intensity of variation of the containership's restoring in waves can be assessed from Figure 8.2 where calculations based on Maxsurf 11 (Figure 8.3). In Figure 8.4 are presented the calculated critical wave amplitudes H_{cr} for the third sub-range of initial roll angles and the first sub-range of speeds. The calculation of probabilities relied again on the JONSWAP spectrum.

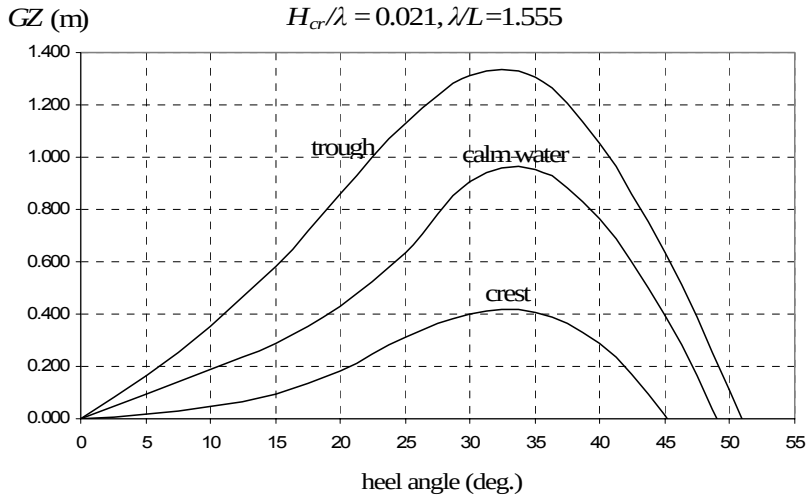

Figure 8.2: Variation of the *GZ* curve on a characteristic steep wave.

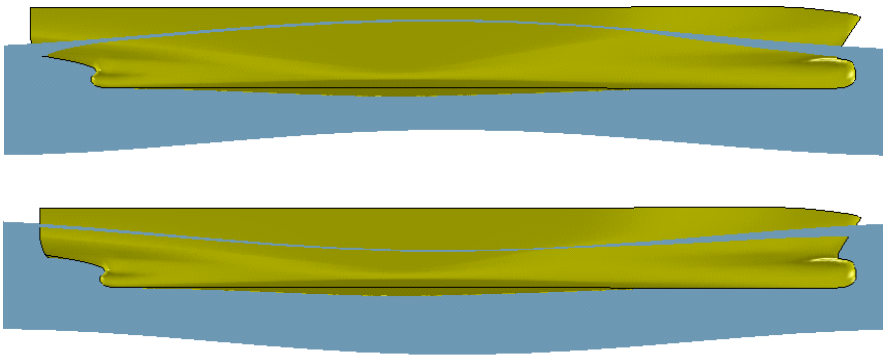

Figure 8.3: Characteristic variation of the wetted part of the hull in a wave.

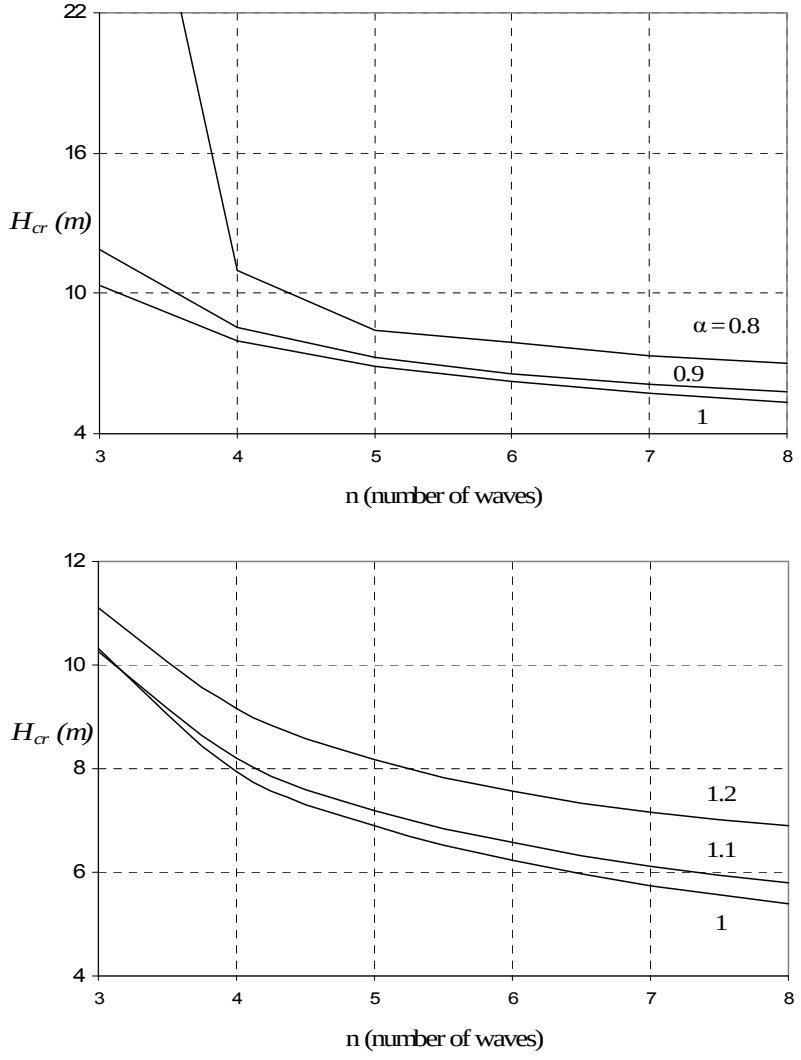

Figure 8.4: Required wave height for reaching the critical roll angle (initial roll angle in range $\varphi_0 = 4^0$ - 6^0 and speed in range $V_S = 0 - 4$ kn).

The principal results of this investigation are summarized in Figure 8.5 and Figure 8.6. As the peak period of the spectrum is shifted to higher values, the probability of occurrence of parametric rolling that exceeds the prescribed amplitude is increased. Nearer to the limit of realistic wave periods this trend is weakened. In general, realistic conditions are encountered where the probability of parametric rolling approaches the level of 10^{-5}. As for the dependence on significant wave height, once a certain threshold level has been exceeded (about 7 m), the probability increases slowly with the wave height. This is explained as follows: as soon as the containership is caught in the parametric rolling regime, she exhibits a tendency for large amplitude rolling (30^0 and above). In consequence, given such a realization, the prescribed roll amplitude is easily surpassed even for the lower (but above critical) wave heights.

Lastly, the probability of exhibiting instability for a fixed time of exposure to a severe sea state characterized by $H_S = 8$ m, $T_P = 16$ s, assuming that the containership encounters the waves always from the bow is estimated. The ensuing probability of critical waves is 9 x 10^{-6}. Assuming a mean ship speed of 4 kn, then the average zero upcrossing encounter wave period is 12.66 s and the number of waves encountered by the ship in one hour should be 3600 (s) / 12.66 (s) = 2.84 x 10^2. Hence the probability of instability for one hour of exposure should be 0.26 % which is a rather high value.

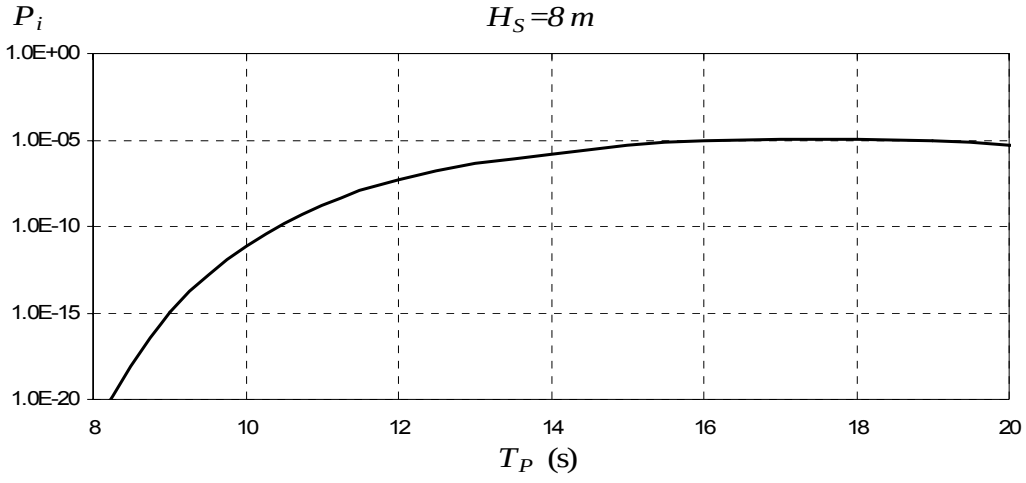

Figure 8.5: Probabilities as functions of T_p.

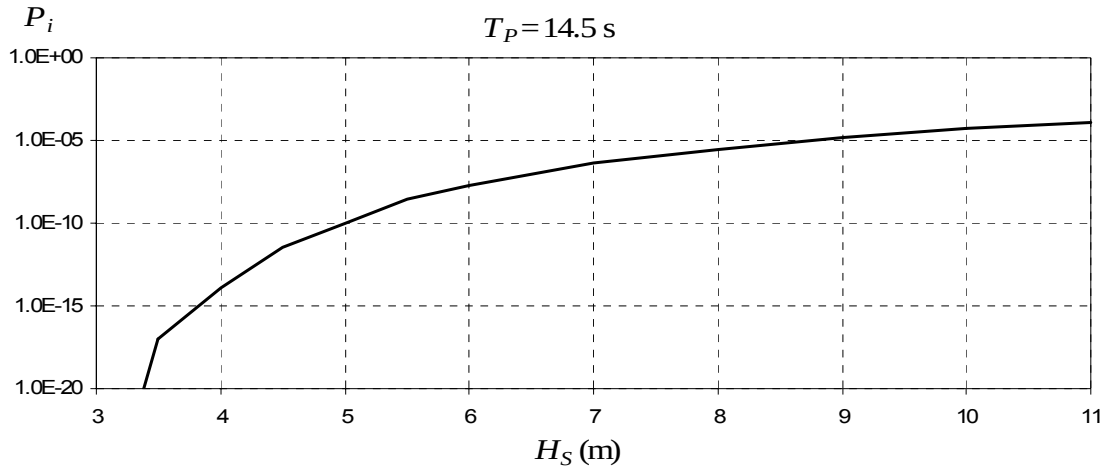

Figure 8.6: Probabilities as functions of H_s.

8.2 Comparative study of detailed and simplified model for parametric rolling

This study focus on a comparison of calculated capsize probabilities using, on the one hand, a simplified model of ship dynamics; and on the other, a detailed panel code, SWAN2. Parametric rolling has been set as the focal point of interest and the investigated ship was the same post - panamax containership of the previous study. Results of the study will regard firstly the differences in critical wave group predictions between the simplified and the detail model, and specifically in terms of the critical wave heights. Then, the effects of the findings of these two methods, in the probability of exhibiting parametric instability, are determined for a realistic sea scenario. Ship data have been inserted in SWAN2 (Figure 8.7).

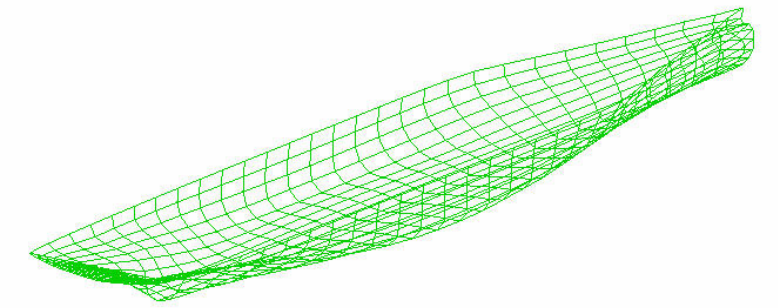

Figure 8.7: 3D plot mesh generation of containership by SWAN2.

8.2.1 Setting the parameters of the problem

Relative speeds for head seas parametric rolling

It was confirmed by both methods, and as shown by the previous study, that the ship is liable to head seas parametric rolling at the low speed range. In Figure 8.8 are shown the critical combinations of ship speed and wavelength where head-sea parametric rolling should be

observed when an exact tuning condition has been realised (in mathematical terms when $a = 4\omega_0^2 / \omega_e^2 = 1$). However, critical combinations of speed and wavelength covering a broad range around $a = 1$ will be taken into account as in the previous study.

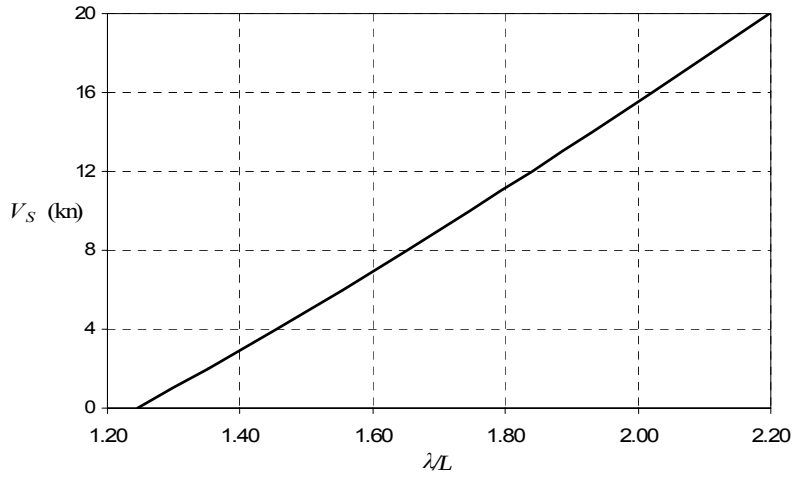

Figure 8.8: Critical combinations of speed and wavelength for head seas paramedic rolling ($a = 1$).

Estimation of roll damping

Roll damping plays an important role for the growth of parametric rolling and, as a matter of fact, in the specification of critical wave groups. In the analytical criterion the linear roll damping coefficient has the same value as in the previous study. On the other hand, numerical decay tests at various speeds have been carried out with SWAN2. Roll damping calculation in SWAN2 follows the well-known method of Ikeda (1978) and Himeno (1981). Corrections due to forward ship speed are taken into account as lifting effects influence significantly roll damping (Sclavounos 1996). In Figure 8.9 and Figure 8.10 are shown two decay tests of the investigated containership; the first with no forward speed and the second with moderate speed. In Figure 8.11 is compared the calculated linear damping coefficient as function of speed, against the constant damping coefficient obtained from the alternative "in-house" method. The damping calculated by SWAN2 is always smaller, and approach the constant value only in the high speed range. Especially in low speeds the damping is excessively small.

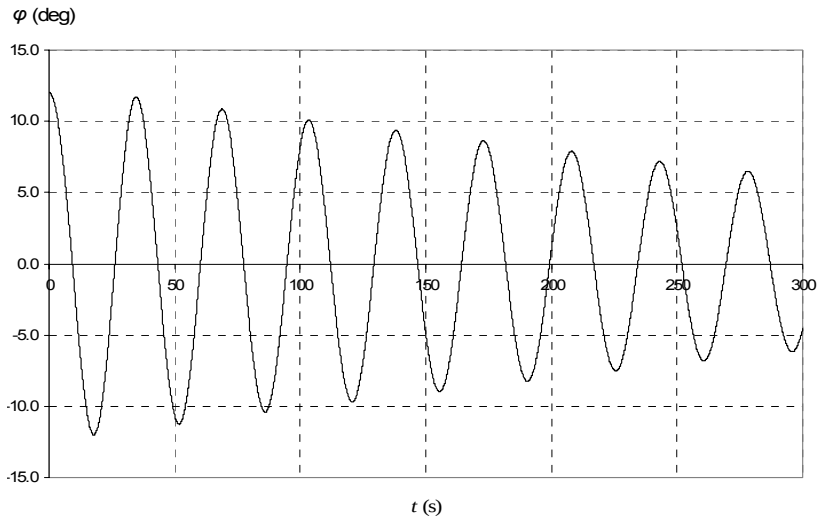

Figure 8.9: Roll decay with no forward speed.

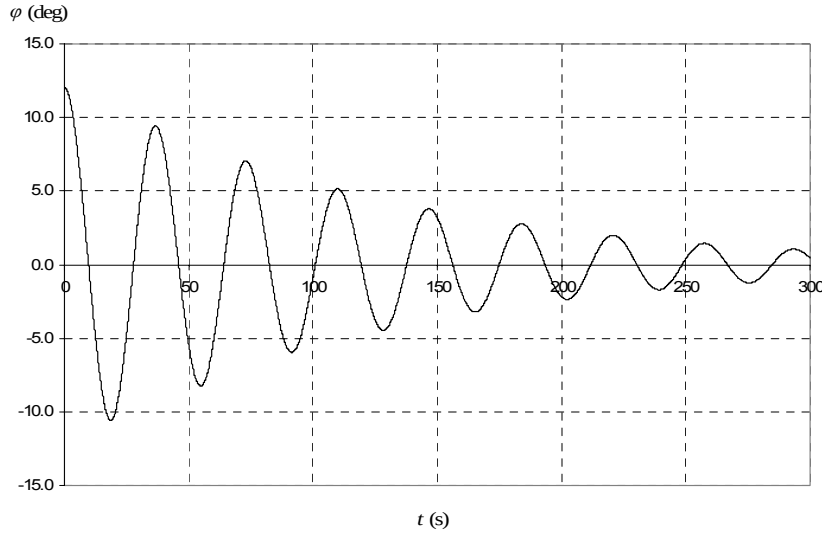

Figure 8.10: Roll decay with forward speed $V_S = 18$ kn.

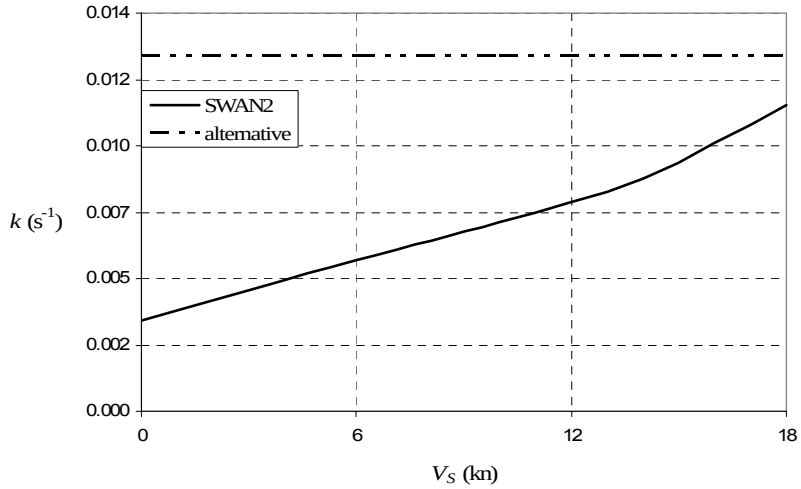

Figure 8.11: Comparison of damping coefficients at various speeds.

Specification of critical wave groups

To ensure that the analytical criterion is applicable with reasonable accuracy, a roll angle of 15^0 has been set as the limiting inclination whose exceedence should be avoided. An uncertain heel disturbance that is necessary for the growth of roll amplitude up to the specified limit is considered, distributed in the range $\varphi_0 = 0^0 - 6^0$. Similarly, a probabilistic speed distributed in the range $V_S = 0 - 20$ kn has been considered.

The analytical criterion has been used similarly with the previous study. In Figure 8.12 one observes the critical parametric amplitudes which correspond to $a = 1$, for three different initial conditions, each assumed to be the representative of a narrow range of initial roll angles. Critical wave heights have been specified by taking into account the geometry of the submerged hull. Thus the variation of restoring between wave crests and troughs needs to be calculated for a range of wavelengths that are near to satisfying the condition $a = 1$, producing similar results as those of Figure 8.2.

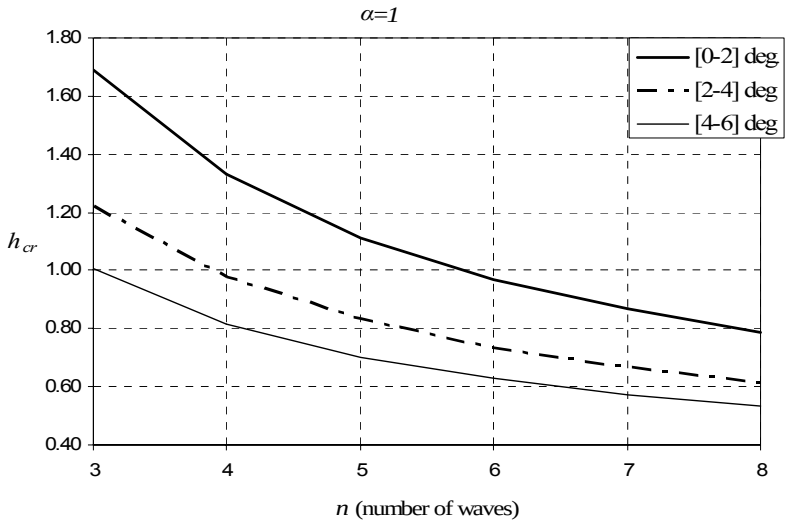

Figure 8.12: Critical parametric amplitudes for $a = 1$.

On the other hand, critical wave group characteristics are identified on the basis of a campaign of numerical simulations, with occasional recording of the occurrence of growth of the roll amplitude up to 15^0 within the allowed number of wave encounters. Nonlinear Froude-Krylov force calculation mode was selected. As manifested by the characteristic time-histories shown in Figure 8.13 to Figure 8.15 referring to the principal instability regime, SWAN2 can capture parametric rolling.

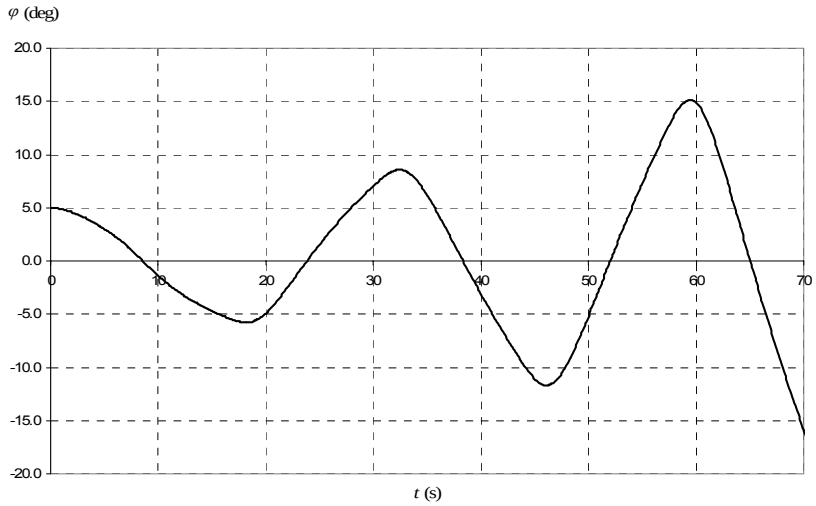

Figure 8.13: Roll response in head waves ($a = 0.8$, $H = 9.9$ m).

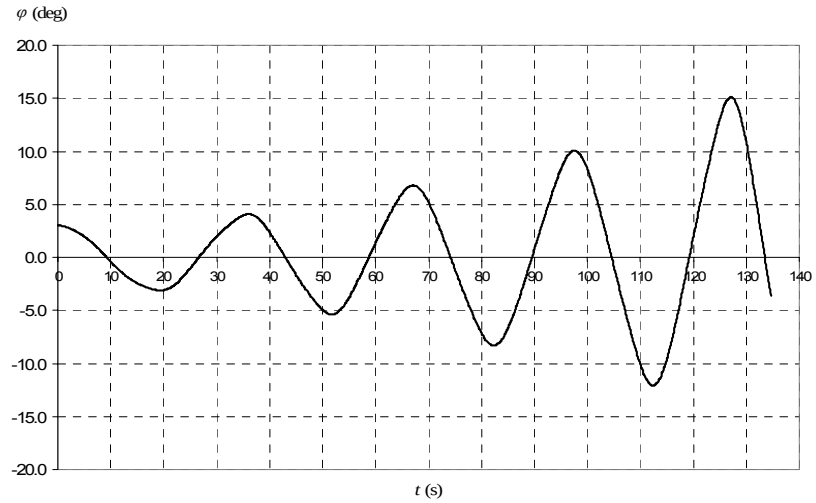

Figure 8.14: Roll response in head waves ($a = 1$, $H = 7$ m).

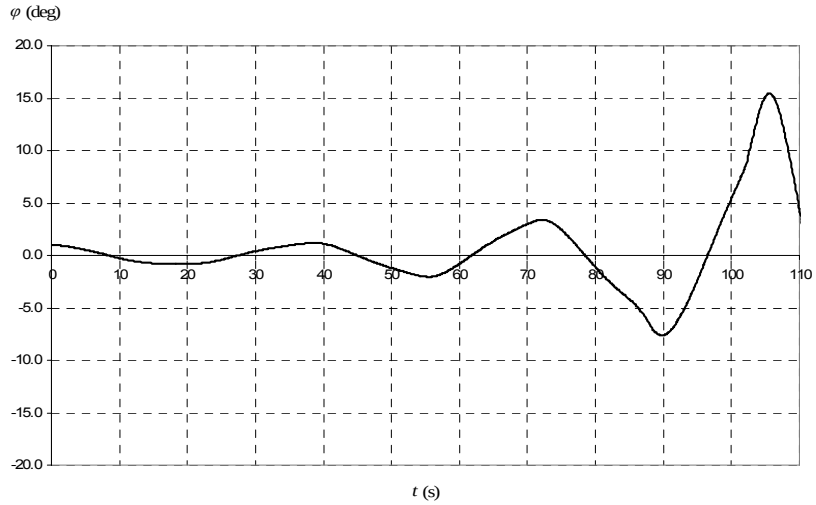

Figure 8.15: Roll response in head waves ($a = 1.2$, $H = 10.4$ m).

8.2.2 Comparison of critical waves

The comparison between analytical and numerical predictions was focused on differences of wave height with all other parameters kept identical. The critical wave heights as calculated by the two prediction techniques are illustrated in Figure 8.16.

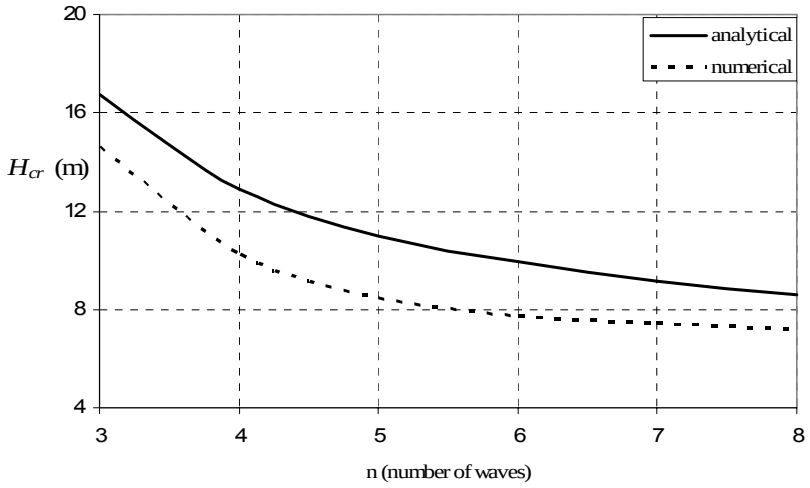

Figure 8.16: Critical wave height as function of run length ($a = 1$, $V_S = 14$ kn , $\varphi_0 = 5^0$).

Critical wave heights, as calculated by the two prediction techniques that generate a 5-fold increase in roll amplitude within $n = 3, 4, ..., 8$ wave encounters have been compared for various speeds. The results are shown in Figure 8.17 to Figure 8.22, varying from one figure to the next the wave group run length n. A trend of wave height increase is noted as the speed is raised, that follows a similar pattern for both prediction methods. In the case of the SWAN2 simulations one could also notice that, despite its increase with speed, roll damping does not seem to affect substantially the critical wave heights. Therefore, the augmentative trend in wave height should be attributed mainly to an increase of the required wavelength; in its turn owed to the higher speed required for achieving frequency tuning at $a = 1$.

An alternative option is to fix the speed, determine those wavelengths that are eligible to incur head-seas parametric rolling when a obtains a value around 1, and then determine the critical wave heights according to the wave group run length. Such diagrams are collected in the set of Figure 8.23 to Figure 8.27, covering a wide range of speeds.

In all cases wave heights estimated by the code proved to be lower without noticing any change in the difference trend regarding the ship's speed and especially in the high speeds where damping was closer to that of analytical method. This could reflect the effect of pitch and heave motions in a way aggravating the effect of restoring variation. Reasonable

coincidence of predictions was found at frequency tuning about $a = 1.2$.

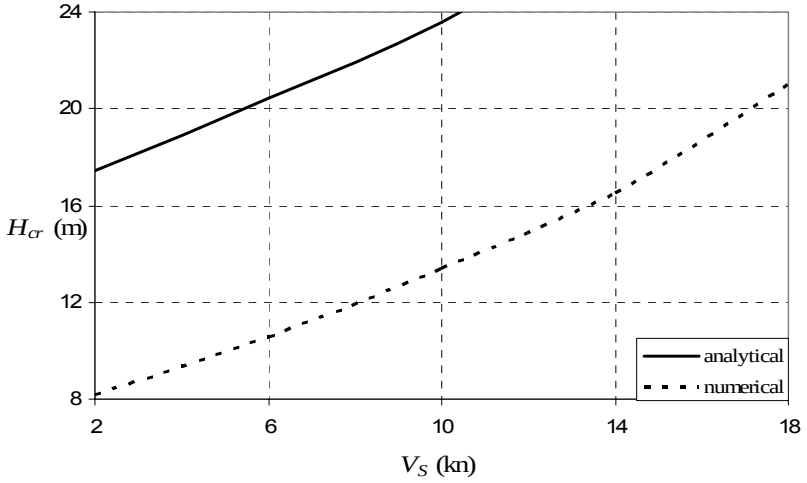

Figure 8.17: Critical wave height as function of speed ($a = 1,\ q = 5$ and $n = 3$ wave encounters).

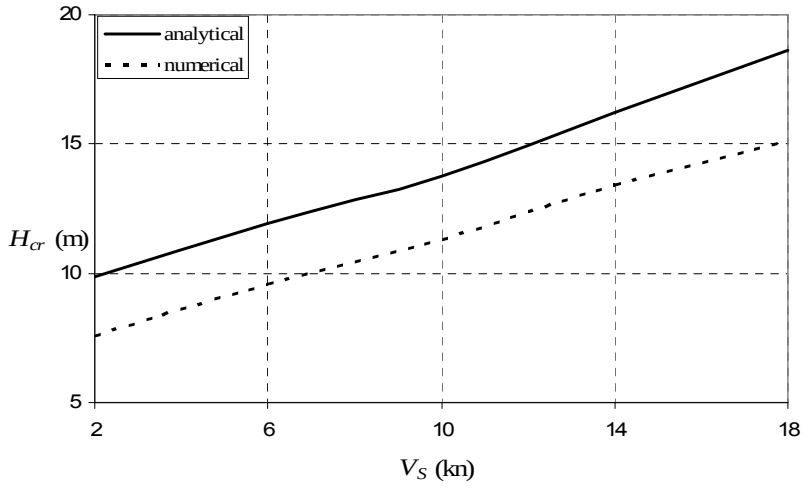

Figure 8.18: Critical wave heights ($a = 1,\ q = 5$ and $n = 4$).

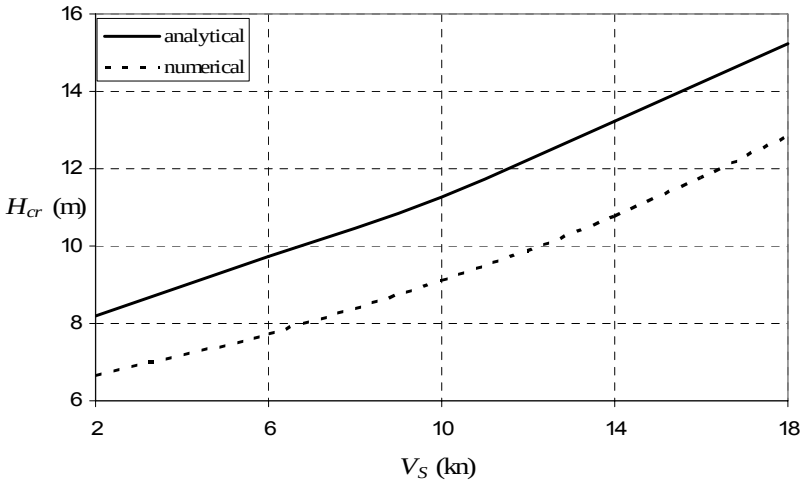

Figure 8.19: : Critical wave heights ($a = 1,\ q = 5$ and $n = 5$).

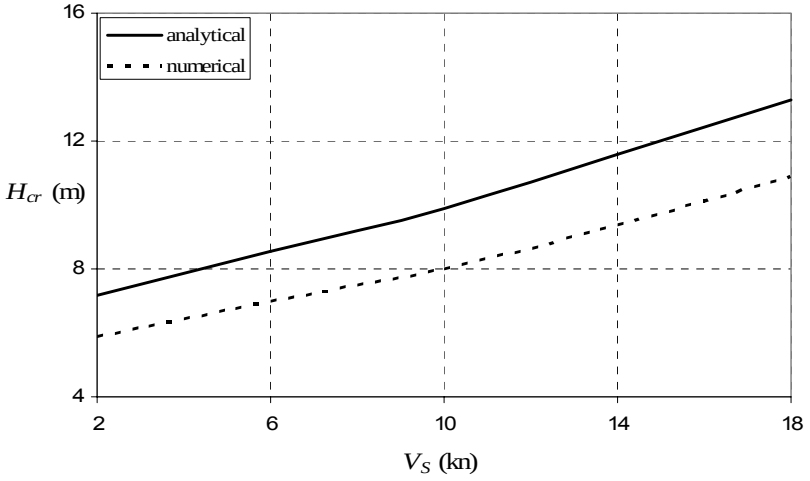

Figure 8.20: Critical wave heights ($a = 1,\ \ q = 5$ and $n = 6$).

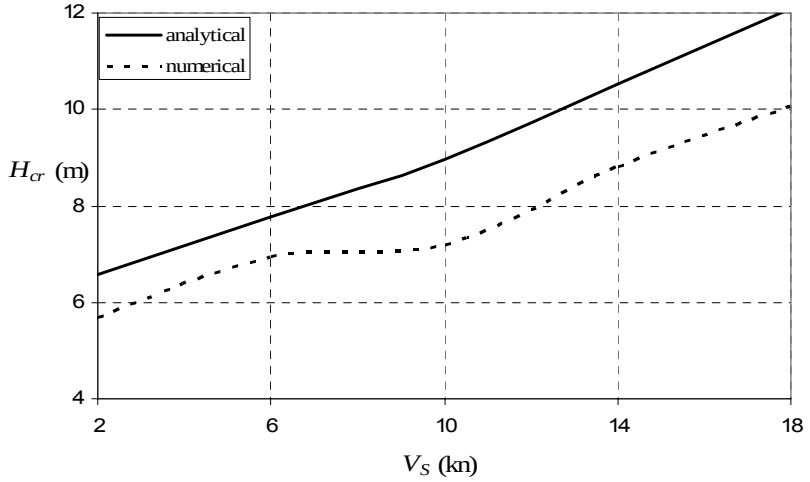

Figure 8.21: Critical wave heights ($a = 1,\ \ q = 5$ and $n = 7$).

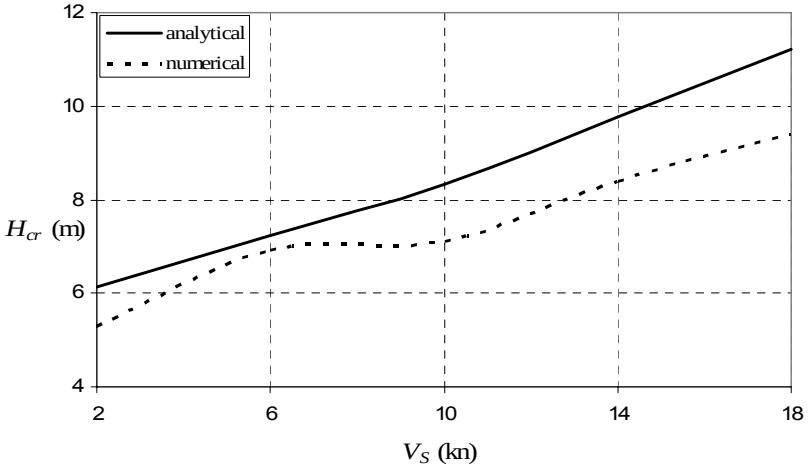

Figure 8.22: Critical wave heights for ($a = 1,\ \ q = 5$ and $n = 8$).

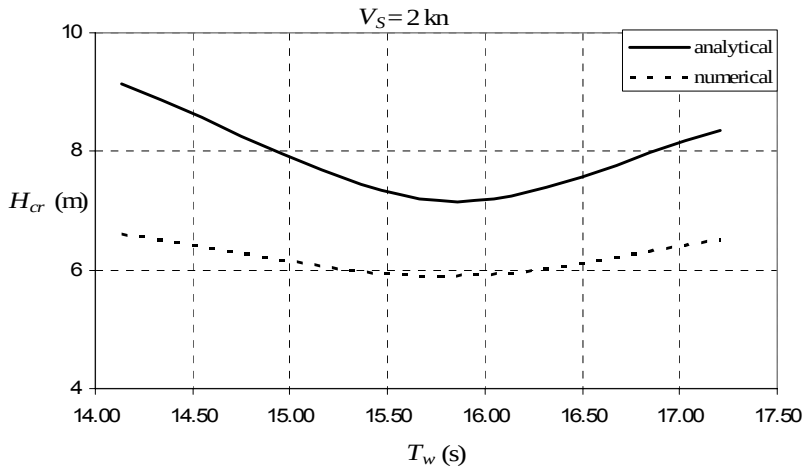

Figure 8.23: Critical wave height as function of wave period ($q = 5$, $V_S = 2$ kn and $n = 6$).

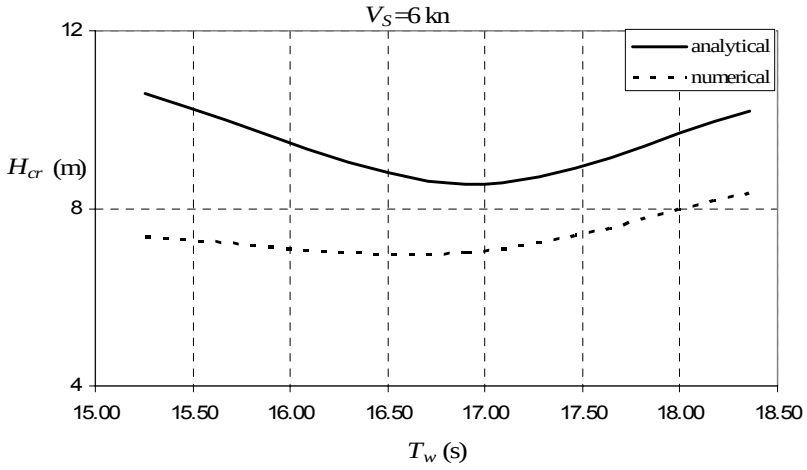

Figure 8.24: Critical wave heights ($q = 5$, $V_S = 6$ kn and $n = 6$).

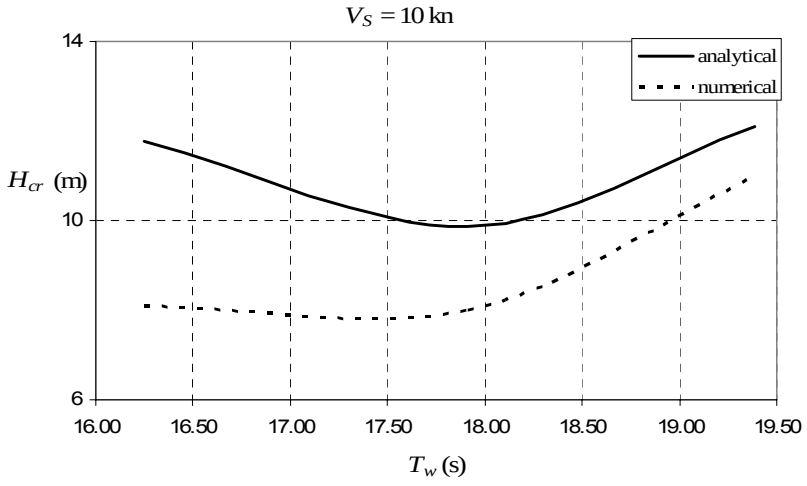

Figure 8.25: Critical wave heights ($q = 5$, $V_S = 10$ kn and $n = 6$).

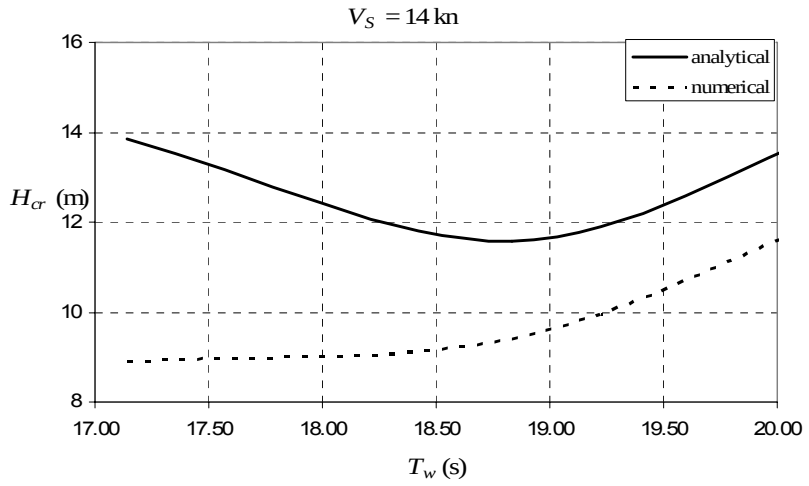

Figure 8.26: Critical wave heights ($q = 5$, $V_S = 14$ kn and $n = 6$).

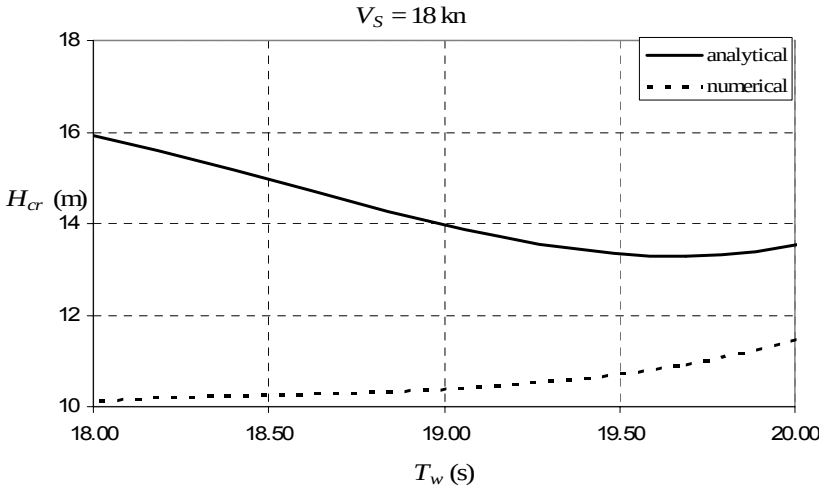

Figure 8.27: Critical wave heights ($q = 5$, $V_S = 18$ kn and $n = 6$).

8.2.3 Calculation of probabilities

In this part of the study, the probabilities to encounter the wave groups specified in the previous paragraphs, for a selected sea state, have been calculated. A sea state with $H_S = 7.6\ m$ and $T_P = 16.4$ s has been picked out of the set of results of a hindcast study which addressed the North Atlantic region (Behrens 2006). Such weather could have prevailed at location 59.5^0N - 7^0W, with a few hours duration on January 14th, 1991. The JONSWAP spectrum was assumed in order to expedite the calculation procedure.

The obtained probability values are illustrated in Figure 8.28 as functions of speed. Concerning initial condition, an assumption was made of some uncertain heel disturbance

with the following distribution: 50% to lie within $0^0 - 2^0$, 30% in $2^0 - 4^0$ and 20% in $4^0 - 6^0$. Lastly, the overall probability values are shown in Table 8.2. To this, the speed was treated as a probabilistic parameter obtaining values in the range 0 – 20 kn. Five successive sub-ranges with length 4 kn were then considered and probabilities were uniformly distributed.

Table 8.2: Total probabilities.

Analytical criterion	1.054×10^{-6}
Numerical simulations	3.159×10^{-5}

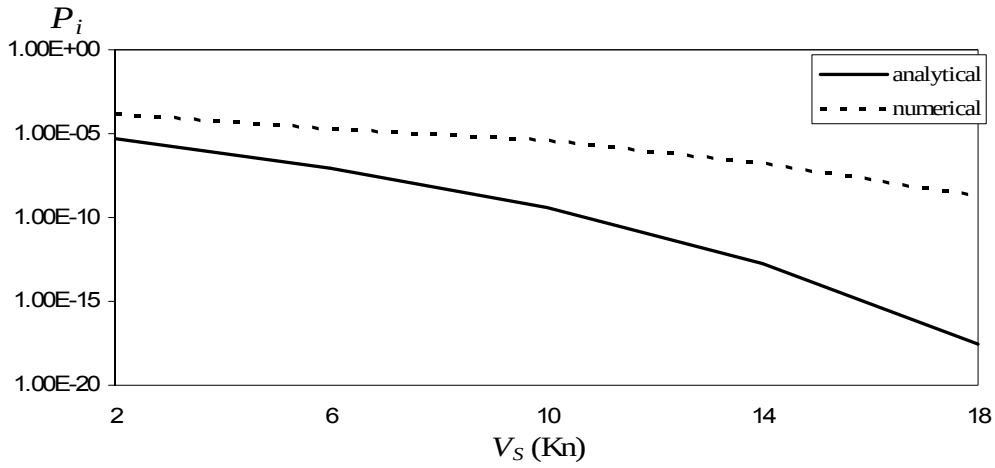

Figure 8.28: Probabilities of encountering the critical wave groups in terms of ship speed.

8.3 Effect of initial state of ship at the moment of wave encounter

As it was mentioned in the introduction of this Chapter, at this stage some issues are discussed concerning the effect of initial conditions on the calculated probability figures, on the basis of a first-principles approach. As becomes obvious, a significant element of the current methodology is the identification of the complete set of critical wave groups by numerical or analytical techniques. Whichever method is selected however, an initial state of the system should be assumed because the assessment is based on transient response. The simplest scenario of course is to assume that the ship is initially upright with zero roll velocity and in vertical equilibrium condition when approached by the wave group. This idea has some

background from ship roll dynamics investigations as it was stated in Chapter 4 (Rainey and Thomson 1991). At this point it should be noticed that for non direct excited modes as parametric rolling in longitudinal seas, an initial roll disturbance is necessary in order rolling motion to occur and in the relevant applications range of initial angles has been considered. Here the study targets mainly the directly excited modes, such as beam seas resonance.

However, a question could be raised whether the assumption of upright initial state is really critical for the deduced probability figure; in which case, one should better treat as probabilistic quantity the initial state, integrating it thereafter with the subsequent calculation of the probability of exceedence of the stability norm. Apparently, the probability is connected to the prevailed weather. Better understanding of the role of initial conditions in the calculation of the probability of instability would be very enlightening.

8.3.1 Setting up the problem and methodology

As any given state $\boldsymbol{\varphi}_0 = \left[\varphi(t_0), \dot{\varphi}(t_0)\right]^{\mathrm{T}}$ of a dynamical system can be regarded as initial condition for any state $\boldsymbol{\varphi}_i$ that belongs to $\boldsymbol{\varphi}_0$'s later time evolution, a system's safe basin could be realistically taken as the appropriate continuum of initial conditions that should be targeted for probabilistic treatment. Given a ship and a sea state, one could sensibly assume that each infinitesimal subregion dA within it could be associated with a probability of being "visited" at the moment when the wave group excitation is applied. Lets then define the encounter of wave group with the condition of being at the trough of the first wave.

Lines of constant potential-plus-kinematic energy of a simple freely oscillating undamped nonlinear oscillator are shown in Figure 8.29. As known, these are approximately cyclic at small energy levels (i.e. linear dynamics), they become elliptic for higher energy. To simplify the calculation process, lets in the first instance confined within linear oscillator dynamics using standard symbols (k is the half dimensionless damping ratio and ω_0 is natural roll frequency):

$$\ddot{\varphi} + 2k\dot{\varphi} + \omega_0^2 \varphi = f \sin(\omega\tau) \tag{8.1}$$

Of course a linear oscillator does not present a basin boundary. However, one could consider, instead, lines of constant energy. A grid of initial conditions may then be created, up to the energy level represented by inclination φ_{cr} that has been identified as critical (Figure 8.30).

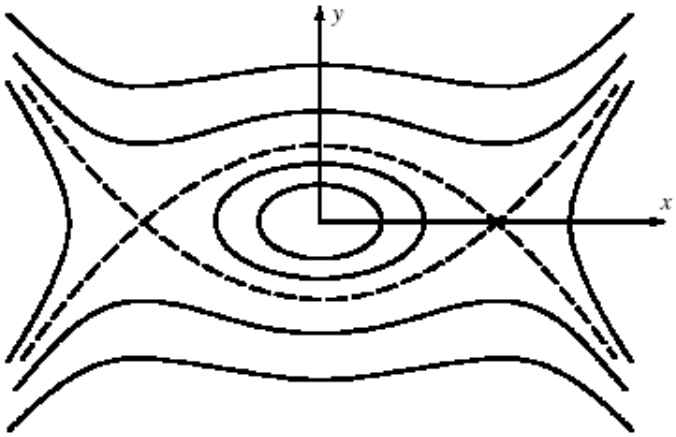

Figure 8.29: Schematic phase-plane trajectories and basin boundary of conservative nonlinear oscillator (taken from Jiang et al. 2000).

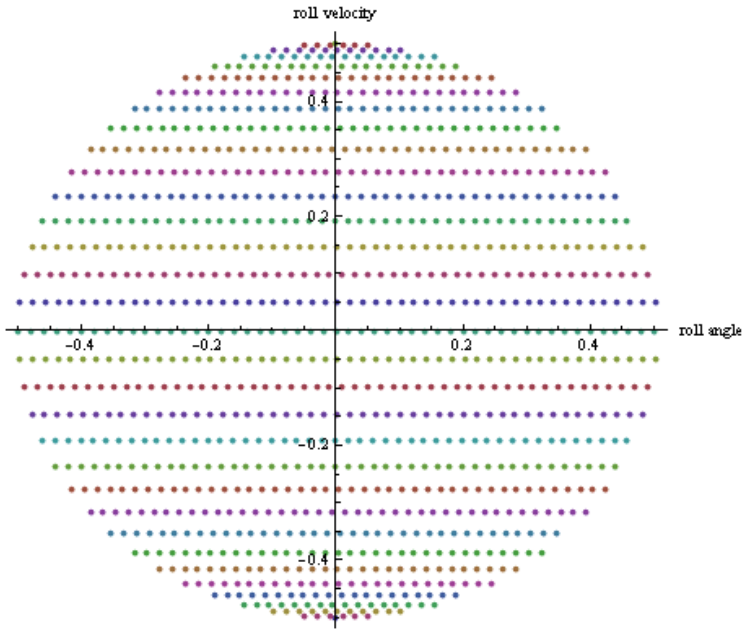

Figure 8.30: Grid of initial conditions.

For each initial state, i.e. a point of the grid, the critical forcing f_{cr} can be calculated analytically from eq. (8.1), using as parameter the considered number n of cycles of periodic excitation. Then, given the assumption of a "Gaussian sea", the probability $P\left(C_{ij}\middle|\boldsymbol{\varphi}_{ij}\right)$ to encounter these wave groups for some wave spectrum S_ζ (represented by H_S and T_P) is straightforward according to the current methodology.

In the ensuing step the probabilistic treatment of initial conditions is introduced. Problems of this kind are not dealt with for the first time; see for example McCue and Troesch (2005). The basic idea is to split the problem in two; the first is governed by the stochastic linear process

and the second the process excited by the wave group. The first one will serve as initial input to the second; therefore it will deduce the probabilistic initial state of the ship when the wave group approaches her, while from the second process the probability of encountering the critical wave group excitation can be estimated.

So, according to the current problem setup, in principle a multivariate pdf of $\varphi(t_0)$, $\dot{\varphi}(t_0)$ is required taking into account the condition that defines wave group's encounter. For example, seek the distribution of roll's initial conditions at the trough before meeting the wave group, $p\left(\varphi,\dot{\varphi}\middle|\dot{\zeta}=0,\ddot{\zeta}>0\right)$. In the next section an analysis of how such a pdf can be derived follows. In Appendix D, the case of a simple joint pdf of roll response $p(\varphi,\dot{\varphi})$ without the condition for the wave trough is considered, where under the assumption of stationary process, the roll angle and velocity are uncorrelated.

The probability for the initial roll angle and velocity to be found in the neighbourhood of state (i,j) is:

$$P\left(\varphi_{ij}\right)=\int_{\varphi_i}\int_{\dot{\varphi}_j} p_{\varphi\dot{\varphi}}\left(\varphi,\dot{\varphi}\right)d\varphi d\dot{\varphi} \tag{8.2}$$

Assuming independence, the total probability can be derived by multiplying the probabilities of wave groups $P\left(C_{ij}\middle|\varphi_{ij}\right)$ with the probability of the initial conditions $P\left(\varphi_{ij}\right)$ and then summing up:

$$P=\sum_i\sum_j P_{(i,j)}=\sum_i\sum_j P\left(C_{ij}\middle|\varphi_{ij}\right)P\left(\varphi_{ij}\right) \tag{8.3}$$

8.3.2 Conditional distribution of roll response on a wave trough

In this section the calculation of the probability density function of the roll angle and velocity response conditioned that the ship lies in a wave trough is presented. This pdf can be a multivariate function of roll angle, roll velocity and of the first two derivatives of wave elevation. Irregular waves are presented in a Fourier series form with a given spectrum resulting in a stationary and ergodic random process.

$$\zeta(t)=\sum_{i=1}^{N}\zeta_i\sin\left(\omega_i t+\delta_i\right) \tag{8.4}$$

where ζ_i is the amplitude of the i^{th} component of Fourier presentation which is calculated

from the spectrum and δ is the phase distributed uniformly in $[0,2\pi]$. Firstly, a linear rolling equation will be assumed

$$\ddot{\varphi}+2k\dot{\varphi}+\omega_0^2\varphi=\sum_{i=1}^{N}f_i\sin\left(\omega_i t+\varepsilon_i\right) \tag{8.5}$$

where f_i is the i^{th} component of wave excitation and ε_i is the phase of the i^{th} harmonic wave component with respect to the wave (in general it may be different from δ_i but here, due to the Froude – Krylov assumption they will be assumed as equal). Therefore:

$$f_i=\omega_0^2\frac{\omega_i^2}{g}\zeta_i \tag{8.6}$$

It is assumed that the joint pdf of $\left(\varphi,\dot{\varphi},\dot{\zeta},\ddot{\zeta}\right)$ can be represented by the multivariate Gaussian distribution, therefore the pdf of the initial ship state to lie in a wave trough will be derived setting the following conditions: $\dot{\zeta}=0$ and $\ddot{\zeta}\geq 0$.

Eq. 8.5 is a linear one, where excitation is represented by a finite Fourier series, therefore the solution of this linear system consists by the general solution of the homogeneous equation and the partial solution of the heterogeneous equation (e.g. Belenky and Sevastianov 2007). If we focus on the process described by the partial solution, in fact this represents the solution of the system after the transition has die out, it could be expressed in the same form as the excitation, thus as a Fourier series:

$$\varphi(t)=\sum_{i=1}^{N}\varphi_i\sin\left(\omega_i t+\beta_i+\varepsilon_i\right) \tag{8.7}$$

where from linear stochastic theory $\varphi_i=\dfrac{f_i}{\sqrt{\left(\omega_0^2-\omega_i^2\right)^2+4\omega_i^2k^2}}$ and $\beta_i=\arctan\left(\dfrac{2\omega_i k}{\omega_0^2-\omega_i^2}\right)$.

In other words, the assumed linear system handles each component of excitation separately.

The multivariate Gaussian of the four variables has the form:

$$f\left(\varphi,\dot{\varphi},\dot{\zeta},\ddot{\zeta}\right)=\frac{1}{(2\pi)^2\sqrt{|\mathbf{\Sigma}|}}\exp\left\{-0.5(\mathbf{x}-\mathbf{m})^T\mathbf{\Sigma}^{-1}(\mathbf{x}-\mathbf{m})\right\} \tag{8.8}$$

where $\mathbf{x}=\left(\varphi,\dot{\varphi},\dot{\zeta},\ddot{\zeta}\right)$, $\mathbf{m}=\left(m_{\phi},m_{\dot{\phi}},m_{\dot{\zeta}},m_{\ddot{\zeta}}\right)$ and $\mathbf{\Sigma}$ is the matrix of variances and covariances:

$$\Sigma = \begin{bmatrix} \sigma_{\varphi}^2 & C(\varphi,\dot{\varphi}) & C(\varphi,\dot{\zeta}) & C(\varphi,\ddot{\zeta}) \\ C(\dot{\varphi},\varphi) & \sigma_{\dot{\varphi}}^2 & C(\dot{\varphi},\dot{\zeta}) & C(\dot{\varphi},\ddot{\zeta}) \\ C(\dot{\zeta},\varphi) & C(\dot{\zeta},\dot{\varphi}) & \sigma_{\dot{\zeta}}^2 & C(\dot{\zeta},\ddot{\zeta}) \\ C(\ddot{\zeta},\varphi) & C(\ddot{\zeta},\dot{\varphi}) & C(\ddot{\zeta},\dot{\zeta}) & \sigma_{\ddot{\zeta}}^2 \end{bmatrix} \tag{8.9}$$

The variances and covariances could be estimated as follows:

$$\sigma_{\varphi}^2 = \frac{1}{2}\sum_{i=1}^{N} \varphi_i^2 \tag{8.10}$$

$$\sigma_{\dot{\varphi}}^2 = \frac{1}{2}\sum_{i=1}^{N} \varphi_i^2 \omega_i^2 \tag{8.11}$$

$$\sigma_{\dot{\zeta}}^2 = \frac{1}{2}\sum_{i=1}^{N} \zeta_i^2 \omega_i^2 \tag{8.12}$$

$$\sigma_{\ddot{\zeta}}^2 = \frac{1}{2}\sum_{i=1}^{N} \zeta_i^2 \omega_i^4 \tag{8.13}$$

$$C(\varphi,\dot{\varphi}) = 0 \tag{8.14}$$

$$C(\varphi,\dot{\zeta}) = \frac{1}{2}\sum_{i=1}^{N} \varphi_i \zeta_i \omega_i \sin(\beta_i) \tag{8.15}$$

$$C(\varphi,\ddot{\zeta}) = -\frac{1}{2}\sum_{i=1}^{N} \varphi_i \zeta_i \omega_i^2 \cos(\beta_i) \tag{8.16}$$

$$C(\dot{\varphi},\dot{\zeta}) = \frac{1}{2}\sum_{i=1}^{N} \varphi_i \zeta_i \omega_i^2 \cos(\beta_i) \tag{8.17}$$

$$C(\dot{\varphi},\ddot{\zeta}) = \frac{1}{2}\sum_{i=1}^{N} \varphi_i \zeta_i \omega_i^3 \sin(\beta_i) \tag{8.18}$$

$$C(\dot{\zeta},\ddot{\zeta}) = 0 \tag{8.19}$$

Of course the matrix is symmetric, for example $C(\varphi,\dot{\varphi}) = C(\dot{\varphi},\varphi)$ and similarly for the other elements. Moreover as the excitation and response are Gaussian processes with zero mean values, therefore $\mathbf{m} = 0$.

For the calculation of the above covariances, the standard calculations of Fourier series and stochastic Gaussian techniques have been followed; see for example Belenky and Sevastianov (2007). An example of how these covariances are derived is provided and specifically the correlation $C(\varphi,\ddot{\zeta})$ of roll amplitude and second derivative of wave amplitude ζ.

The first two time derivatives of eq 8.4 are respectively:

$$\dot{\zeta}(t) = \sum_{i=1}^{N} \zeta_i \omega_i \cos(\omega_i t + \varepsilon_i) \tag{8.20}$$

$$\ddot{\zeta}(t) = -\sum_{i=1}^{N} \zeta_i \omega_i^2 \sin(\omega_i t + \varepsilon_i) \tag{8.21}$$

As mentioned above, the response can be represented by eq. 8.7, whose derivatives are

$$\dot{\varphi}(t) = \sum_{i=1}^{N} \varphi_i \omega_i \cos(\omega_i t + \beta_i + \varepsilon_i) \tag{8.22}$$

$$\ddot{\varphi}(t) = -\sum_{i=1}^{N} \varphi_i \omega_i^2 \sin(\omega_i t + \beta_i + \varepsilon_i) \tag{8.23}$$

Furthermore, as linear systems hold ergodicity and irregular waves are assumed to represent an ergodic random process, the response will be also an ergodic random process. The correlation moment $C(\varphi, \ddot{\zeta})$ will be in general:

$$C(\varphi, \ddot{\zeta}) = \int_{-\infty}^{\infty} \int_{-\infty}^{\infty} (\varphi - m_{\varphi})(\ddot{\zeta} - m_{\ddot{\zeta}}) f(\varphi, \ddot{\zeta}) d\varphi d\ddot{\zeta} \tag{8.24}$$

Because of the ergodicity and since the mean value of wave elevation m_{ζ} and thus of all other related parameters is zero $(\mathbf{m} = 0)$, the correlation moment will be:

$$C(\varphi, \ddot{\zeta}) = \frac{1}{T} \int_{0}^{T} \varphi \ddot{\zeta} dt \tag{8.25}$$

Taking into account the Fourier representation:

$$C(\varphi, \ddot{\zeta}) = \frac{1}{T} \int_{0}^{T} \left(\sum_{i=1}^{N} \varphi_i \sin(\omega_i t + \beta_i + \varepsilon_i) \sum_{j=1}^{N} -\zeta_j \omega_j^2 \sin(\omega_j t + \varepsilon_j) \right) dt \tag{8.26}$$

$$C(\varphi, \ddot{\zeta}) = -\frac{1}{T} \int_{0}^{T} \left(\sum_{i=1}^{N} \sum_{j=1}^{N} \varphi_i \zeta_j \omega_j^2 \sin(\omega_i t + \beta_i + \varepsilon_i) \sin(\omega_j t + \varepsilon_j) \right) dt \tag{8.27}$$

With some manipulation it will be transformed to:

$$\begin{aligned} C(\varphi, \ddot{\zeta}) = &-\frac{1}{2T} \sum_{i=1}^{N} \sum_{j-1}^{N} \int_{0}^{T} \varphi_i \zeta_j \omega_j^2 \cos\left[(\omega_i - \omega_j) t + \beta_i + (\varepsilon_i - \varepsilon_j) \right] dt + \\ &+ \frac{1}{2T} \sum_{i=1}^{N} \sum_{j-1}^{N} \int_{0}^{T} \varphi_i \zeta_j \omega_j^2 \cos\left[(\omega_i + \omega_j) t + \beta_i + (\varepsilon_i + \varepsilon_j) \right] dt \end{aligned} \tag{8.28}$$

Let us call the first part of the sum of eq 8.28 as A and the second as B, then in order to estimate the integrals, the indices i, j could be equal or non equal. Taking into account the orthogonality of trigonometric functions it can be derived that:

$$\begin{aligned} &i \neq j \Rightarrow A = B = 0 \\ &i = j \Rightarrow A = -\frac{1}{2}\sum_{\mathrm{i}}^{\mathrm{N}} \varphi_{\mathrm{i}}\zeta_{\mathrm{i}}\omega_{\mathrm{i}}^2 \cos(\beta_{\mathrm{i}}),\ B = 0 \end{aligned} \tag{8.29}$$

$$C\left(\varphi,\ddot{\zeta}\right) = -\frac{1}{2}\sum_{i}^{N} \varphi_i\zeta_i\omega_i^2 \cos(\beta_i) \tag{8.30}$$

Similarly the other covariance parameters can be derived.

The joint pdf of $\left(\varphi,\dot{\varphi}\right)$ given the conditions $\dot{\zeta} = 0$ and $\ddot{\zeta} \geq 0$ will be derived, according to (Price and Bishop, 1974) as:

$$f_c\left(\varphi,\dot{\varphi}\right) = f\left(\varphi,\dot{\varphi}\middle|\dot{\zeta} = 0, \ddot{\zeta} > 0\right) = \frac{\int_0^{\infty} \ddot{\zeta} f\left(\varphi,\dot{\varphi},0,\ddot{\zeta}\right) d\ddot{\zeta}}{\int_{-\infty}^{\infty}\int_{-\infty}^{\infty}\int_0^{\infty} \ddot{\zeta} f\left(\varphi,\dot{\varphi},0,\ddot{\zeta}\right) d\varphi d\dot{\varphi} d\ddot{\zeta}} \tag{8.31}$$

8.3.3 Application

For an initial application the scaled critical angle was set at $z_{\mathrm{cr}} = \varphi_{\mathrm{cr}} / \varphi_{\mathrm{v}} = 0.5$, where φ_{v} is the angle of vanishing stability, the natural roll period T_0 at 15 s and the half dimensionless damping ratio k at 0.021 s^{-1}. The grid density was kept constant in polar coordinates. The domain of initial conditions was parameterised by the radius r of the circle within which the grid was built. As it is obvious, r reflects up to how "far" from the quiescent state initial conditions have been considered. Furthermore, the ratio r / z_{cr} should present an interesting relationship with the calculated total probability value.

For each initial condition the critical wave groups were determined with run lengths successively $n = 2,3,...8$, under the assumption of a JONSWAP spectrum. In Figure 8.31 can be observed the calculated variation of the critical wave group probability $P\left(C_{ij}\middle|\mathbf{z}_{ij}\right)$ for the case where $H_S = 7$ m and $T_P = 15$ s for different initial conditions. Probabilities of the initial conditions $P\left(\mathbf{z}_{ij}\right)$ are shown in Figure 8.32.

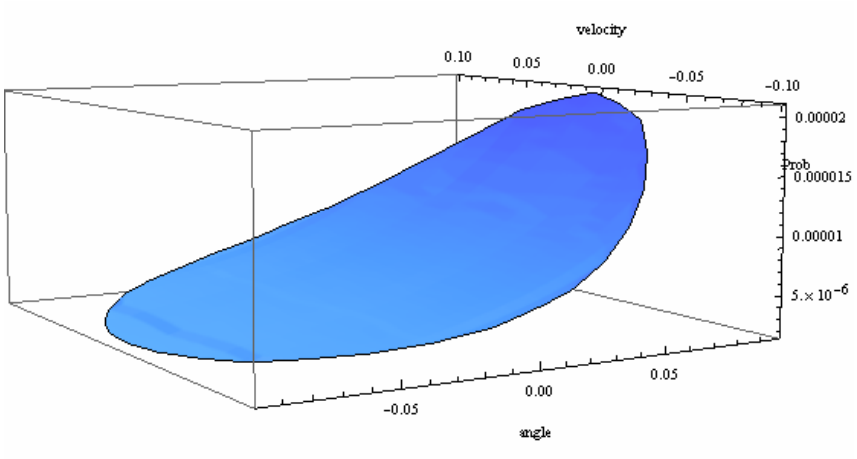

Figure 8.31: Probabilities of critical wave groups from different initial conditions. $H_S = 7$ m **and** $T_P = 15$ s **.**

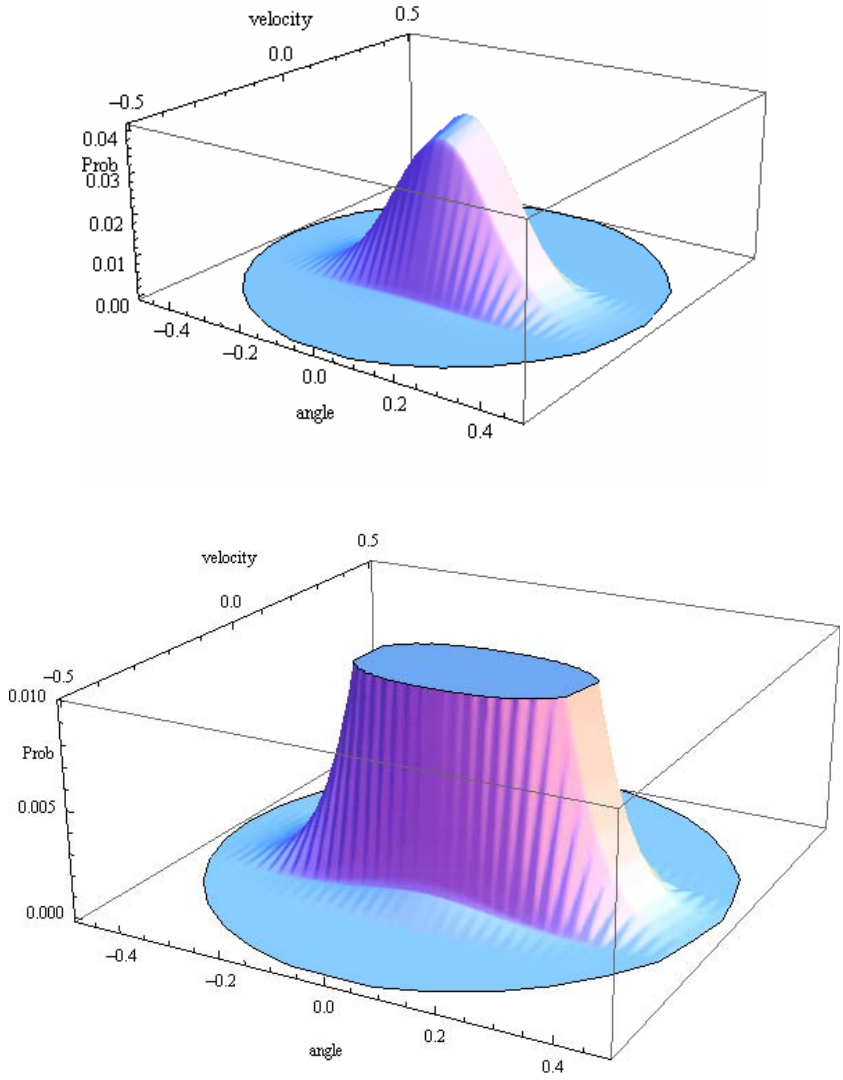

Figure 8.32: Probability distribution of initial conditions within the circle for $H_S = 7$ m **and** $T_P = 15$ s **. The lower picture shows details in the region of smaller probability values.**

However the main purpose of this analysis was to understand whether a probabilistic distribution of the initial conditions affects significantly the value of total probability, in comparison with the assumption of quiescent initial state. The result of parametric studies based on the total probability according to the two calculation procedures, are shown in Figure 8.33 and Figure 8.34 , firstly with respect to H_S and secondly to T_P. One could observe that the "quiescent case" presents always lower values. In order to have a more enlightening view of these results, the difference in probability (dP) between the two cases are calculated for various values of r/z_{cr}. Results are collected in Figure 8.35. Positive difference means here larger value for the "joint" case.

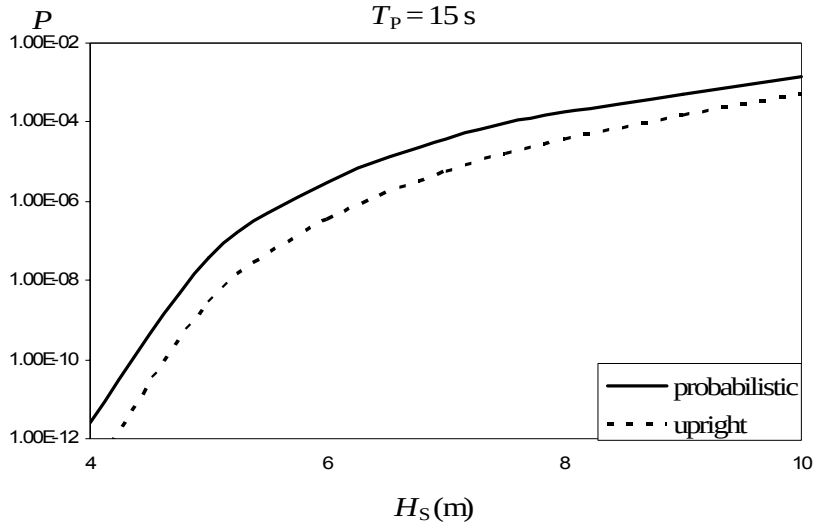

Figure 8.33: Total probabilities for the "quiescent" and for the joint case ($r/z_{cr} = 1$) varying H_S.

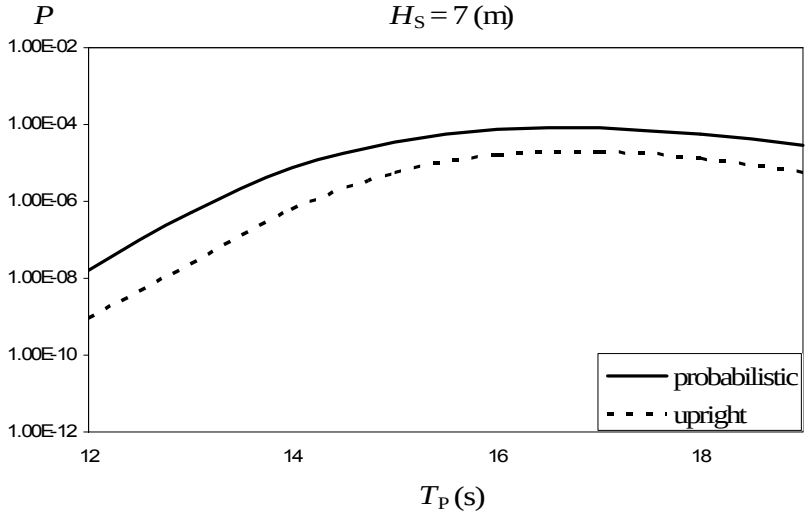

Figure 8.34: Total probabilities for the "quiescent" and for the joint case ($r/z_{cr} = 1$) varying T_P.

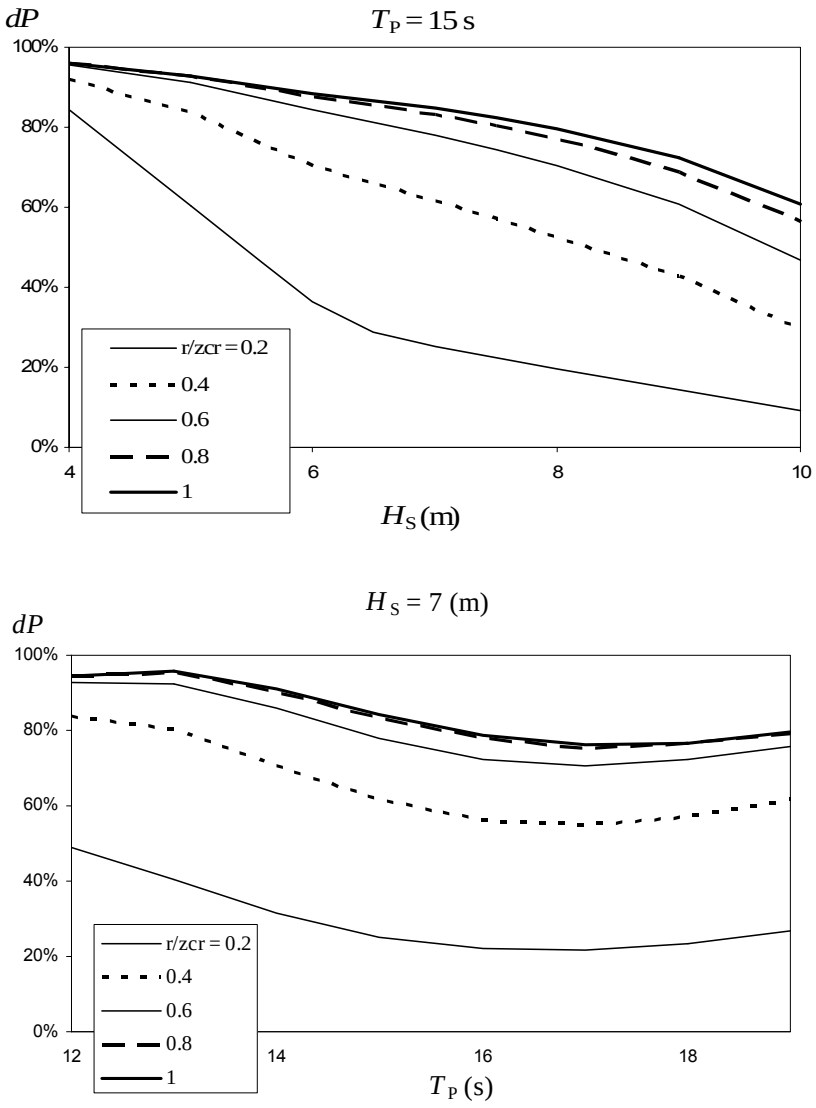

Figure 8.35: Difference in probabilities as the ratio r/z_{cr} is varied.

It is observed that there is a decreasing trend in the difference when H_S is raised. The difference is more pronounced for the small grid radius cases r/z_{cr}. Here it should be mentioned that in order the comparison with to be meaningful, the sample space of each r/z_{cr} case is supposed to have probability one. For a constant ratio r/z_{cr}, when H_S is low, the positions of the ship not so far away from the "quiescent case" incur a more significant "disturbance"; because even though their wave group probability is not so much different from the "quiescent case", their probability of existence is high. This results from the assumed gaussian nature of the response and is more valid for the small values of H_S as the shape of the response curve is sharper than for larger H_S where it becomes broader. In these cases, even though initial states of the ship significantly different from the "quiescent case" have

higher wave group probability, their probability of lying at these positions is not so high in order to modify substantially the total probability figure compared with the upright case. Changing T_P does not bring about major differences, however a minimum is observed in a value near to the natural roll period. On the other hand, increasing the ratio r/z_{cr} while keeping constant the weather parameters results in increase of the difference in the probability with the "quiescent case", as Figure 8.36 shows.

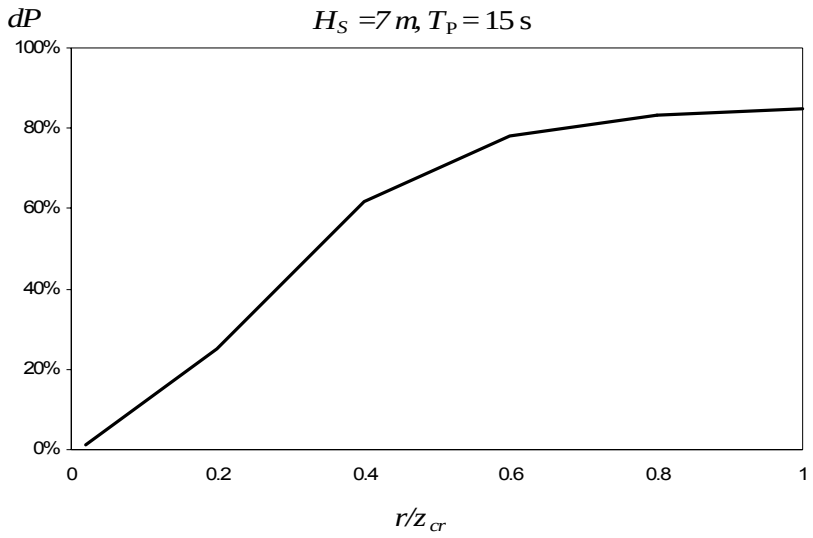

Figure 8.36: Effect of the ratio r/z_{cr}.

Chapter 9:

Conclusions

A novel method for the probabilistic assessment of ship stability has been developed. By exploiting the groupiness characteristic of high waves, the method combines the strengths of deterministic analyses of ship dynamics with state-of-the-art probabilistic analysis of the seaway. It is believed that all basic established ship capsize modes can be handled by the current method.

To facilitate understanding, the method was laid out as a number of specific steps. Mathematical models of ship motions of different level of detail have been used. In general, the proposed method does not depend exclusively on a specific mathematical model and predictions of instability based on different tools or techniques can be combined for reaching a more informed decision. Especially, a mathematical model for the coupled roll motion in beam seas has been developed from first principles focusing on large amplitude transient motion and taking into account important parameters of the problem such as drift motion and viscous forces. Furthermore, key techniques for specific instabilities have been incorporated, providing a rational interface between ship's parameters (e.g. damping and restoring variation) and the key wave group characteristics.

Wave group statistics and models have been studied and properly integrated into the framework of the approach. Refinements in terms of alternative distributions for example different joint pdf of wave height and periods, can be easily employed since this part is not automatically tied to the ship dynamics calculations and thus to the specification of critical wave groups.

Practicality was proven through two applications. In the first one a ROPAX ferry was set to operate on an invented long route across the Mediterranean Sea where statistical wave data has been used. In the second application, a post-panamax containership was examined in a North Atlantic route for days of "bad weather" extracted from hindcast data. A new type of stability assessment diagram has been generated providing information for ship's tendency to exhibit certain types of instabilities in specific parts of the route. These diagrams could support decision-making at various levels.

Further studies have been carried out for several aspects of the assessment. A systematic study for the effect of weather parameters in a post-panamax's propensity for head seas parametric rolling has been performed, resulting in quite logical probability figures. Furthermore a comparative study between the prediction of a numerical code and an analytical method for head-seas parametric rolling, and the reflection of the differences in the probability figures for a specific sea state has been carried out. The potential use of tools incorporating different viewpoints in the modelled physics can lead to a more prudent estimation of the characteristics of critical wave groups while one should keep in mind to regard these predictions with caution and should not rush to consider as more correct those produced by detailed tools.

A preliminary investigation of the effect of initial state of the ship when the wave group is encountered, on the derived probabilities has been also carried out. The simplified model of a forced linear oscillator has been assumed and a grid of possible roll angle and velocities has been created where each pair serves as an initial condition of the problem. The probability of occurrence of these pairs are linked with the weather conditions and then, taking into account the probability of occurrence of critical wave groups in each case, the total probability can be derived. It was found that the degree of influence of initial conditions on the overall probability figure depends mainly on the severity of the sea state. However it is notable that, in a logarithmic scale, the difference appears insignificant. It accrues therefore that beyond the purely technical part of such an investigation, it is essential to clarify what is the "right" scale that one should use for assessing the importance of the several factors that play a role in the modelled physical process.

Refinements at various aspects of the developed methodology could be examined as future work. Other instabilities should be incorporated in the process, utilizing or developing also the necessary calculation tools for their study. An analytical criterion for broaching can be derived for instance. Another issue that could be considered is the determination of more "realistic" wave groups, in terms of their shape; for example each wave in the group could exceed a different height level. However as many combinations will be able to satisfy the critical norm, this would blow up the calculations required for their specification. Then, even if the relevant probabilistic calculations are not time consuming, practicality of the method could be lessened. The current method targets the estimation of the lowest height level that each wave in the group should exceed, leading to a more facile procedure.

Another point that could be further investigated is the involvement of additional probability

density functions for the calculation of wave group's probability which can be sought from the literature or even be developed to suit the examined stability criterion. Thus a breaking wave event or instability due to accumulation of water on deck may be treated by more appropriate, to the nature of these instability modes, probabilistic tools.

Implementation of new analytical techniques and methods for the specification of critical wave groups are desirable in order to complement the current tools portfolio. Improved understanding of the dynamics of instability modes and connection of their source mechanism with characteristics of critical wave events will enhance this direction.

The methodology could be easily embodied in a risk assessment framework. This option is feasible because the developed approach calculates the probability of occurrence of some specified undesirable event. By coupling with the consequences one can calculate risk. One idea is to set then levels of risk. The region of unsafe behaviour could be segmented into a number of subregions whose realization will induce escalating consequences. Thereafter, upper and lower bounds of critical wave groups' characteristics should be specified for each subregion.

Last but not least, the current approach could possibly contribute to the forthcoming new stability requirements, as IMO has recently reopened the issue, anticipating that these will have a probabilistic character. The sound scientific basis, the flexibility of the methodology in terms of use of calculation tools and the potential to treat all known ship instabilities, allow one to be optimistic about its prospects for practical application.

Chapter 10:

References

ABS *Guide for the parametric roll for the design of container carriers*, Houston, T.X, (2004).

ARHAN, M. AND EZRATY, R. "Statistical relationship between successive wave heights." *Oceanologica Acta*, 1 (1978): 151 – 158.

ARNOLD, L., CHUESHOV, I. AND OCHS, G. "Stability and capsizing of ships in random sea – a survey." *Nonlinear Dynamics,* 36 (2004): 135 – 179.

ATHANASSOULIS, G.A., SKARSOULIS, E.K. AND BELIBASSAKIS, K.A "Bivariate distribution with given marginals with an application to wave climate description." *Applied Ocean Research*, 16 (1994): 1-14.

ATHANASSOULIS ET AL. *Metadlas: Wind and wave atlas of the Mediterranean Sea*, WEAU (consortium: CS, NTUA, CNR/ISMAR, THETIS, Semantic, MeteoFrance), 2004, ISBN 2-11-095674-7.

ATHANASSOULIS, G.A., BELIBASSAKIS, K.A. AND GEROSTATHIS, T.P." Description of wave data along ship routes in the Mediterranean Sea." *NTUA Internal Report, SAFEDOR S.P. 2.3.6*, Athens, (2006).

AYYUB, B.M., KAMINSKIY, M., ALMAN, P.R., ENGLE, A., CAMPBELL, B.L. AND THOMAS, W.L. III. "Assessing the probability of the dynamic capsizing of the vessels." *Journal of Ship Research*, 50 (2006): 289-310.

BAARHOLM, G.S. AND JENSEN, J.J. "Influence of whipping on long-term vertical bending moment." *Journal of Ship Research*, 28 (2004): 261-272.

BATTJES, J.A AND VAN VLEDDER, G.PH. "Verification of Kimura's theory for wave group statistics." *Proceedings*, 19th International Coastal Engineering Conference, (1984): 642- 648.

BECK, R.F. AND REED, A.M. "Modern Computational Methods for Ships in a Seaway." *Transactions*, Society of Naval Architects and Marine Engineers, 109 (2001): 1-52.

BEHRENS, A. "Environmental data: Inventory and new data sets." *SAFEDOR S.P. 2.3.2 deliverable report,* (2006).

BELENKY, V.L " Piece – wise linear method for the probabilistic stability assessment for ship in a seaway." *Proceedings*, 5th International Conference on Stability of Ships and Ocean Vehicles, Melbourne, (1994): 13-30.

BELENKY, V.L., DEGTYAREV, A. B. AND BOUKHANOVSKY, A. V. "Probabilistic quantities of nonlinear stochastic rolling." *Ocean Engineering*, 25 (1998): 1 – 25.

BELENKY, V.L., WEEMS, K.M., LIUT, D., SHIN, Y.S. "Nonlinear roll with water-on-deck: numerical approach." *Proceedings,* 8th International Conference on the Stability of Ships and Ocean Vehicles*,* (2003).

BELENKY, V., SEVASTIANOV, N. *Stability and safety of Ships: Risk of Capsizing*, 2nd Edition, Society of Naval Architects and Marine Engineers (SNAME), New Jersey, USA, 2007, ISBN 0-939773-61-9.

BELENKY, V., YU, HAN-CHANG AND WEEMS, K. "Numerical procedures and practical experience of assessment of parametric roll of container carriers." *Proceedings*, 9th International Conference on Stability of Ships and Ocean Vehicles, Rio de Janeiro, (2006): 119-130.

BELENKY, V. AND WEEMS, K. "Numerical procedure for evaluation of capsizing probability with time split method." *Proceedings*, 27th Symposium on Naval Hydrodynamics, Seoul, Korea, (2008), to be presented.

BLOCKI, W. "Ship safety in connection with parametric resonance on the roll." *International Shipbuilding Progress*, 27 (1980): 36 – 53.

BOUKHANOVSKY, A.V. AND DEGTYAREV, A.B. "Nonlinear stochastic ship motion stability in different wave regime." *Proceedings*, CFR'96: 3rd International Conference in Commemoration of the 300th Anniversary of creating Russian fleet by Peter the Great, St. Petersburg, (1996): 296 – 306.

BRETSCHNEIDER, C.L. “Wave variability and spectra for wind generated waves.” Technical Memo 118, Beach Erosion Board, U.S. Army Corps of Engineers, (1959).

BROWN, A.J. AND DEYBACH, F. “Towards a rational intact stability criteria for naval ships.” *Naval Engineers Journal*, (1998): 56 – 77.

CAVANIÉ, A., ARHAN, M. AND EZRATY, R. “A statistical relationship between individual heights and periods of storm waves.” *Proceedings*, Conference on Behaviour of Offshore Structures, Trondheim, Norwegian Institute of Technology, (1976): 354-360.

CHEN, S., SHAW, S.W. AND TROESCH, A.W. “A systematic approach to modelling nonlinear multi – d.o.f ship motions in regular seas.” *Journal of Ship Research,* 25 (1999): 25 – 37.

CUMMINS W. E. “The impulse response function and ship motions.” *Schiffstechnik*, 9 (1962): 101–109.

DEKAT, J.O. “Irregular waves and their influence on extreme ship motions.” Report No. 208883-OP1, ONR’94 (1994).

DEKAT, J.O AND PAULLING J.R. “The Simulation of Ship Motions and Capsizing in Severe Seas.” *Transactions*, Society of Naval Architects and Marine Engineers, 97 (1989): 139 – 168.

DET NORSKE VERITAS. “*DNV MaxWave*.” Report No. 2001 – 1491, (2002a).

DET NORSKE VERITAS. *Cargo Securing Manual*: *model manual.* Version 3.1, (2002b).

DRAPER, L. “Severe wave conditions at sea.” *Journal of the Institute of Navigation*, 24 (1971): 273- 277.

FALZARANO, J., SHAW S. AND TROESCH, A. “Application of global methods for analyzing dynamical systems to ship rolling motion and capsizing.” *International Journal of Bifurcation and Chaos,* 2 (1992): 101-115.

FRANSCESCUTTO, A, SERRA, A AND SCARPA, S. “A critical analysis of weather criterion for intact stability of large passenger vessels.” *Proceedings*, 20th International Conference on Offshore Mechanic and Artic Engineering, (2001).

FROUDE, W. “On the rolling of ships.” *Transactions,* Institute of Naval Architects, 2 (1861).

GERASIMOV, A.V. “*Energy statistical theory of nonlinear irregular ship motion*.” Sudostroenie Publishing, Leningrad (1979), (in Russian).

GODA, Y. “On wave groups.” *Proceedings*, 1st International Conf. on Behavior of Offshore Structures, Trondheim, Norway, (1976): 115–128.

GOOGLE EARTH, “http://earth.google.com” (2005).

GROCHOWALSKI, S., HSIUNG, C.C., HUANG, Z.J. AND CONG, L.Z. “Theoretical Modeling of Ship Motions and Capsizing in Large and Steep Waves.” *Transactions*, Society of Naval Architects and Marine Engineers, 106 (1998): 241 – 267.

HADDARA, M.R. “A modified approach for the application of Fokker - Planck equation to the nonlinear ship motions in random waves.” *International Shipbuilding Progress*, 21 (1974): 283 – 288.

HADDARA, M.R. AND ZHANG, Y. “On the joint probability density function of nonlinear rolling motion.” *Journal of Sound and Vibration*, 169 (1994): 562- 569.

HADDARA, M.R. AND NASSAR, M.A. “A stochastic model for the analysis of rolling motion in a realistic seaway.” *International Shipbuilding Progress*, 33 (1986): 144- 150.

HASSELMANN, K. et al “Measurements of wind-wave growth and swell decay during the Joint North Sea Wave Project (JONSWAP).” *Deutschen Hydrographischen Zeitschrift,* A.12 (1973): 1 – 95.

HAYASHI, C. *Nonlinear Oscillations in Physical Systems*, Princeton University Press, Princeton, New Jersey, 1986, ISBN 0691083835.

HIMENO, Y. “Prediction of ship roll damping- State of Art”, Department of Naval Architecture and marine Engineering, University of Michigan, Ann Arbor, MI, Report No. 239., (1981).

HOLLAPA, K.W. AND FALZARANO, J.M. “Application to extended state space to nonlinear ship rolling.” *Ocean Engineering*, 26 (1999): 227 – 240.

HSIEH, S.R., SHAW, S.W. AND TROESCH, A.W. "A nonlinear probabilistic method for predicting vessel capsizing in random beam seas." *Proceedings A,* The Royal Society, London, 446 (1994): 195 – 211.

IBRAHIM, M.R. *Parametric Random Vibration*, Research Studies Press, Letchworth, England, 1985, ISBN 0471908304.

IMO Code *of Safe Practice for Cargo Stowage and Securing and Amendments Thereto*, Resolution A.714 (with 1994/95 amendments, Annex 1-13), London, (1991).

IMO Code *on Intact Stability for All Types of Ships Covered by IMO Instruments*, Resolution A.749 (18), London, (1993).

IMO *Guidance to the Master for Avoiding Dangerous Situations in Following and Quartering Seas,* MSC. Circ. 707, London, (1995).

IKEDA, Y., HIMENO, Y. AND TANAKA, N., "A prediction method for ship roll damping, Report No. 00405 of Department of Naval Architecture, University of Osaka Prefecture, (1978).

ITTC "Report of The Specialist Committee on Prediction of Extreme Ship Motions and Capsizing Stability." 23rd ITTC, Italy, (2002).

ITTC "Report of The Specialist Committee Stability in Waves" 24th ITTC, Edinburgh, UK, (2005).

JEFFREYS, E.R. "Simulation of wave power devices." *Applied Ocean Research*, 6 (1984): 31 – 39.

JIANG, C., TROESCH, A.W. AND SHAW, S.W. "Highly nonlinear rolling motion of biased ships in random beam seas." *Journal of Ship Research,* 40 (1996): 125 – 135.

JIANG, C., TROESCH, A.W. AND SHAW, S.W. "Capsize criteria for ship models with memory – dependent hydrodynamics and random excitation." *Philosophical transactions of the Royal Society,* Series A 358 (2000):1761 – 1791.

KATO, H. "On the frictional resistance to the roll of ships." *JSNAJ*, 102 (1958).

KIMURA, A. “Statistical properties of random wave groups.” *Proceedings*, 17th International Conference on Coastal Engineering, Sydney, Australia, (1980): 2955 – 2973.

KOBYLINSKI, L.K. AND KASTNER, S. *Stability and safety of Ships: Regulation and operation*, Vol. 1, Elsevier, Ocean Engineering Book Series, Kidlington, UK, 2003, ISBN 0080443540.

KOTZ, S., BALAKRISHNAN, N. AND JOHNSON, N.L. *Continuous multivariate distributions*, John Wiley & Sons, New York, 2000, ISBN 0471183873.

KURODA, T., IKEDA, Y. “Extreme roll motion in wide frequency range due to rapid drift motion.” *Proceedings,* 6th International Ship Stability Workshop*,* Webb Institute, Long Island, (2002).

LINDGREN, G. AND RYCHLIC, I. “Wave characteristics distributions for Gaussian waves – wavelength, amplitude and steepness.” *Ocean Engineering*, 9 (1982): 411 – 432.

LLOYD, A.R.J.M. *Seakeeping: Ship Behavior in Rough Weather*, Ellis Horwood Series in Marine Technology, 1989, ISBN 0953263401.

LONGUET-HIGGINS, M.S. “The statistical analysis of a random moving surface.” *Philosophical transactions of the Royal Society,* Series A, London*,* 249 (1957): 321 – 387.

LONGUET-HIGGINS, M.S. “On the joint distribution of the periods and amplitudes of sea waves.” *Journal of Geophysical Research*, 80 (1975): 6778–89.

LONGUET-HIGGINS, M.S. “On the joint distribution of wave periods and amplitudes in a random wave field.” *Proceedings A*, The Royal Society, London, 389 (1983): 241–258.

LONGUET-HIGGINS, M.S. “Statistical properties of wave groups in random sea state.” *Philosophical transactions of the Royal Society,* Series A, London, 312 (1984): 219 – 250.

LUGOVKY, V.V. “ New method of estimation of stipulated amplitude of rolling of transport ships in stability standards.” *Transactions*, Russia Register of Shipping, (1963): 3 – 45 (in Russian).

MARUO, H. “The drift of a body floating on waves.” *Journal of Ship Research***,** 4 (1960): 1 – 10.

MASSEL, S.R. *Ocean surface waves: their physics and predictions*, World Scientific, Singapore, 1998, ISBN 9810216866.

MASSON, D. AND CHANDLER, P. "Wave groups: a closer look at spectral methods." *Coastal Engineering*, 20 (1993): 249-275.

MATHIESEN, J. AND BITNER – GREGERSEN, E. "Joint distribution for significant wave height and zero crossing period." *Applied Ocean Research*, 12 (1990): 93-103.

MEDINA, J.R. AND HUDSPETH, R.T. "A review of the analyses of wave groups." *Coastal Engineering*, 14 (1990): 515 – 542.

MEMOS, C.D. "On the theory of joint probability of heights and periods of sea waves." *Coastal Engineering*, 22 (1994): 201 – 215.

MCCREIGHT, W.C. "Ship maneuvering in waves." *Proceedings*, 16th Symposium on Naval Hydrodynamics, (1986).

MCCUE, L.S., TROESCH, A.W. "The effect of coupled heave/heave velocity or sway/sway velocity initial conditions on capsize modelling." *Proceedings*, 8th International Conference on the Stability of Ships and Ocean Vehicles, (2003).

MCCUE, L. AND TROESCH, A. "Probabilistic determination of critical wave height for a multi-degree of freedom capsize model." *Ocean Engineering,* 32 (2005): 1608-1622.

MCTAGGART, K. AND DEKAT, J.O. "Capsize risk of intact frigates in irregular seas." *Transactions*, Society of Naval Architects and Marine Engineers, 108 (2000): 47 – 177.

MIDDLETON, D. *An introduction to statistical communication theory*, McGraw – Hill Book Company, New York, 1960.

MOLLO-CHRISTENSEN, E. AND RAMAMONJIARISOA, A. "Modelling the presence of wave groups in a random wave field." *Journal of Geophysical Research*, 83 (1978): 4117 – 4122.

MOSELEY, H. "On the dynamical stability and on the oscillation of floating bodies." *Philosophical transactions of the Royal Society,* Series A, London, 207 (1850): 609–643.

MYRHAUG, D. AND RUE, H. “Note on a joint distribution of successive wave periods.” *Journal of Ship Research*, 37 (1993): 208 -212.

MYRHAUG, D. AND RUE, H. “Joint distribution of successive wave periods revisited.” *Journal of Ship Research*, 42 (1998): 199 -206.

MYRHAUG, D., DAHLE, E.A., RUE, H. AND SLAATTELID, O.H. “Statistics of successive wave periods with application to rolling of ships.” *International Shipbuilding Progress,* 47 (2000): 253-266; errata: 425-426.

NAITO, S. MINURA, M. HAMANAKA, S. AND YAMAMOTO, T. “Long-term prediction method based on ship operation criteria.” *International Shipbuilding Progress*, 53 (2006): 229-252.

NAMACHCHIVAYA, SRI, N, AND RAMAKRISHNAN, N. “Stochastic dynamics of parametrically excited two d.o.f systems with symmetry.” *Journal of Sound and Vibration*, 262 (2003): 613-631.

NESS, O.B., MATHISEN, J., MCHENRY, G. AND WINTERSTEIN, S. “Nonlinear analysis of ship rolling in random beam waves.” *Proceedings*, STAR Symposium, New Orleans, (1989).

NEWMAN, J.N. “The drift force and moment on ships in waves.” *Journal of Ship Research*, 11 (1967): 51 – 60.

NOLAN, V.J. AND NAMACHCHIVAYA, SRI, N. “Almost sure stability of linear gyroscopic systems.” *Journal of Sound and Vibration*, 227 (1999): 105-130.

OCHI, M. “On long term statistics for ocean and costal waves.” *Proceedings*, 16th Conference on Coastal Engineering, Hamburg, (1978): 59-75.

OCHI, M. *Ocean Waves: The Stochastic Approach*, Cambridge University Press, Cambridge, England, 1998, ISBN 052156378X.

OCHI, M.K. AND SAHINOGLOU, I.I. “Stochastic characteristics of wave group in random seas; Part 1: Time duration of and number of waves in a group.” *Applied Ocean Research*, 11 (1989a): 39 - 50.

OCHI, M.K. AND SAHINOGLOU, I.I. "Stochastic characteristics of wave group in random seas; Part 2: Frequency of occurrence of wave groups." *Applied Ocean Research*, 11 (1989b): 89 - 99.

PAROKA, D. AND UMEDA, N. "Capsizing probability prediction for a large passenger Ship in irregular beam wind and waves: comparison of analytical and numerical methods." *Journal of Ship Research*, 50 (2006): 371 – 377.

USA "Rules and regulations for passengers vessels." United States Coast Guard, Treasury Department (1962), also IMO (1963).

USSR "Standards of stability of sea – going vessels and floating cranes." Register of shipping of the USSR, (1961). Also IMO (1988) Document SLF 33/ INF .4

PRICE, W. G. & BISHOP, R.E.D. *Probabilistic theory of ship dynamics*, Chapman and Hall, London, 1974, ISBN 0412124300.

RAHOLA, J. "The judging of the stability of ships*." Transactions* I.N.A (1935).

RAINEY, R.C.T AND THOMPSON, J.M.T. "Transient capsize diagram – a new method of quantifying stability in waves." *Journal of Ship Research*, 41 (1991): 58 – 62.

RICE, S.O. "Mathematical analysis of random noise." *Bell Systems Technology*, 24 (1945): 46 – 156.

ROBERTS, J.B. "A stochastic theory for nonlinear ship motion in irregular seas." *Journal of Ship Research*, 26 (1982): 229 – 245.

RODRIGUEZ, G.R. AND SOARES C.G. "Correlation between successive wave heights and periods in a mixed sea state." *Ocean Engineering*, 28 (2001): 1009 – 1030.

RYE, H. "Wave group formation among storm waves." *Proceedings*, 14th International Conference on Coastal Conference, Copenhagen, (1974): 164 – 183.

SAWHNEY, M.D. "A study of ocean wave amplitudes in terms of the theory of runs and a Markov chain process." *Technical repor*t, Dept. Meteor. and Oceanography, New York University (1962).

SCLAVOUNOS, P., "Computations of wave ship interactions." *Advances in Marine*

Hydrodynamics, Computational Mechanics Publications, (1996).

SCHMITKE, R.T, "Ship sway, roll and yaw motions in oblique seas", *TSNAME*, 86 (1978).

SIMIU E. *Chaotic Transitions in Deterministic and Stochastic Dynamical Systems – Applications of Melnikov Processes in Engineering, Physics and Neuroscience. Princeton Series in Applied Mathematics*, Princeton University Press, New Jersey, 2002, ISBN 0691050945.

SOBEY, R.J. "Correlation between individual waves in a real sea state." *Coastal Engineering*, 27 (1996): 223 – 242.

SOLIMAN, M.S., "An analysis of ship stability based on transient motions*." Proceedings*, 4th International Conference on the Stability of Ships and Ocean Vehicles, (1990).

SPYROU, K.J. "Pure – loss of stability revisited: analytical and numerical design aids." *NTUA Internal Report*, Athens, (2000).

SPYROU, K.J. "A basis for a developing a rational alternative to the weather criterion: problems and capabilities." Proceedings, 6th International Ship Stability Workshop, Webb Institute, New York, (2002).

SPYROU, K.J. "Design criteria for parametric rolling." *Oceanic Engineering International*, 9 (2005): 11-27.

SPYROU, K.J. "Asymmetric rolling of ships in following seas and its repercussions for safety." *Nonlinear Dynamics*, 43 (2006): 149 – 172.

SPYROU, K.J. AND THEMELIS, N. "Probabilistic assessment of intact stability." *Proceedings*, 8th International Ship Stability Workshop, Istanbul, (2005).

SPYROU, K.J. AND THEMELIS, N. Development of probabilistic procedures and validation – Alternative 2: capsize mode analysis." *SAFEDOR S.P. 2.3.5 deliverable report,* (2006).

SPYROU, K.J. THEMELIS, N. AND NIOTIS, S. "Towards a Full Risk-Based Assessment of Ship Stability." *Proceedings*, RINA, SAFEDOR Midterm Conference, Brussels, May, (2007a).

SPYROU, K.J., THEMELIS, N, AND NIOTIS, S. "Probabilistic assessment of parametric rolling: comparative study of detailed and simplified models", *Proceedings*, 9th International Ship Stability Workshop, Hamburg, (2007b).

SPYROU, K.J. AND THOMPSON, J.M.T. "The nonlinear dynamics of ship motions: a field overview and some recent developments." *Philosophical transactions of the Royal Society,* Series A, London, 358 (2000):1735 – 1760.

SPYROU, K.J. AND THOMPSON, J.M.T. (eds) "The nonlinear dynamics of ships." *Philosophical transactions of the Royal Society,* Series A (Theme issue 1771) 358 (2000): 1733-1981.

SPYROU, K.J., POLITIS, K., LOUKAKIS, T. AND GRIGOROPOULOS, G. "Towards a risk – based system for the departure control of passengers ships in rough weather in Greece." *Proceedings*, 2nd International Maritime Conference on Design for Safety, Sakai, Japan, (2004): 255 – 261.

SROKOSZ, M.A. AND CHALLENOR, P.G. "Joint distribution of wave height and period: a critical comparison." *Ocean Engineering*, 14 (1987): 295 – 311.

ST. DENIS, M. AND PIERSON, W. "On the motion of ship in confused ship." *Transactions*, Society of Naval Architects and Marine Engineers, 61 (1953): 280-357.

STANSELL, P., WOLFRAM, J. AND LINFOOT, B. "Statistics of wave groups measured in the northern North Sea; comparisons between time series and spectral predictions." *Applied Ocean Research*, 24 (2002): 91–106.

STANSELL, P., WOLFRAM, J. AND LINFOOT, B. "Improved joint probability distribution for joint wave heights and periods.", *Journal of Fluid Mechanics*, 503 (2004): 273 – 297.

SWAN2, *User Manual*, Boston Marine Consulting, Ship Flow Simulation in Calm Water and in Waves., (2002).

TAKAISHI, Y., WATANABE, K. AND MASUDA, K. "Probability to encounter high run of waves in the dangerous zone shown on the operational guidance IMO for following/quartering seas." Contemporary ideas on ship stability (ed. D. Vassalos et al.), 2000, Oxford, Elsevier, ISBN0080436528.

TANAKA, N. “A study on the bilge keels (Part 4 – On the eddy making resistance to the rolling of a ship hull).” *JNSAJ,* 109 (1960).

TAYFUN, M.A. “Distribution of large wave heights.” *Journal of Waterway, Port, Coastal and Ocean Engineering*, 116 (1990): 686–707.

TAYFUN, M.A. “Joint distributions of large wave heights and associated periods.” *Journal of Waterway, Port, Coastal and Ocean Engineering*, 119 (1993): 261–273.

THEMELIS N. AND SPYROU K.J. “The nonlinear dynamics of the coupled ship rolling in steep beam waves.” *THALES Project deliverable report*, (2005).

THEMELIS N. AND SPYROU K.J. “Lashing of trailers on board Ro/Ro ships under intensive rolling.” *Proceedings*, 8th International Conference on Stability of Ships and Ocean Vehicles, Madrid, (2003).

THEMELIS, N. AND SPYROU, K.J. “A coupled heave-sway-roll model for the analysis of large amplitude ship rolling and capsize of ships in beam seas on the basis of a nonlinear dynamics approach*.” Proceedings*, 16th International Conference on Hydrodynamics in Ship Design, Gdansk, Poland, (2005): 314 – 325.

THEMELIS, N. AND SPYROU, K. “Probabilistic Assessment of Resonant Instability.” *Proceedings*, 9th International Conference on Stability of Ships and Ocean Vehicles, Rio de Janeiro, (2006): 37-48.

THEMELIS, N., SPYROU, K. AND NIOTIS, S. “Implementation and application of probabilistic procedures.” *SAFEDOR S.P. 2.3.6 deliverable report,* (2007).

THEMELIS, N. AND SPYROU, K. “Probabilistic assessment of ship stability.” *Transactions,* Society of Naval Architects and Marine Engineers, (SNAME) 115 (2007).

THOMPSON, J.M.T, RAINEY, R.C.T. AND SOLIMAN, M.S. “Mechanics of ship capsize under direct and parametric wave excitation.” *Philosophical Transactions of the Royal Society*, Series A 338 (1992): 471 – 490.

THOMPSON, J.M.T AND SOLIMAN, M.S. “Fractal control boundaries of driven oscillators and their relevance to safe engineering design.” *Proceedings A*, The Royal Society, London, 428 (1990): 1-13.

THOMPSON, J.M.T. “Designing against capsize in beam seas: Recent advantages and new insights.” *Applied Mechanics Review,* 50 (1997): 307-325.

TIGKAS, I. “Dynamic stability of ships in longitudinal seas and wind and development of criteria.” *PhD thesis under development,* National Technical University of Greece*,* (2007).

TIKKA, K.K AND PAULLING, J.R. “Prediction of critical wave conditions for extreme vessel response in random seas.” *Proceedings*, 4th International Conference on the Stability of Ships and Ocean Vehicles, Naples, (1990).

UMEDA N., HAMAMOTO M., TAKAISHI Y., CHIBA Y., MATSUDA A., SERA W., SUZUKI S., SPYROU K. AND WATANABE K. “Model Experiments of ship capsize in astern seas.” *Journal of the Society of Naval Architects of Japan*, 177 (1995): 207 – 217.

VASSILOPOULOS, L. “Ship rolling at zero speed in random seas with nonlinear damping and restoration.” *Journal of Ship Research*, 15 (1971): 289 – 294.

VANMARCKE, E.H. “On the distribution of the first – passage time for normal stationary random process.” *Journal of Applied Mechanics*, 42 (1975): 215 – 220.

VAN VLEDDER, G.P. “Statistics of wave groups parameters.” Proceedings, 23rd International Conference on Coastal Engineering, Venice, (1992): 946 – 959.

VIRGIN, L.N. “The nonlinear rolling response of a vessel including chaotic motions leading to capsize in regular seas.” *Applied Ocean Research,* 9 (1987): 89-95.

VINJE, T. “On stability of ships in irregular following sea.” *Norwegian Maritime Research*, 2 (1976): 15-19.

WATANABE, Y. “Some contributions to the theory of rolling.” *Transactions* I.N.A (1938).

WIGGINS, S. *Global Bifurcations and Chaos: Analytical Methods*, Springer-Verlag, New York, 1988, ISBN 0387967753.

WIST, H. MYRHAUG D. AND RUE H. “Statistical properties of successive wave heights and successive wave periods.” *Applied Ocean Research*, 26 (2004): 114–136.

YAMAGATA, M. “Standard of stability adopted in Japan.” *Transactions,* INA, 101 (1959): 417-443.

Appendix A:

The concept of the effective gravitational field

After Froude, it has been quite common to investigate ship rolling with a single-degree of-freedom model, assuming that the ship tends to follow the rotational motion of water particles. This allows use of the concept of "effective gravitational field" where the effective gravity force can be assumed to work always perpendicular to the instantaneous water surface (Thompson et al. 1992). The concept is valid for long incident waves relatively to the beam of the ship and it implicitly assumes a slave variation of heave in order to maintain a constant immersed volume. However, these assumptions have limitations as the wave steepness is increased. Furthermore, in the shorter wave range (length comparable to the ship's beam) the method deviates and may not be fully representative of the physical system.

A.1 Analysis of the concept – limitations

When a body follows the circular motion of water particles on a sinusoidal wave in deep water, a time varied gravitational acceleration $\vec{g}_e(t)$ acts on it, which is often assumed as nearly perpendicular to the wave slope. Figure A.1 shows the circular motion of a particle on the wave surface in deep water. It is assumed that a surface particle stays on the surface. The surface elevation of a simple sinusoidal wave is:

$$\eta(y,t) = \mathrm{A}\cos(ky - \omega_w t) \tag{A.1}$$

where A, k, ω_w are, respectively, wave amplitude, wavenumber and frequency. Initially the particle is at position 1 (see Figure A.1) and after time t, it will be transferred to position 2 having run an angle $\omega_w t$ on a circular trajectory, while the distance covered will be $\mathrm{c}\cdot\mathrm{t}$, where c is the wave velocity:

$$c = \frac{\lambda}{T_w} = \frac{\omega_w}{k} \tag{A.2}$$

λ, T_w are the wavelength and period respectively. For linear waves on deep water the dispersal relation is valid and allows for one independent parameter for the problem.

$$\omega_w^2 = gk \tag{A.3}$$

The accelerations that act on the wave particle at position 2 are: the acceleration of gravity $\vec{g}$ and the centrifugal acceleration $\overrightarrow{-\omega_w^2 A}$. The vector sum of these two is the effective gravitational acceleration $\vec{g}_e(t)$, which forms an angle β with $\vec{g}$ (Figure A.1). The effective gravitational acceleration is calculated then as follows:

$$g_e(t) = g - A\omega_w^2 \cos(\omega_w t) \tag{A.4}$$

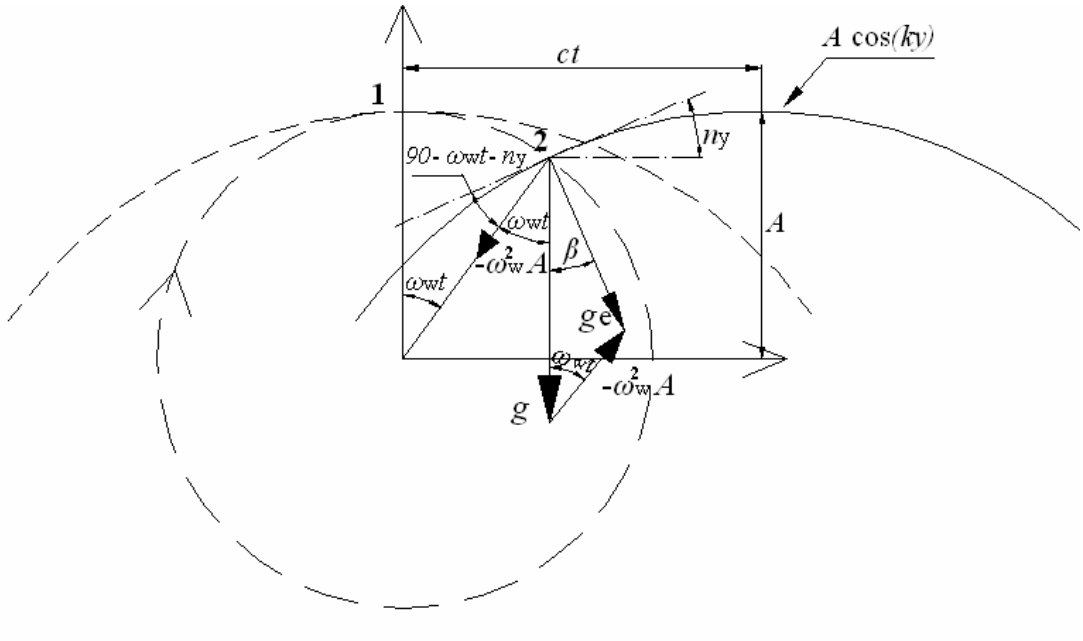

Figure A.1: The rotational motion of a water particle for a wave in deep water.

The slope n_y of a sinusoidal wave is:

$$\eta_y(y,t) = Ak \sin(ky - \omega_w t) \tag{A.5}$$

Assuming that for all points of the circle $y = 0$ and using eq. A.3, the wave slope becomes:

$$\eta_y = A\frac{\omega_w^2}{g}\sin(\omega_w t) \tag{A.6}$$

According to Figure A.1, the condition of perpendicularity between the effective gravitational acceleration and the wave slope is expressed as follows:

$$\gamma = \beta - n_y = 0 \tag{A.7}$$

where γ is the angle that characterizes the error from perpendicularity. For the angle β stands:

$$\frac{g_e}{\sin(\omega_w t)} = \frac{\omega_w^2 A}{\sin\beta} \Rightarrow \sin\beta = \frac{\omega_w^2 A \sin(\omega_w t)}{g_e} \tag{A.8}$$

According to Figure A.1:

$$g_e^2 = g^2 + A^2\omega_w^4 - 2.gA\omega_w^2 \cos(\omega_w t) \tag{A.9}$$

And so, from eq. A.8 the angle β is calculated as follows:

$$\beta = \arcsin\left(\frac{\omega_w^2 A \sin(\omega_w t)}{\sqrt{g^2 + A^2\omega_w^4 - 2gA\omega_w^2 \cos(\omega_w t)}}\right) \tag{A.10}$$

A.2 Effect of wave steepness and wavelength

The effect of the wave steepness H/λ on the maximum calculated values of the angle γ is shown in Figure A.2. For more enlightening presentation of the results γ is scaled over the wave slope Ak. The wavelength was kept constant at $\lambda/B = 6$ where above this value the long wave assumption is customarily valid, thus the presence of the ship does not disturbs the wave pressure. As all the calculations performed in non dimensional form, the value of the breadth of the ship B does not play any role.

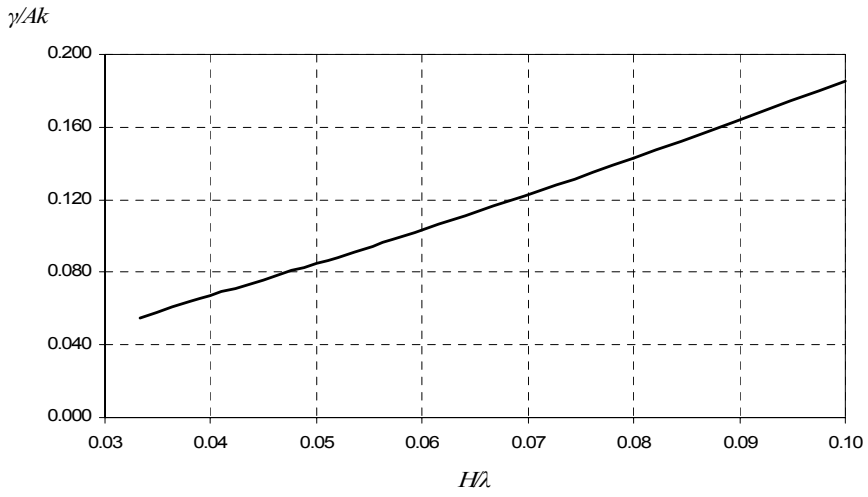

Figure A.2: Effect of wave steepness.

Figure A.3 shows the variation of the angle γ, in terms of the ratio λ/B. From these figures, it becomes clear that the assumption of perpendicularity is not valid (the error is greater than

10% of Ak) when the wave steepness is greater than 1/20; and also, when the wave length is shorter than about five times the beam of the ship.

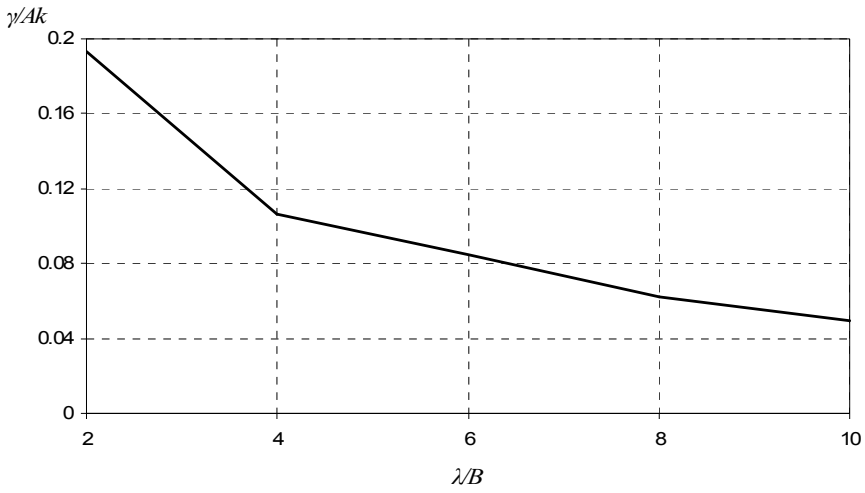

Figure A.3: Effect of wavelength.

From this analysis it can be deduced that if the body is not following the motion of water particles then it should be drifting, i.e. sway coupling should be taken into account. Furthermore, in shorter waves the ship should also be heaving. As a matter of fact, a roll-sway-heave model should be more suitable for investigating ship dynamic response in beam seas, especially for shorter waves.

Appendix B:

Further analysis of the developed mathematical model

In this section more details about the developed mathematical model for the coupled roll motion in beam seas will be presented. The basic modelling has been provided in Chapter 6, however some issues regarding the calculation of radiation and viscous forces decided that it would be better to presented separately in an Appendix.

B.1 Radiation forces with memory effects

As it was referred in Chapter 6, the radiation force involves frequency dependent added mass and damping coefficient. So, in the time domain the linear radiation forces are estimated using an impulse response function, obtained as the Fourier transform of the frequency dependent radiation transfer function. Thus the radiation forces will be (Cummins 1962):

$$F_{Ri}(t) = -A_{ij}(\infty)\dot{v}_j - \int_0^{+\infty} K_{ij}(\tau)v_j(t-\tau)d\tau, \text{ for } i, j = 2,3,4 \tag{B.1}$$

where the impulse response function or else retardation function is considered as

$$K_{ij}(\tau) = \frac{2}{\pi}\int_0^{\infty} B_{ij}(\omega)\cos(\omega\tau)d\omega \tag{B.2}$$

It should be noticed that the damping $B_{ij}(\infty)$ at infinite frequency is negligible and v_j is the velocity in the j direction. However, the solution of the convolution integrals in the time-domain is a repetitive and time-consuming process. Thus an alternative approach has been proposed and used in the past, for example (Jeffreys, 1984; McGreight, 1986; Holappa and Falzarano, 1999). In this procedure, added mass and damping are modelled by a filter with approximately the same frequency as the forces and moments. This filter is created in the frequency domain and can be implemented in the time-domain. The technique mentioned above is sufficiently accurate but it increases the order of the equations of the system, specifically all equations are transformed into first-order differential equations by employing the state-space approximation technique. Nevertheless, the increasing of the equations of the

system does not delay significantly the simulation process.

The relevant analysis and calculation procedure at this stage has been performed by Tigkas (2007), during his currently developing PhD thesis, so more details are provided there.

By using a discrete form for the equation B.2, the impulse response function for a time in the past (τ) can be transformed into:

$$K_{ij}(\tau) = \frac{2}{\pi}\sum_{0}^{\infty} b_{ij}(\omega)\cos(\omega\tau)d\omega \tag{B.3}$$

The Kernels $K_{ij}(\tau)$ are calculated at each time-step in the past, where it can be observed that the effect of the retardation functions attenuates as moving backwards and eliminates after a few seconds. An example of a Kernel function for rolling of a fishing vessel is presented next (Tigkas 2007).

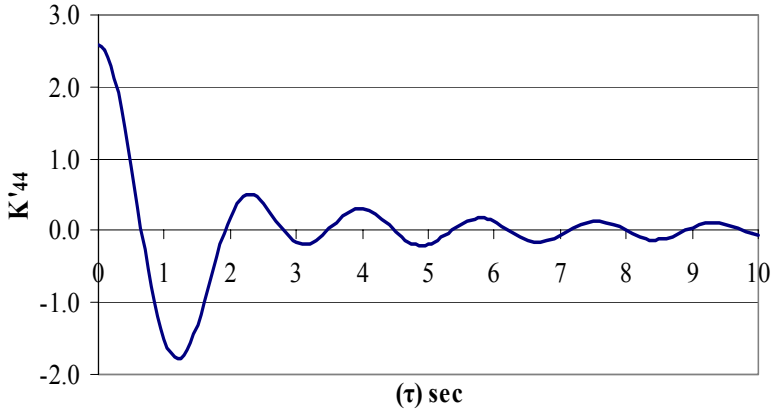

Figure B.1: Kernel function for roll (Tigkas 2007).

A brief description of the construction of the filter and the method of extended state space variables follows. In order to derive the filter that can model the memory effects of the forces and moments, it is necessary to express the impulse response function as an inverse Laplace transform of the transfer function:

$$K_{ij}(t) = L^{-1}[G_{ij}(s)] \tag{B.4}$$

This transfer function is obtained from the total radiation hydrodynamic force $f_{ij}(t)$ that has the following form:

$$f_{ij}(t) = -\left\{\left[A_{ij}(\omega) - A_{ij}(\infty)\right]\dot{v}_j(t) + \left[B_{ij}(\omega) - B_{ij}(\infty)\right]v_j(t)\right\} \tag{B.5}$$

In the Laplace domain the above equation can be transformed as below:

$$f_{ij}(s) = -\left\{ s\left[A_{ij}(\omega) - A_{ij}(\infty) \right] + \left[B_{ij}(\omega) - B_{ij}(\infty) \right] \right\} v_j(s) \tag{B.6}$$

The above transfer function can be written in the frequency domain:

$$G_{ij}(s) = \frac{f_{ij}(s)}{v_j(s)} = -\left\{ i\omega\left[A_{ij}(\omega) - A_{ij}(\infty) \right] + \left[B_{ij}(\omega) - B_{ij}(\infty) \right] \right\} \tag{B.7}$$

A filter then can be constructed for the transfer function with unknown a_{kij} and b_{kij} coefficients, as shown below (Holappa and Falzarano 1999):

$$G_{ij}(s) = \frac{\sum_{k=0}^{n} (i\omega)^k a_{kij}}{(i\omega)^{n+1} + \sum_{k=0}^{n} (i\omega)^k b_{kij}} \tag{B.8}$$

Equalizing B.7 with B.8, the coefficients a_{kij} and b_{kij} can be estimated by the simultaneous fit of equations using a suitable least square technique and taking into account stability criteria in order to keep the set of the recursive equations always stable. The extended state space representation then, for example for a one degree of freedom system, will be obtained as following, assuming for the curve fit $k = 3$:

$$\begin{aligned}
\dot{y}_1 &= y_2 \\
\dot{y}_2 &= \mathbf{f} + y_3 \\
\dot{y}_3 &= y_4 - a_3 y_3 - b_3 y_2 \\
\dot{y}_4 &= y_5 - a_2 y_3 - b_2 y_2 \\
\dot{y}_5 &= y_6 - a_1 y_3 - b_1 y_2 \\
\dot{y}_6 &= -a_0 y_3 - b_0 y_2
\end{aligned} \tag{B.9}$$

where y_1, y_2 is the displacement and velocity variables respectively, $\mathbf{f}$ represents external forces except radiation and y_3 is the radiation force.

B.2 Viscous forces calculation method

In this section, more details about the calculation procedure and the related parameters for the estimation of the viscous forces are presented. The analysis is based on Lloyd (1989) respective method. As pointed in Chapter 6, where the mathematical model for the coupled roll motion described, viscous damping forces are decomposed in three parts: eddy making damping, skin friction damping and bilge keel or appendage damping. Their calculation

methodology follows.

B.2.1 Eddy making damping

According to Tanaka (1960) and Schmitke (1978), the force due to the making of eddies is generated at the point where the geometry of the hull is sharply changed and whose distance from ship's center of gravity is r_b according to the next figure for various types of hull sections.

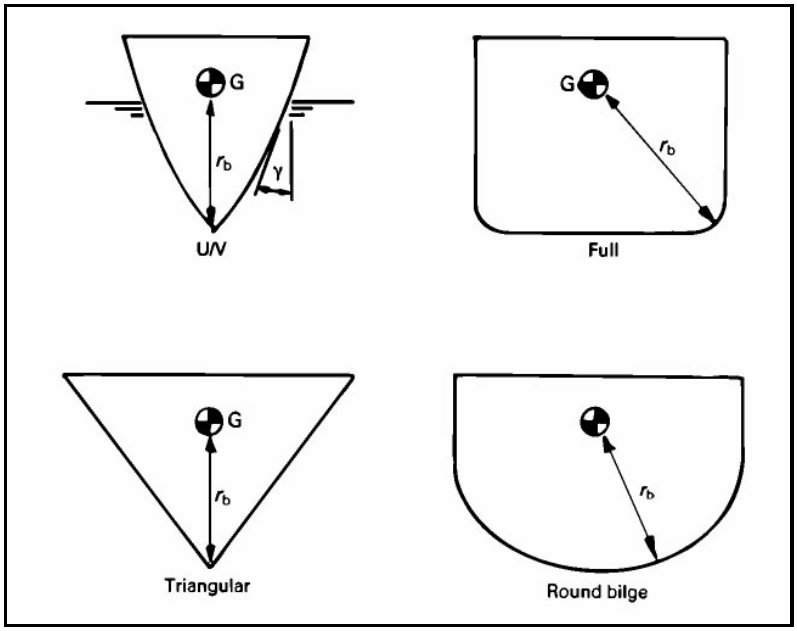

Figure B.2: Parameters for different hull sections, extracted from Lloyd (1989).

If $\dot{\varphi}$ is the rolling velocity, then the force at this point will be derived from:

$$F = \frac{1}{2}\rho r_b \dot{\varphi} |r_b \dot{\varphi}| s C_E dx_b \tag{B.10}$$

where s, dx_b are the radius of curvature and the length of the section respectively and ρ is water's density. The drag coefficient is estimated according to Schmitke (1978) with the following empirical formula:

$$C_E = Z_1 Z_2 \exp\left(-u r_e / D\right) \tag{B.11}$$

where Z_1, Z_2 are functions of B_S/KG, γ and r_e/D and estimated by Figure B.3. γ is the slope of the hull in the waterline, B_S and D are ship's breadth and depth respectively, u is a function of the roll amplitude and r_e is the active radius down to the keel and estimated by:

$$r_e = \frac{B_S}{2}\left[4.12 - 2.69\frac{KG}{B_S} + 0.823\left(\frac{KG}{B_S}\right)^2\right] \text{ in (m), } \frac{KG}{B_S} < 2.1 \tag{B.12}$$

$$r_e = 0\ ,\ \frac{KG}{B_S} > 2.1 \tag{B.13}$$

$$u = 14.1 - 46.7\varphi + 61.7\varphi^2 \tag{B.14}$$

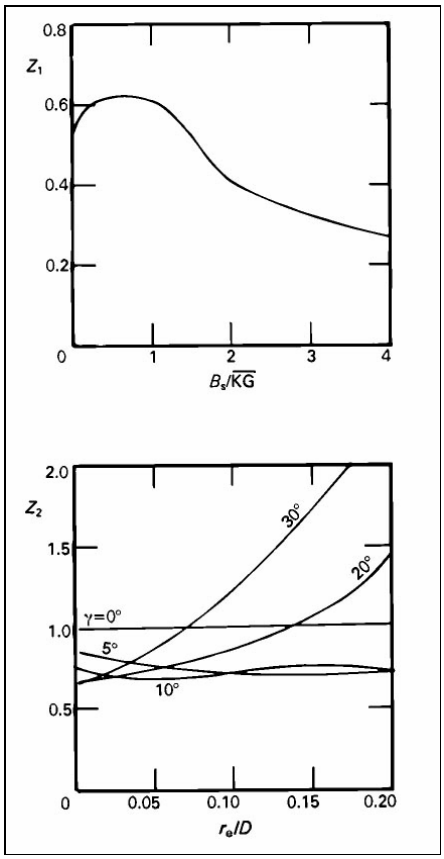

Figure B.3: Estimation of Z_1, Z_2 , extracted from Lloyd (1989).

B.2.2 Skin friction damping

The flow of the fluid on the hull incurs surface friction forces. The force generated on a element δs whose distance from the center of gravity is r and the tangential velocity on his element due to rolling motion is $r\dot{\varphi}\sin(\theta_1 + \theta_2)$, see Figure B.4, is given by:

$$F = \frac{1}{2}\rho r\dot{\varphi}\sin(\theta_1 + \theta_2)\left|r\dot{\varphi}\sin(\theta_1 + \theta_2)\right|\delta s C_F dx_B \tag{B.15}$$

where the friction coefficient C_F calculated when ship's forward ship is zero by the formula of Kato (1958):

$$C_F = 1.328R_N^{-0.5} + 0.014R_N^{-0.014} \tag{B.16}$$

Where R_N is a Reynolds number that depends on the mean roll velocity $\bar{\dot{\varphi}}$ and the mean distance from the center of gravity $\bar{r}$:

$$R_N = \frac{0.515\rho\left(\bar{r}\bar{\dot{\varphi}}\right)^2 \omega_{roll}}{\mu_w} \tag{B.17}$$

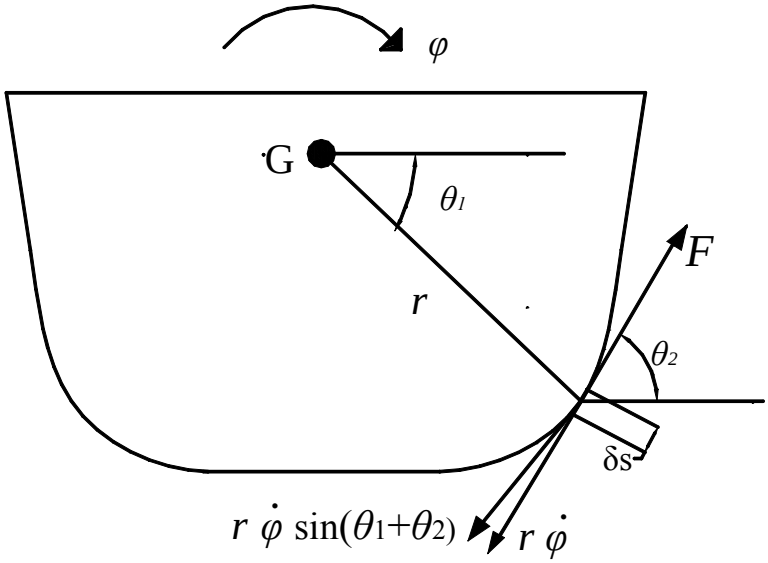

Figure B.4: Skin friction force.

$$\bar{r} = \frac{1}{\pi}\left[(0.887 + 0.145C_B)(1.7D + B_S C_B) + 2(KG - D)\right] \text{ in (m)} \tag{B.18}$$

where μ_w is viscosity coefficient, ω_{roll} is the rolling response frequency and C_B is hull coefficient. In the case where ship's forward ship exists, then Schmitke (1978) proposed the formula of Schoenherr for the estimation of the mean friction coefficient which is based on the calculations of ship resistance.

$$C_F = 0.004 + \left[3.36\log_{10}\left(R_N\right) - 5.6\right]^{-2} \tag{B.19}$$

where the Reynolds number depends on ship speed U and on her length L_S :

$$R_N = \frac{\rho U L_S}{\mu_w} \tag{B.20}$$

B.2.3 Damping due to bilge keels

The case where ship's speed is zero is taken into account, so bilge keels generate only drag force. This force, considering rolling motion is estimated by:

$$F_B = \frac{1}{2}\rho r_A \dot{\varphi} \left| r_A \dot{\varphi} \right| C_D A_{BK} \tag{B.21}$$

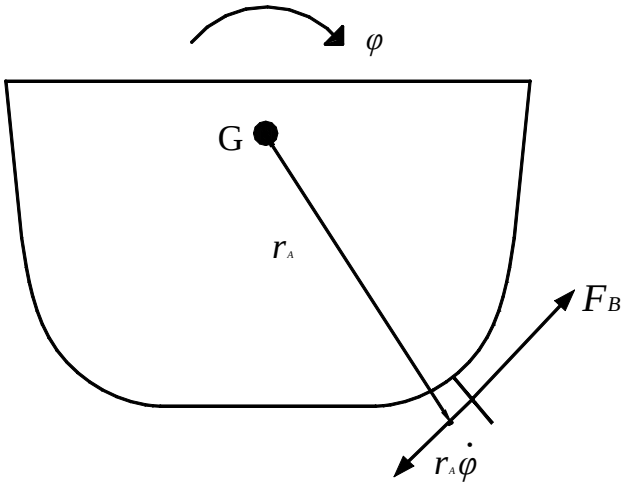

Figure B.5: Bilge keel force.

Where the distance of bilge keels from the center of gravity G is r_A, A_{BK} is the total bilge keel area and C_D is a drag coefficient whose value according to Lloyd (1989) is 1.17 .

Appendix C:

Application of the mathematical model for coupled rolling motion of a fishing vessel

The developed mathematical model for the simulation of the coupled rolling motion in beam seas has been employed by the assessment as a calculation tool for the critical wave group identification. However it can be also used as a standard time domain numerical simulation code. For this reason an application studying the dynamic stability of a fishing vessel has been carried out. The effect of various parameters on the roll response such as the wave steepness, the wave frequency as well as different initial states of the ship on the wave has been examined. Furthermore the impact of drift motion on the mean roll angle will be discussed.

C.1 General ship characteristics

A Japanese fishing vessel, which has been used by the International Towing Tank Conference (ITTC) as a reference ship for intact stability, has been studied. Her body plan and basic particulars (Umeda et al. 1995) are shown in Figure C.1 and Table C.1 respectively. The distribution of panels on the hull as generated by the code is presented in Figure C.2 . Due to symmetry the half hull is provided.

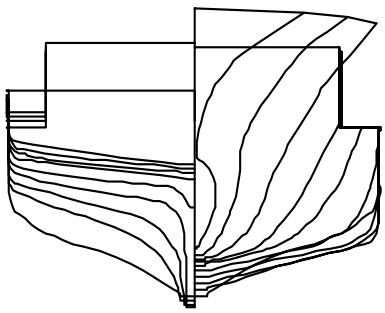

Figure C.1: Body plan.

Table C.1: Main particulars of investigated ship.

L_{bp} (length)	34.5 m	GM (metacentric height)	0.75 m
B (beam)	7.60 m	T_0 (natural roll period)	9.7 s
D (depth)	3.07 m	b_{BK} (breadth of bilge keels)	0.35 m
T (mean draft)	2.65 m	KG (vertical position of centre of gravity above keel)	3.36 m
C_b (block coef.)	0.597		

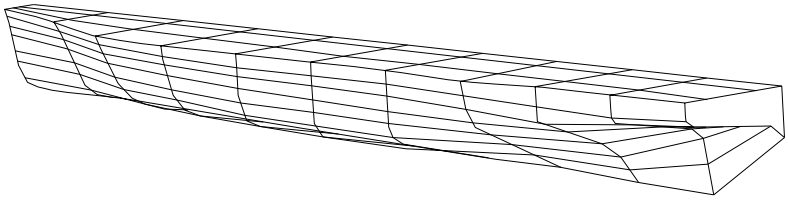

Figure C.2: Half-hull panelization.

The GZ curve in calm water as calculated numerical from the code, is shown in Figure C.3. The code provides the capability of the calculation of the restoring forces in case of static stability, thus for a given value of heel angle and for an appropriate value of the vertical distance of the center of gravity from the free surface in order the vertical balance of forces to be satisfied.

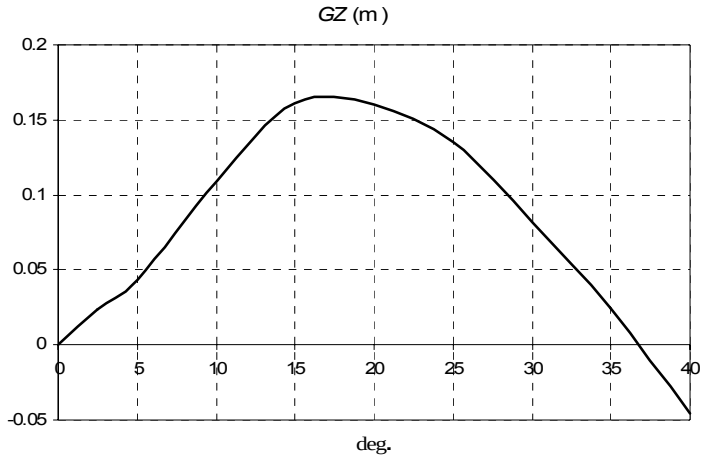

Figure C.3: The GZ curve.

The angle of vanishing stability is about 37.5^0. Simulation of a roll decay test from extreme angle of release, approximately 85% of the angle of vanishing stability, is illustrated in Figure C.4.

C.2 Numerical simulations and response results

In Figure C.5 to Figure C.7 are shown the time histories of roll, heave and sway response respectively near resonance, for moderate wave steepness. Heave is measured from the inertial coordinate system (Chapter 6) and therefore starts from a non zero value. From the corresponding sway response per wave period, it is apparent that there is significant drifting motion that cannot be neglected.

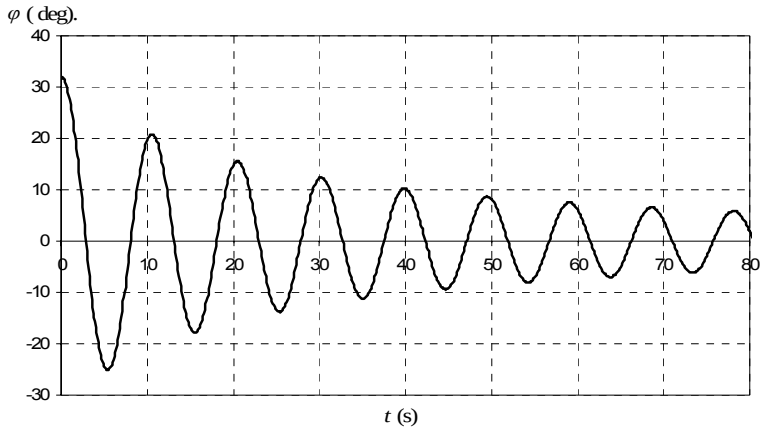

Figure C.4: Roll decay test.

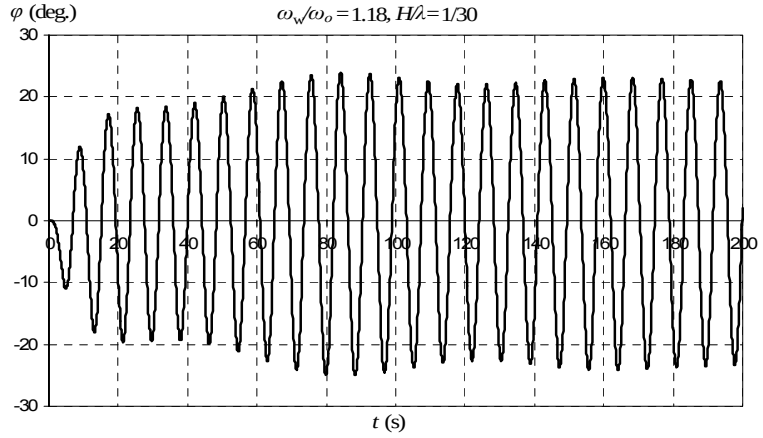

Figure C.5: Roll response for $\omega_w / \omega_o = 1.18$ and $H/\lambda = 1/30$.

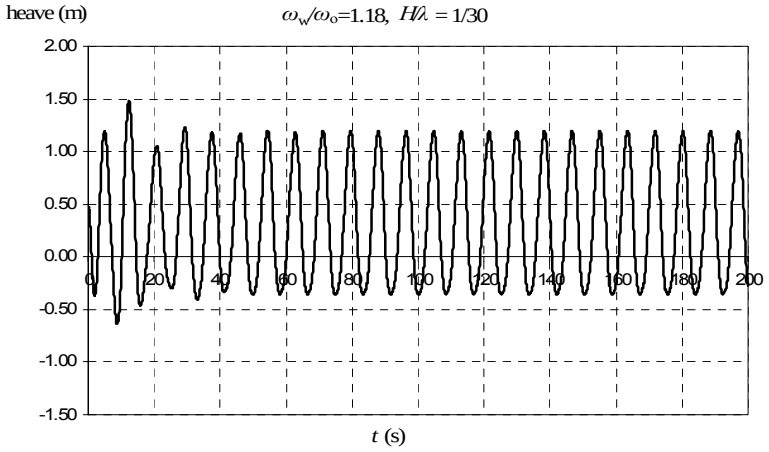

Figure C.6: Heave response for $\omega_w / \omega_o = 1.18$ and $H/\lambda = 1/30$.

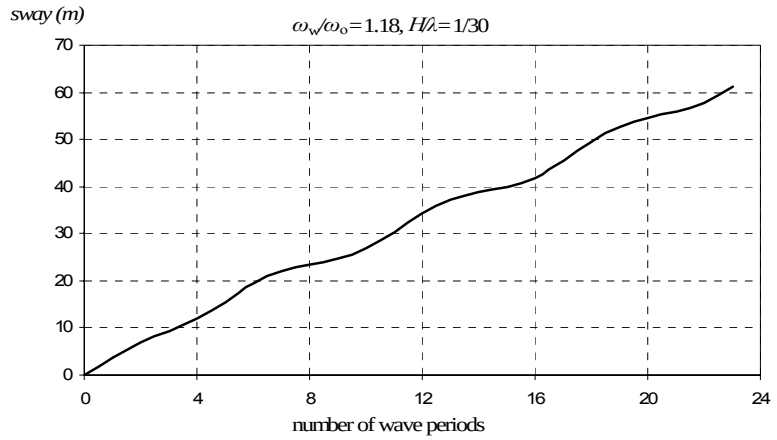

Figure C.7: Respective sway response.

Next, the effect of wave steepness on the amplitude of steady roll (Figure C.8) and also on the mean roll angle is examined (Figure C.9). There seems to be a near linear relationship between the amplitude of roll and wave steepness. Furthermore, there is an increase of a similar nature concerning the mean roll angle (towards the weather side), which, for $H/\lambda = 1/12$, can become about 16% of the roll amplitude. It is believed that the mean roll angle comes from the lateral wave drift force combined with the lateral resistance force, so this pair produces an extra roll moment that tends to rotate the ship towards the weather side. This bias in rolling motion should be seriously taken into account as it may reduce disproportionally the dynamic stability of the ship (Thompson 1997).

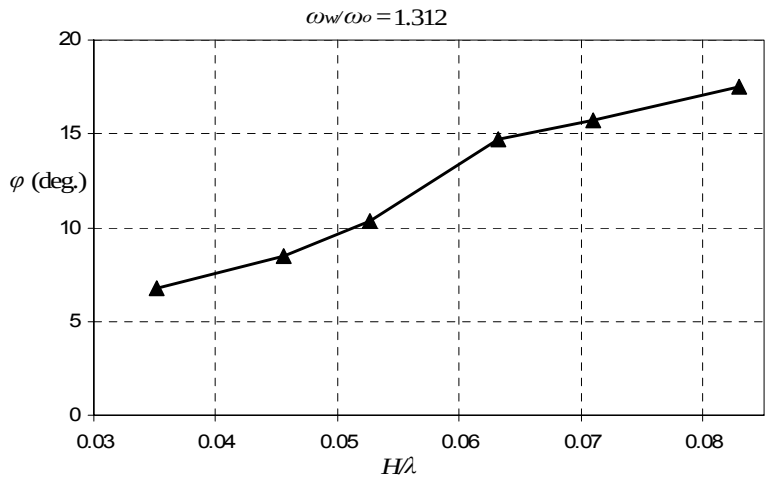

Figure C.8: Effect of wave steepness on roll amplitude ($\omega_w / \omega_o = 1.312$).

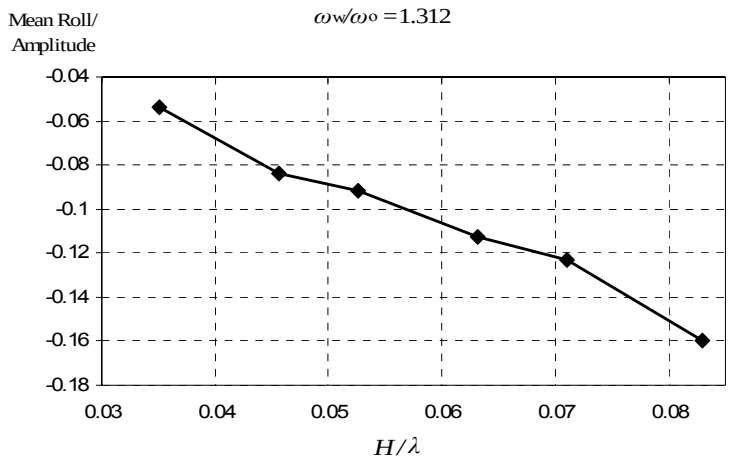

Figure C.9: Effect of wave steepness on the mean roll angle ($\omega_w / \omega_o = 1.312$).

The drift motion tends to lower the encounter frequency and, as a result, larger amplitude motion appears later in terms of wave frequency. This effect is shown in Figure C.10 where it presents points of the roll response curve taking into account the mean drift velocity in the calculation of encounter frequency, k is the wavenumber.

$$\omega_e = \omega_w - k\overline{v}_{drift} \tag{C.1}$$

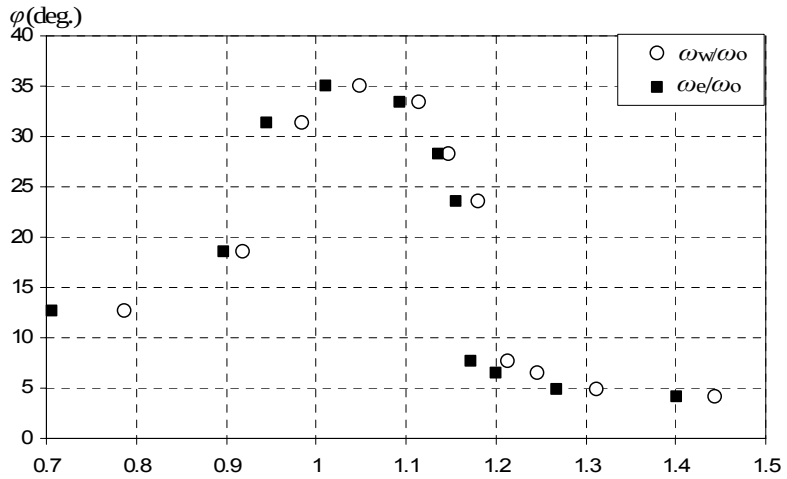

Figure C.10: Roll response diagram for constant wave steepness $H/\lambda = 1/30$.

C.3 Different initial states of the ship on wave

It is well known that different initial conditions can affect the amplitude of transient (and some times also of steady-state) motion. In order to investigate this effect, various scenarios are examined for the initial roll angle and the lateral initial position of the ship on waves. When there is an initial heel to the lee side the obtained max roll is significantly higher than

that of heel to the weather side and therefore the propensity to capsize is affected (Figure C.11). Concerning the initial lateral position of the ship on the wave, the maximum transient roll angle is reached when the ship is placed on a trough (Figure C.12). It should be noted that initially there was balance in the vertical direction and in steady state the roll amplitude was the same for all scenarios.

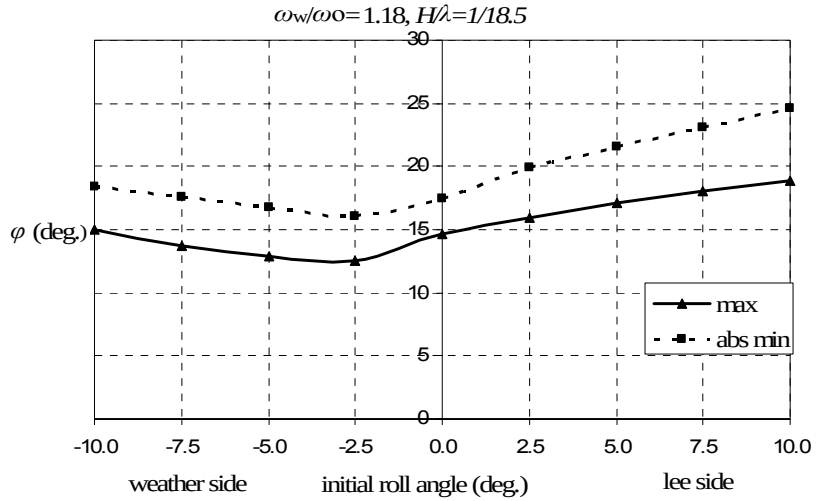

Figure C.11: Maximum and minimum roll angles (transient response) for different initial heel ($\omega_w / \omega_o = 1.18$, $H/\lambda = 1/18.5$).

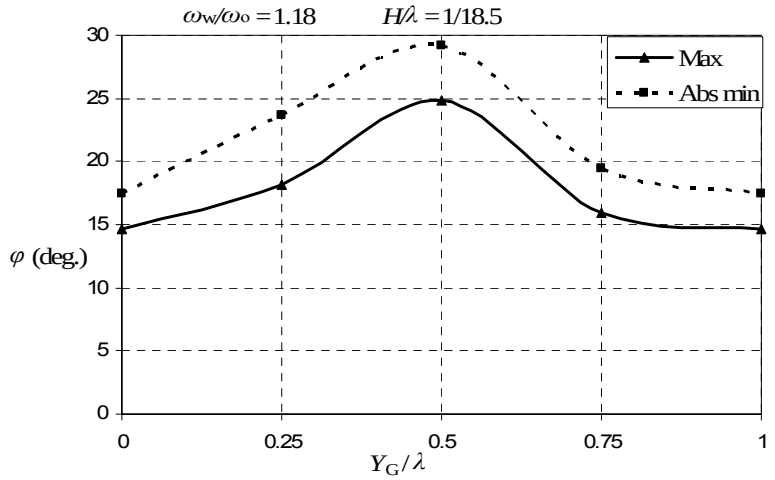

Figure C.12: Effect on transient response of the initial lateral position ($\omega_w / \omega_o = 1.18$, $H/\lambda = 1/18.5$).

Appendix D:

Effect of initial conditions for the uncorrelated roll angle – roll velocity distribution

In this section, the case of a joint pdf $p(\varphi,\dot{\varphi})$ without the condition for the wave trough is considered, where under the assumption of stationary process, the roll angle and velocity are uncorrelated.

$$p_{\varphi\dot{\varphi}}(\varphi,\dot{\varphi}) = p_{\varphi}(\varphi)\, p_{\dot{\varphi}}(\dot{\varphi}) \tag{D.1}$$

The response spectrum can then be derived in the usual manner for linear processes:

$$S_z(\omega) = \left|F(\omega)\right|^2 S_{\zeta}(\omega) \tag{D.2}$$

which is in fact the Wiener – Khinchin theorem (Price and Bishop 1974) providing the relationship among spectra of excitation and response for linear systems.

$$F(\omega) = \frac{(\omega\cdot\omega_0)^2}{g\sqrt{(\omega_0^2-\omega^2)^2+4\omega k^2}} \tag{D.3}$$

The probability density function of the response will be Gaussian (x can be φ or $\dot{\varphi}$):

$$p_x(x) = \frac{1}{\sigma_x\sqrt{2\pi}}\, e^{-0.5\left(\frac{x}{\sigma_x}\right)^2} \tag{D.4}$$

where the standard deviation is:

$$\sigma_x^2 = \int_0^{\infty} S_x(\omega)\, d\omega \tag{D.5}$$

The respective results assuming the above pdf and the same parameters as in the application of section 8.3.3 are presented next (Figure D.1 to Figure D.5)

Comparing the corresponding diagrams, it is revealed that both the case of the uncorrelated roll angle – roll velocity distribution and the conditional joint distribution of roll response in a wave trough present a similar quantitatively behaviour in the probability figures. However the assumption of the uncorrelated roll angle – roll velocity distribution leads to lower difference in the probability figures with the “quiescent case” which is about 10% - 15% compared with

the conditional roll response distribution.

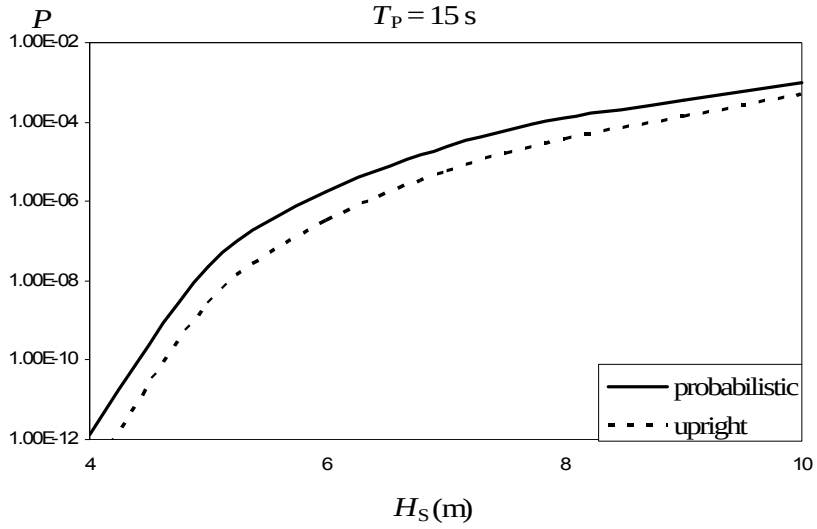

Figure D.1: Total probabilities for the "quiescent" and for the joint case ($r / z_{cr} = 1$) varying H_S .

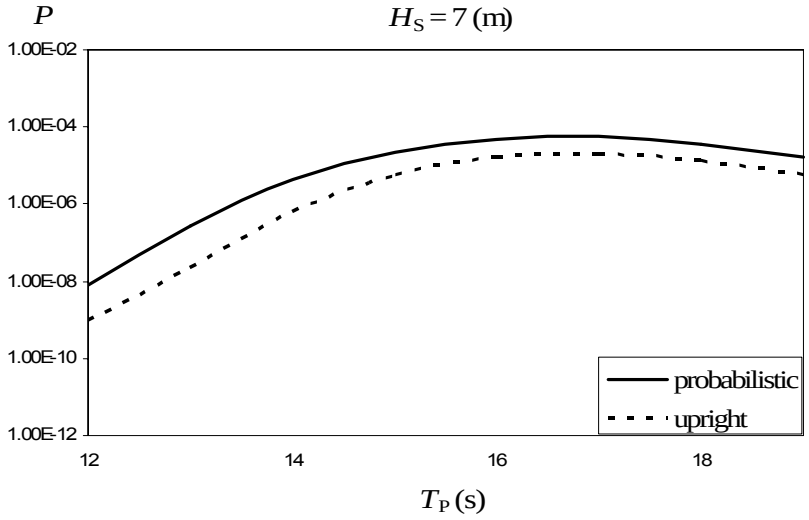

Figure D.2: Total probabilities for the "quiescent" and for the joint case ($r / z_{cr} = 1$) varying T_P .

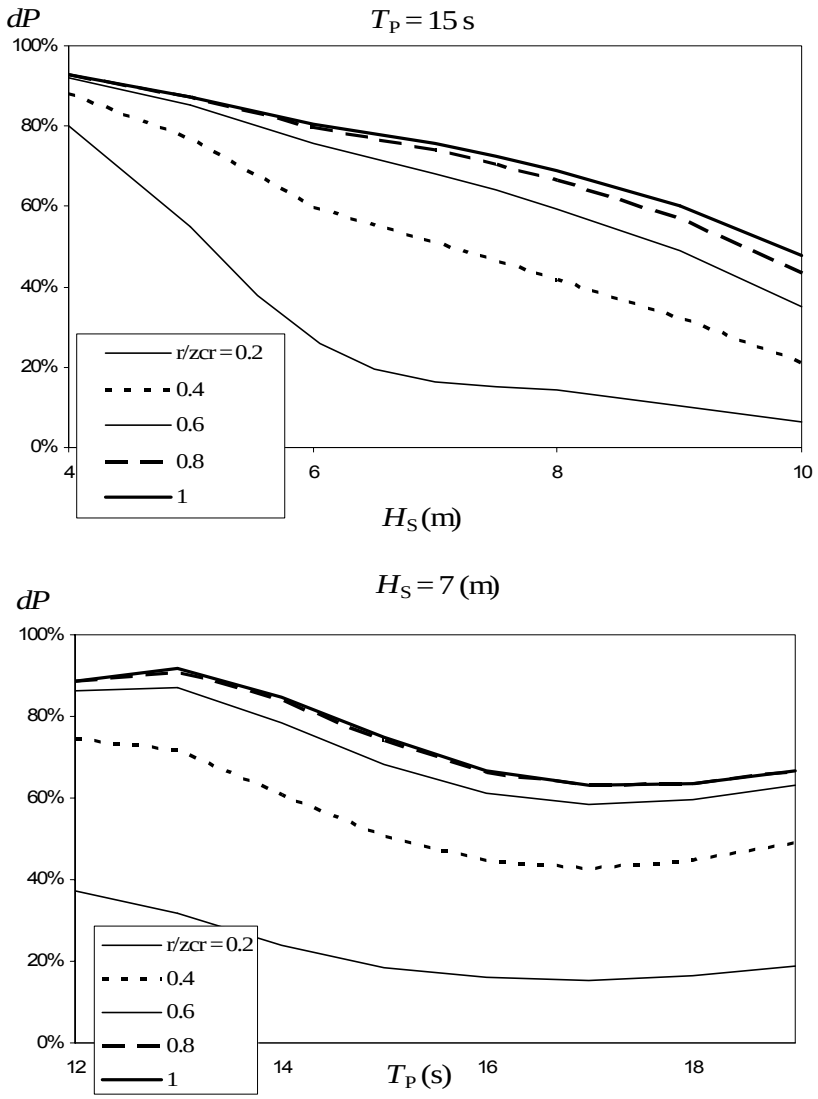

Figure D.3: Difference in probabilities as the ratio r/z_{cr} is varied.

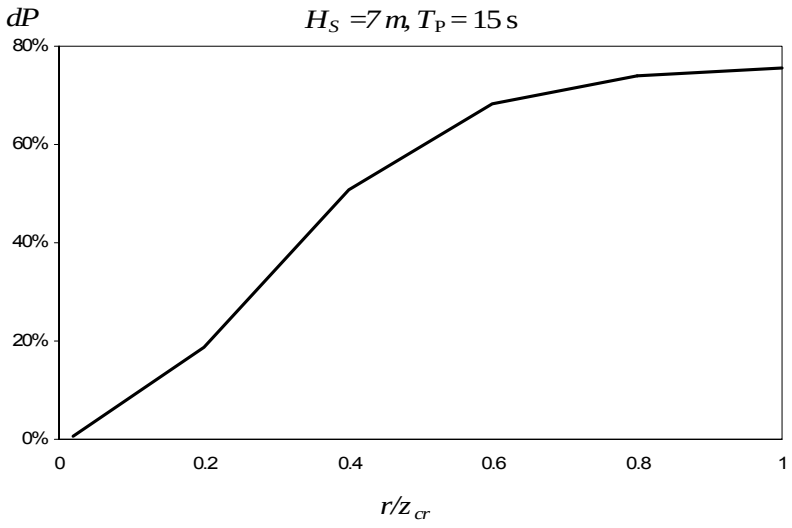

Figure D.4: Effect of the ratio r/z_{cr}